UNIVERSITÀ DEGLI STUDI DI PAVIA

DOTTORATO IN SCIENZE CHIMICHE E FARMACEUTICHE E INNOVAZIONE INDUSTRIALE

XXXIII CICLO

Coordinatore: Chiar.mo Prof. Piersandro Pallavicini

HIGHLY ATOM-ECONOMIC AND ECO-COMPATIBLE GOLD(I)-CATALYZED INTRAMOLECULAR ENANTIOSELECTIVE CYCLIZATION REACTION FOR THE TOTAL SYNTHESIS OF SATURATED HETEROCYCLES

Tesi di Dottorato di

Massimiliano Andreoli

a.a. 2019-2020

Tutor:

Chiar.mo Prof. Giuseppe Zanoni

Sommario

1 Overview on natural products containing saturated heterocycles

Heterocycles are noteworthy because of their biological activity and their applications in diverse fields, reflected by the fact that heterocycles constitute more than half of known organic compounds. Heterocyclic moieties are ubiquitous in important classes of naturally occurring compounds, for example, alkaloids, vitamins, hormones, and antibiotics. They are also widely prevalent in pharmaceuticals, herbicides, dyes and many other application-oriented materials. Many natural products possess heterocyclic moieties, and many of them are important in terms of their biological activities and application in different fields.

1.1 Oxygen-containing saturated heterocycles

1.1.1 Natural products containing Tetrahydrofurans and Tetrahydropyrans

Several natural products and biologically active compounds present oxygenated five-atom rings as structural motif. In particular, substituted tetrahydrofurans (THFs) and tetrahydropyrans (THPs) are sub-structures commonly found in both terrestrial and marine metabolites. These substances possess a wide range of biological activities, including anti-tumoral and anti-microbial activity.

For example, Communiols are natural products isolated for the first time by Malloch and collaborators in 2004, during their studies on coprophil mushrooms[1]. This extract of the *Podospora communis* mushroom, obtained from horse manure, was purified by reverse phase HPLC, allowing to isolate three new compounds, called Communiols A-C. They are characterized by the presence of a tetrahydrofuranic scaffold and by a high antibacterial activity towards *Bacillus subtilis* and *Staphylococcus aureus*.

The configuration (3S, 5S, 6S) was initially attributed to Communiol C, while (5R, 7S, 8S) to Communiols A and B, relying exclusively on NMR spectroscopy. Kuwahara and Enomoto[2] subsequently attempted to synthesize the Communiol C with the structure proposed by Gloer. However, the spectroscopic data of the synthetic Communiol did not correspond with those of the isolated natural compound.

They therefore modified their synthesis in order to obtain the communiol diastereoisomer C (3R, 5R, 6S), whose experimental data are in agreement with the molecule isolated by Gloer. As a consequence, they also obtained the correct structures for the communiols A and B, the diastereoisomers (5S, 7R, 8S).

[1] Che, Y.; Gloer, J.B.; Scott, J.C.; Malloch, D. *Tetrahedron Lett.* **2004**, *45*, 6891
[2] Kuwahara, S.; Enomoto, M. *Tetrahedron Lett.* **2005**, *46*, 6297

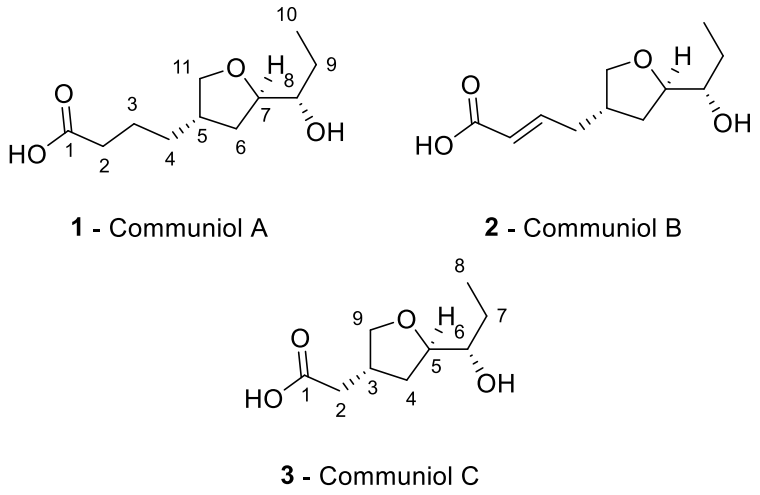

Figure 1.1 - Communiols with correct structures

Communiols' structures contain a 2,4-disubstituted tetrahydrofuran, a unit structurally quite rare among natural products. This structural peculiarity and the high antibacterial activity render intriguing the production of an easy and efficient synthetic route, also for the purpose of any large-scale production.

Another example is the family of *Acetogenine Annonacee* (ACG), a group of secondary metabolites isolated from a genus of typically tropical plants called *Annonaceous*. These compounds possess a wide range of biological activities, in particular antitumor, cytotoxic, antiparasitic, pesticide, antimalarial and immunosuppressive activity.

The general structure of these natural products is characterized by a linear hydrocarbon chain (C_{32} or C_{34}) with a terminal γ-lactone. Over the years, different types of ACG have been isolated and characterized. Their classification[3] is based on the type of functional groups present on the linear chain. In most cases there are oxygenated substituents, such as hydroxyl groups, ketones, epoxides, tetrahydropyranes and tetrahydrofurans, but it is also possible to observe double and triple bonds.

ACGs containing tetrahydrofuranic nuclei are generally classified according to the number of heterocycles present: mono-THF-ACG, bis-THF-ACG and tri-THF-ACG. Only one component belongs to the latter class, namely goniocin, while for the other two there are more compounds. There is also the THP-ACG class, in which belongs the ACGs presenting a tetrahydropyran scaffold in the structure.

[3] Zafra-Polo, M.C.; Figadère, B.; Gallardo, T.; Tormo, J.R.; Cortes, D. *Phytochemistry* **1998**, *48* (7), 1087

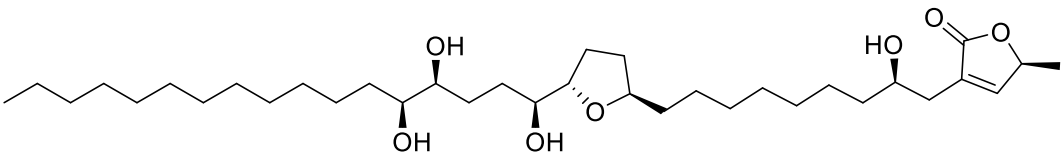

4 - Muricatetrocin B

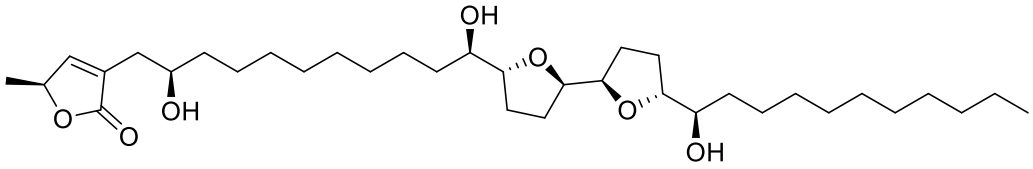

5 - Parviflorin

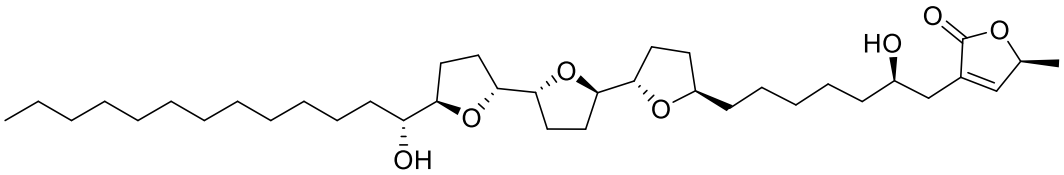

6 - Goniocin

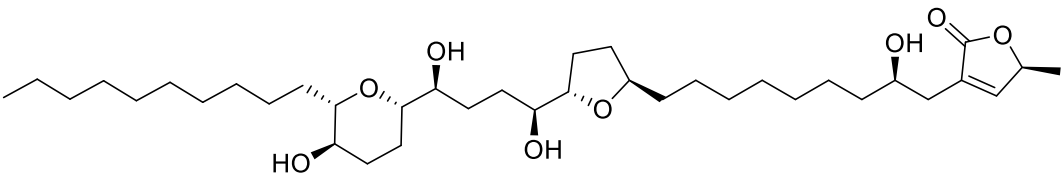

7 - Mucocin

Figure 1.2 - Some examples of ACGs

Recent studies allowed to define the biological activity of these compounds, which differs simply based on their structure[4]. A too much short spacer between the lactone and the tetrahydrofuran ring induces a decrease in the activity of the molecule, as well as a terminal alkyl chain, too much hydrophobic. This is most likely due to the fact that the oxygenated heterocycle strongly interacts with the liposomal lipid membrane, acting as an anchor and optimizing the position and conformation of the functional groups present on the ACGs[5].

1.1.2 Natural Products containing lactones

THFs and THPs are not the only oxygen-containing saturated heterocycles found in natural products. As described above, in most of the ACGs the linear Carbon chain is terminated by a γ-lactone. However, they are just an example among a large variety of natural products.

[4] Miyoshi, H.; Ohshima, M.; Shimada, H.; Akagi, T.; Iwamura, H.; McLaughlin, J. L. *Biochim Biophys Acta*, **1998**, *1365*, 443

[5] Shimada, H.; Grutzner, J. B.; Kozlowski, J. F.; McLaughlin, J. L. *Biochemistry*, **1998**, *37*, 854

In the Amazonian forest of French Guiana, some woody species are commercialized for residential construction and other outdoor applications because of their excellent resistance to decay. From the extracts of commercial waste of this durable wood, a large number of compounds has been isolated, showing antifungal activity. For instance, extracts from the trunk wood of the Amazonian tree *Nectandra Rubra* allowed the isolation of unique lactones rubrenolide and rubrynolide[6] (Figure 1.3).

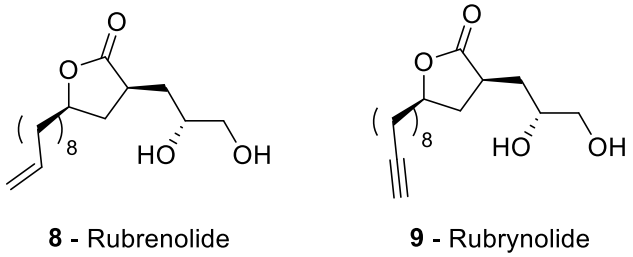

8 - Rubrenolide **9** - Rubrynolide

Figure 1.3 - Lactones isolated from N. Rubra

Some years after their isolation and characterization, Stien and Espìndola[7] discovered that both these compounds displayed rather low cytotoxicities, with IC_{50} values > 100 µg/mL against several fungi. For this reason, both these metabolites have some potential as lead compounds in the search of new antifungal agents, especially considering the very high potency against dermatophytes.

Limonoids are modified triterpenes derived from a precursor with a 4,4,8-trimethyl-17-furanysteroid skeleton. It has been suggested that limonoids present in the Citrus seeds are translocated from the fruit tissue and that consequently juices extracted from seedless fruits suffer severely from limonoids bitterness[8]. The three major representatives of this class of compounds are limonin, nomilin and obacunone (*Figure 1.4*).

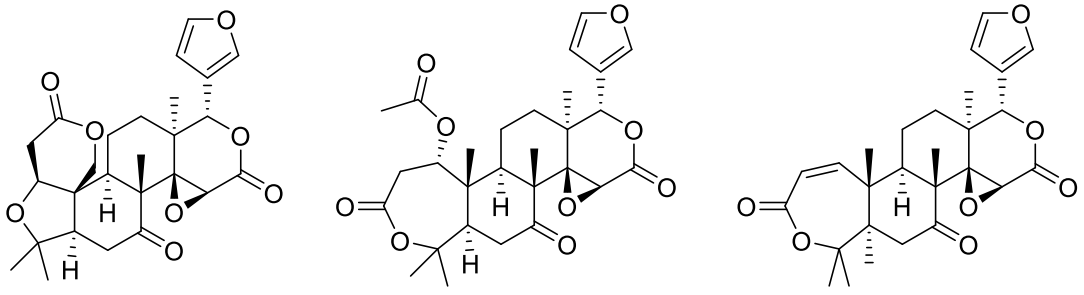

10 - Limonin **11** - Nomilin **12** - Obacunone

Figure 1.4 - Limonoids found in Citrus seeds

Bitterness is not the only characteristic of this class of compounds. Some recent studies demonstrate the cytotoxic activity of these natural products, especially towards MCF-7 cell lines, corresponding to

[6] Franca, N.C.; Gottlieb, O.R.; Coxon, D.T. *Phytochemistry* **1977**, *16*, 257
[7] Rodrigues, A.M.S.; Theodoro, P.N.E.T.; Eparvier, V.; Basset, C.; Silva, M.R.R.; Beauchene, J.; Espìndola, L.S.; Stien, D. *J. Nat. Prod* **2010**, *73*, 1706
[8] Hasegawa, S.; Bennett, R.D.; Verdon, C.P. *J. Agric. Food. Chem.* **1980**, *28* (5), 922

breast cancer cell lines[9]. Some years after, in 2003, Vullo and coworkers found that limonin and nomilin showed an inhibitory effect on HIV. They demonstrated that this two limonoids were able to inhibit *in vitro* HIV-1 protease activity, preventing cell replication at all the concentrations studied[10].

1.1.3 Stereoselective synthesis of oxygen-containing heterocycles

Due to the importance of biologically active compounds containing oxygenated rings presented above, over the last decades considerable efforts have been devoted towards the development of stereoselective strategies for the construction of resembling systems.

In this section, the attention will be focused on methods involving the formation of the C- O bond as key step. As a matter of fact, they are inherent in the methodology developed in this PhD thesis, which will be described in the next chapters.

In 2015, Wolfe and his research group developed a Pd-catalyzed coupling of γ-hydroxyalkenes with aryl bromides, affording enantiomerically enriched 2-(arylmethyl)tetrahydrofuran derivatives[11]. This transformation was achieved through the development of a new TADDOL-derived chiral phosphite ligand (*Scheme 1.1*). The transformations are effective with several aryl bromides, and can be used for the production of THFs bearing quaternary stereocenters.

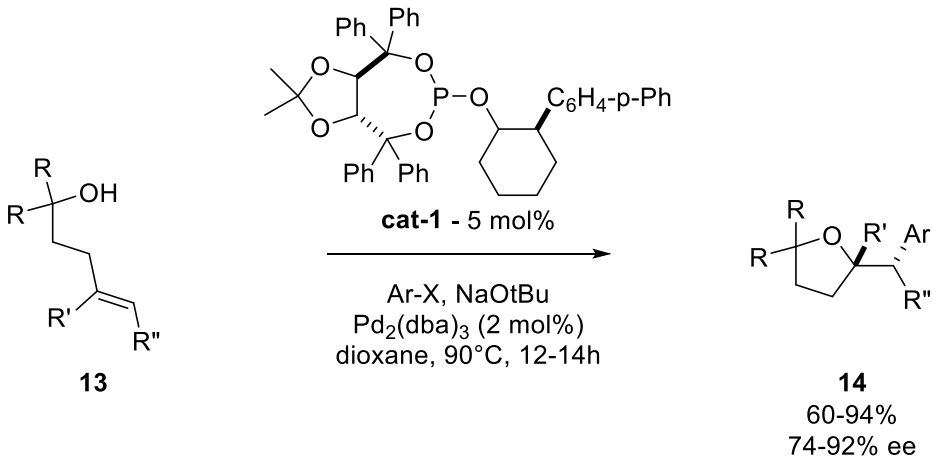

Scheme 1.1 - Enantioselective Pd-Catalyzed Carboalcoxylation

In a similar fashion, also lactones can be obtained. Buchwald and coworkers, in the same year, designed a versatile method for the rapid synthesis of diverse enantiomerically enriched lactones based on Cu-catalyzed enantioselective radical oxyfunctionalization of alkenes[12]. A wide range of radicals were found to participate in this type of reaction, including azidyl, arylsulfonyl, aryl, acyloxyl, and alkyl radicals. This

[9] Tian, Q.; Miller, E.G.; Ahmad, H.; Tang, L.; Patil, B.S. *Nut. Cancer* **2001**, *40* (2), 180
[10] Battinelli, L.; Mengoni, F.; Lichtner, M.; Mazzanti, G.; Saija, A.; Mastroianni, C.M.; Vullo, V. *Planta Med* **2003**, *69*, 910
[11] Hopkins, B.A.; Garlets, Z.J.; Wolfe, J.P. *Angew. Chem. Int. Ed.* **2015**, 54, 13390
[12] Zhu, R.; Buchwald, S.L. *J. Am. Chem. Soc.* **2015**, 137, 8069

method provides rapid access to a broad spectrum of interesting enantiomerically enriched lactones through tandem C-C and C-Hetero bond formation.

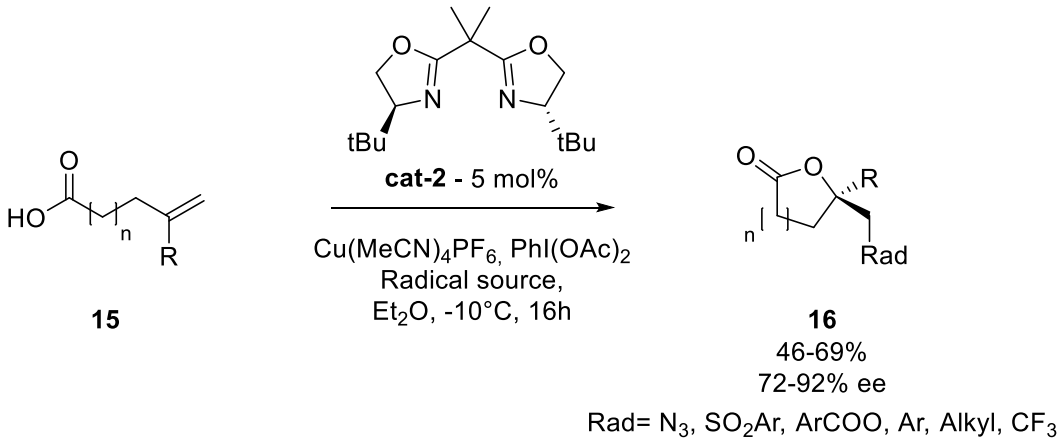

Scheme 1.2 - Enantioselective Cu-Catalyzed Radical Oxyfunctionalization

In 2016, List and coworkers described the development of the first catalytic asymmetric vinylogous Prins cyclization[13]. This transformation represents an efficient approach for highly diastereo- and enantioselective synthesis of tetrahydrofurans and is catalyzed by a confined chiral imidodiphosphoric acid (IDP) (*Scheme 1.3*). Aromatic and heteroaromatic aldehydes react with various 3,5-dien-1-ols to afford 2,3-disubstituted THFs with d.r. values up to >20:1, and e.r. values up to 99:1.

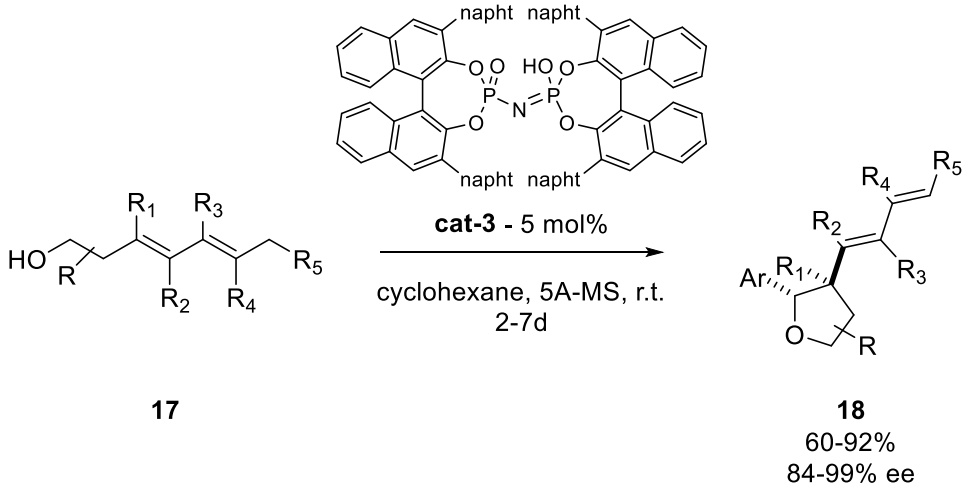

Scheme 1.3 - Enantioselective Vinylogous Prins Cyclization

The same research group, a couple year after, developed a catalytic chemo- and enantioselective nucleophilic additions to ketoaldehydes[14]. The selective addition of nucleophiles toward ketones over aldehydes was observed, thanks to the oxonium-ion intermediate (*Scheme 1.4*). Five- and six-membered rings with both aromatic and aliphatic substituents, as well as an alkynyl substituent, are obtained.

[13] Xie, Y.; Cheng, G-J.; Lee, S.; Kaib, P.S.J.; Thiel, W.; List, B. *J. Am. Chem. Soc.* **2016**, 138, 14538
[14] Lee, S.; Bae, H.Y.; List, B. *Angew. Chem. Int. Ed.* **2018**, 57, 12162

Moreover, multisubstituted THFs are synthesized with excellent stereoselectivities, exploiting ion-pair catalysis.

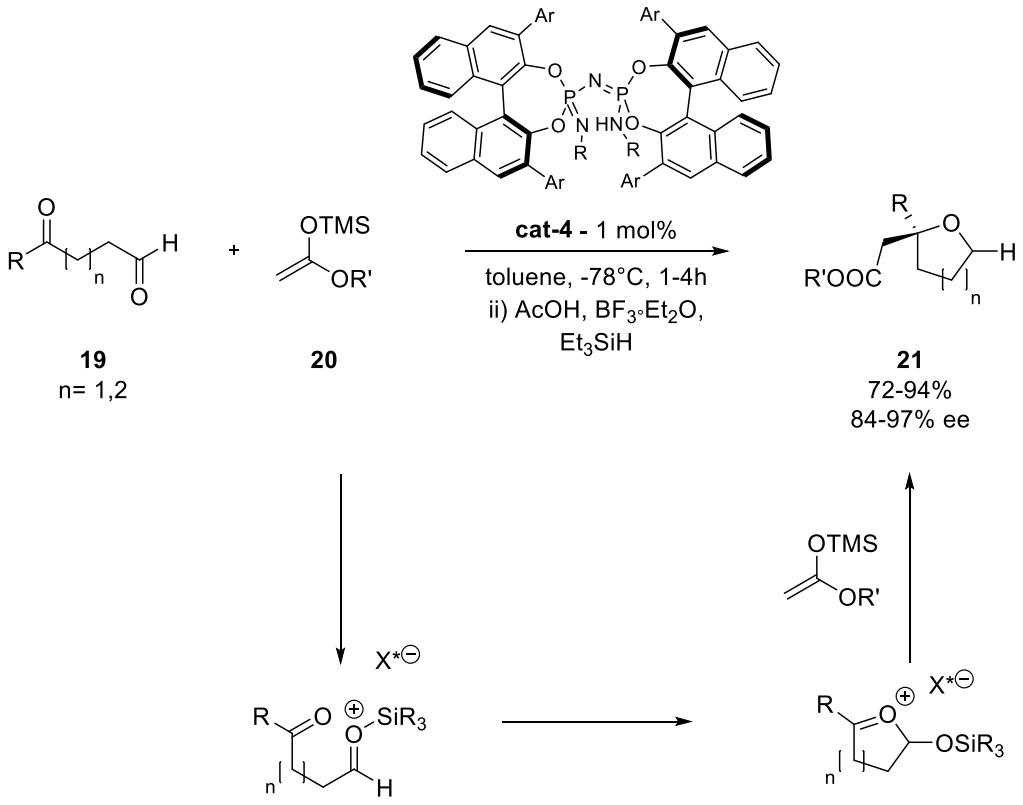

Scheme 1.4 - Regio- and Enantioselective Nucleophilic Addition

In 2017, Biju and his research group developed a N-Heterocyclic Carbene (NHC) catalyzed enantioselective synthesis of cyclopentane-fused β-lactones by the intramolecular aldol lactonization of ketoacids[15]. The reaction proceeds under mild conditions thanks to the chiral NHC catalyst along with HATU for the activation of acid. This process afforded the β-lactones in moderate to good yields and with excellent *ee* values.

[15] Mondal, S.; Mukherjee, S.; Das, T.K.; Gonnade, R.G.; Biju, A.T. *J. Org. Chem.* **2017**, 82, 9223

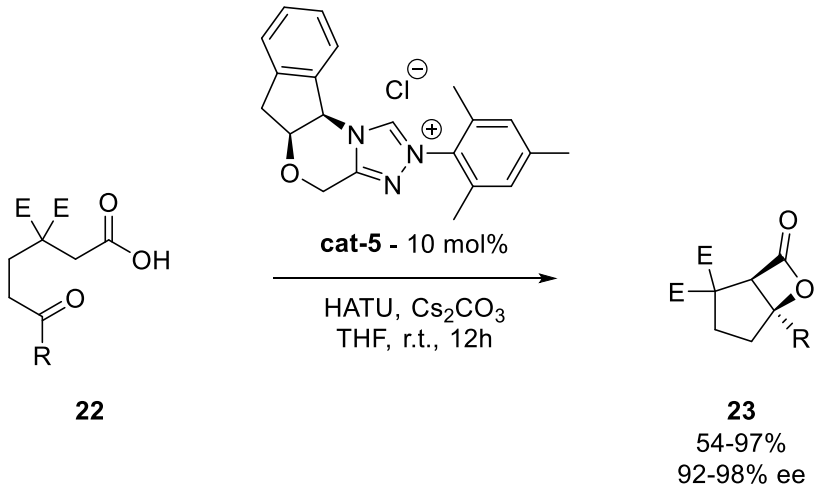

Scheme 1.5 - Enantioselective NHC-Catalyzed Aldol Lactonization

Another example of enantioselective synthesis of oxygen-containing heterocycles is represented by Johnson and coworkers' paper[16]. They developed a protocol for the preparation of enantioenriched THF derivatives through a dynamic kinetic asymmetric [3 + 2] cycloaddition of racemic malonate-derived cyclopropanes and aldehydes. A variety of cyclopropanes bearing electron-rich donor groups undergo cycloaddition with aryl, cinnamyl, and aliphatic aldehydes to afford products in good yields and enantioselectivities.

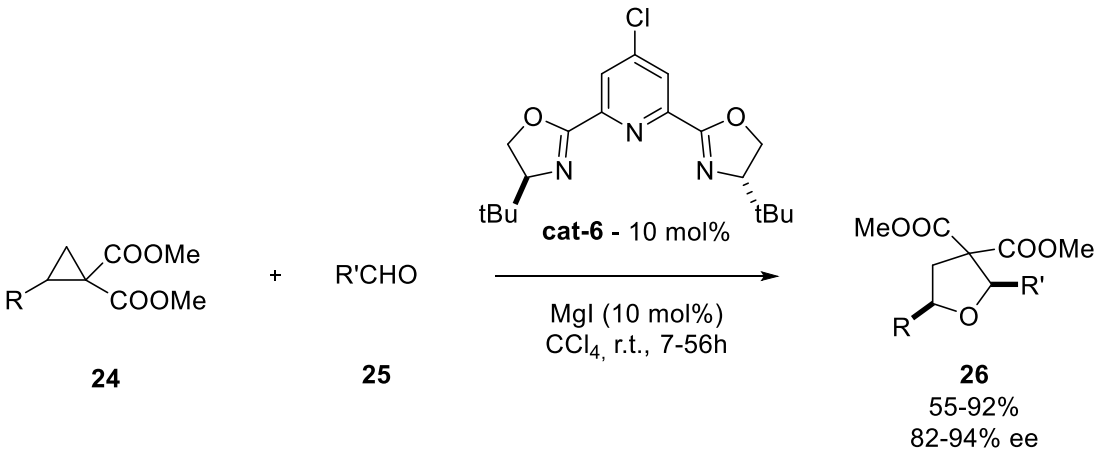

Scheme 1.6 - Enantioselective [3+2] Cycloaddition

In 2020, Lv and his research group achieved a Ru-Catalyzed asymmetric transfer hydrogenation of γ-keto carboxylic acids[17]. They exploited the formic acid–triethylamine azeotrope as the hydrogen source, affording chiral multicyclic γ-lactones in high yields with excellent diastereo- and enantioselectivities.

[16] Parsons, A.T.; Johnson, J.S. *J. Am. Chem. Soc.* **2009**, 131, 3122
[17] Xiong, Z.; Tian, J.; Xue, P.; Zhang, X.; Lv, H. *Org. Chem. Front.* **2020**, 7, 104

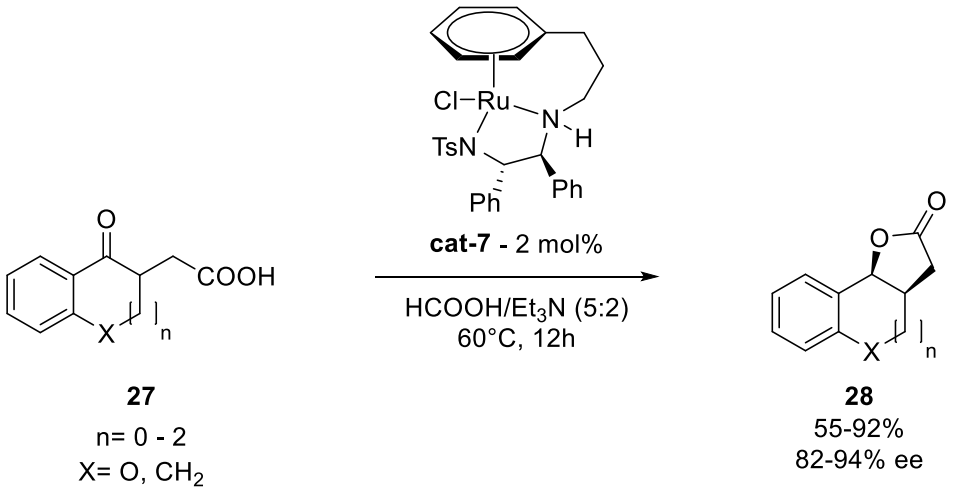

27
n= 0 - 2
X= O, CH_2

28
55-92%
82-94% ee

Scheme 1.7 – DKR-Mediated Tandem Reduction/Lactonization

In 2011, Marini and coworkers described an organocatalytic protocol for the synthesis of spirolactones from cyclic β-ketoesters and an easily accessible vinyl selenone[18]. This process, a one-pot Michael addition/cyclization sequence, is based on the peculiar properties of the phenylselenonyl substituent, which acts both as an electron-withdrawing group, during the addition step, and as a leaving group during the cyclization by intramolecular nucleophilic substitution.

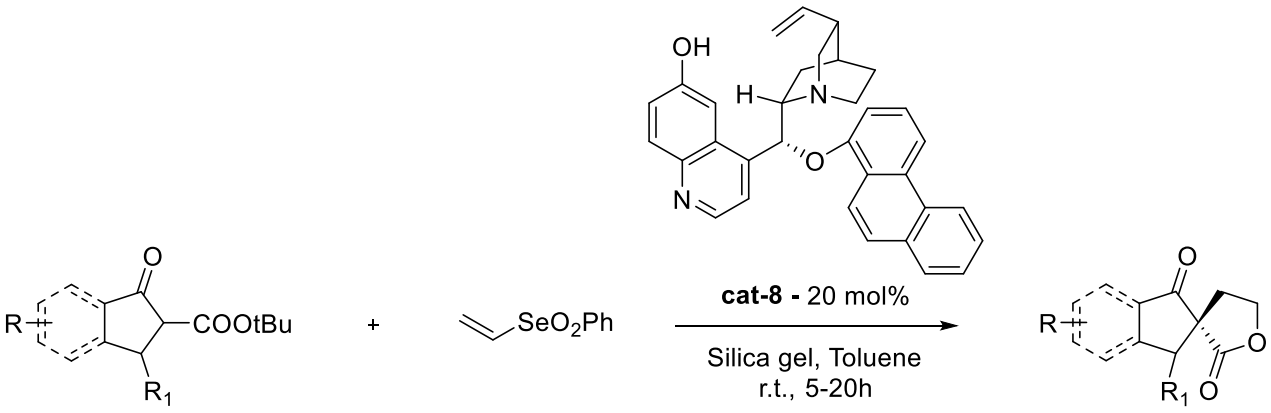

29 **30** **31**
71-99%
90-98% ee

Scheme 1.8 - Enantioselective One-pot Micheal Addition/Cyclization

[18] Sternativo, S.; Calandriello, A.; Costantino, F.; Testaferri, L.; Tiecco M.; Marini, F. *Angew. Chem. Int. Ed.* **2011**, 50, 9382

1.2 Nitrogen-containing saturated heterocycles

1.2.1 Natural products containing pyrrolidines

Different natural products and biologically active metabolites present azotate rings as structural motif. In particular, substituted pyrrolidines are sub-structures commonly found in natural alkaloids. These substances possess a wide range of biological activities, including anti-tumoral and anti-microbial activity. For this reason, over the last twenty years numerous studies have been carried out on the development of efficient and stereoselective synthetic strategies for the construction of substituted azotate rings.

The term lincomycin is based on Lincoln, Nebrasca, where the antibiotic was first isolated from *Streptomyces lincolnensis* in a soil sample. Lincosamides constitute a relatively small group of antibiotics with a chemical structure consisting of amino acid and sugar moieties. The naturally occurring members of the group are lincomycin and celesticetin, but there are some other of semisynthetic nature[19].

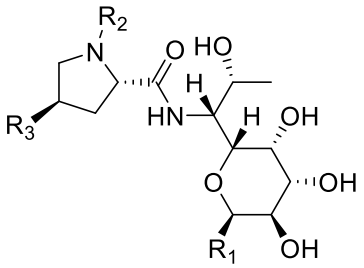

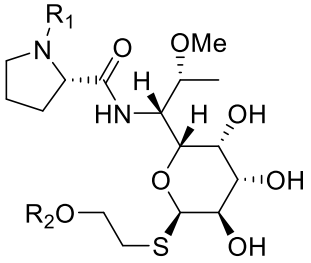

31a - Lincomycin A: R_1= SMe, R_2= Me, R_3= $CH_2CH_2CH_3$
31b - Lincomycin B: R_1= SMe, R_2= Me, R_3= CH_2CH_3
31c - Lincomycin C: R_1= SEt, R_2= Me, R_3= $CH_2CH_2CH_3$
31d - Lincomycin D: R_1= SMe, R_2= H, R_3= $CH_2CH_2CH_3$
31e - Lincomycin S: R_1= SEt, R_2= Et, R_3= $CH_2CH_2CH_3$
31f - Lincomycin K: R_1= SEt, R_2= H, R_3= $CH_2CH_2CH_3$

32a - Celesticetin: R_1= Me, R_2= COC_6H_4(o-OH)
32b - Celesticetin B: R_1= Me, R_2= COiPr
32c- Celesticetin C: R_1= Me, R_2= COC_6H_4(o-NH_2)
32d - Celesticetin D: R_1= Me, R_2= $COCH_3$
32e - Desalicetin: R_1= H, R_2= H

Figure 1.5 – Lincosamides

Another naturally occurring antibiotic of this group is desalicetin, the alkaline hydrolysis product of celesticetin[20]. Both compounds are in vitro and in vivo less effective against a number of microorganisms than lincomycin, although celesticetin exhibits a broad antibacterial spectrum, particularly against Gram-positive bacteria[21].

Since its discovery in 1967, serine protease DPP-4 has been a popular subject of research. Several research groups participated in the DPP-4 inhibitor rush, because of its effect on different type of diabetes. In 1998[22], Novartis synthetized for the first time a novel N-substituted glycinyl-cyanopyrrolidine, that exhibited a powerful inhibitory effect on DPP-4.

[19] Spizek, J.; Rezanka, T. *Biochem. Pharmacol.* **2017**, *133*, 20
[20] Hoeksema, H. *J. Am. Chem. Soc.* **1968**, *90*, 755
[21] Mason, D.J.; Lewis, C. *Antimicrob. Agents Chemoter.* **1964**, *10*, 7
[22] Villhauer, E.B. WO2000034241 A1, June 15, 2000

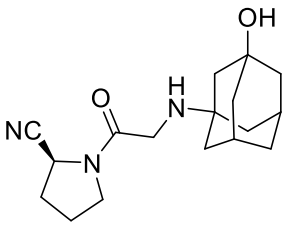

33 - Vildagliptin
(Galvus)

Figure 1.6 - DPP-4 inhibitor developed by Novartis

Vildagliptin inhibits the inactivation of Glucagon-Like Peptide 1 (GLP-1)[23] and Gastric Inhibitory Polypeptide (GIP) by DPP-4, allowing GLP-1 and GIP to potentiate the secretion of insulin in the beta cells and suppress glucagon release by the alpha cells of the islets of Langerhans in the pancreas. Moreover, Vildagliptin has been shown to reduce hyperglycemia in type 2 diabetes mellitus[24]. Today is a well-known commercial drug under the name Galvus®, distributed all over the world.

1.2.2 Natural products containing lactams

The γ-lactam moiety is present in a large number of natural and non-natural biologically active compounds. The range of biological activities covered by these compounds is very broad. Therefore, functionalized γ-lactams are thus of high interest and have great potential in medicinal chemistry[25].

Penmacric acid was isolated by two independent teams[2627] in 1975 from *Pentaclethra macrophylla*, an African leguminous tree. It has an interesting structure composed of a pyroglutamic acid linked to a glycine via a carbon–carbon bond.

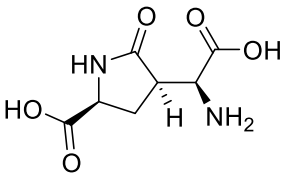

34 - Penmacric acid

Figure 1.7 - Structure of penmacric acid

This natural compound could find applications as an anti-inflammatory agent, knowing that the extracts of the plant show significant anti-inflammatory activity against acute inflammation[28]. It could also find application in food, by being a potential nutritive component in cereal mixture-based food[29].

---

[23] Ahrén, B.; Landin-Olsson, M.; Jansson, P-A.; Svensson, M.; Holmes, D.; Schweizer, A. *J. Clin. Endocrinol. Metab.* **2004**, *89* (5), 2078
[24] Mentlein, R.; GallWitz, B.; Schmidt, W.E. *Eur. J. Biochem.* **1993**, *214*, 829
[25] Caruano, J.; Muccioli, G.G.; Robiette, R. *Org. Biomol. Chem.* **2016**, *14*, 10134
[26] Welter, A.; Jadot, J.; Dardenne, G.; Marlier, M.; Casimir, J. *Phytochemistry* **1975**, *14*, 1347
[27] Mbadiwe, E.I. *Phytochemistry*, **1975**, *14*, 1351
[28] Akah, P.A.; Nwambie, A.I.; *J. Ethnopharmacol.* **1994**, *42*, 179
[29] Isichei, M.O.; Achinewhu, S.C. *Food Chem.* **1988**, *30*(2), 83

In 2008, Stierle and co-workers[30] isolated several microbes from the Berkeley Pit Lake System. From one of the first being studied, Penicillum rubrum, they obtained an organic extract capable of inhibition on some different enzyme matrices. Going deeper, they found a large variety of compounds and among them they discovered the Berkeleyamides.

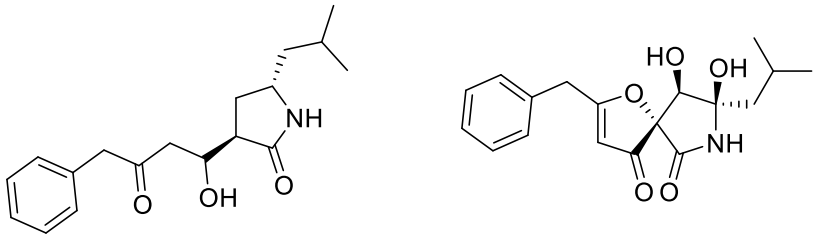

35 - Berkeleyamide A **36 -** Berkeleyamide D

Figure 1.8 - Examples of Berkeleyamides

Berkeleyamide A and D, among all, exhibit the greatest potency, inhibiting MMP-3 and caspase-1 in the low-micromolar/high-nanomolar range. These two enzymes are involved in tumor cell metabolism and proliferation, therefore Berkeleyamides can be used as antitumoral against the majority of tumors.

1.2.3 Stereoselective synthesis of Nitrogen-containing heterocycles

As mentioned above in paragraph 1.1.3, over the last decades considerable efforts have been devoted towards the development of stereoselective strategies for the construction of nitrogen-containing heterocycles resembling the natural products presented above.

In this section, the attention will be focused on methods involving the formation of the C- N bond as key step. As a matter of fact, they are inherent in the methodology developed in this PhD thesis, which will be described in the next chapters.

In 2015, Zeng and coworkers described a Cu(II)-mediated asymmetric intramolecular cyclization of N-alkenylureas[31]. This process provides a useful tool for the rapid assembly of chiral vicinal diamino bicyclic heterocycles in moderate to good yields with high to excellent enantioselectivity. The readily available N,N-chelating bidentate oxazoline ligand in conjunction with alkali metal lithium carbonates plays a key role for obtaining high enantioselectivity (*Scheme 1.9*).

[30] Stierle, A.A.; Stierle, D.B.; Patacini, B. *J. Nat. Prod.* **2008**, *71*, 856
[31] Fu, S.; Yang, H.; Li, G.; Deng, Y.; Jiang, H.; Zeng, W. *Org. Lett.* **2015**, 17, 1018

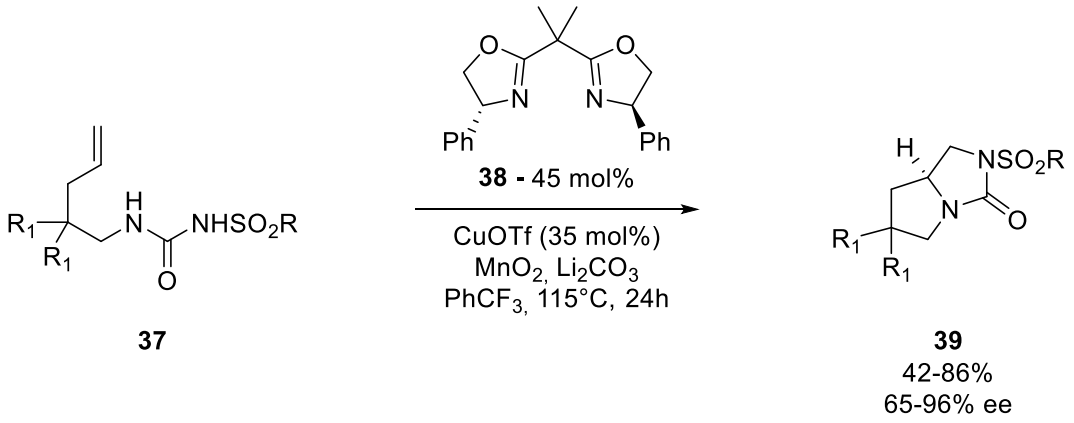

Scheme 1.9 - Enantioselective Cu(II)-mediated Diamination

In 2019, Yu and coworkers developed a chemoselective Ru-catalyzed γ-C(sp3)-H bond amidation of dioxazolones for the production of enantioenriched γ-lactams[32]. With chiral diphenylethylene diamine as scaffold, enantioselectivities have been achieved involving benzyl, propargyl and allyl C-H amidation. Noted that the dioxazolones **40** can be easily prepared from readily available carboxylic acids, this asymmetric Ru-catalyzed C-H bond amidation strategy represents a promising tool for the transformation of hydrocarbon feedstocks to chiral γ-lactams core (*Scheme 1.10*).

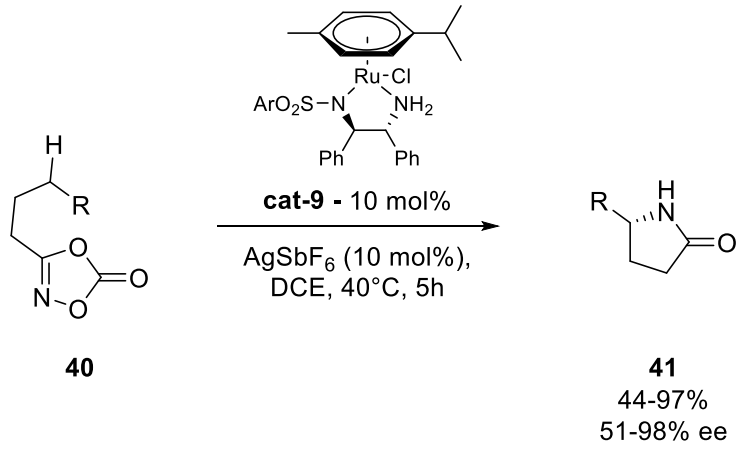

Scheme 1.10 - Enantioselective C-H bond Amination

In 2014, Singh and his research group reported an enantioselective one-pot alkynylation/lactamization cascade as a new entry to a wide range of isoindolinones[33]. The use of an easily accessible pybox as a catalyst and the operational simplicity of the method provide enantiomerically enriched isoindolinones with high to excellent levels of enantioselectivity under additive-free conditions (*Scheme 1.11*).

[32] Xing, Q.; Chan, C-M.; Yeung, Y-W.; Yu, W-Y. *J. Am. Chem. Soc.* **2019**, 141, 3849
[33] Bisai, V.; Suneja, A.; Singh, V.K. *Angew. Chem. Int. Ed.* **2014**, 53, 10737

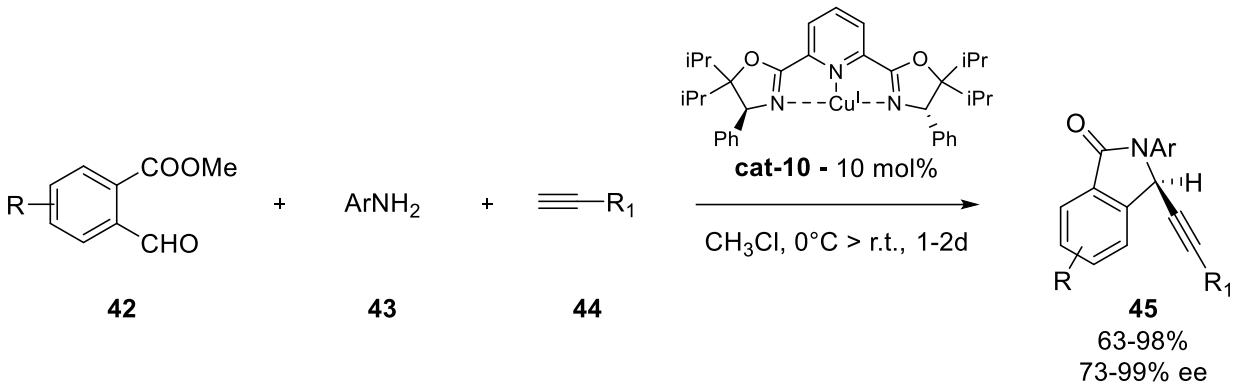

Scheme 1.11 - Enantioselective One-pot Alkynylation/Lactamization

The same research group, in 2018, disclosed an efficient diastereo- and enantioselective route to access a wide range of highly substituted pyrrolidine and pyrrolizidine derivatives[34]. The (R)-DM-SEGPHOS (**cat-11**)–Ag(I) complex (*Scheme 1.12*) has been developed as a common catalytic system for (1,3)-dipolar cycloaddition reactions. After an extensive substrate scope, the desired products were obtained in high yields with good to excellent stereoselectivities.

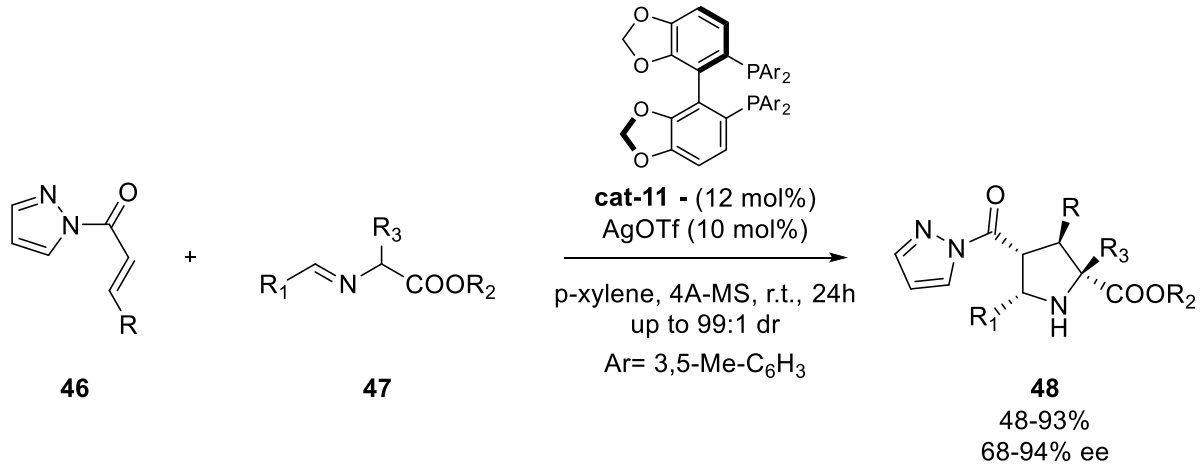

Scheme 1.12 - Enantioselective Ag-catalyzed (1,3)-Dipolar Cycloaddition

In 2017, Zhou and coworkers reported an asymmetric (3 + 2) annulations of δ-acetoxy allenoates with β-carbonyl amides by using the (R)-SITCP catalyst (**cat-12**, *Scheme 1.13*)[35]. The δC and γC positions of allenoate serve as two electrophilic sites engaging in the annulation with the αC and N of the amide, respectively. The protocol features a wide substrate scope, providing a promising tool for synthesis of various γ-lactams and spirocyclic β-keto lactams with high to excellent stereoselectivity.

[34] Ray, S.K.; Biswas, R.G.; Suneja, A.; Sadhu, M.M.; Singh, V.K. *J. Org. Chem.* **2018**, 83, 2293
[35] Ni, C.; Chen, J.; Zhang, Y.; Hou, Y.; Wang, D.; Tong, X.; Zhu, S-F.; Zhou, Q-L. *Org. Lett.* **2017**, 19, 3668

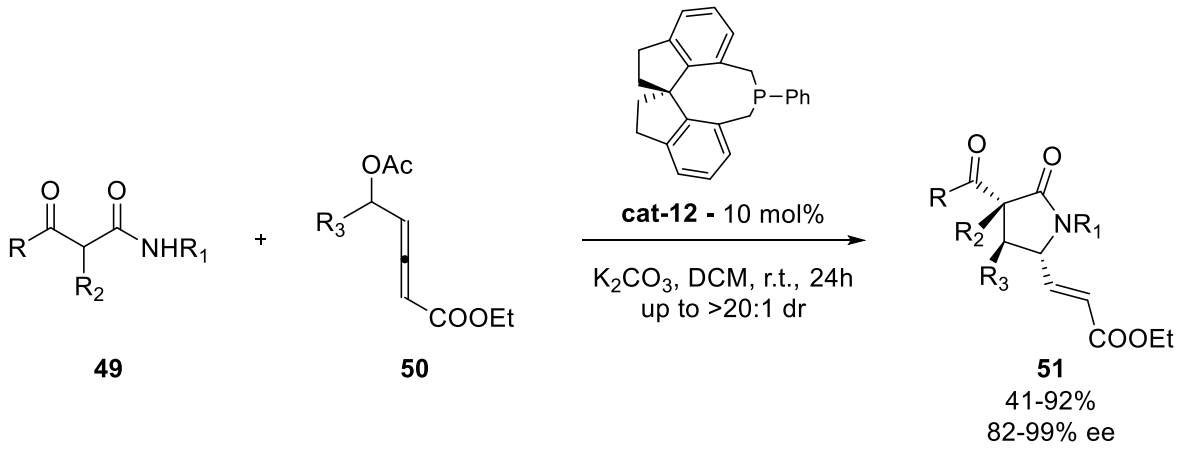

Scheme 1.13 - Enantioselective Phosphine-catalyzed [3+2] Annulation

In 2013, Yu and his research group described a highly enantioselective intramolecular aza-Michael addition with enone carbamates catalyzed by chiral Brønsted acids. However, the precursors of Michael addition were prepared through cross metathesis and the reaction yields were not always satisfactory. For this reason, they also developed a domino cross-metathesis/intramolecular aza-Michael addition promoted by the cooperation of chiral phosphoric acid **cat-13** and the Hoveyda–Grubbs II catalyst (*Scheme 1.14*)[36].

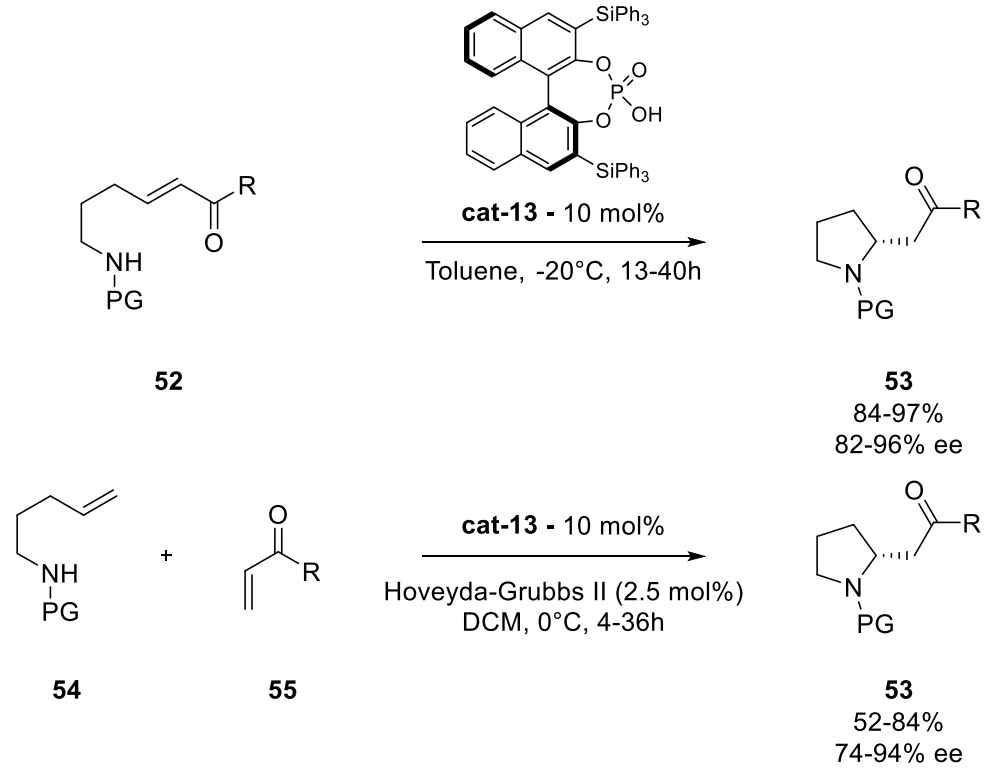

Scheme 1.14 - Enantioselective aza-Micheal Addition and Tandem Cross-Metathesis/aza-Micheal Addition

[36] Liu, H.; Zeng, C.; Guo, J.; Zhang, M.; Yu, S. *RSC Advances* **2013**, 3, 1666

2 Homogeneous Gold(I) catalysis

2.1 Gold(I) electronic and chemical properties

Gold is a transition metal belonging to the XI group of the periodic table presenting some interesting properties. To begin with, it is the most ductile and malleable element on our planet, meaning it can be stretched into a wire, pounded into other shapes, and cut into slices[37]. It also has the lowest electrochemical potential of any metal so that gold in cationic form is easily reducible and will accept electrons from virtually any reducing species to form metallic gold. It is the most electronegative of all metals: on the Pauling scale, the electronegativity of gold, the highest among the metallic elements, is 2.4, which is the same as Se and close to that of S (2.5) and I (2.5).

The two most common oxidation states for gold complexes are +1 and +3, with outer electronic configuration $[Xe]5d^{10}6s^{0}$ and $[Xe]5d^{8}$, although some Au^{II} species have been reported[38]. It is generally observed that gold complexes do not cycle between these states, in fact the redox potential for the couple Au^{I}/Au^{0} is about 1.69 V and for the couple Au^{III}/Au^{I} is about 1.41V[39]. This points out that Au^{I} species do not undergo oxidative addition and reductive elimination processes easily. Moreover, for the same reason, these species generally tolerate oxygen and moisture, therefore it is possible to run reactions without the need of inert atmosphere.

The preferential coordination mode for Au^{I} ion, a d^{10} species with 14 electrons in the valence shell, is a linear dicoordinated geometry, in which the two ligands are anti-parallel to each other at about 180°. This geometry is utterly different from Cu(I) and Ag(I), belonging to the XI group of the periodic table, both of which adopt tricoordinate or tetracoordinate geometries. In order to activate the "dormant" metal centre to catalytic activity, it is necessary to remove one of the two ligands from the neutral or cationic species. The linear structure can be explained by the high stabilization of the 6s orbital compared to the 6p. Since the LUMO is exclusively composed by the 6s and the 6p orbitals, it has more s-character, making the linear geometry the preferred one. Instead, Au^{III} is a d^{8} ion with 16 electrons in the valence shell and it adopts a square planar structure[40].

The poor tendency to be oxidized, the peculiar high stability of metallic gold as well as the preference for a linear coordination mode exhibited by Au^{I} are all manifestations of the same phenomenon, *i.e.* a general contraction of the s and p orbitals, which is often referred to as 'relativistic effect'. The term was introduced in 1928 by Dirac[41], who considered relativity to formulate an equation which calculates the

[37] Concepciòn Gimeno, M. The Chemistry of Gold. In *Modern Supramolecular Gold Chemistry*; Laguna A. Ed.; Wiley-VCH, Weinheim, 2008; pp 1-64;
[38] Mirzadeh, N.; Bennett, M.A.; Bhargava, S.K. *Coord. Chem. Rev.* **2013**, *257*, 2250
[39] Bratsch, S.G. *J. Phys. Chem. Ref. Data* **1989**, *18* (1), 1;
[40] Leyva-Perez, A.; Corma, A. *Angew. Chem. Int. Ed.* **2012**, *51*, 614
[41] Dirac, P.A.M.; Fowler, R.H. *Proc. R. Soc. Lond. A.* **1928**, *117*, 610

energy of atomic orbitals for systems in which electrons move at speeds which approach the speed of light.

2.1.1 The Relativistic Effect

Post-lanthanide elements are characterized by a large number of protons in their atomic nuclei; therefore, the electrons move in a field of very high nuclear charge, which leads to velocities approaching that of light and, consequently, they have to be treated according to Einstein's theories of relativity. This is particularly true for electrons that are in s orbitals, which have wavefunctions that correspond to a finite electron density at the atomic nucleus, but it is less important for electrons in p or d orbitals. Electrons moving at a speed close to the speed of light are assigned a relativistic mass that is larger than the mass of the electron at rest. The effect on the 6s electrons, in the post-lanthanide elements, is that the orbital radius is contracted and the distance of the electrons from the nucleus is reduced.

Figure 2.1 shows a plot where the ratio of the relativistic radius of the valence electrons to their non-relativistic radius is presented as a function of atomic number.

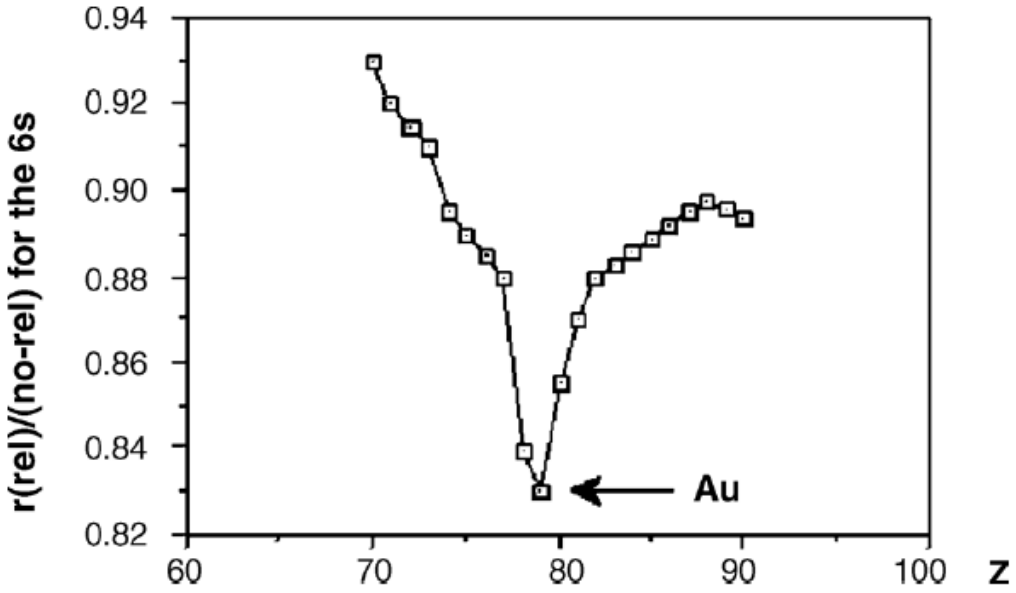

Figure 2.1 - Ratio of r(rel)/r(non-rel) versus atomic number for the 6s electron

It is clear that this ratio strongly deviates from unity as Z increases, and it reaches a pronounced local minimum for gold.

According to the special relativity, the relativistic mass of the electron m_{rel} is defined by equation 3.1:

$$m_{rel} \frac{m_e}{\sqrt{(1 + {}^{v_e}/_{c})^2}}$$

Equation 2.1 -

where m_e is the mass of the electron at rest, v_e is the velocity of the electron and c the speed of light.

In non-relativistic conditions c is approximated to $c = \infty$ and no mass correction should be applied to the mass of the electron, thus $m_{rel} = m_e$. In ultimate relativistic conditions we consider that electrons move at the speed of light. Hence if v_e is equal to c, m_{rel} of the electron is approximated to ∞. For these reasons, in general, the higher the value of v_e, the bigger the value of m_{rel} of the electron is.

Since the Bohr radius of an electron orbiting around a nucleus is inversely proportional to m_e, the increase in mass corresponds to a decrease in radius, which will lead to an orbital contraction, in particular for s and p orbitals.

The process is significant for elements with $Z > 70$, as described in Fig. 3.1: the high positive charge of these nuclei exerts a strong attraction on the electrons, which increments their velocity to a significant fraction of c. Furthermore, the tightly bound s and p orbitals are shielded, leading to a partial deshielding of d and f orbitals.

In the case of gold, whose atomic number is $Z = 79$, relativistic effects play an important part in the description of the energy of the 5d and 6s frontier orbitals, the HOMO (Highest Occupied Molecular Orbital) and the LUMO (Lowest Unoccupied Molecular Orbital), respectively (Fig. 2.2). The former is destabilized, promoting Au-Au interactions, a phenomenon called 'aurophilicity'. This aspect would be unexpected in a closed-shell state such as a d^{10}, but can occur thanks to London forces.[42] The LUMO, on the other hand, is stabilized in energy, conferring gold its extreme soft Lewis acidity. As a result it can interact with soft Lewis bases, such as multiple bonds (alkynes, allenes and alkenes).

[42] Schmidbaur, H. *Nature* **2001**, *413*, 31

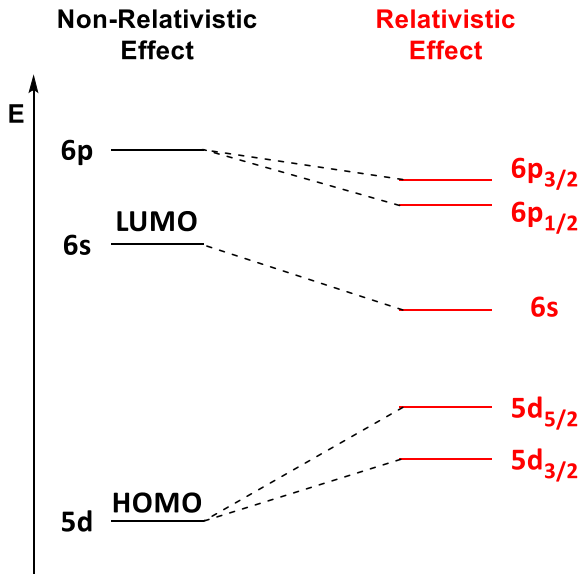

Figure 2.2 - The relative energies of the atomic frontier orbitals of gold in the non-relativistic case (black) and in the relativistic case (red).

Thus, the relativistic effect on gold has some fundamental consequences:

1. The colour of gold. Gold has an absorption beginning at 2.4 eV, attributed to a transition from the filled 5d band to the Fermi level (essentially the 6s band). It therefore reflects red and yellow light and strongly absorbs blue and violet.

2. A marked reduction in the lengths of covalent bonds involving gold atoms.

3. The closed shell $5d^{10}$ is no longer chemically inert and can interact with other elements, that is, with other gold atoms in molecules or clusters. Bonding between two gold(I) centers (equilibrium distance is between 2.7 and 2.2 Å) with equal charge cannot be understood in terms of classical bonding.

4. The small difference in energy between the s, p and d orbitals leads to the efficient formation of linear two-coordinate complexes in gold(I).[43]

5. The destabilization of the 5d orbitals allows the formation of the oxidation state III in gold to be explained (this is almost absent in silver), and the stabilization of the 6s orbitals explains the formation of the gold(-I) oxidation state (which is unknown in silver).

For all these reasons gold can be considered as an element with unique chemical features, and gold catalysis can be seen as one of the most important breakthroughs in organic synthesis during the last decades.[44]

[43] Wang, L-S. *Phys. Chem. Chem. Phys.* **2010**, *12*, 8694
[44] Hashmi, A.S.K. *Chem. Rev.* **2007**, *107*, 3180

2.1.2 The Chirality Transfer Problem

As it is already described in the previous paragraph, Gold(I) relativistic effect outilines several consequences on its behaviour and reactivity. Homogeneous Gold catalysis saw literally a "gold rush" in the beginning of this century, however asymmetric Gold catalysis had been a lot slower to emerge. The difficulties in developing efficient asymmetric transformations with chiral gold catalysts may be attributed to the linear coordination favored by Au(I). This geometrical constraint generally places the chiral ligand and the substrate on opposite sides of the metal center; therefore, the substrate is displaced from the chiral atmosphere, even if both the ligand–Au and Au–substrate bonds retain free rotation and unrestricted bonding. Moreover, gold-catalyzed addition reactions of nucleophiles to π-bonds are generally proposed to proceed through out-sphere pathways. All these features render chirality transfer and consequently enantioselective Gold(I)-catalysis a tough challenge.

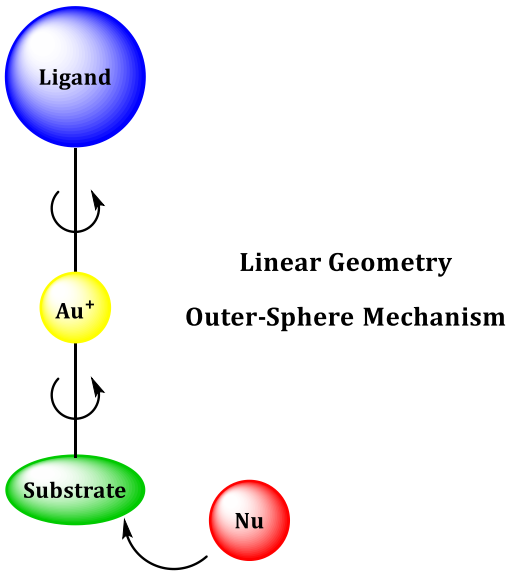

Figure 2.3 – Coordination mode for Gold(I)-catalysis

One of the very first attempts in developing a Gold(I)-catalyzed enantioselective reaction is represented by Toste's work in 2007[45]. He described an Au(I)-mediated hydroalkoxylation on a variety of allenols (*Scheme 2.1*), in which the induction of asymmetry is possible thanks to the interaction of the cationic gold catalyst with a chiral silver counter ion associated with the metal in an ion pair.

[45] Hamilton, G.L.; Kang, E.J.; Mba, M.; Toste, F.D. *Science* **2007**, 317, 496

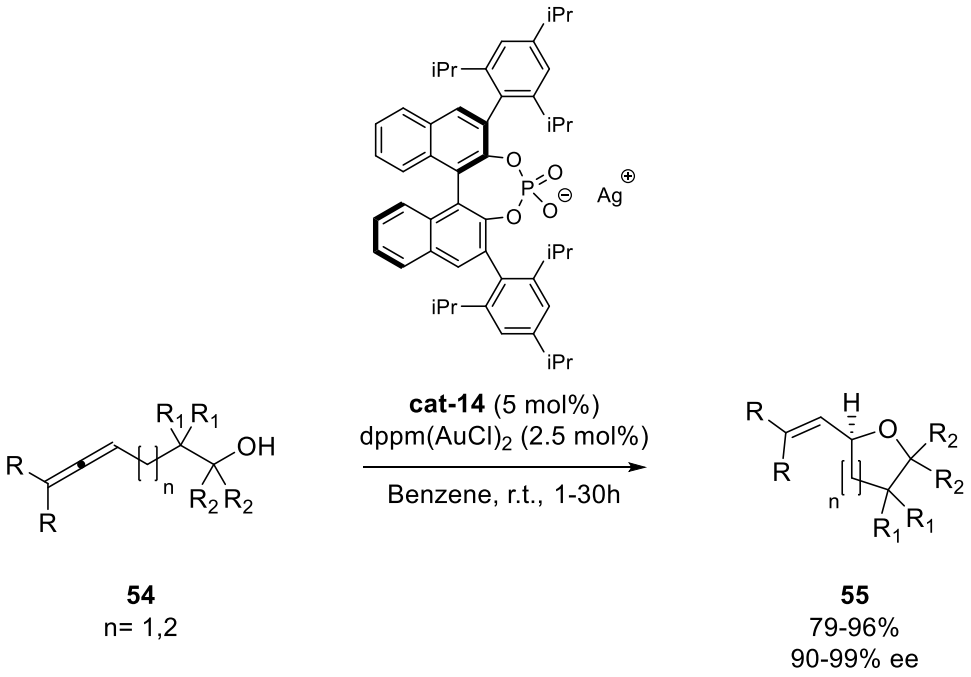

Scheme 2.1 - Toste's Enantioselective Hydroalkoxylation

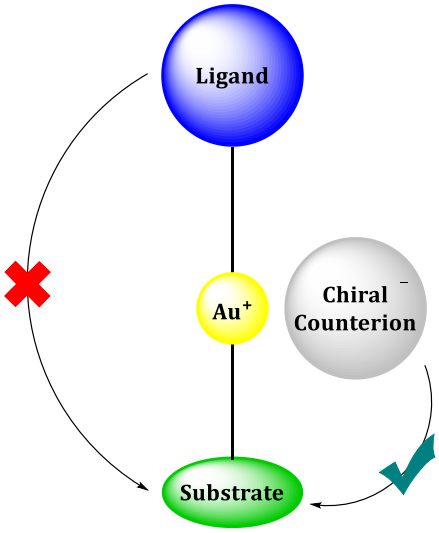

Figure 2.4 -Chirality Transfer Path Differences With and Without Chiral Counterion

In this way, the chirality transfer has to follow a shorter and faster path. Therefore, it is possible to use the same or a small library of chiral counter ions to make a wide range of cationic catalysts enantioselective.

In the same year, Widenhoefer and his research group disclosed a different approach to the problem. They achieved the same results as Toste by using binuclear gold(I)catalysts activated by achiral silver salts[46]. His strategy is focused on what's called "Aurophilicity", that refers to the tendency of gold(I) complexes to aggregate via formation of weak gold-gold bonds. It is a very useful property of gold

[46] Zhang, Z.; Widenhofer, R.A. *Angew. Chem. Int. Ed.* **2007**, 46, 283

especially in catalysis, because, as Echavarren already described in his paper[47] and then Toste later confirmed[48], those weak bonds permit the modulation of the catalyst's redox behaviour and probably this involves modifications of the accessible conformational space that modify stereoinduction in enantioselective gold(I)-catalysed reactions.

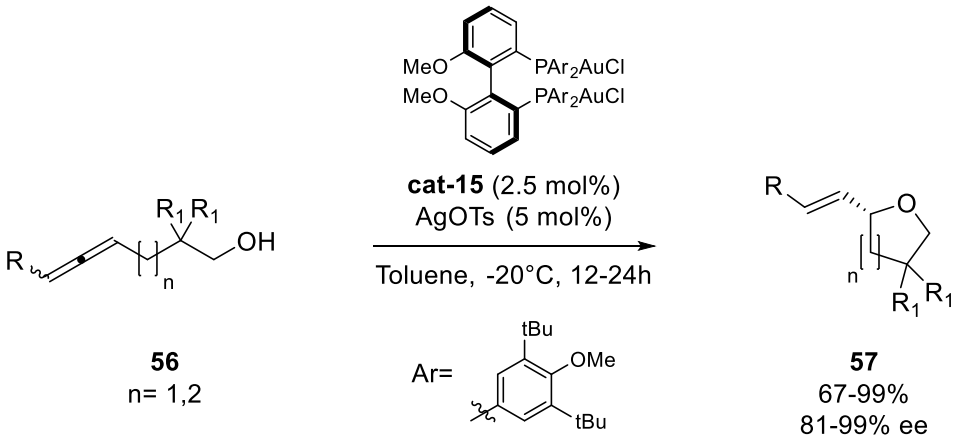

Scheme 2.2 - Wiedenhofer's Enantioselective Hydroalkoxylation

As example here it's reported a proposed mechanism for the Au(I)-catalyzed hydroalkoxylation on allenols. The formation of the Au-π-allene η2 complex **II** favors the *anti* nucleophilic attack of the hydroxyl group on the unsaturated system, followed by deprotonation of the nucleophile. The complex **III** undergoes the step of protonolysis of the Au-C bond, to obtain the tetrahydrofuran system **V** and with regeneration of the catalytically active complex. With the formation of intermediate **III** it is possible to witness the above-mentioned phenomenon of aurophilicity, which can positively interfere on the stereochemical induction.

[47] Munoz, M.P.; Adrio, J.; Carretero, J.C.; Echavarren, A.M. *Organometallics* **2005**, 24, 6, 1293
[48] Tkatchouk, E.; Mankad, N.P.; Benitez, D.; Goddard, W.A.; Toste, F.D. *J. Am. Chem. Soc.* **2011**, 133, 14293

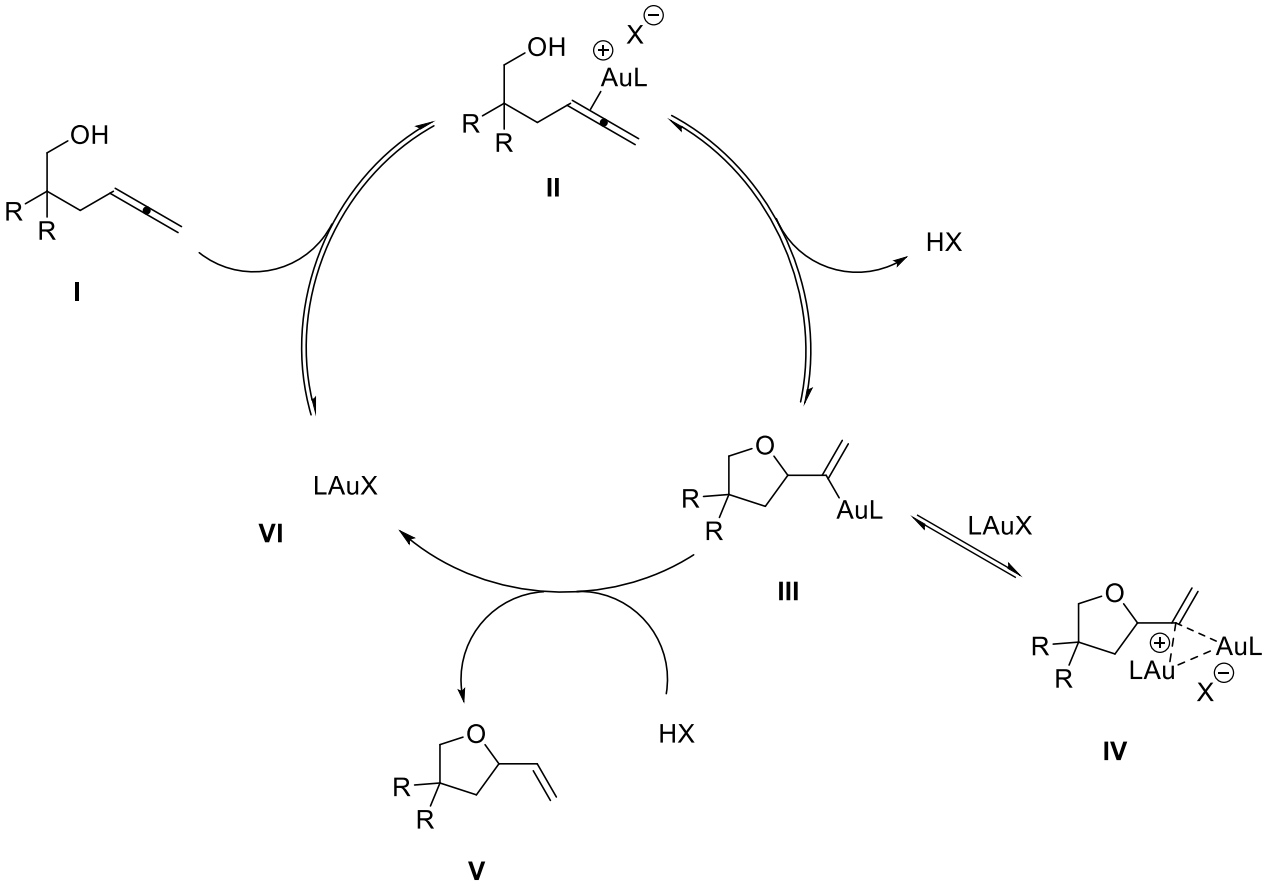

Scheme 2.3 - Wiedenhofer Proposed Mechanism

In 2010, Mikami and his coworkers took advantage of both Toste and Widenhoefer works. In fact, in his paper he describes a synergistic effect in Gold(I)-catalyzed intramolecular hydroalkoxylation[49] of allenols. The combination of the enantiopure binuclear Au(I) complex with a chiral phosphate anion can lead to a match pair, increasing considerably the level of enantioselectivity.

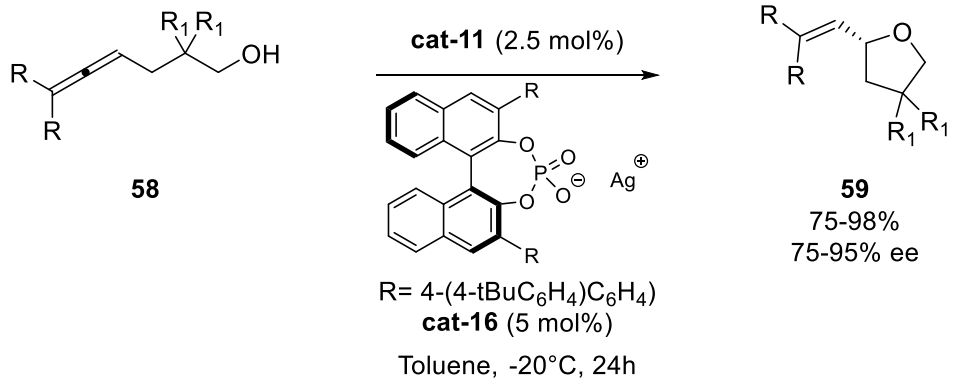

Scheme 2.4 - Mikami's Enantioselective Hydroalkoxylation

[49] Aikawa, K.; Kojima, M; Mikami, K. *Adv. Synth. Catal.* **2010**, 352, 3131

More recently, Prof. Zhang, in collaboration with our research group, has developed a new strategy based on Ligand Accelerative Catalysis[50]. In his reaction, the formation of one enantiomer is accelerated via asymmetric ligand-substrate interaction that enables ligand-metal cooperation, thanks to the new design of the ligand. The catalyst itself bears an amidic moiety which coordinates the incoming nucleophile through H-bond and guides the hydroalkoxylation onto one of the two allene faces. The utility of the LAC is demonstrated by the very low catalyst loadings, as low as 100 ppm, and the generally excellent stereoselectivities in the cyclization of 4-allen-1-ols.

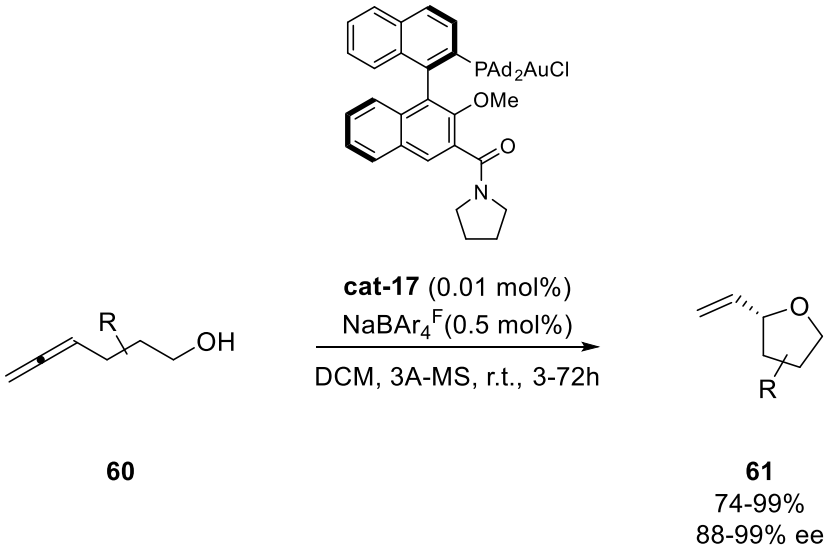

Scheme 2.5 - Zhang's Enantioselective Hydroalkoxylation

[50] Wang, Z.; Nicolini, C.; Hervieu, C.; Wong, Y-F.; Zanoni, G.; Zhang, L *J. Am. Chem. Soc.* **2017**, *139*, 16064

2.2 Gold(I)-catalyzed reactions

As mentioned above, the soft carbophilic nature of gold(I) towards functionalities bearing multiple bonds makes this metal extremely useful for activation of allenyl, alkynyl and alkenyl groups.

In particular, Au^{I} catalysis has been initially exploited for the functionalization of alkenes and alkynes, forming C-O and C-N bonds by nucleophilic attack of –OH and -NH_2 groups. Only after some years this type of reaction was employed on allenic substrates.

The allenic system, as far as reactivity is concerned, may be classified as a strong σ donor and a weak π acceptor. As a consequence, metal-allene complexes are characterized by a strong σ donation from the filled p orbitals of the allene to the empty orbital of the metal. This donation causes either a weakening of one of the two allenyl double bonds and a marked increase of the electrophilicity of the allenyl functionality.

Compared to other metal catalyst belonging to X-XII group, Au^{I} shows three main advantages: firstly, the Au^{I} species is much more prone to switch from the η^2 coordination mode to the η^1 one. Secondly, Au^{I} catalysts are mostly air-stable, affording to run reactions without the use of inert atmosphere. Finally, Au^{I} catalysis affords a remarkable selectivity control of the reaction, since the catalytic cycle does not involve a β-elimination step, unlike many others do.

Thanks to the aforementioned advantages, gold(I) catalysis has emerged as a powerful tool in organic synthesis to promote novel transformations accessing elaborated structures from simple starting materials.

Several applications of gold(I) chemistry are well known, like (cyclo)isomerization reactions[51,52], catalysis through gold-oxonium intermediates[53,54], carbene transfer reactions[55,56] or dearomatization of arenes and heteroarenes[57,58].

The attention, however, will be drawn towards gold(I)-catalyzed heterofunctionalization reactions, which represent the main topic of this thesis. Moreover, these transformations represent a valuable tool in organic chemistry to make C-Hetero bond in an inter- or intramolecular fashion.

[51] Wang, Z.; Ying, A.; Fan, Z.; Hervieu, C.; Zhang, L. *ACS Catal.* **2017**, *7*, 3676;
[52] Brooner, R.E.M.; Brown, T.J.; Wiedenhofer, R.A. *Angew. Chem. Int. Ed.* **2013**, *52*, 6259;
[53] Wang, T,; Shi, S.; Vilhelmsen, M.H.; Zhang, T.; Rudolph, M.; Rominger, F.; Hashmi, A.S.K., *Chem. Eur. J.* **2013**, *19*, 12512;
[54] Liu, L.P.; Malhotra, D.; Jin, Z.; Paton, R.S.; Houk, K.N.; Hammond, G.B. *Chem. Eur. J.* **2011**, *17*, 10690;
[55] Kawade, R.K.; Huang, P-H.; Kara, S.N.; Liu, R-S. *Org. Biomol. Chem.* **2014**, *12*, 737;
[56] Shapiro, N.D., Toste, F.D. *J. Am. Chem. Soc.* **2007**, *129*, 4160
[57] An, J.; Lombardi, L.; Grilli, S.; Bandini, M. *Org. Lett.* **2018**, *20* (23), 7380;
[58] Liu, K.; Xu, G.; Sun, J. *Chem. Sci.* **2018**, *9*, 634;

2.2.1 Oxygen as Nucleophile

Reactions involving rearrangement of vinyl gold intermediates generated via the addition of oxygen nucleophiles to alkynes have attracted intense research during the last decade. For example, in 2006 Toste and coworkers[59] reported a gold(I)-catalyzed carboalkoxylation of alkynes, affording substituted indenes with good chirality transfer. Some years later, in 2013, the same group[60] developed a ligand-controlled asymmetric variant of this reaction (*Scheme 2.1*).

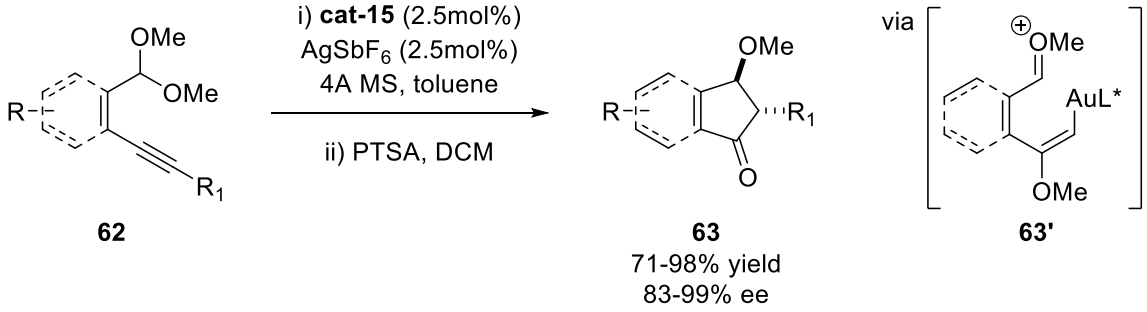

Scheme 2.6 - Toste's carboalcoxylation of alkynes (2013)

Utilizing acetals as the nucleophile instead of ether group circumvents the chirality transfer process, presumably due to the stronger resonance stabilization in the proposed oxocarbenium ions **63'**. Various optically active beta-alkoxyindanone derivatives **63** were obtained in good yields with high enantioselectivities using this reaction.

In 2014, Zhang and co-workers[61] developed a new class of chiral gold(I) complexes for the intermolecular acid addition to alkynes to obtain vinyl-esters **66** (*Scheme 2.2*).

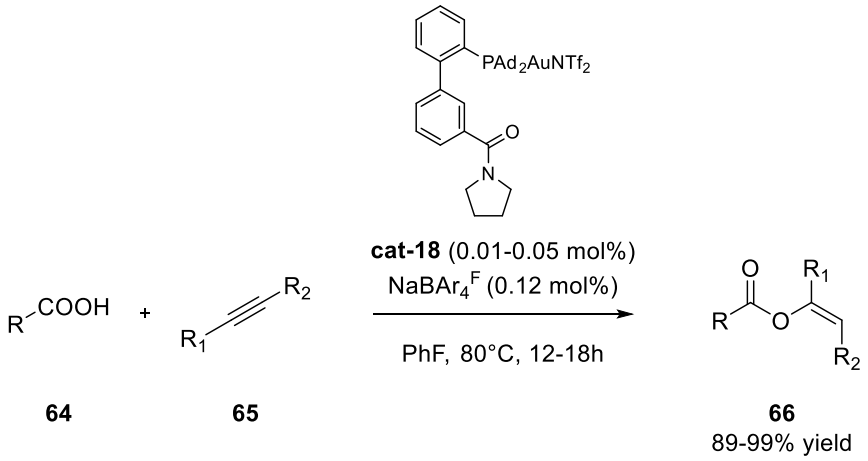

Scheme 2.7 - Zhang's acid addition to alkynes (2014)

[59] Dubé, P.; Toste, F.D. *J. Am. Chem. Soc.* **2006**, *128*, 12062
[60] Zi, W.; Toste, F.D. *J. Am. Chem. Soc.* **2013**, *135*, 12600
[61] Wang, Y.; Wang, Z.; Li, Y.; Wu, G.; Cao, Z.; Zhang, L. *Nat. Commun.* **2014**, *5*, 3470

They advanced a novel ligand design based on the privileged (1,1'-biphenyl)-2-ylphosphine framework that could dramatically improve gold catalysis. It employs FGs at the remote 3'-position to direct and promote nucleophilic attack of gold-activated alkynes, with its TON up to 99,000.

Lipshutz and his group in 2014 developed an asymmetric Gold(I)-catalyzed lactonization in water at room temperature exploiting a surfactant with traces of organic solvent as additive[62].

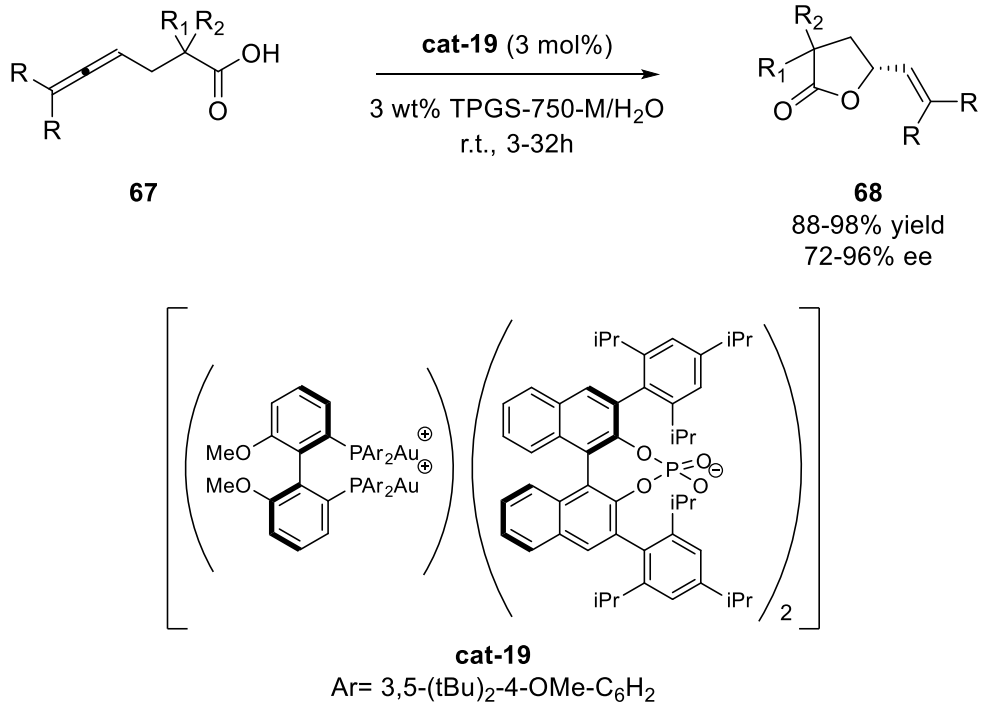

Scheme 2.8 - Lipshutz's asymmetric lactonization (2014)

The hydrophobic effect associated with in situ-formed aqueous nanomicelles gives good to excellent *ee* of product lactones. In-flask product isolation, along with the recycling of the catalyst and the reaction medium, are combined to arrive at an especially environmentally friendly process.

2.2.2 Nitrogen as Nucleophile

Hydroamination reactions of double and triple bonds are among the most well-studied transformations in gold catalysis. Since the heterocycles formed by these methods are widespread in nature products and bioactive molecules, it's appealing to apply these atom economical transformations to complex organic target synthesis.

The first successful asymmetric hydroamination of alkynes via desymmetrization strategy appeared in 2012. Czekelius and co-workers disclosed a chiral anion-induced gold(I)-catalyzed enantioselective cyclization of diynamides **69** to pyrrolidines **70**[63].

[62] Handa, S.; Lippincott, D.J.; Aue, D.H.; Lipshutz, B.H. *Angew. Chem. Int. Ed.* **2014**, *53*, 10658
[63] Mourad, A.K.; Leutzow, J.; Czekelius, C. *Angew. Chem. Int. Ed.* **2012**, *51*, 11149

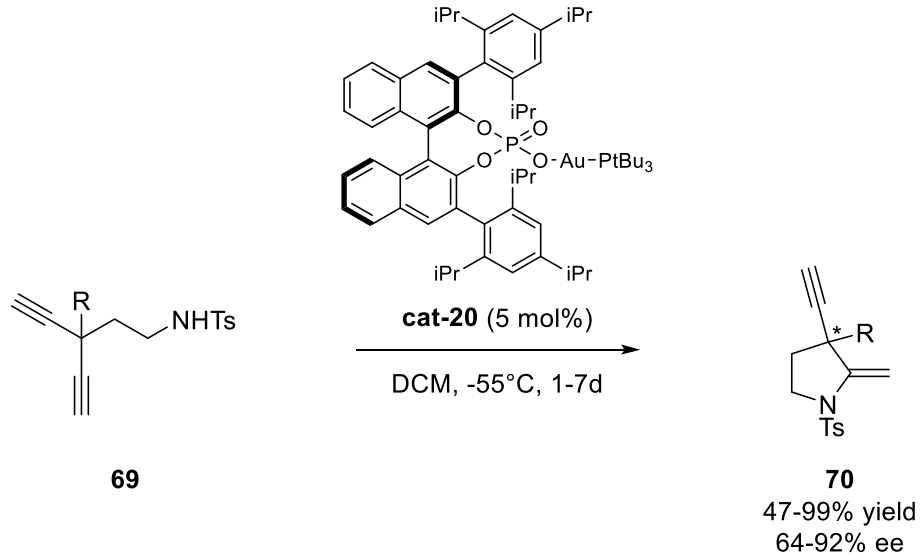

Scheme 2.9 - Czekelius's desymmetrization (2012)

Although the reaction scope was limited, good enantioselectivities were obtained and pyrrolidines with all-carbon quaternary stereocenter are highly valuable building blocks in organic synthesis. More importantly, unlike most reported gold-catalyzed desymmetrization reactions based on desymmetrization of two nucleophiles, this work represented rare examples of enantioselective desymmetrization of two electrophilic π-bonds.

The amine group has also been employed as the nucleophile in the gold-catalyzed allylic substitution reactions. As disclosed by Widenhoefer and co-workers in 2012, the dehydrative amination of allylic alcohols with carbamates formed five- and six-membered nitrogen heterocycles[64].

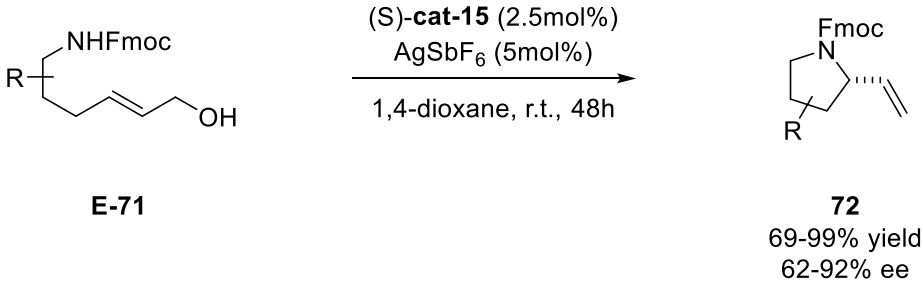

Scheme 2.10 - Wiedenhofer's hydroamination (2012)

Notably, only E-allylic alcohols **71** were competent in this enantioselective transformation. When **Z-71** was employed, racemic cyclization product was formed. This result is consistent with the hypothesis that the E-configured alkenes can form an intramolecular hydrogen-bond between the amine moiety and the hydroxyl, which is proposed to be crucial for the proton transfer step.

[64] Mukherjee, P.; Wiedenhofer, R.A. *Angew. Chem. Int. Ed.* **2012**, *51*, 1405

In 2010, Toste and his research group developed a Gold(I)-catalyzed enantioselective synthesis of pyrazolidines and isoxazolidines, exploiting hydroamination on allenes with hydrazines or hydroxylamines as nucleophiles[65].

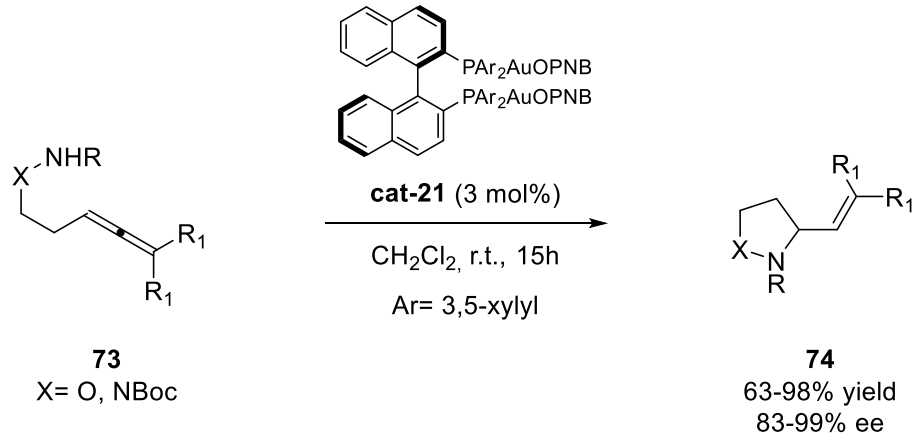

Scheme 2.11 - Toste's hydroamination (2010)

With this new protocol it is possible to access to saturated heterocycles with more than one heteroatom in the cycle with high level of stereoselectivities.

2.2.3 Sulfur as Nucleophile

Not only oxygen and nitrogen have been exploited for the heterofunctionalization of double and triple bonds. Even if it is largely known that S-Au bond is one of the strongest, Sulfur-based nucleophiles are still interesting for the production of thiophene derivatives.

Nakamura and his group developed a protocol for the gold(I)-catalyzed carbothiolation of 1-arylethyl sulfides, obtaining multisubstituted benzo[b]thiophenes with retention of the stereochemistry[66].

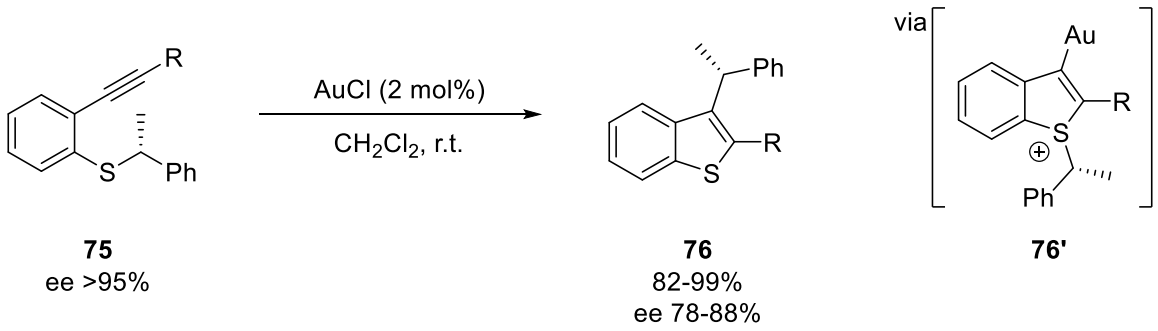

Scheme 2.12 - Nakamura's carbothiolation (2008)

[65] LaLonde, R.L.; Wang, Z.J.; Mba, M.; Lackner, A.D.; Toste F.D. *Angew. Chem. Int. Ed.* **2010**, *49*, 598
[66] Nakamura, I.; Sato, T.; Terada, M.; Yamamoto, Y. *Org. Lett.* **2008**, *10* (13), 2649

The reaction proceeds in a two-step fashion: the first step is the nucleophilic attack of the Sulfur atom on the Au-alkyne complex, producing intermediate **76'**. The second step is a direct [1,3] shift of the α-phenethyl group forming the desired product with retention of the configuration.

Some years before, in 2006, Krause and his group reported a highly efficient synthesis of 2,5-dihydrothiophenes by stereoselective cycloisomerization of α-thioallenes[67].

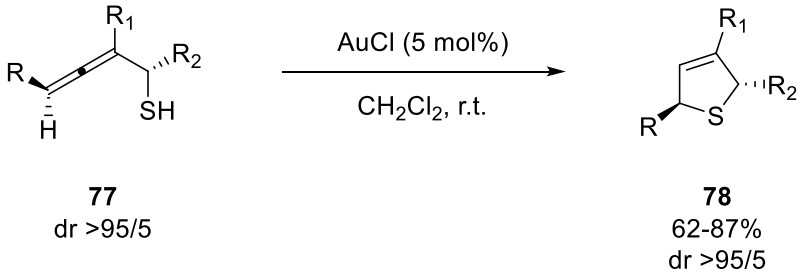

77
dr >95/5

78
62-87%
dr >95/5

Scheme 2.13 - Krause's hydrothiolation (2006)

In this protocol, also Gold(III) catalyst promoted the hydrothiolation reaction. However, yields were affected by the formation of the disulfide as a side product. The presence of this product may indicate that the Gold(III) catalyst promoted the oxidation to disulfide, reducing itself to Au(I), which is the catalytically active species.

[67] Morita, N.; Krause, N. *Angew. Chem. Int. Ed.* **2006**, *45*, 1897

3 Aim of the Thesis

The studies carried out in this thesis deal with the construction of substituted saturated heterocycles, which, as mentioned in previous chapters, represent fundamental building blocks in several biologically active molecules. The main strategy for the production of these scaffolds will be focused on Gold(I)-catalysis, with a particular attention pointed towards the principles of eco-compatibility and atom-economy.

In particular, this project will examine Gold(I)-catalyzed intramolecular enantioselective heterofunctionalization of allenyl moieties, as depicted in *Scheme 3.1*, performing a complete methodological study to comprehend the mechanistic features of these reactions.

Moreover, this work will include the conclusion of an already started project on the Gold(I)-catalyzed intramolecular enantioselective desymmetrization of achiral bis-allenols, depicted in the scheme below.

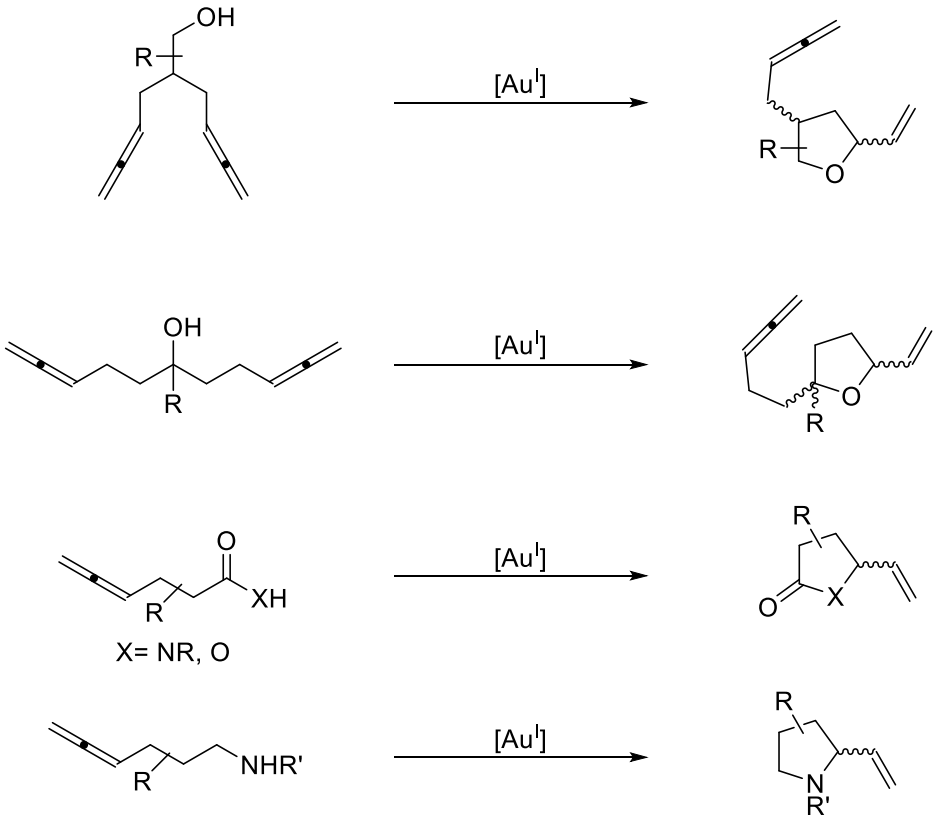

Scheme 3.1 - Gold(I)-catalyzed Enantioselective Heterofunctionalization

We will then exploit these transformations for the development of new chiral bifunctional ligands, similar to those used by Zhang (*Chapter 2.1.2*), in order to achieve a broader substrate applicability and improvements in both yield and stereoselectivity.

Furthermore, we will explore the unprecedented Gold(I)-catalyzed intramolecular enantioselective cyclization on other functionalities than allenes, such as ene-ynes and allylic alcohols (*Scheme 3.2*). Both

these transformations represent promising tools for the production of different saturated heterocycles, broadening Gold(I)-catalysis applications towards the total synthesis of biologically relevant molecules.

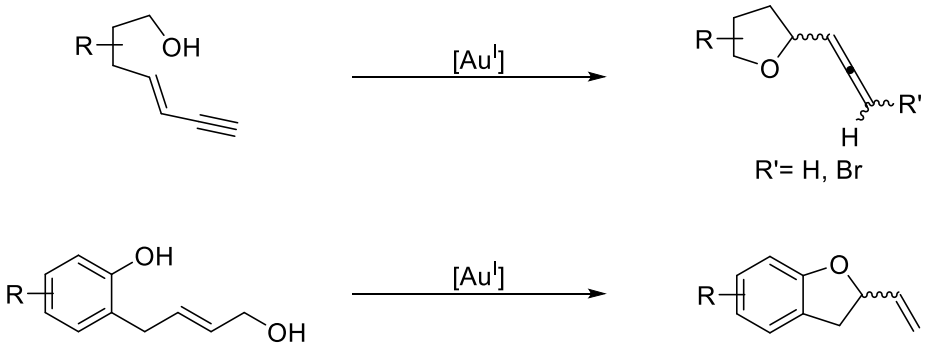

Scheme 3.2 - Gold(I)-catalyzed Enantioselective Cyclizations

Eventually, for all the reactions explored we will develop an analytical method for the chiral HPLC analysis, in order to understand the diastereo- and enantioselective features.

4 Gold(I)-catalyzed Desymmetrization of Bisallenols

Taking into account Zhang's paper described in Chapter 2.1.2 in collaboration with our research group, we would like to investigate on a challenging enantioselective desymmetrization of achiral bisallenyl alcohols to obtain 2,4- and 2,5-di-substituted tetrahydrofurans.

In a previous Ph.D. Thesis, written by Dott. Corrado Nicolini, were described the substrates synthesis, along with some results and the assignment of the absolute configuration. After briefly presenting the substrate synthesis, in this Ph.D. Thesis will be described some improvements in both results and synthesis for the assignment of the absolute configuration.

4.1 Substrate Synthesis

We designed two different substrates, which we named *Medius* **79** and *Remotus* **80** in respect to the distance between the two allenyl moieties (*Figura 4.1*).

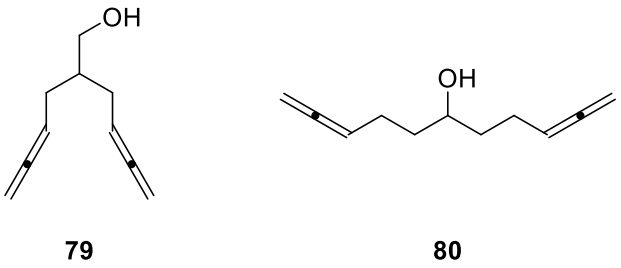

*Figure 4.1 - Medius **79** and Remotus **80***

In the schemes below are described the synthesis for Medius, along with the synthesis of all the other substrates prepared to test the applicability of the reaction.

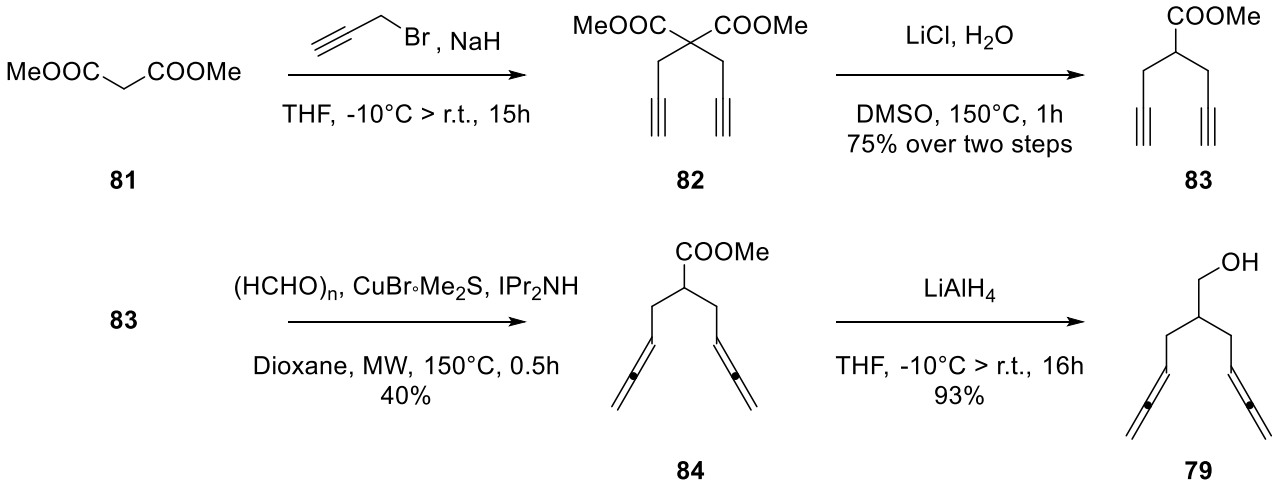

*Scheme 4.1 - Synthesis of Medius **79***

Starting from commercially available dimethyl malonate, we performed a double alkylation using propargyl bromide to obtain bis-alkyne **82**. Slightly modified Kraptcho's decarboxylation allowed us to obtain compound **83**, which undergoes then a Crabbè reaction to give bisallene **84**. Lastly, reduction with $LiAlH_4$ gave us bisallenol *Medius* **79**, ready for the Gold(I)-catalyzed cyclization.

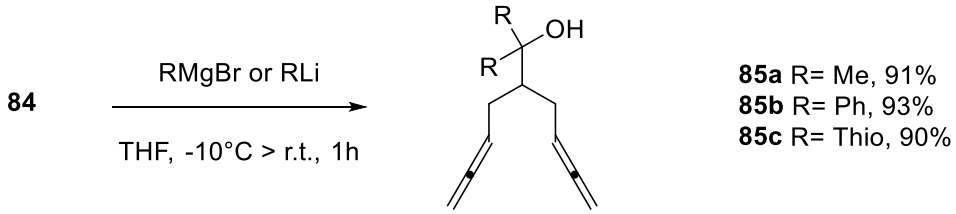

*Scheme 4.2 - Synthesis of substrates **85a-c***

Treating compound **84** with two equivalents of organomagnesium or organolithium compounds, enable the obtainment of substrates **85a-c** easily with almost quantitative yields.

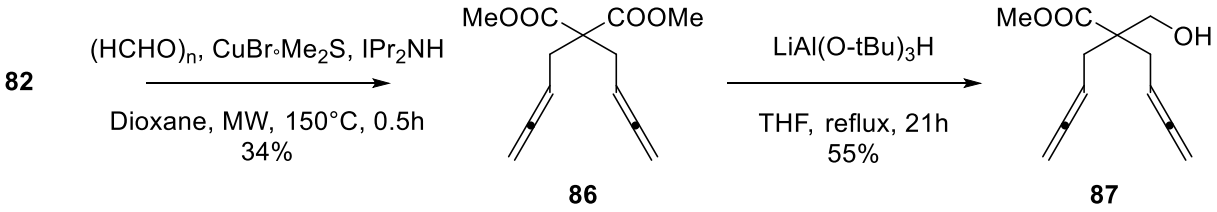

*Scheme 4.3 - Synthesis of substrate **87***

Starting from compound **82**, instead, we could perform the Crabbè reaction to obtain bisallene **86**, which then undergoes mono-reduction with $LiAl(O\text{-}tBu)_3H$ to obtain substrate **87**.

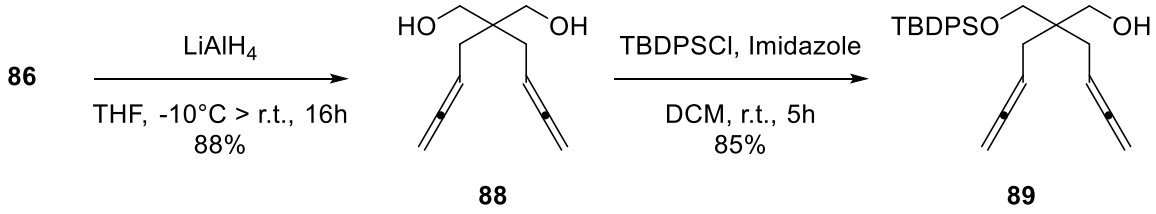

*Scheme 4.4 - Synthesis of substrate **89***

From compound **86** we could perform a full reduction of both ester moieties, and perform a mono-protection with bulky silyl group TBDPS. Both reactions were performed smoothly and substrate **89** was obtained easily.

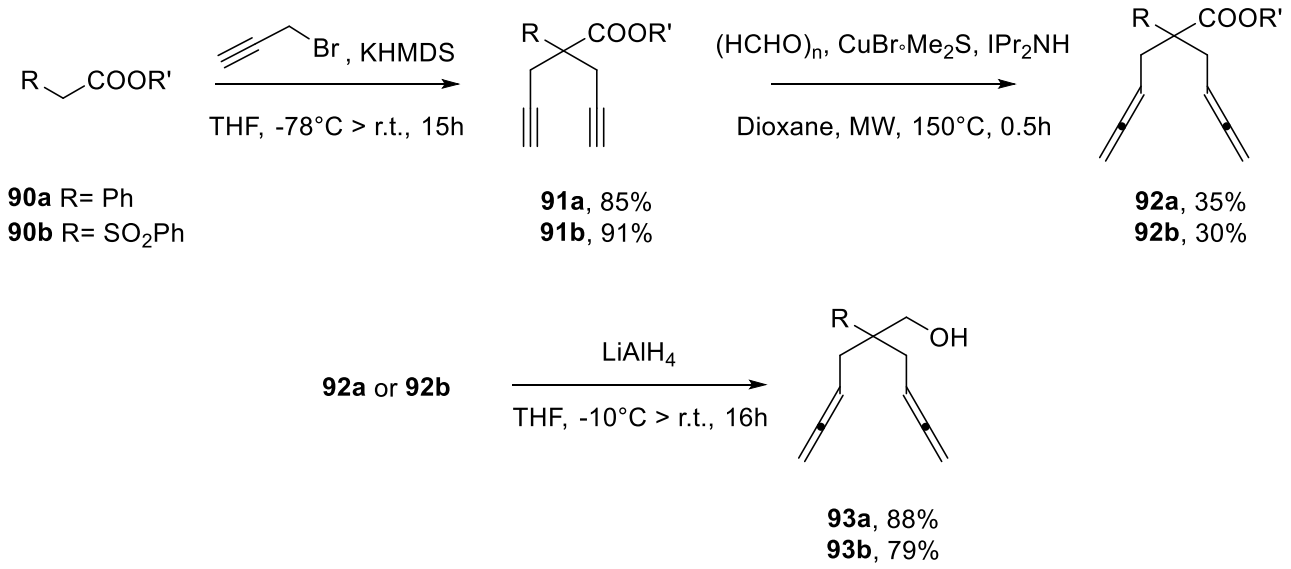

*Scheme 4.5 - Synthesis of substrates **93a** and **93b***

We also envisioned two different substrates bearing different substituents in β-position. We started from ethyl phenylacetate and methyl phenylsulfonylacetate and followed *Medius* synthesis in order to obtain, respectively, substrate **93a** and **93b**.

In the schemes below are presented the synthesis for Remotus and all the other substrates prepared.

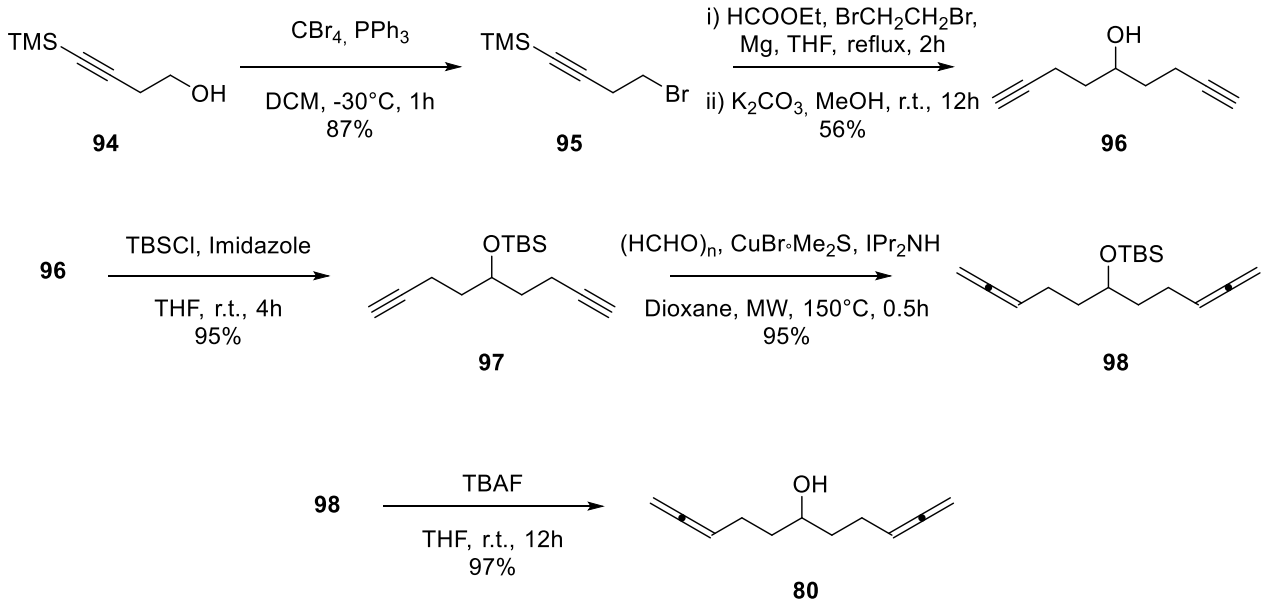

*Scheme 4.6 - Synthesis of Remotus **80***

Starting from commercially available 4-trimethylsilyl-3-butyn-1-ol, we performed a bromination reaction to obtain bromide **95** in almost quantitative yield. Grignard formation, treatment with ethyl formate and deprotection of the trimethylsilyl groups allowed us to obtain bis-alkyne **96**. After

protection with TBS group, Crabbè reaction e deprotection with TBAF we obtained substrate *Remotus* **80**, ready for the Gold(I)-catalyzed cyclization.

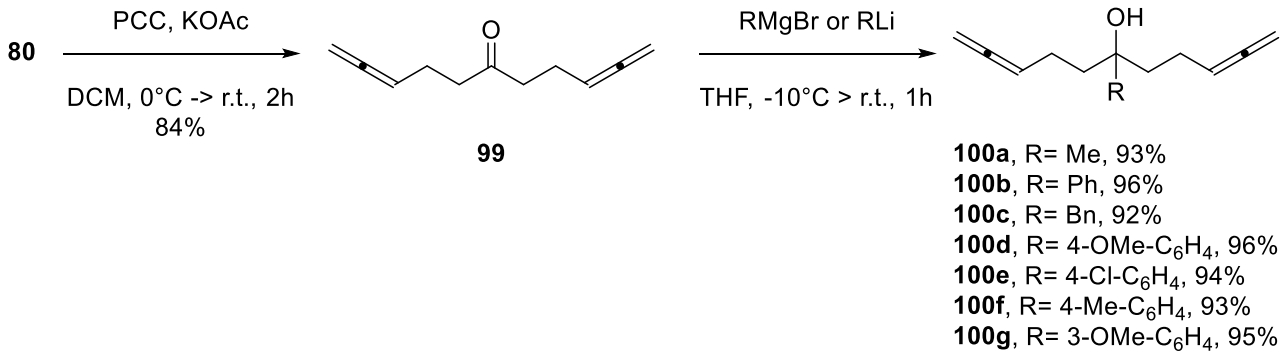

*Scheme 4.7 - Synthesis of substrates **100a-g***

Owing the quite long synthesis for the production of *Remotus*, we decided to synthetize only α-substituted derivatives. **80** was submitted to oxidation condition to obtain ketone **99**, which underwent alkylation with several Grignard and organolithium reagents to produce substrates **100a-g** in almost quantitative yields.

4.2 Gold(I)-catalyzed Desymmetrization

After an extensive methodological study described in the previous Ph.D. Thesis, in which all the strategies presented in Chapter 2.1.2 were tested, we found the optimal conditions for both Medius and Remotus.

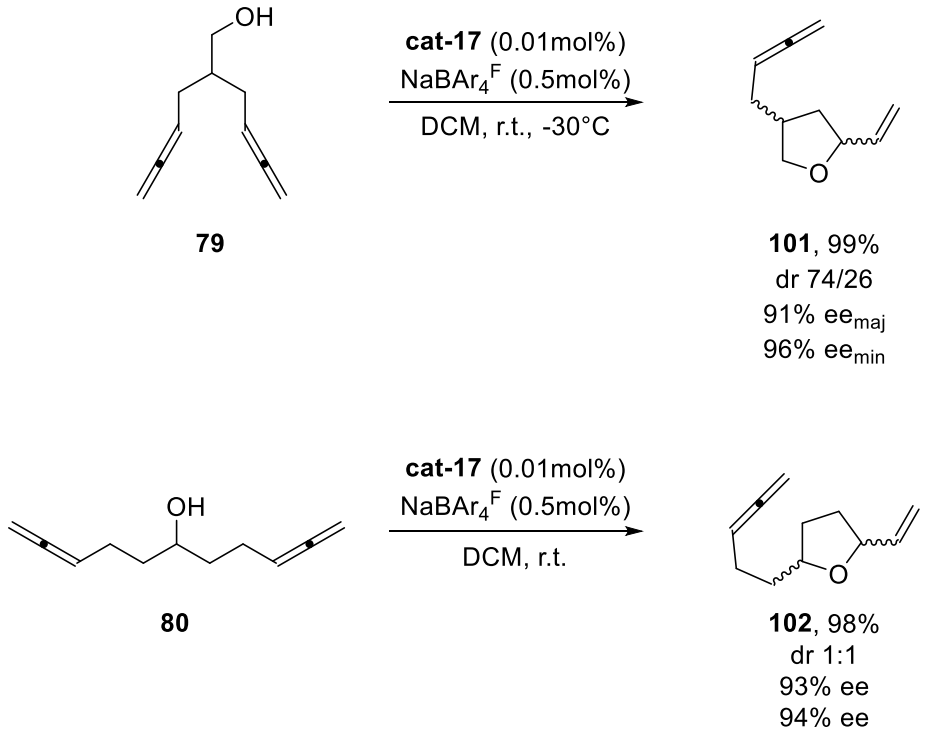

*Scheme 4.8 - Gold(I)-catalyzed Enantioselective Desymmetrization of Medius **79** and Remotus **80***

Zhang's catalyst proved to be the best regarding both yield and enantioselectivity in both transformations, in combination with $NaBAr_4^F$ as counterion in dichloromethane. Moreover, we managed to keep the same incredibly low catalyst loading as described in Zhang's paper.

Since our HPLC system works in combination with a Photo-Diode Array (PDA), we need a solid method to functionalize products without a chromophore, in order to obtain the stereoselectivity data. We managed to perform a Gold(I)-catalyzed intermolecular hydroalkoxylation on the allene moiety, which would not change nor touch the stereogenic centers. The functionalization reaction is performed right after the main cyclization.

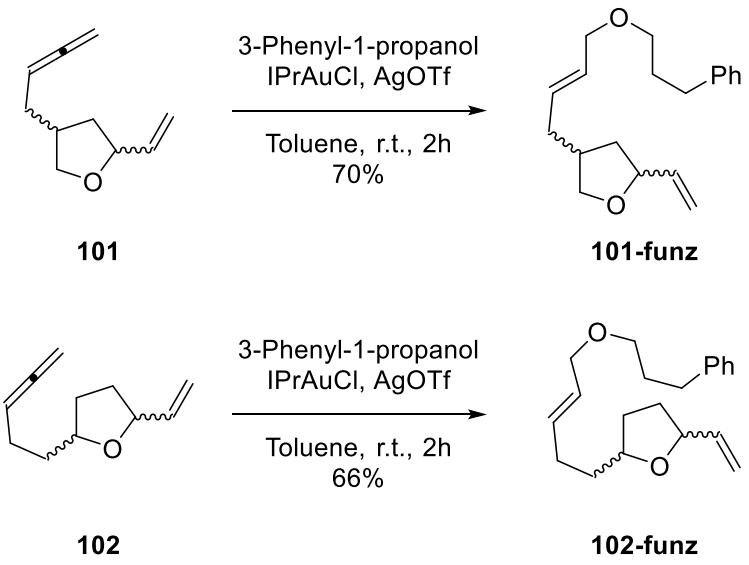

Scheme 4.9 - Gold(I)-catalyzed Functionalization

We then applied both protocols to the corresponding substituted substrates, to test the applicability of the reaction.

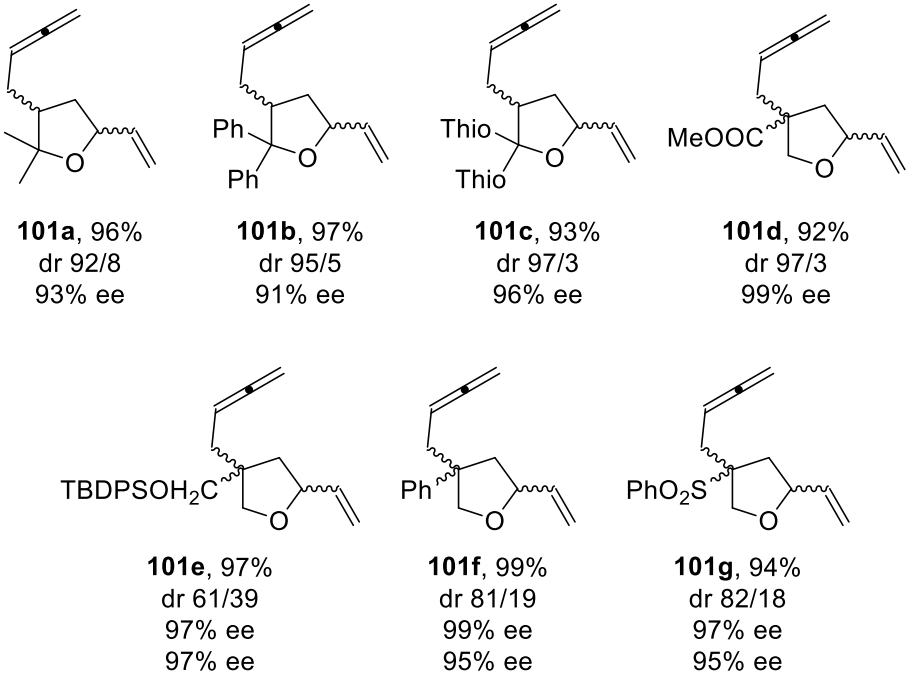

101a, 96%
dr 92/8
93% ee

101b, 97%
dr 95/5
91% ee

101c, 93%
dr 97/3
96% ee

101d, 92%
dr 97/3
99% ee

101e, 97%
dr 61/39
97% ee
97% ee

101f, 99%
dr 81/19
99% ee
95% ee

101g, 94%
dr 82/18
97% ee
95% ee

Table 4.1 - Medius Desymmetrization Substrate Scope

As shown in *Table 4.1*, α-substituted bisallenols (**101a-c**) exhibited excellent yields, high diastereoselectivities and excellent enantioselectivities. Clearly, Thorpe-Ingold Effect plays a primary role in the reaction and, at the same time, it shows how tertiary alcohols are well tolerated.

For what it concerns β-substituted bisallenols, we observed a general decrease in diastereoselectivity especially for product **101e** bearing the sterically hindered TBDPS group. Aryl and even sulfone groups (**101f** and **101g**) are very well tolerated and gave excellent results both in yield and enantioselectivity.

In particular, product **101d** exhibited excellent yield, excellent diastereoselectivity and excellent enantioselectivity.

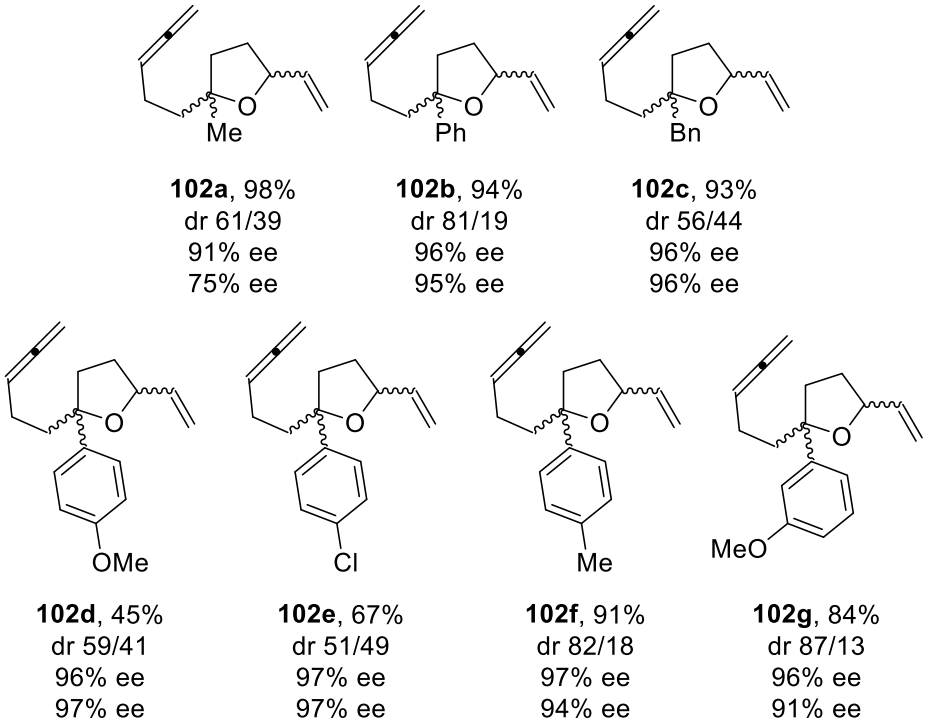

102a, 98%	**102b**, 94%	**102c**, 93%
dr 61/39	dr 81/19	dr 56/44
91% ee	96% ee	96% ee
75% ee	95% ee	96% ee

102d, 45%	**102e**, 67%	**102f**, 91%	**102g**, 84%
dr 59/41	dr 51/49	dr 82/18	dr 87/13
96% ee	97% ee	97% ee	96% ee
97% ee	97% ee	94% ee	91% ee

Table 4.2 - Remotus Desymmetrization Substrate Scope

As shown in Table 4.2, generally Remotus derivatives showed moderate to excellent yields, excellent enantioselectivities and low to moderate diastereoselectivities.

The decrease in yield and stereoselectivity for some products can be explained as a consequence of a collateral reaction, giving by-products we were not able to isolate and characterized. Notably, the collateral reaction seems to assume more importance by increasing the stability of the carbocation that can be formed in the substrate if the hydroxyl group is lost as OH-. In fact, the more the carbocation is stabilized, the higher is the by-products yield, lowering the yield of the desired product. In this scenario, the methoxy group present in the para position of the phenyl ring in product **102d** exerts a strong mesomeric stabilization of the carbocation, causing a dramatic decreasing of the reaction yield. The same could happen for product **102e**, but of slight lesser extent due to the weaker donation of the chloride group.

4.3 Absolute Configuration Determination

After having carried out a complete methodological work and substrate scope for the Gold(I)-catalyzed cyclization reaction of Medius and Remotus, we focused on the determination of the absolute and relative configuration of the stereogenic centers present in the cyclized products of Medius. In this context, we envisioned to synthetize **101-funz** starting from commercially available enantiopure lactone **103**, proceeding through reaction pathways which could afford a complete control over the formation of the second stereogenic center.

In the first two steps of the synthesis (*Scheme 4.10*) we performed the protection as silyl ether of the hydroxyl group of enantiopure lactone **103**, followed by an allylation reaction with allyl bromide leading to lactone **105**.

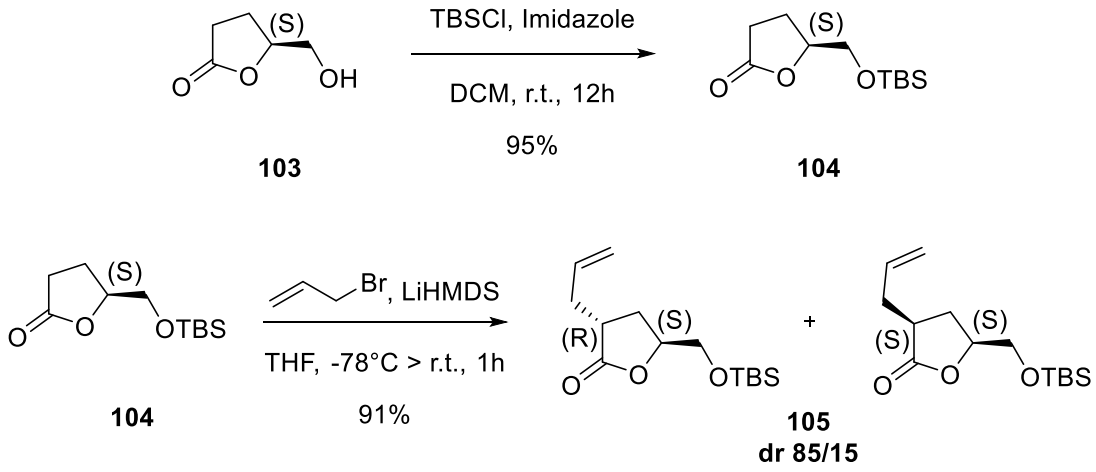

*Scheme 4.10 - Synthesis of compound **105***

The two diastereomeric products have been separated through flash column chromatography, and the major one was subjected to 1H-NMR analysis. The spectroscopic data were in accordance with those known in literature[68] for the trans diastereoisomer. We then performed a GC-MS analysis in order to evaluate the diastereomeric ratio, which turned out to be 85/15 = *trans*/*cis*.

Compound **107** has been prepared treating 3-phenyl-1-propanol with sodium hydride and subsequently allyl bromide in a classical substitution reaction (*Scheme 4.11*) allowing us to obtain compound **107**, ready for the next cross-metathesis step.

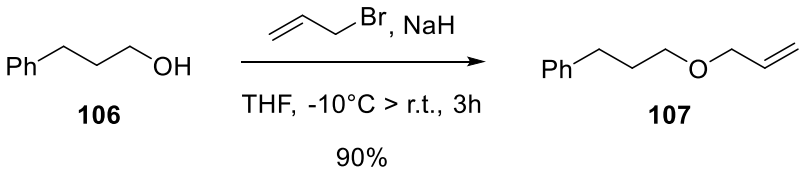

*Scheme 4.11 - Synthesis of compound **107***

[68] Sells, T.B.; Nair, V. *Tetrahedron* **1994**, 50, 1, 117

We then performed the cross-metathesis (*Scheme 4.*12) catalyzed by 2nd generation Hoveyda-Grubbs catalyst to obtain the diastereomeric mixture **108**, which was evaluated by GC-MS analysis to be still 85/15 in favor of the *trans* diastereomer. We then performed the two-step lactone reduction treating compound 108 first with DIBAl-H at -78°C and then with Et_3SiH in combination with $BF_3{\cdot}Et_2O$. From this step until the formation of the desired product **101-funz**, we managed to perform all the steps without any purification step.

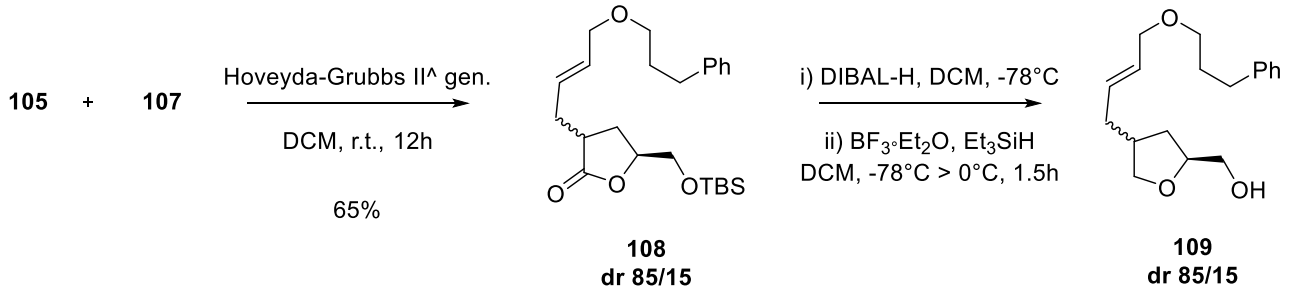

*Scheme 4.12 - Synthesis of compound **109***

The hydroxyl group in compound **109** was then oxidized to aldehyde by treatment with IBX, and subsequently compound **110** underwent an olefination reaction to obtain **101-funz** in 55% yield over four steps (*Scheme 4.13*).

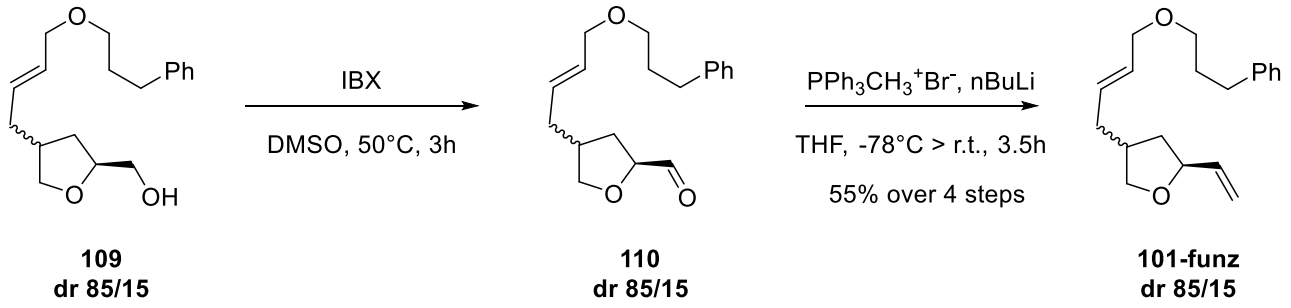

*Scheme 4.13 - Synthesis of compound **101-funz***

We subjected compound **101-funz** to a GC-MS analysis (*Figure 4.x*) along with a 1H-NMR analysis and we obtained a diastereomeric mixture of 88.3/11.7 in favor of the *trans* diastereomer.

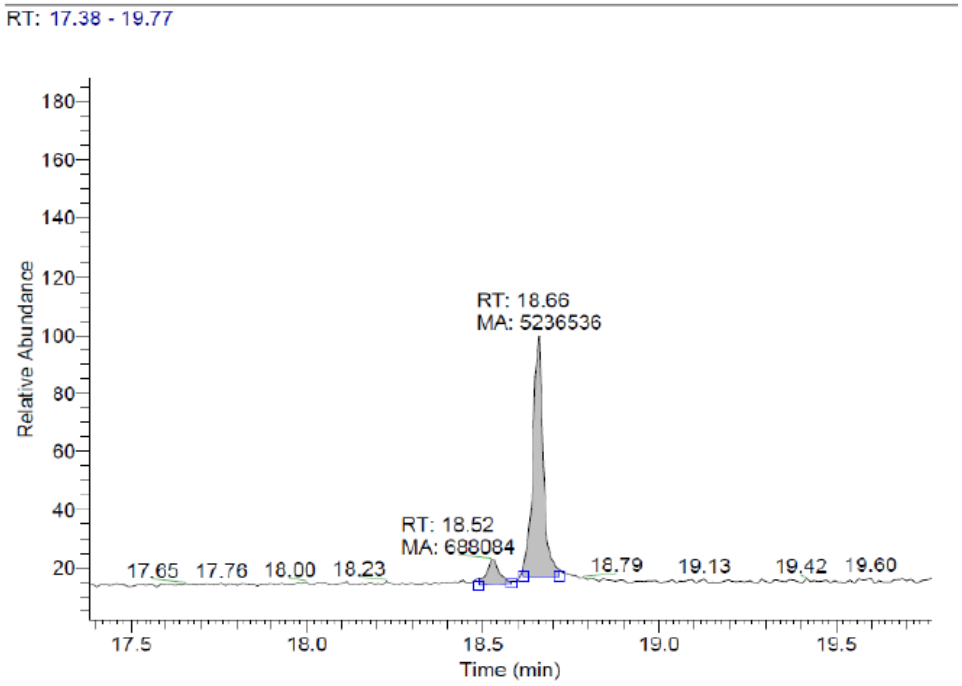

*Figure 4.2 - GC-MS analysis of compound **101-funz***

The diastereomeric mixture was then subjected to chiral HPLC analysis. Comparing it with the HPLC analysis of racemic and enantioenriched **101-funz** obtained from the Gold(I)-catalyzed cyclization (*Figure 4.3-4.4*) and knowing the diastereomeric ratio of the products, it is possible to assign the absolute configuration for each of the peaks in the chromatogram.

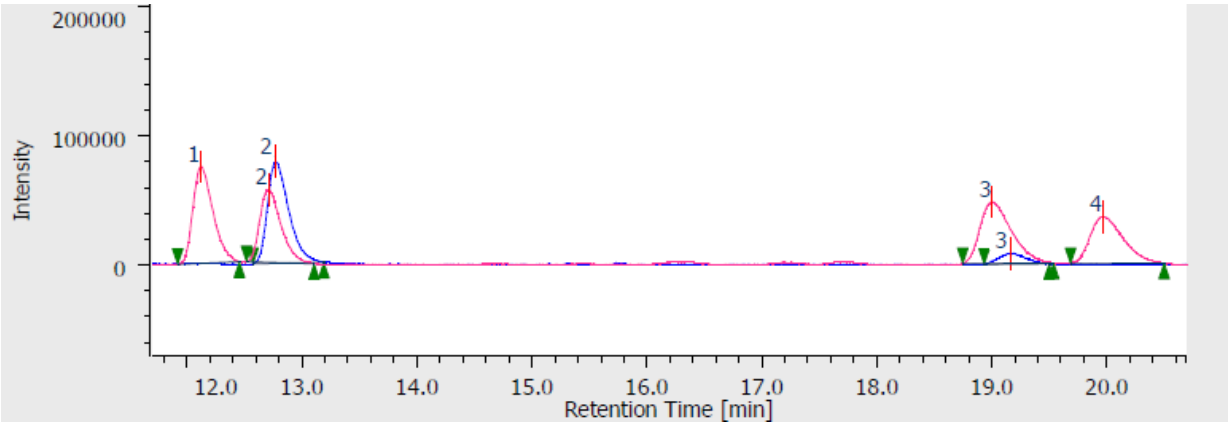

*Figure 4.3 – Chiral HPLC comparison between **101-funz** from racemic Gold(I)-catalyzed cyclization (pink) and from the synthesis presented above (blue)*

	Racemic 101-funz (pink)			Synthetized 101-funz (blue)		
Peak	**t_R (min)**	**Area (µV·sec)**	**Area %**	**t_R (min)**	**Area (µV·sec)**	**Area %**
1	12.120	902542	27.878	-	-	-
2	12.707	721396	22.283	12.773	1008130	88.363
3	19.000	892609	27.571	19.160	132760	11.637
4	19.960	720925	22.268	-	-	-

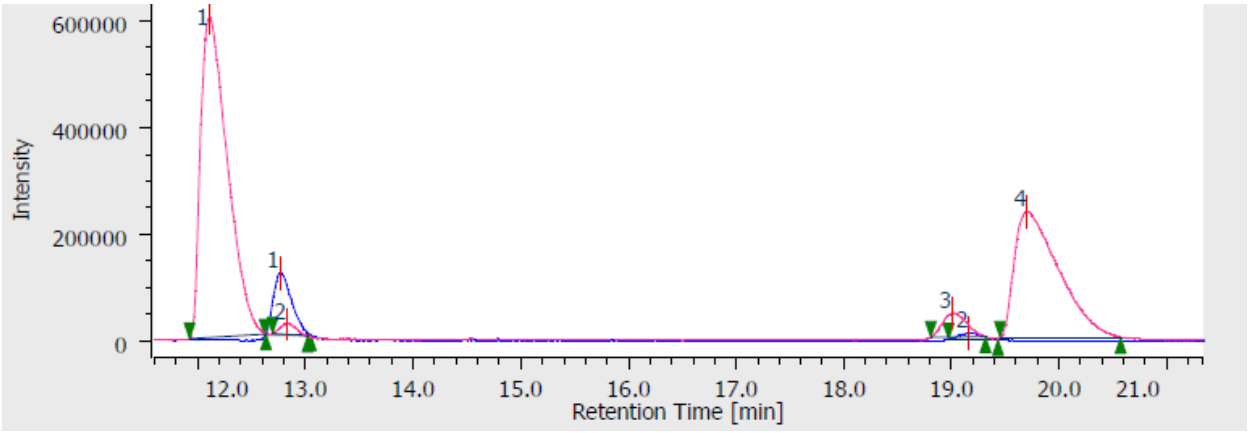

*Figure 4.4 - Chiral HPLC comparison between **101-funz** from enantioenriched Gold(I)-catalyzed cyclization (pink) and from the synthesis presented above (blue)*

	Enantioenriched 101-funz (pink)			Synthetized 101-funz (blue)		
Peak	**t_R (min)**	**Area (μV·sec)**	**Area %**	**t_R (min)**	**Area (μV·sec)**	**Area %**
1	12.000	10386382	57.698	-	-	-
2	12.720	208515	1.158	12.773	1008130	88.363
3	18.893	702600	3.903	19.160	132760	11.637
4	19.587	6703723	37.240	-	-	-

Relying on retention times, it can be seen that the major peak in the diastereomeric mixture matches with the second peak in both racemic and enantioenriched chromatograms, while the minor peak corresponds to the third peak in the chromatograms of **101-funz**. Moreover, observing the racemic HPLC analysis we can recognize from the areas the enantiomers, coupled as peaks 1-3 and 2-4. For what stated above, the structure assignment for each of the peaks are represented in *Figure 4.5*.

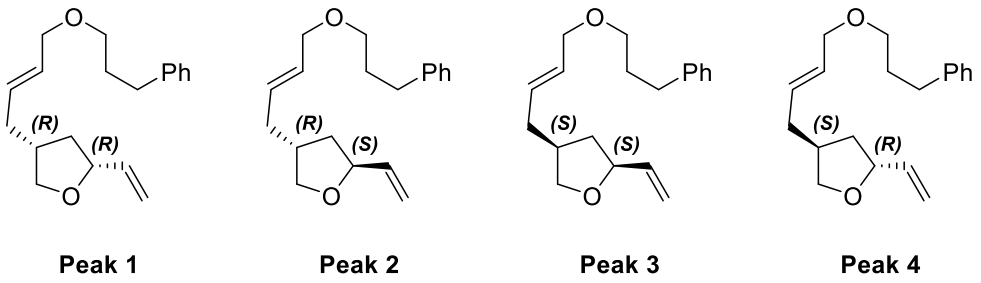

*Figure 4.5 – Determination of the Absolute Configuration of **101-funz***

Since the major product in the optimized reaction conditions of Medius (*Scheme 4.x*) is Peak 1 (2R,4R), we can state that this method exploiting gold(I) catalysis affords the enantioselective construction of cis-2,4-disubstituted THF systems. This represents a novel way to access this type of products, knowing that *cis* 2,4-substitution is, in general, much more difficult to achieve in comparison with the *trans*, as proved by the synthesis for the assignment of the absolute and relative configuration of the products.

5 Gold(I)-catalyzed Heterofunctionalization of allenes

Having deeply examined the hydroalkoxylation reaction on allenes and bis-allenes, our attention turned to other nucleophiles. Acids and protected amines have fully explored by different research group, as described in Chapter 2. However, we would like to test these nucleophiles with the new design of Zhang's ligand and possibly find some variant in order to enhance the reactivity. Amides will also be checked, since there is no report for a Gold(I)-mediated lactamization reaction on allenes.

5.1 Gold(I)-catalyzed Lactonization

5.1.1 Substrate Synthesis

We started with our analysis on acid allenes. We began synthetizing a quite simple substrate following an already known route, in order to compare our ligand with commercially available ones.

Starting from commercially available 4-pentynoic acid **111**, treating with benzyl bromide and potassium carbonate in dimethylformamide provided the corresponding benzyl ester **112** in quantitative yield.

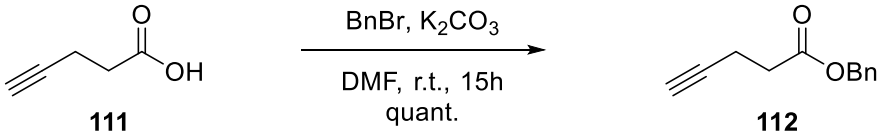

Scheme 5.1 - Protection as benzyl ester

Benzyl ester **112**, then, underwent Crabbè reaction with paraformaldehyde and diisopropylamine, following a known protocol, optimized for a microwave equipment. This process gave us allenyl benzyl ester **113** in quite good yield.

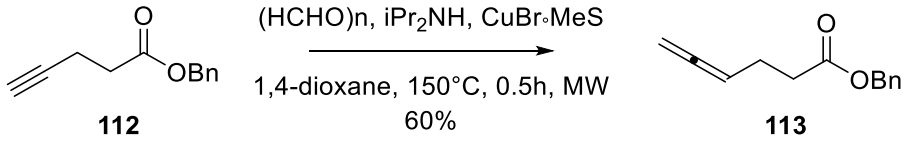

Scheme 5.2 - Crabbè reaction

As for the last step of this synthesis, we performed the hydrolysis of the benzyl ester to obtain the desired allenyl acid **114**. This would be the first substrate to be tested in the following paragraph.

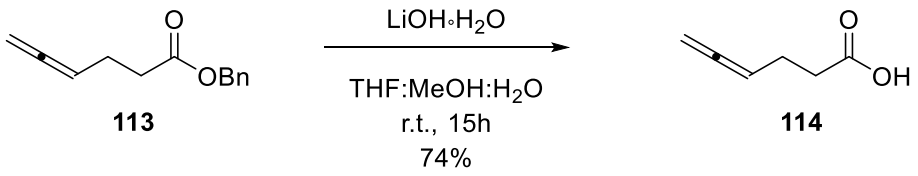

113 114

Scheme 5.3 - Ester hydrolysis

We then thought to allocate some substituents on the substrate, in order to better analyze the interactions between the substrate and the ligand.

First, we tried to accomodate some substituents on the allenyl moiety. Following an already known route, diketone **115** was treated with triflic anhydride to access enol triflate **116** in moderate yield.

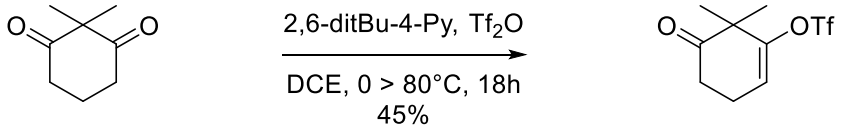

115 116

Scheme 5.4 - Production of the enol triflate

The enol triflate **116** was then treated with water and potassium carbonate in order to obtain the allenyl acid **117** through a Grob fragmentation.

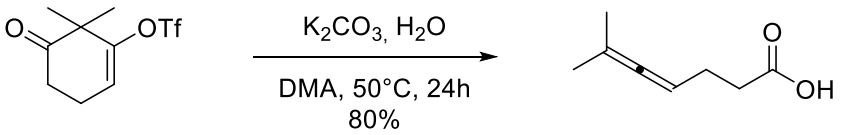

116 117

Scheme 5.5 - Grob fragmentation

We also wanted to synthetize a substrate without any substituent on the allenyl moiety. We thought that leaving the allene with only hydrogen atoms will produce a monosubstituted double bond, easier to undergo late stage functionalization. However, we would like to exploit Thorpe-Ingold effect forcing a better outcome on the cyclization reaction.

Therefore, following an already known route for the preparation of allenols, we started from diphenyl methyl acetate **118** and propargyl bromide reacting together in presence of a strong base. Alkylation of the starting material proceeded smoothly, thanks to a precise control in temperature.

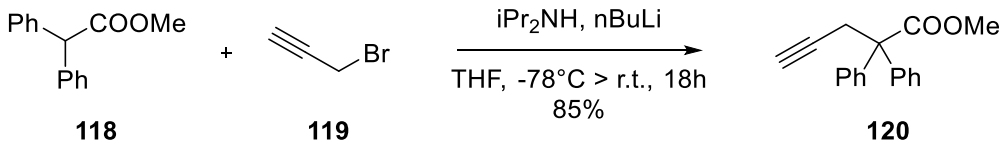

Scheme 5.6 – Alkylation

We, then, performed the already known Crabbè allenylation in a microwave flask achieving allenyl ester **121** in quite good yield.

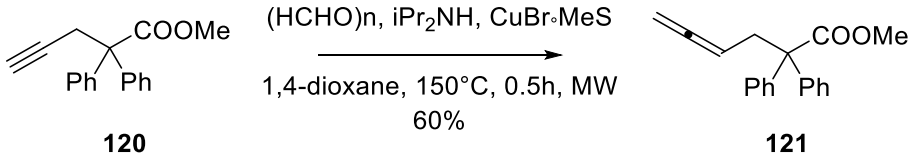

Scheme 5.7 - Crabbè reaction

To get the desired product we performed the hydrolysis of the methyl ester. We tried different methods, such as lithium hydroxide or potassium carbonate in methanol and water, but none of them allowed us to obtain the desired product. Finally using potassium hydroxide in refluxing ethanol were the right reaction conditions for our case.

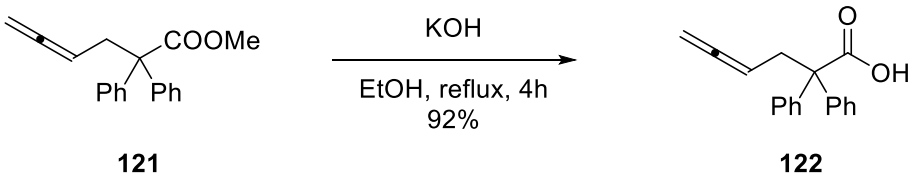

Scheme 5.8 - Ester hydrolysis

5.1.2 Methodological study

Having all the substrates ready, we tried different conditions starting from allenyl acid **114**. All the results are described in *Table 5.1*, while ligands are presented in *Figure 5.1*.

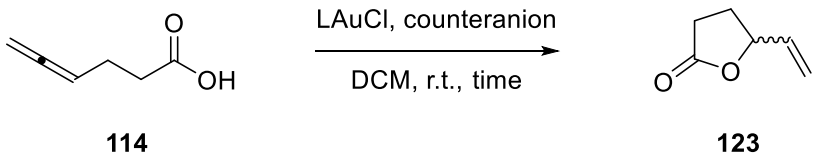

114 **123**

Scheme 5.9 - Gold(I)-catalyzed Lactonization of 114

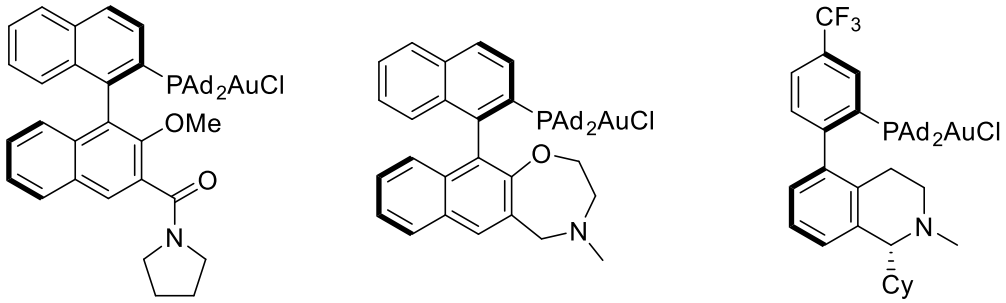

cat-17 **cat-22** **cat-23**

Figure 5.1 - Catalysts used for the cyclization

Entry	Catalyst	Counteranion	T	t(h)	Conversion (%)	123 (Y%)
1[a]	**PPh_3AuCl**	AgOTs	rt	2	>95	34
2[b]	**cat-17**	$NaBAr_4^F$	rt	15	>95	nd
3[b]	**cat-22**	$NaBAr_4^F$	rt	7	>95	nd
4[b]	**cat-23**	$NaBAr_4^F$	rt	48	>95	nd

Table 5.1 – 0.1 mmol scale. a) PPh_3AuCl 5mol%, AgOTs 5mol%, DCM 0.05M; b) catalyst 100 ppm, $NaBAr_4^F$ 0.5mol%, DCM 0.05M

For all of these reactions has been really difficult to isolate the desired product. The TLC plate showed a complex mixture of inseparable compounds. Only by crude ^{1}H-NMR was possible to identify some characteristic signals of the desired product, however their intensity was too low to consider the THF moiety as the main product. Only in Entry 1 in *Table 5.1* was possible to isolate the desired product in low yield, together with another compound which at the moment wasn't identified yet.

We decided, then, to try the cyclization with the second acid substrate, trying to compare our ligand with commercially available ones.

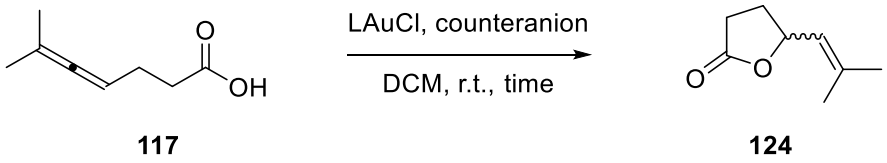

Scheme 5.10 - Gold(I)-catalyzed Lactonization of 117

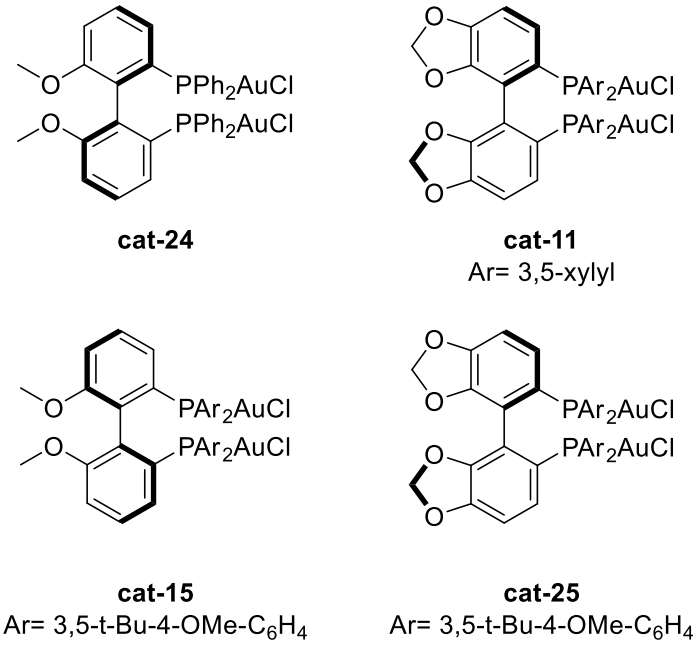

Figure 5.2 - Additional Catalyst tested

Entry	Catalyst	Counteranion	T	t(h)	Conversion (%)	124 (Y%)	ee (%)
1[a]	**PPh_3AuCl**	AgOTs	rt	0,5	>95	>95	nd
2[a]	**cat-25**	AgOTs	rt	7	>95	75	43,4
3[a]	**cat-24**	AgOTs	rt	1,5	>95	>95	<5
4[a]	**cat-11**	AgOTs	rt	1	>95	>95	<5
5[a]	**cat-15**	AgOTs	rt	0,5	>95	>95	<5
6[b]	**cat-17**	$NaBAr_4^F$	rt	24	50	>95	<5
7[b]	**cat-22**	$NaBAr_4^F$	rt	12	>95	>95	50

Table 5.2 – 0.1 mmol scale. a) catalyst 5mol%, counterion 5mol%, DCM; b) catalyst 100 ppm, $NaBAr_4^F$ 0.5mol%, DCM;

As described in Table 5.2, in this case we had more consistent results. In most of the entries, the desired product is the only compound formed during the reaction. However, we observed a lack of enantioinduction in almost all the entries, even we were using chiral ligands. Moreover, our catalysts seemed to be quite slow comparing with the commercially available ones (*Entry 6* and *7*), but still we had some encouraging results.

As the last substrate described above, we tried the diphenyl substituted one, thinking that Thorpe-Ingold effect would help us accelerating the reaction.

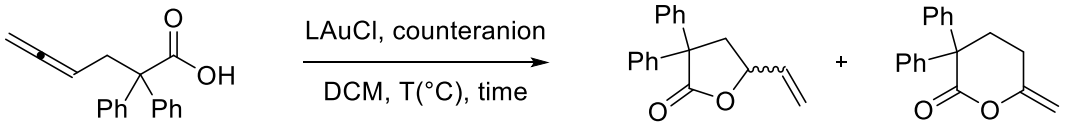

122 **125a** **125b**

Scheme 5.11 - Gold(I)-catalyzed Lactonization of 122

Entry	Catalyst	Counteranion	T	t(h)	Conversion (%)	125a (Y%)	125b (Y%)	ee (%)
1[a]	**PPh_3AuCl**	AgOTs	rt	2	>95	>95	<5	nd
2[b]	**cat-17**	$NaBAr_4^F$	rt	2	>95	77	23	43.3
3[b]	**cat-22**	$NaBAr_4^F$	rt	2	>95	77	23	43.7
4[b]	**cat-23**	$NaBAr_4^F$	rt	16	>95	58	42	11

Table 5.3 – 0.1 mmol scale. a) PPh_3AuCl 5mol%, AgOTs 5mol%, DCM 0.05M; b) catalyst 100 ppm, $NaBAr_4^F$ 0.5mol%, DCM 0.05M

With this new substrate the reaction is incredibly faster compared with the other ones. Moreover, there is a moderate enantioinduction that could be improved optimizing the reaction conditions. However, besides the desired cyclized product, we found a second cyclized product. We manage to isolate it and fully characterize and we identified that as the six-membered lactone **125b**. Possibly, it can arise by nucleophilic attack on the central carbon of the allene moiety. We, thus, decided to perform an optimization study to better understand the mechanistic aspect of this reaction.

Entry	Catalyst	Counteranion	Solvent	T	t(h)	Conversion (%)	125a (Y%)	125b (Y%)	ee (%)
1[a]	-	AgOTs	DCM	rt	15	>95	75	nd	nd
2[b]	**PPh_3AuCl**	$NaBAr_4^F$	DCM	rt	2	>95	<5	>95	nd
3[c]	**cat-17**	AgOTs	DCM	rt	5	>95	93	7	<5
4[c]	**cat-17**	AgOTf	DCM	rt	2	>95	>95	<5	<5
5[c]	**cat-17**	$AgNTf_2$	DCM	rt	2	>95	>95	<5	<5
6[c]	**cat-17**	$NaBAr_4^F$	Toluene	rt	2	>95	85	15	24.7
7[c]	**cat-17**	$NaBAr_4^F$	DCM	-10	2	>95	89	11	45.9
8[c]	**cat-22**	$NaBAr_4^F$	DCM	-10	2	>95	87	13	46.4
9[c]	**cat-17**	$NaBAr_4^F$	DCM	-30	2.5	>95	88	12	61.2
10[c]	**cat-22**	$NaBAr_4^F$	DCM	-30	4.5	>95	66	44	33.2
11[c]	**cat-17**	$NaBAr_4^F$	DCM	-50	24	<5	nd	nd	nd
12[c]	**cat-22**	$NaBAr_4^F$	DCM	-50	24	<5	nd	nd	nd

Table 5.4 - 0.1 mmol scale. a) AgOTs 5mol%, DCM 0.05M; b) PPh_3AuCl 5mol%, AgOTs 5mol%, DCM 0.05M; c) catalyst 100 ppm, $NaBAr_4^F$ 0.5mol%, solvent 0.05M

Firstly, we tried the reaction without any source of Gold (*Table 5.4, entry 1*). In the presence of only silver tosylate, lactone **125a** is formed in good yield after 15 hours. In this case, we could cut out the role of silver as catalyst just by comparing the reaction time. We then tried to understand if $NaBAr_4^F$ could influence the formation of this secondary product (*entry 2*). Running the reaction with 5 mol% of PPh_3AuCl and $NaBAr_4^F$ in DCM at room temperature, the only product formed was **125b**. We then tried to use silver salts in combination with our chiral Gold(I)-catalyst (*entries 3-5*) and we observed an increased selectivity toward the formation of the 5-membered lactone. However, looking at chiral HPLC

analysis, only racemic compounds were formed. For this reason, we decided to stick with $NaBAr_4^F$, trying to increase the formation of **125a** over the 6-membered lactone.

Having explored the role of the counteranion, we then tried the reaction by changing solvent and temperature. Toluene (*entry 6*) at room temperature gave us a better selectivity than the previous entries (*Table 5.3*), but with a lower stereoselectivity. Lowering the temperature at -10°C in DCM (*entries 7-8*) resulted in a slightly better selectivity for the formation of the 5-membered lactone, but no significant improvement in the *ee* values. At -30°C (*entries 9-10*) **cat-17** gave us almost the same distribution of products as the previous entry, while the enantioselectivity arose to a 61% value. **Cat-22**, instead, did not bring any improvement to the reaction. Finally, we tried the reaction at even lower temperature, at -50°C (*entries 11-12*), but in these cases both the reaction did not give any sign of conversion, possibly meaning that the energy system is not enough for the cyclization to happen.

Considering these results, we decided to run some computational calculation in order to understand the possible reaction pathways as regard of regio- and enantioselectivity. We used M062X as DFT method with a standard Gaussian distribution for the common atoms and effective core potential with relativistic effect for Gold. All the calculations are done considering DCM as solvent, using PCM theory, and all the energy values you can see are relative values. Considering H-bonding between the nucleophile and the ligand, we found two possible transition states leading to the two different products. In each of them, the OH group of the acid reacts with the allene moiety. As you can see the TS leading to the 5-membered ring has a lower activation energy than the other one and it leads to an enantiopure product. However, this difference energy doesn't reflect the experimental distribution of the products.

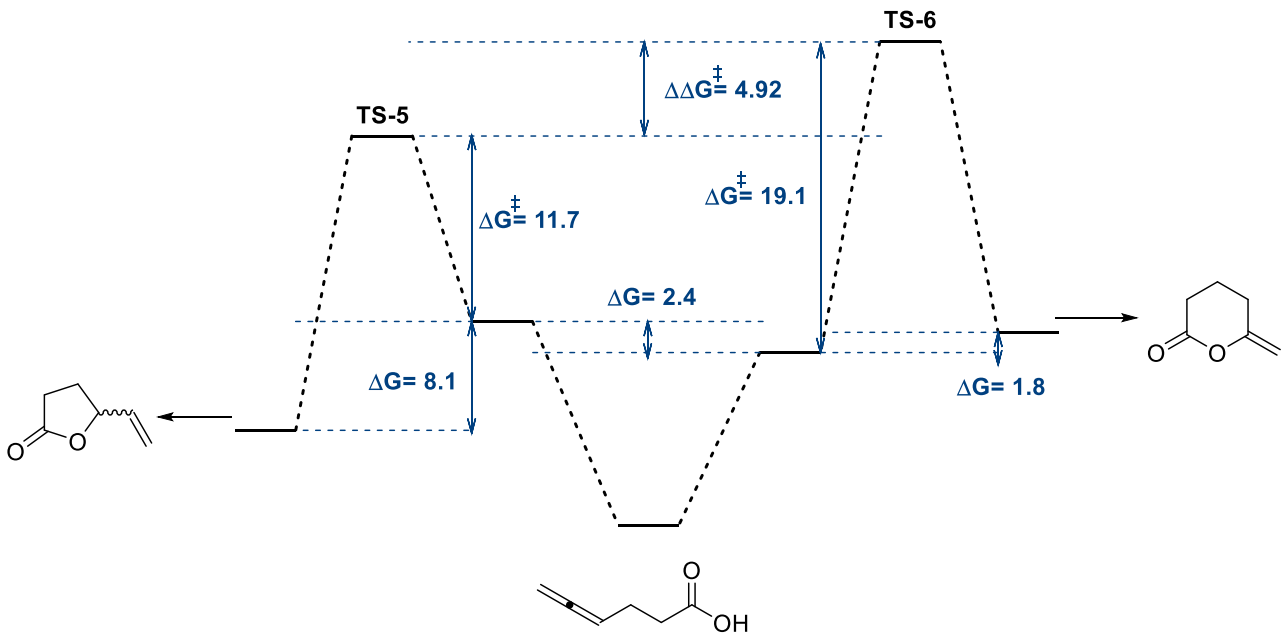

Scheme 5.12 - Energy differences for the pathways leading to 5-membered and 6-membered lactone

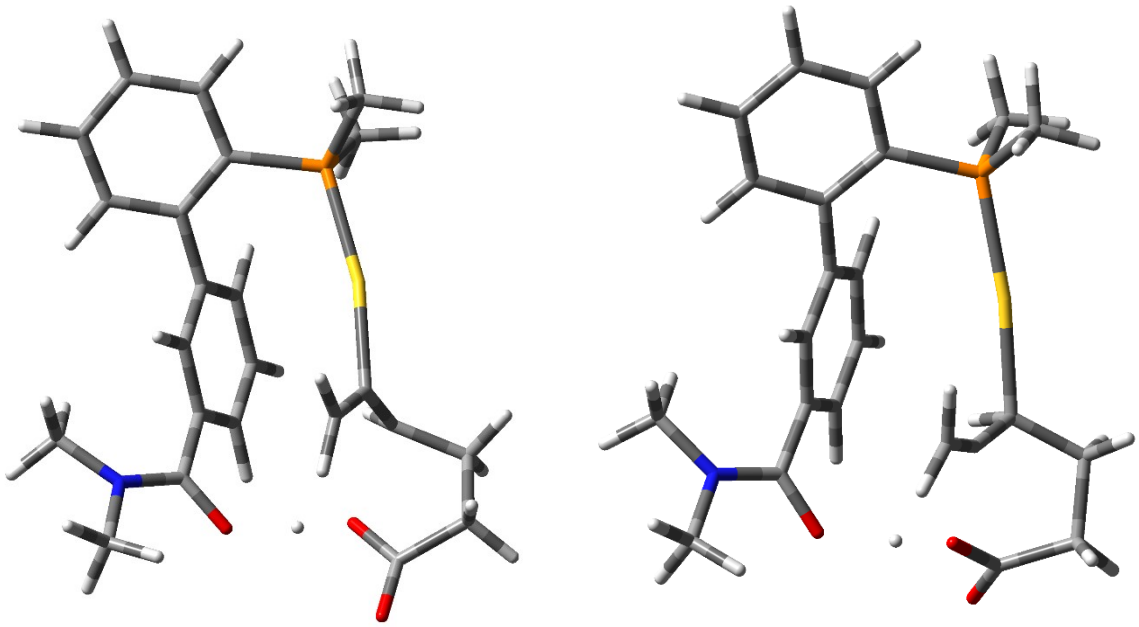

TS-5 (ν= -393.8)

TS-6 (ν= -453.3)

Figure 5.3 - Calculated TSs for the formation of 5-membered and 6-membered lactones.

For this reason, we evaluate the possibility that the C=O double bond could be involved in the nucleophilic attack. To do so we had to eliminate the H-bond, otherwise the energy of the starting point was too high to be considered a realistic pathway. We found then two pathways leading to the same product as before, but in this case the 5-membered ring is in a racemic mixture due to the uncontrollable attack of the carboxyl group.

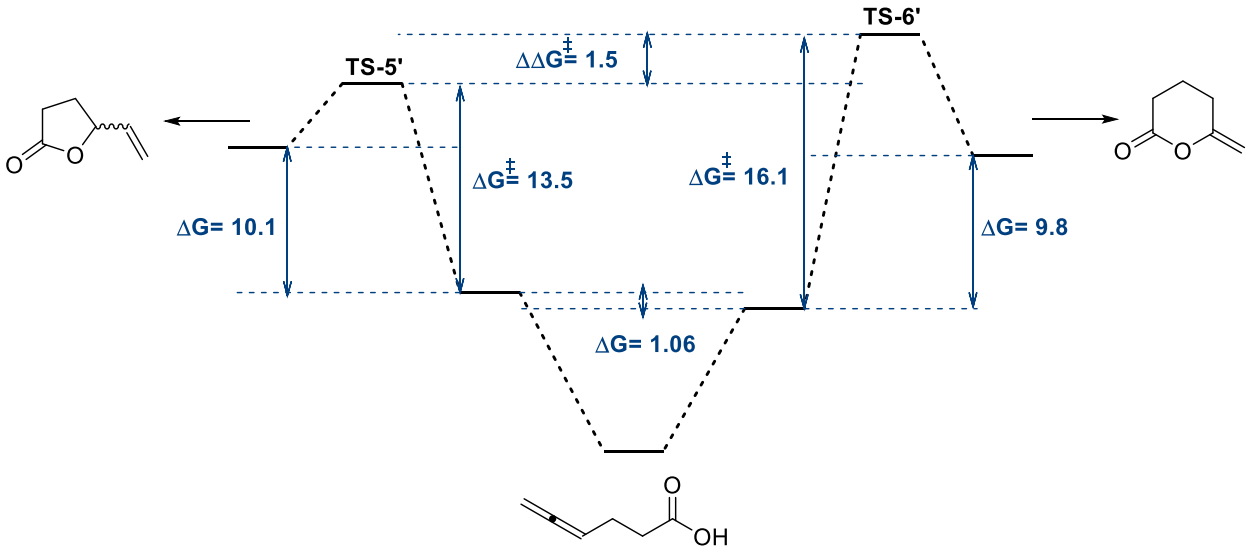

Scheme 5.13 - Energy differences for the pathways leading to 5-membered and 6-membered lactone

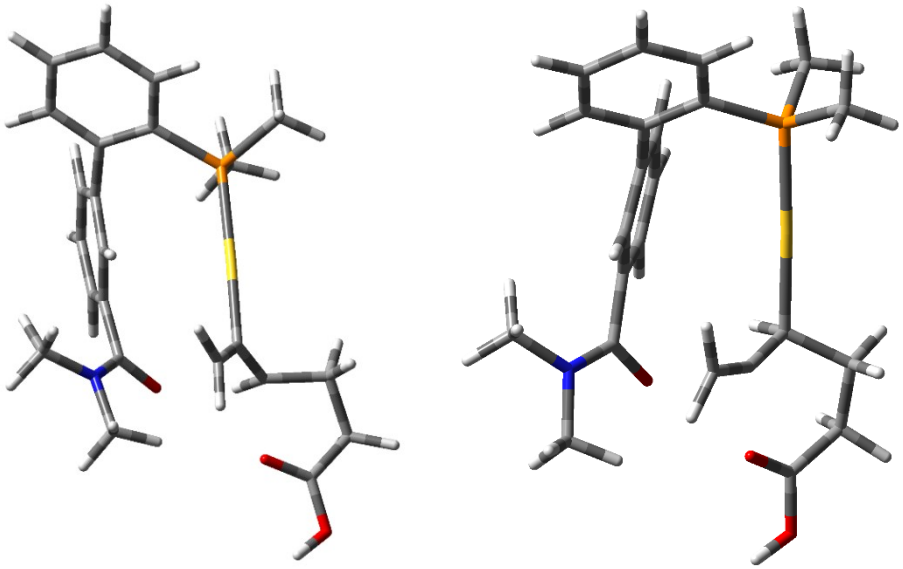

TS-5' (ν= -295.6) TS-6' (ν= -387.4)

Figure 5.4 – Calculated TSs for the formation of 5-membered and 6-membered lactones.

Making a comparison between the two graphs, we can see that the difference between racemic and enantiopure leading TS is about 0.7 kcal/mol and between enantiopure and 6-membered ring leading TS is about 0.8 kcal/mol. At this moment, the energetic situation is very close to the experimental data collected. Moreover, calculating Boltzmann's distribution considering 5-membered ring TS we found that it quite similar to the experimental ee values.

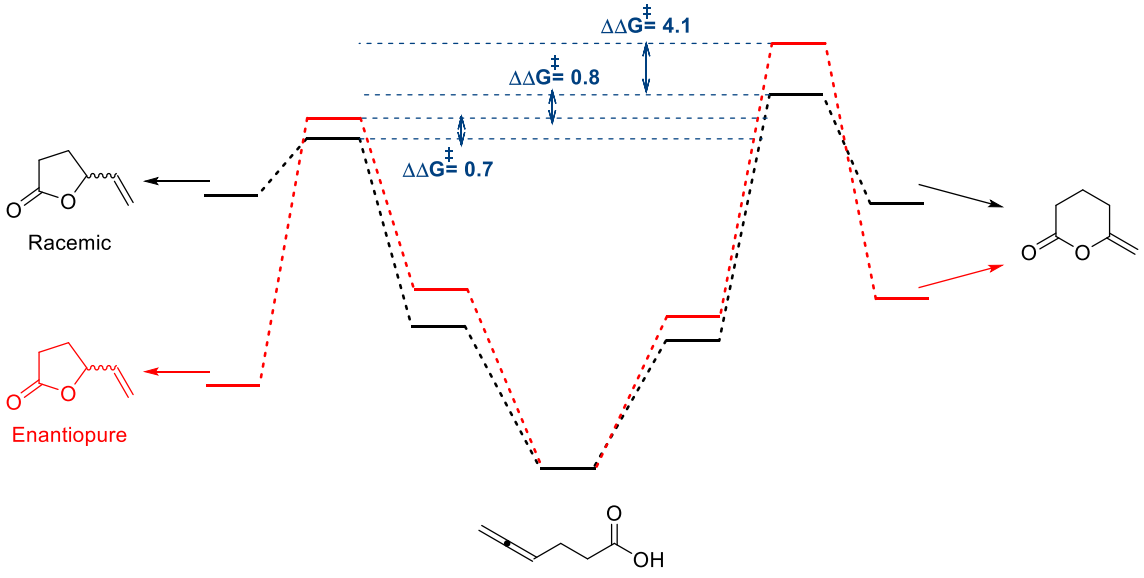

Scheme 5.14 - Energy differences for the pathways leading to 5-membered and 6-membered lactone

In order to have a comprehensive overview of the reaction mechanistic aspects, in the future we will also perform calculation with carboxylate instead of the acid. On the other hand, starting from this preliminary data, we will increase the level of theory (6-311+G(d,p) for all atoms and def2TZVP for gold) to obtain a better accordance between experimental and computational data.

5.2 Gold(I)-catalyzed Hydroamination

5.2.1 Substrate Synthesis

After exploring the lactonization reaction, our attention turned to the Gold(I)-catalyzed intramolecular hydroamination. Observing the results on allenyl acids, we decided to focus directly on the diphenyl substituted allenyl amines.

Following a reported procedure by Wiedenhofer and coworkers[69], we treated diphenyl acetonitrile with propargyl bromide in the presence of lithium diisopropylamide as strong base.

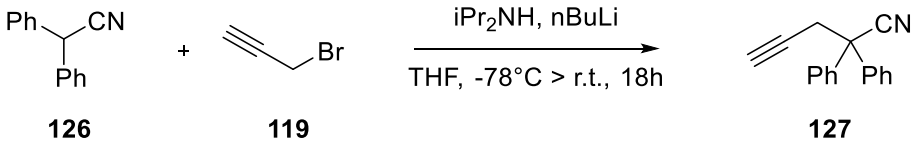

126 **119** **127**

Scheme 5.15 – Alkylation

Without purifying the desired product, we performed directly the Crabbè reaction on alkyne **127**, exploiting a microwave equipment, achieving allene **128**.

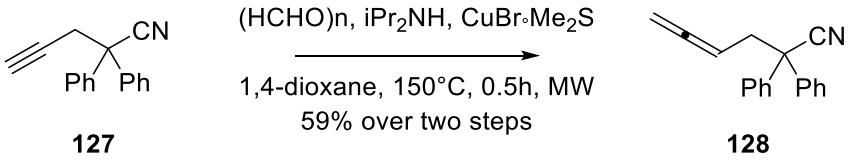

127 **128**

Scheme 5.16 - Crabbè reaction

We, then, reduced the nitrile moiety to free amine using lithium aluminum hydride. We could not isolate the desired product, probably because of degradation during purification on silica gel. In order to overcome this problem, we decided to perform the amine protection directly after the reduction step. Protections were carried out with two different protecting group such as *p*-toluensulfonyl (Ts) and *tert*-butyloxycarbonyl (Boc), to study the different interactions in the cyclization reaction.

[69] Zhang, Z.; Bender, C.F.; Widenhofer, R.A. *Org. Lett.* **2007**, 9, 15, 2887

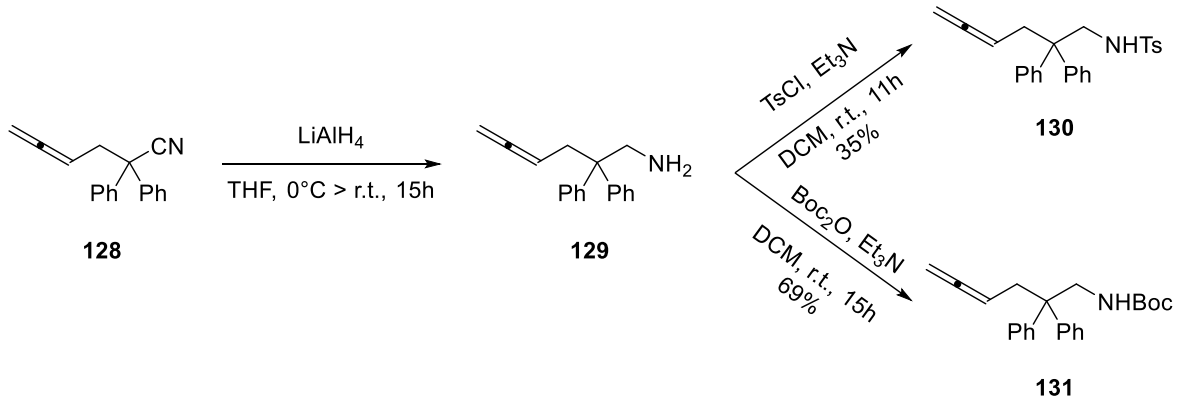

Scheme 5.17 – Reduction and protected amine formation

5.2.2 Methodological study

We began our study by exploring the Gold(I)-catalyzed hydroamination reaction on tosyl-protected amine **130**. We used the same catalytic systems described in the lactonization study (*Chapter 5.1.2*).

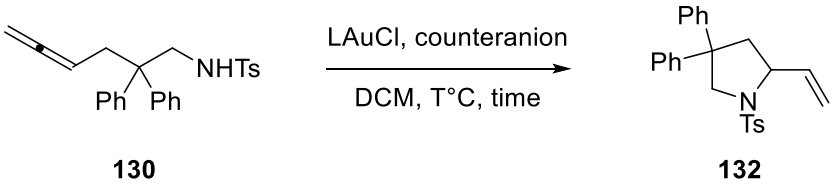

Scheme 5.18 – Gold(I)-catalyzed Hydroamination of 130

Entry	Catalyst	Counteranion	T	t(h)	Conversion (%)	132 (Y%)	ee (%)
1[a]	**PPh_3AuCl**	AgOTs	rt	24	>95	40	nd
2[a]	**PPh_3AuCl**	$NaBAr_4^F$	rt	24	<5	nd	nd
3[b]	**cat-17**	AgOTs	rt	24	>95	90	35.8
4[b]	**cat-17**	$NaBAr_4^F$	rt	15	>95	80	59.2
5[b]	**cat-22**	$NaBAr_4^F$	rt	24	<5	nd	nd
6[b]	**cat-17**	$NaBAr_4^F$	-10	24	>95	97	65.1
7[b]	**cat-17**	$NaBAr_4^F$	-30	48	<5	nd	nd

Table 5.5 – 0.1 mmol scale; a) catalyst 5mol%, counteranion 5mol%, DCM 0.05M; b) catalyst 100 ppm, counteranion 0.5mol%, DCM 0.05M

Firstly, we tried the racemic version of the reaction, using PPh_3AuCl as Gold(I)-catalyst in combination with either Silver tosylate or $NaBAr_4^F$ (*Table 5.5, entries 1-2*). Surely the counterion plays a pivotal role in this transformation since in $NaBAr_4^F$ case the reaction did not even start, while with AgOTs we obtained a 40% yield of the desired product. Nonetheless, we tried the hydroamination in the same conditions but this time we exploited a chiral Gold(I)-catalyst (*entries 3-4*). In reverse as the racemic version, $NaBAr_4^F$ gave better results in terms of reaction time and enantioselectivity than Silver tosylate, even though it still produced a slightly higher yield. Changing the catalyst to **cat-22** (*entry 5*), we did not get any desired product nor any conversion of the substrate at all. These results suggest us that the H-

bond catalysis is essential for a positive outcome for this transformation. In *entry 1*, tosylate anion in the mixture could probably give a weak but helpful H-bond in order to facilitate the nucleophilic attack on the Au-allene system. Moreover, the different results obtained between **cat-17** and **cat-22** could be related to the different H-bond acceptor. The C=O present in **cat-17** is a stronger H-bond acceptor than the tertiary N-sp3 in **cat-22**.

We then decided to lower the temperature in order to increase the enantioselectivity (*entries 6-7*). Unfortunately, only at -10°C we could get a little improvement in the ee values, along with an almost quantitative yield, while at -30°C we could not get any conversion of the substrate, even after 48h.

At this point, we decided to switch substrate and to begin the study on the Boc-protected amine.

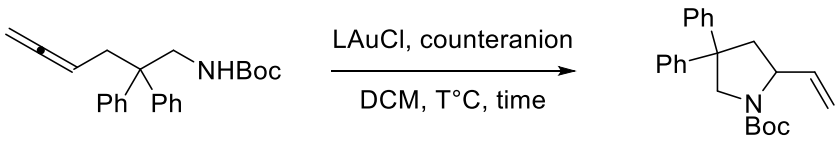

131 **133**

Scheme 5.19 - Gold(I)-catalyzed Hydroamination of 131

Entry	Catalyst	Counteranion	T	t(h)	Conversion (%)	133 (Y%)	ee (%)
1[a]	**PPh_3AuCl**	AgOTs	rt	48	<5	nd	nd
2[a]	**PPh_3AuCl**	$NaBAr_4^F$	rt	24	20	>95	nd
3[b]	**cat-17**	AgOTs	rt	24	>95	83	45.3
4[b]	**cat-17**	$NaBAr_4^F$	rt	24	>95	71	88.9
5[b]	**cat-22**	$NaBAr_4^F$	rt	24	50	30	35.1
6[b]	**cat-17**	$NaBAr_4^F$	-10	30	>95	91	47.0
7[b]	**cat-17**	$NaBAr_4^F$	-30	48	<5	nd	nd

Table 5.6 – 0.1 mmol scale; a) catalyst 5mol%, counteranion 5mol%, DCM 0.05M; b) catalyst 100 ppm, counteranion 0.5mol%, DCM 0.05M

In the same way as before, we started from racemic Gold(I)-catalyst PPh_3AuCl, in combination with two different counteranion (*Table 5.6, entries 1-2*). Surprisingly, Silver tosylate did not produce any product at all, even after 48 hours. $NaBAr_4^F$, instead gave a 20% conversion of the substrate leading to only one product which is the desired pyrrolidine **133**. We, then, switched to the chiral catalysts and we observed some significant improvements. **Cat-17** in combination with AgOTs gave the best results in term of yield with a moderate enantioselectivity (*entry 3*), while in combination with $NaBAr_4^F$ we obtained a slightly lower yield along with a huge improvement in the ee value, up to 89% (*entry 4*). We then decided to try the same conditions with **cat-22**. However, it did not give the hoped results and lower conversion and enantioselectivity was found. We then tried to lower the temperature, just as we did with the previous substrate, trying to replicate the best conditions. At -10°C, we obtained a slightly higher yield along with a longer reaction time, but the enantioselectivity incredibly dropped at a 47% ee value (*entry 5*). Lowering the temperature even more at -30°C (*entry 6*), we could not observe any product nor any conversion of the substrate, just as the previous amine.

We decided to stop at this moment of the study, considering the good results exploiting only 0.01 mol% of the Gold(I)-catalyst and 0.5 mol% of the counteranion, and to begin exploring the lactamization reaction.

5.3 Gold(I)-catalyzed Lactamization

Finally, we would explore the cyclization of allenyl amides in order to obtain enantioenriched substituted γ-lactam. We were quite interested in this Gold(I)-catalyzed reaction as there is no precedent in the literature and the products eventually formed could be useful for designing new total synthesis of natural products.

5.3.1 Substrate Synthesis

Starting from the already synthetized allenyl acid **122**, we prepared three differently substituted amides.

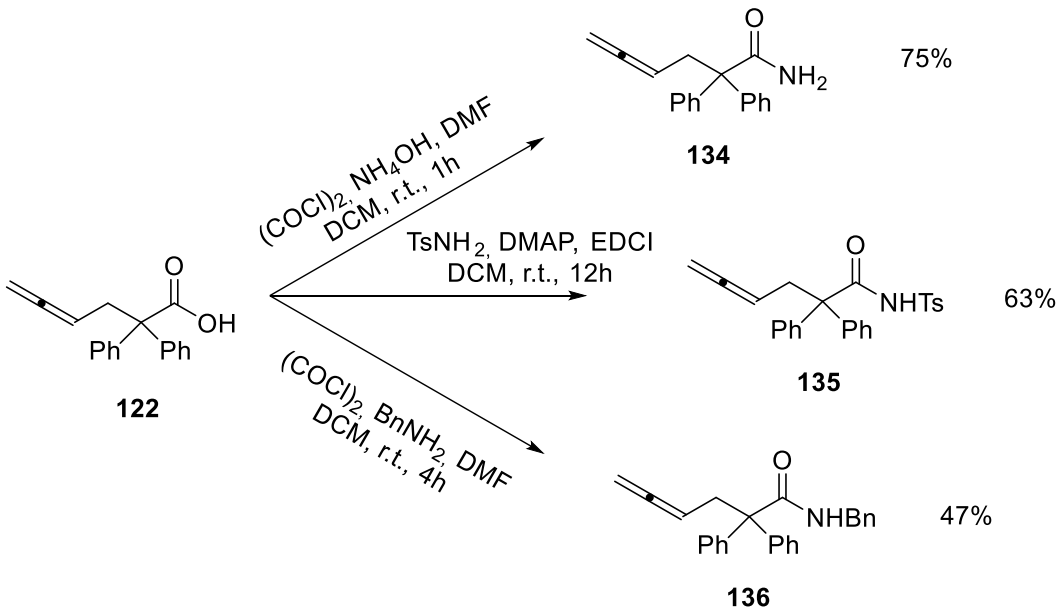

*Scheme 5.20 - Synthesis of amide substrates **134-136***

Free amide **134** was synthetized by treatment of acid **122** with oxalyl chloride and ammonium hydroxide. A condensation reaction mediated by 1-ethyl-3-(3-dimethylaminopropyl)carbodiimide and *p*-toluensulfonamide allowed the obtainment of tosyl-protected amide **135** in moderate yield. Lastly, we obtained benzyl amide **136** upon treatment of the acid with oxalyl chloride and benzylamine, similarly to the procedure of the free amide.

5.3.2 Methodological study

We began our study by exploring the Gold(I)-catalyzed lactamization reaction on free amide **134**. We used the same catalytic systems described in the lactonization (*Chapter 5.1.2*) and hydroamination study (*Chapter 5.2.2*).

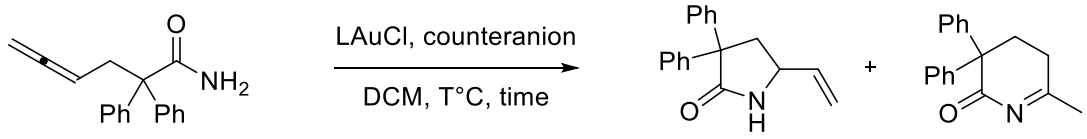

134 **137a** **137b**

Scheme 5.21 - Gold(I)-catalyzed Lactamization of 134

Entry	Catalyst	Counteranion	Additive	T	t(h)	Conversion (%)	137a (Y%)	137b (Y%)	ee (%)
1[a]	**PPh_3AuCl**	AgOTs	none	rt	15	>95	nd	81	nd
2[a]	**PPh_3AuCl**	$NaBAr_4^F$	none	rt	48	<5	nd	nd	nd
3[b]	**cat-17**	AgOTs	none	rt	48	<5	nd	nd	nd
4[b]	**cat-17**	$NaBAr_4^F$	none	rt	48	<5	nd	nd	nd

Table 5.7 - 0.1 mmol scale; a) catalyst 5mol%, counteranion 5mol%, DCM 0.05M; b) catalyst 100 ppm, counteranion 0.5mol%, DCM 0.05M; c) catalyst 5mol%, counteranion 5mol%, additive 5mol%, DCM 0.05M

We started our study with free amide **134**. We performed some screening with different conditions and catalyst but only with PPh_3AuCl in combination with silver tosylate (*Table 5.7, entry 1*) we managed to obtain 81% yield of the 6-membered lactam **137b**. Although it is not the desired product, this compound it is quite interesting firstly it is unknow in the literature and also because it can act as an α,β-unsaturated system, undergoing some other reactions increasing the molecular complexity.

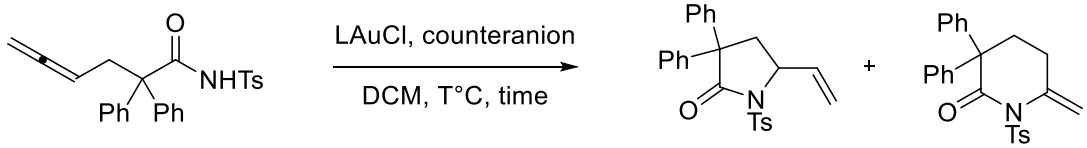

135 **138a** **138b**

Scheme 5.22 - Gold(I)-catalyzed Lactamization of 135

Entry	Catalyst	Counteranion	Additive	T	t(h)	Conversion (%)	138a (Y%)	138b (Y%)	ee (%)
1[a]	**PPh_3AuCl**	AgOTs	none	rt	15	25	nd	>95	nd
2[a]	**PPh_3AuCl**	$NaBAr_4^F$	none	rt	48	<5	nd	nd	nd
3[b]	**cat-17**	$NaBAr_4^F$	none	rt	24	53	>95	<5	<5
4[b]	**cat-22**	$NaBAr_4^F$	none	rt	15	>95	89	11	<5
5[b]	**cat-23**	$NaBAr_4^F$	none	rt	24	37	67	33	<5
6[b]	**cat-22**	$NaBAr_4^F$	none	-10	48	<5	nd	nd	nd

Table 5.8 - 0.1 mmol scale; a) catalyst 5mol%, counteranion 5mol%, DCM 0.05M; b) catalyst 100 ppm, counteranion 0.5mol%, DCM 0.05M; c) catalyst 5mol%, counteranion 5mol%, additive 5mol%, DCM 0.05M

We then moved to the tosyl-protected amide **135**, and we observed some more consistent results. Also in this case, PPh_3AuCl and silver tosylate gave us the 6-membered ring, although in low conversion (*Table 5.8, entry 1*), while using $NaBAr_4^F$ no substrate conversion happened (*entry 2*). We tried with some chiral catalysts and we observed a change in selectivity towards the formation of the 5-membered lactam. Most probably the presence of the directing group on the ligands helped the reaction for the production of compound 138a. However, we could not observe any stereoinduction on the system.

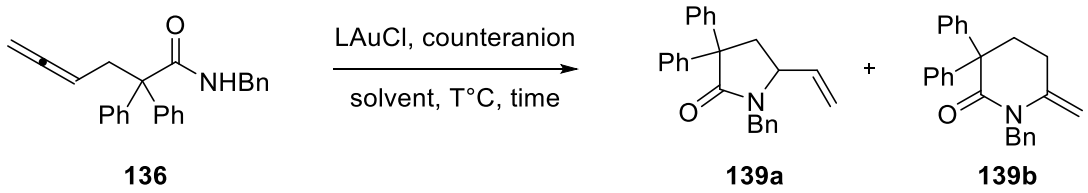

136 **139a** **139b**

Scheme 5.23 - Gold(I)-catalyzed Lactamization of 136

Entry	Catalyst	Counteranion	Additive	T	t(h)	Conversion (%)	139a (Y%)	139b (Y%)	ee (%)
1[a]	**PPh_3AuCl**	AgOTs	none	rt	48	<5	nd	nd	nd
2[a]	**PPh_3AuCl**	AgOTs	none	rt	48	<5	nd	nd	nd
3[b]	**cat-22**	$NaBAr_4^F$	none	rt	48	<5	nd	nd	nd
4[b]	**cat-22**	$NaBAr_4^F$	none	rt	48	<5	nd	nd	nd

Table 5.9 - 0.1 mmol scale; a) catalyst 5mol%, counteranion 5mol%, DCM or THF 0.05M; b) catalyst 100 ppm, counteranion 0.5mol%, DCM or THF 0.05M.

Last substrate we studied was benzyl-protected amide **136**. We tried different conditions, even changing solvent to a more polar one, such as THF, but we could not obtain any desired product nor substrate conversion at all.

At this point we thought of having enough results to move our attention to the development of new chiral bifunctional ligands described in the next chapter.

6 New Ligands design and synthesis

After gaining insight on all these reactions described above, we observed a tendency linked to the acidity of the nucleophile. The lower the pK_a, the faster the reaction. Moreover, since LAC is based on reaction kinetics, the faster the reaction, the higher the enantioselectivity will be. Thus, if we want to improve the reaction effectiveness, we must use either a quite acid nucleophile or a stronger hydrogen bond acceptor. The latter is the most attractive option as it could hypothetically allow us to perform different reaction with the same catalyst system. Until now, we used tertiary amines and secondary amides as hydrogen-bond acceptor, as shown in Figure 6.1.

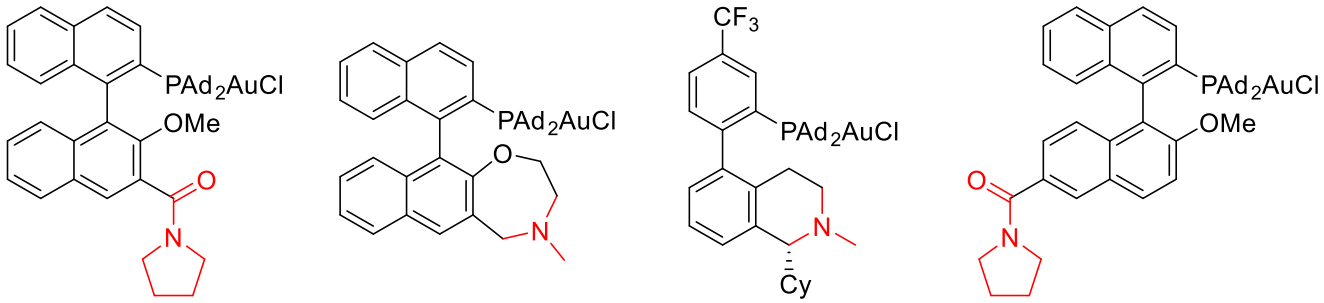

cat-17 **cat-22** **cat-23** **cat-24**

Figure 6.1 - Directional groups in ligands

Searching in the literature, we found a pk_{HB} acceptor scale[70], based on the Gibbs energy change for the formation of hydrogen bonding complexes between hydrogen bond acceptors (HBA) and a reference hydrogen bond donor (4-fluorophenol) in tetrachloromethane at 298 K. They described how the HBA strength is influenced by several factors, including the position of the acceptor atom in the periodic table, polarizability, field/inductive and resonance effects of substituents around the acceptor atom and proximity effects including steric hindrance of the acceptor site, intramolecular hydrogen bonding and lone-pair–lone-pair repulsions. For these reasons the pk_{HB} scale differs completely from pk_a scale of proton transfer. Looking into the pk_{HB} scale reported we can link our ligands to the nearest functional group. Thus, secondary amide contained in L_1-AuCl and L_4-AuCl can be related to dimethylacetamide, with a pk_{HB} value of 2.44, while tertiary amines contained in L_2-AuCl and L_3-AuCl can be related both to triethylamine, with a pk_{HB} value of 1.99. Going down the scale we found some functional group of great interest for the design of new ligands. Some functional group examples are dimethylsulfoxide (2.58), N-methylimidazole (2.72), 4-N,N-dimethylaminopyridine (2.80) and triethylphosphine oxide (3.16).

To test these data, we ran some other hydroamination reactions (*Scheme 6.1*), since we had some difficulties in obtaining consistent results with this transformation. We exploited the racemic version and we added some additives, in catalytic quantities, to test if the reaction time and yield could get any

[70] Laurence, C.; Berthelot, M. *Perspect. Drug Discov.* **2000**, 18, 39

improvement (*Table 6.1*). We used both DMAP and triethylphosphine oxide with all the allenyl amides, since these two functional groups are between the strongest H-bond acceptor.

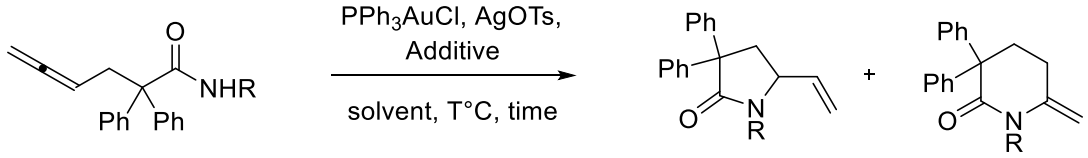

Scheme 6.1 - Gold(I)-catalyzed Lactamization in presence of additives

Entry	R	Additive	T	t(h)	Conversion (%)	γ-lactam (Y%)	δ-lactam (Y%)
1	**H**	DMAP	rt	24	15	nd	>95
2	**H**	Et_3PO	rt	24	90	nd	92
3	**Ts**	DMAP	rt	15	>95	71	nd
4	**Ts**	Et_3PO	rt	15	>95	11	88
5	**Bn**	DMAP	rt	48	<5	nd	nd
6	**Bn**	Et_3PO	rt	48	<5	nd	nd

Table 6.1 - 0.1 mmol scale; catalyst 5mol%, counteranion 5mol%, additive 5mol%, DCM 0.05M

Looking at the lactamization performed on free amide **134** (*Table 6.1, entries 1-2*), we obtained a huge improvement exploiting Et_3PO as additive, while DMAP was not so effective. In the tosyl-protected amide case, we could observe how both additives gave a complete conversion of the substrate. Benzyl-protected amide **136**, instead, did not gave any product nor conversion at all. Comparing these entries with the same without additives for both substrates, we can confirm the effective improvement in the lactamization reaction mediated by DMAP and Et_3PO.

The latter one attracted us the most, since phosphine oxides are quite stable functional groups in several reaction conditions and pyridine could be too much basic.

6.1 Functional groups

We started designing the synthesis for the new ligand including a tertiary phosphine oxide in place of the secondary amide. We thought of installing a diphenylphosphine oxide in order to further control the electronic effect with several substituents. Our first attempt mimicked **cat-17** synthesis reported by Zhang's coworkers in 2017.

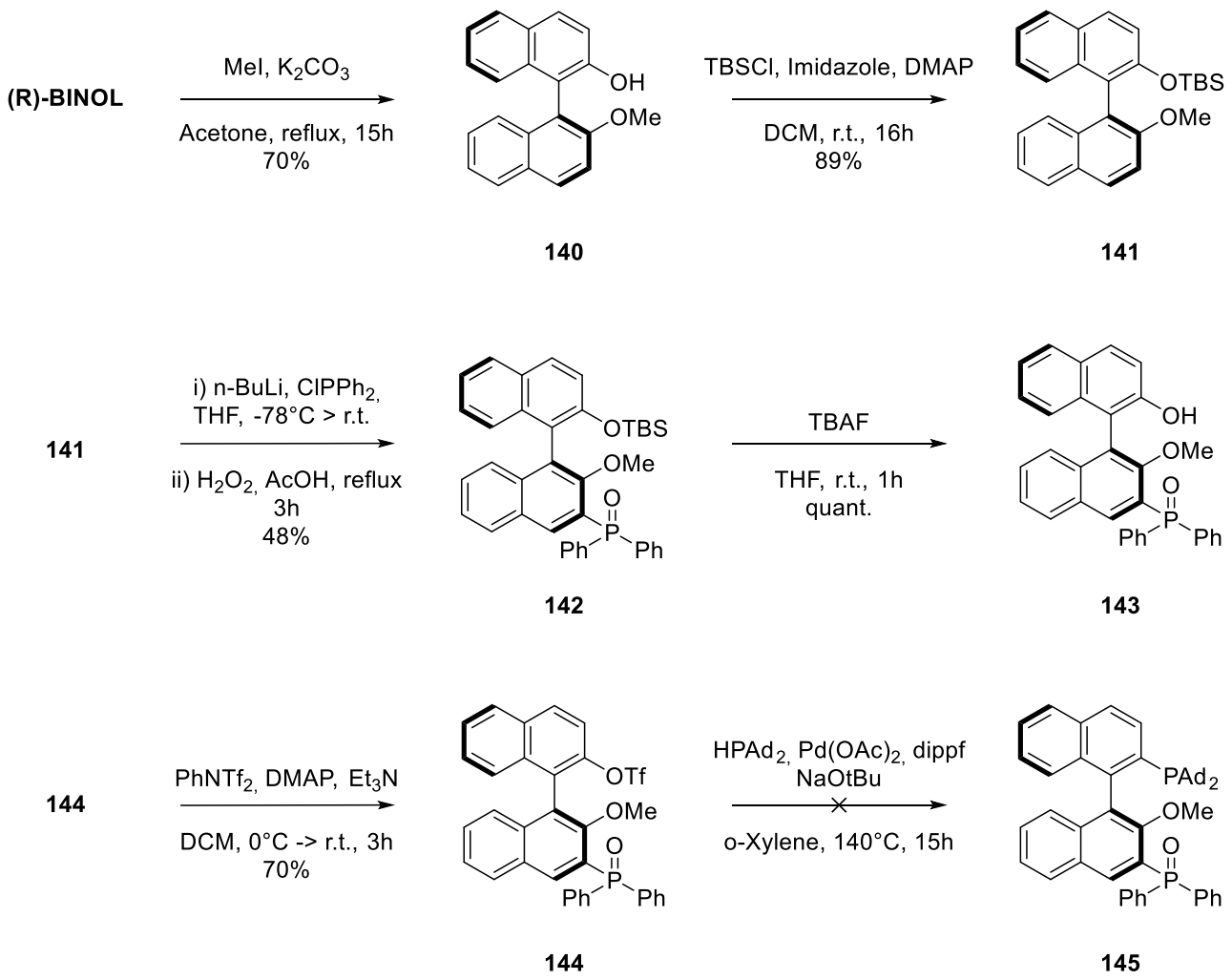

Scheme 6.2 - First attempt in Phosphine-Oxide catalyst synthesis

Starting from commercially available (*R*)-Binol, we performed the methylation of one of the hydroxyl group and the protection as tert-butyldimethylsilyl ether of the other one in two different steps. *Ortho*-litiation with butyllithium and diphenylphosphine with subsequent oxidation to phosphine oxide proceeded in moderate yield to obtain compound **142**. Deprotection with TBAF and triflation led to compound **144**, ready for the difficult Pd-mediated phosphine coupling. We tried different conditions, always using Schlenk technique, changing bases, Palladium sources and ligands but none of them gave us the desired product. In all the attempts we recollected triflate **144** in 50-60% yield and we managed to isolate compound **143** in 20-30% yield, probably due to some traces of water in the reaction mixture.

We, then, decided to change the design of our synthesis by performing first the formation of the phosphine and then inserting the phosphine oxide.

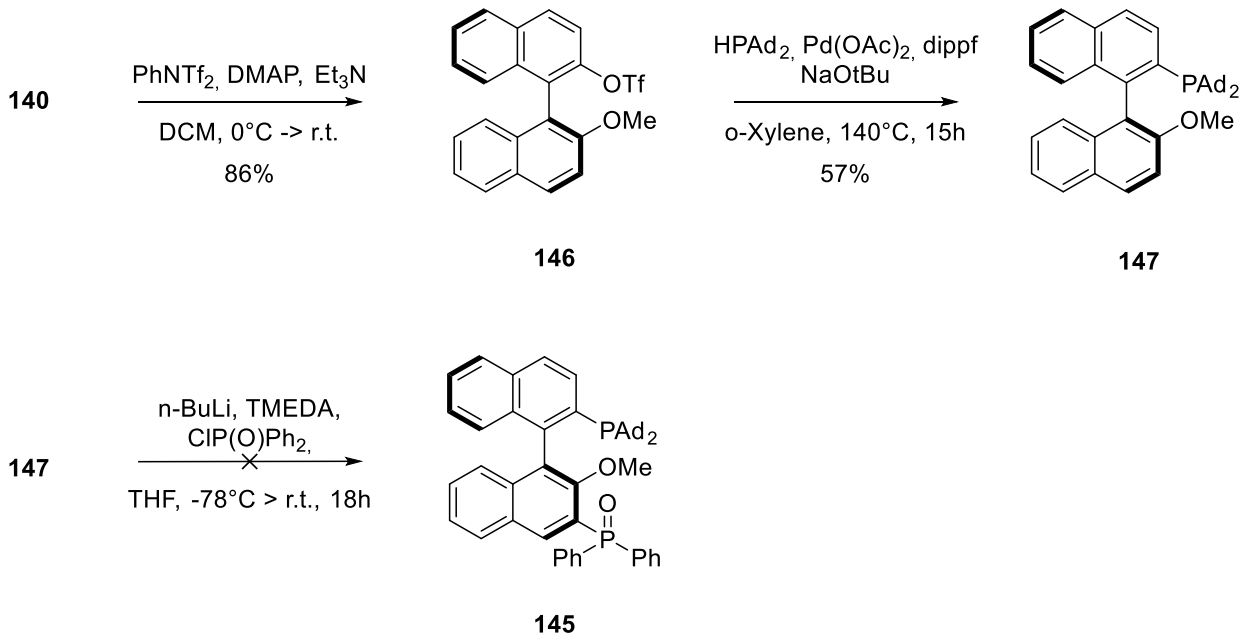

After having prepared compound **140**, we subjected to a triflation protocol exploiting bis(trifluoromethanesulfonyl)aniline in DCM. Triflate **146**, then, underwent the Pd-mediated phosphine coupling with di-1-adamantylphosphine to obtain compound **147**. We noted that the higher the scale of this reaction, the higher the yield. In fact, we ran this reaction at gram-scale, while in the previous synthesis the same step was performed at a 200-milligram scale. In order to insert the phosphine oxide group, we thought of an ortolithiation reaction in combination with chlorodiphenylphosphine oxide. The anion formation should be directed primarly in *ortho* to the methoxy group, because of stereoelectronic effects. Unfortunately, also in this case the reaction did not give any desired product. However, at the same time, no substrate was consumed. We tried again the reaction by increasing the equivalent of n-butyllithium and TMEDA, but we could not obtain any trace of product nor any consumption of the starting material.

Since we were not able to put the selected directing group on the catalyst, we decided to change completely our strategy.

6.2 Modifying directing group position

We then thought of moving the directing group to another position and we thought that the 6 position could be useful to restrain the TS conformational space and enhance the stereoselectivity. For these reasons we developed a new synthesis.

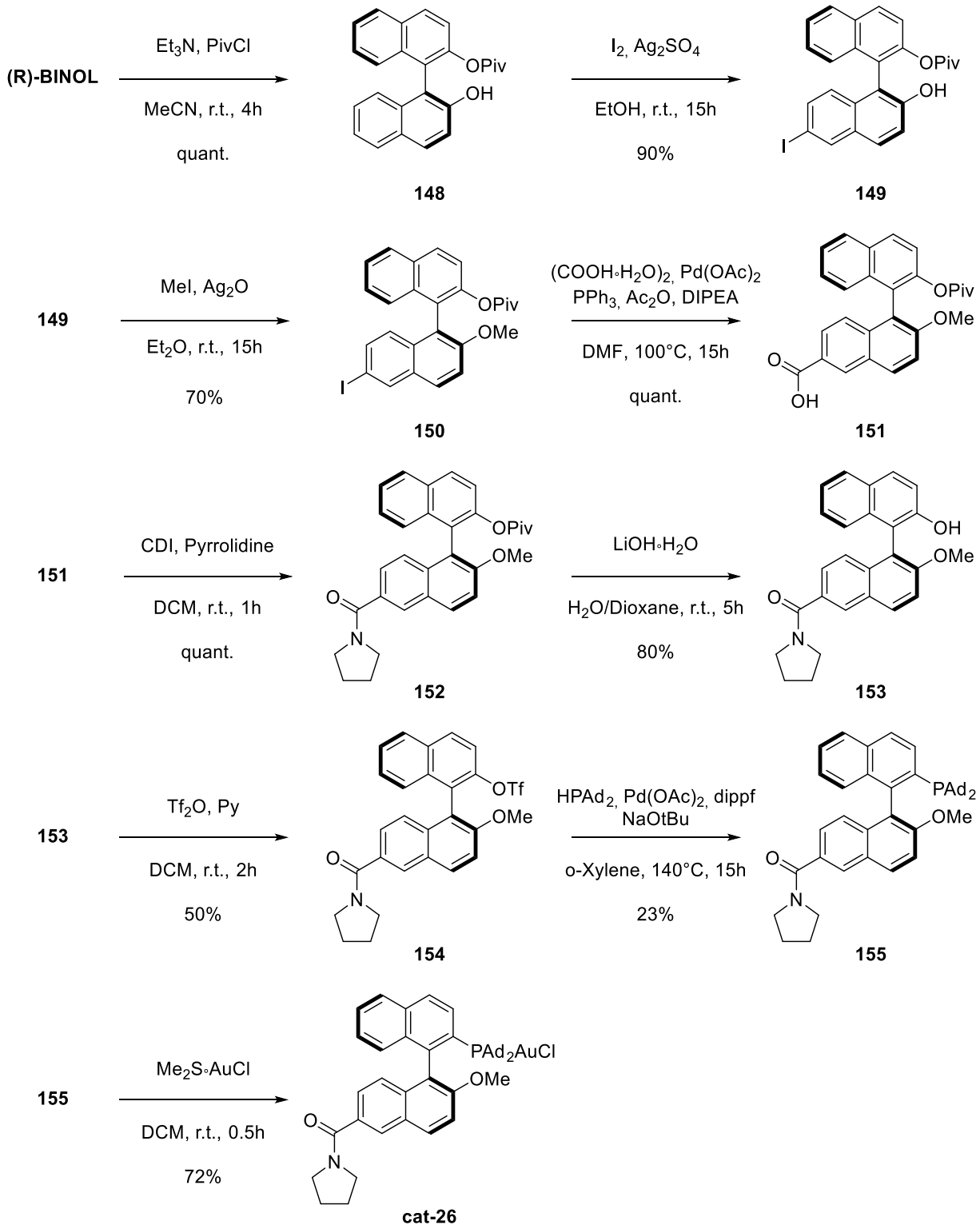

*Scheme 6.3 – **cat-24** synthesis*

Starting from the commercially available (*R*)-BINOL, we followed an already known procedure to obtain iodide **149**. Protection of a hydroxyl group as pivalate allowed us the correct regiochemistry for the subsequent iodination step. Performing the methylation was quite tricky. Following classical methylation conditions, such as CH_3^+-source in basic conditions, gave us a complex mixture of compounds, almost impossible to identify. Using silver oxide instead of bases was the key and we managed to obtain the desired compound **150**. We then performed a carbonylation reaction exploiting oxalic acid as CO source obtaining acid **151** quantitively which was then transformed in the amide **152** through a condensation. After deprotection of pivalate and transformation of the hydroxyl group into the triflate we could perform the P-coupling, obtaining finally the ligand **155**. Last step of the synthesis was placing the metal on the phosphine group. To prove the successful attach of Gold, we run P^{31}-NMR experiments, observing the chemical shift from 27.6ppm to 62.4ppm.

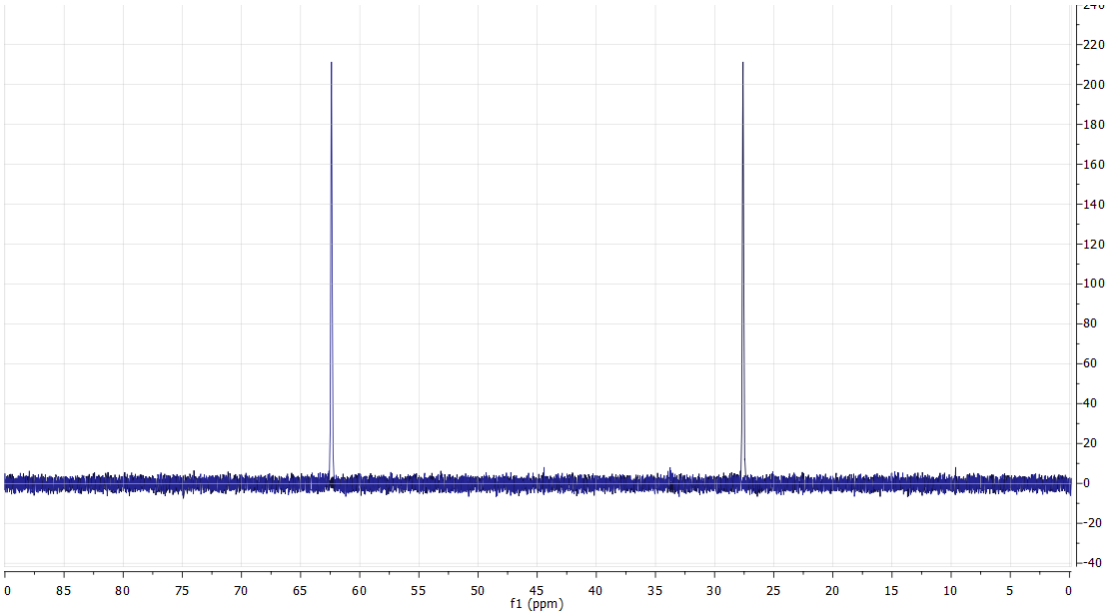

Figure 6.2 - P^{31}-NMR chemical shifts of L_4 and L_4-AuCl

7 Gold(I)-catalyzed Cyclization of ene-ynes

Having established the heterofunctionalization reactions on allene, we sought for similar reaction on different and under-explored electrophilic sites. The idea is to extend the applicability of the Gold(I)-catalyzed heterofunctionalization on other functional groups and to obtain different substituents on the saturated heterocycles, other than vinyl. Thereby, we can possibly extend and increase the molecular complexity by accessing to multiple tools for late-stage functionalization.

We took inspiration looking at Braddock's work[71]. In 2008, with his coworkers described an intramolecular bromoetherification reaction on ene-ynes (*Scheme 7.1)*.

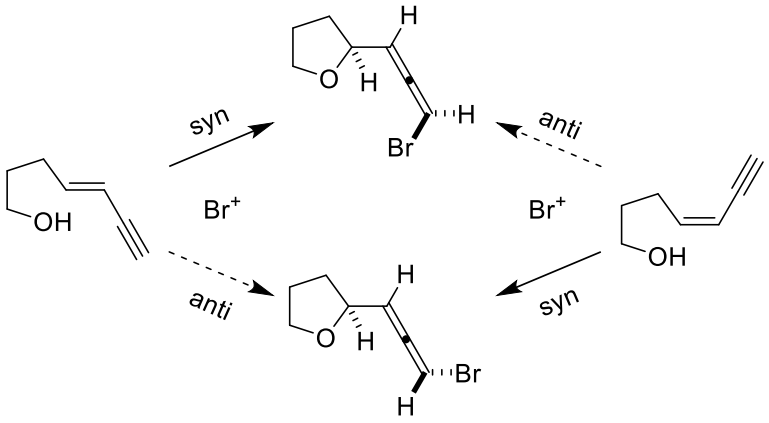

Scheme 7.1 - Braddock's Bromoetherification of Ene-ynes

Since we found no example in literature about a Gold(I)-catalyzed version of this transformation, we were intrigued into exploring this new reaction. We wanted to study also the Gold(I)-catalyzed intramolecular hydroalkoxylation reaction in the absence of the Br^+-source to obtain an allene moiety as substituent on the THF core.

7.1 Substrate Synthesis

We then started with the synthesis of the simplest ene-yne substrate. Starting from 4-pentyn-1-ol, we performed a hydroiodination reaction, in presence of DIBAl-H and iodine, to obtain vinyl iodide **157** (*Scheme 7.2*).

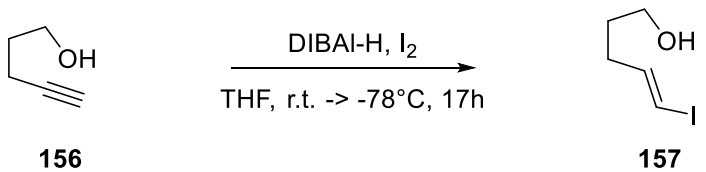

Scheme 7.2 – Hydroiodination reaction

[71] Braddock, D.C.; Bhuva, R.; Pérez-Fuertes, Y.; Pouwer, R.; Roberts, C.A.; Ruggiero, A.; Stokes, E.S.E.; White, A.J.P. *Chem. Commun.* **2008**, 1419

Since we could not isolate the product because of its instability, we subjected it directly in the next step. A Sonogashira cross-coupling reaction had been performed in combination with trimethylsilylacetylene to produce ene-yne **158**. From NMR analysis, we could observe a complete selectivity for the E configuration of the double bond.

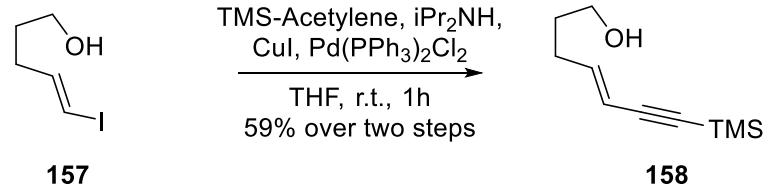

157 **158**

Scheme 7.3 – Sonogashira Cross-Coupling

As last step of the synthesis, we performed the deprotection of the alkyne moiety in the presence of potassium carbonate in methanol.

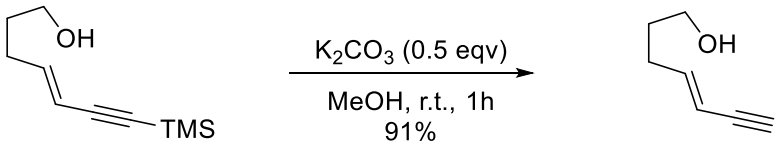

158 **159**

Scheme 7.4 - Deprotection of the alkyne moiety

We also developed a synthesis for a substrate bearing substituents on the β position to the hydroxyl group. These substituents will allow us an easier development of a HPLC analytical method and should also assist the cyclization reaction thanks to the Thorpe Ingold effect.

Starting from propargyl alcohol, we performed the same reactions for the obtainment of vinyl iodide **161**, as described for the previous substrate. However, the yield for the two steps was incredibly lower than the one for the other substrate. The reason could be appointed to the volatility of the vinyl iodide intermediate and, as consequence, the Sonogashira cross-coupling produced a complex mixture of compounds.

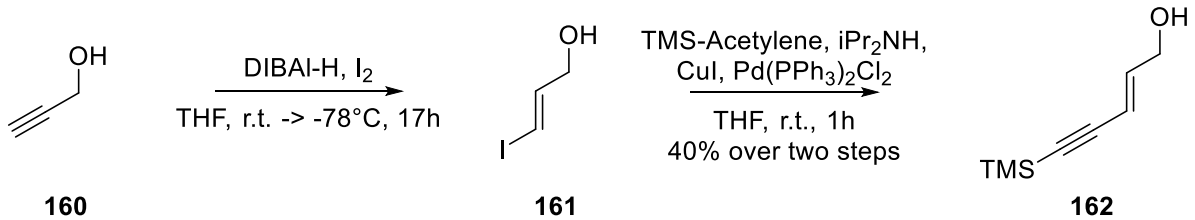

160 **161** **162**

Scheme 7.5 - Synthesis of ene-yne 160

To overcome this problem, we found another protocol for the production of compound **162**. We exploited the *in situ* formation of the Schwartz reagent, from zirconocene dichloride and DIBAl-H. This protocol gave us a cleaner reaction, by TLC analysis and a higher yield of the intermediate. We also

modified the Sonogashira reaction, by degassing both the solvent and the diisopropylamine, in order to eliminate the oxygen in the mixture and increasing the stability of the metal catalysts. Also in this case, we observed complete selectivity toward E configuration of the double bond.

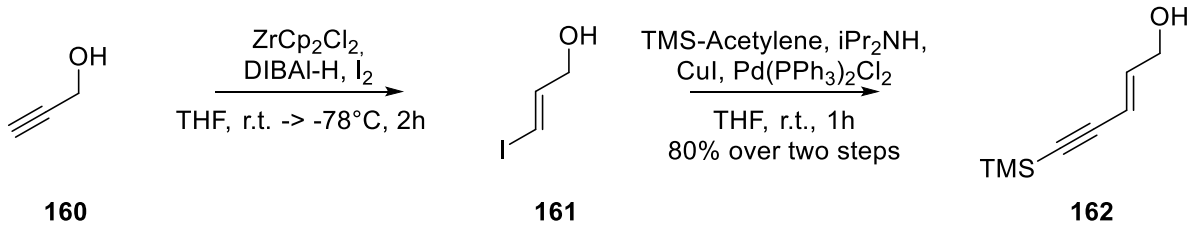

Scheme 7.6 - Optimized synthesis of ene-yne 160

Next step of the synthesis is the bromination reaction, using PBr_3. In this way bromide **163** is ready for the alkylation reaction in combination with methyl diphenyl acetate and LDA. Ester **164** was obtained in almost quantitative yield.

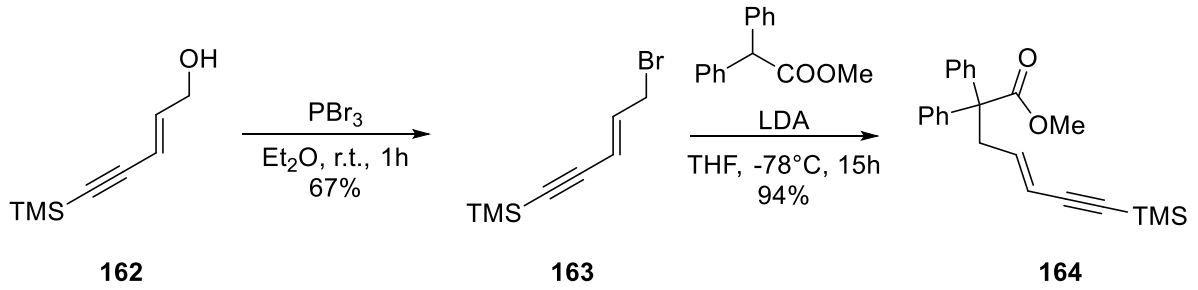

Scheme 7.7 - Synthesis of ester 162

Last two steps of the synthesis are the reduction with DIBAl-H of the ester moiety to hydroxyl group and the deprotection of the TMS-protected alkyne to obtain substrate **166**.

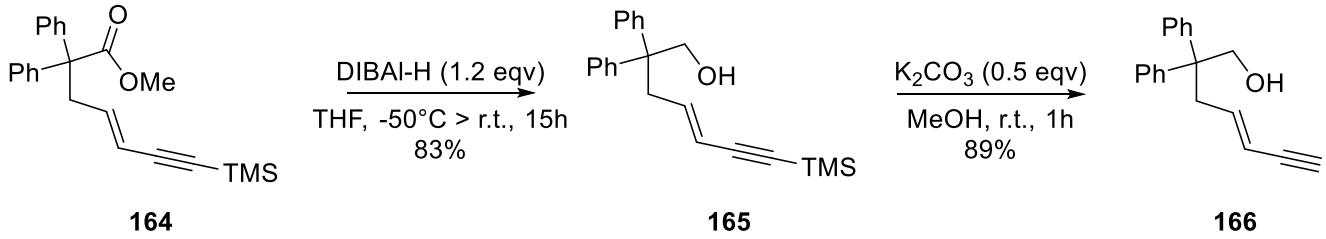

Scheme 7.8 - Synthesis of substrate 164

7.2 Gold(I)-catalyzed Hydroalkoxylation methodological study

As mentioned above, for the intramolecular Gold(I)-catalyzed hydroalkoxylation of ene-ynes we took inspiration from Braddock's work about bromoetherification of this kind of substrates. Since no example in literature is reported on a Gold(I)-catalyzed version of this transformation, we began a methodological study, considering the mechanism proposed below (*Scheme 7.9*)

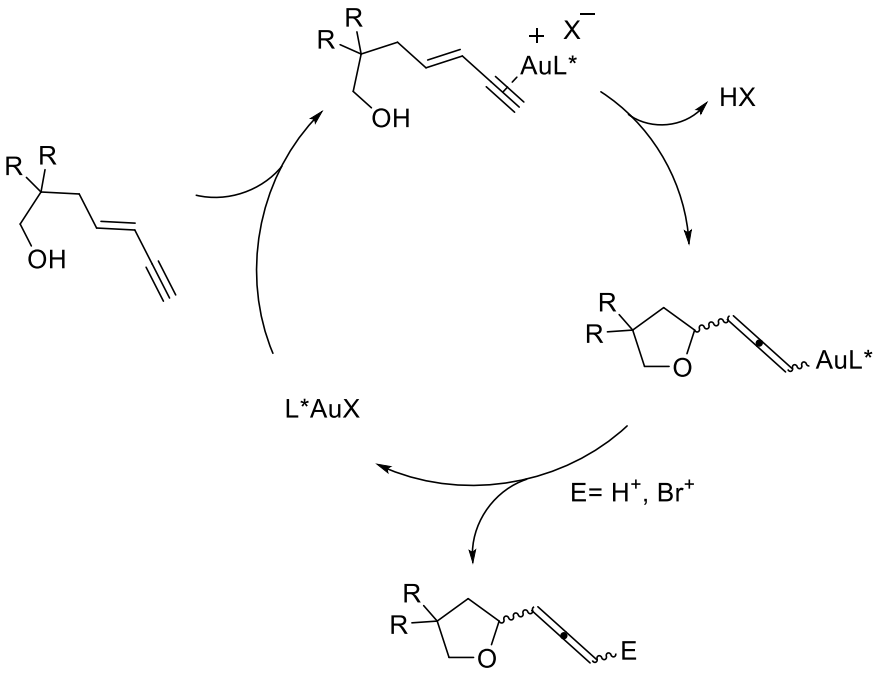

Scheme 7.9 - Proposed mechanism for the Gold(I)-catalyzed hydroalkoxylation

Exploiting these substrates, the expected products present one stereogenic center in the case of the unsubstituted allene, while a mixture of two diastereomer is expected if N-bromosuccinimide is used, since the allene formed possesses axial chirality.

We began the methodological study by observing the reaction of **159** and **166** in the presence of achiral Gold(I)-catalysts, an Ag-based counterion in DCM or Toluene.

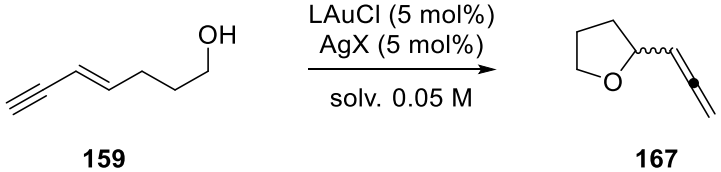

*Scheme 7.10 - Gold(I)-catalyzed cyclization reaction on substrate **159***

Entry	Catalyst	Counteranion	Solvent	T	t(h)	Conversion (%)	167 (Y%)
1	**PPh_3AuCl**	$AgNTf_2$	DCM	rt	4	<5	nd
2	**JohnPHOSAuCl**	$AgNTf_2$	DCM	rt	4	<5	nd

Table 7.1 - 0.1 mmol scale; catalyst 5 mol%, counterion 5 mol%, solvent 0.05M.

For what concerns substrate **157**, we could not observe the formation of any desired compound nor any advancement in the conversion.

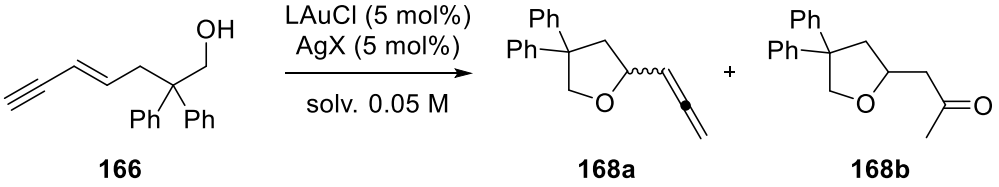

166 **168a** **168b**

*Scheme 7.11 - Gold(I)-catalyzed cyclization reaction on substrate **166***

Entry	Catalyst	Counteranion	Solvent	T	t(h)	Conversion (%)	168a (Y%)
1	**PPh_3AuCl**	$AgNTf_2$	DCM	rt	5	82	35
2	**JohnPHOSAuCl**	$AgNTf_2$	DCM	rt	5	79	37
3	**JohnPHOSAuCl**	$AgNTf_2$	Toluene	rt	2	39	29

Table 7.2 - 0.1 mmol scale; catalyst 5 mol%, counterion 5 mol%, solvent 0.05M.

Looking at the hydroalkoxylation reaction on ene-yne **166**, we could observe the formation of the desired product in low yield along with almost a complete conversion. Together with the substituted THF **168a**, we found a second product we identified as ketone **168b**. Most probably it derives from a background alkyne hydration reaction, promoted by water traces inside the reaction vessel.

We, then, began to study the Gold(I)-catalyzed cyclization on substrate **159**, by exploiting chiral catalysts along with 3Å-molecular sieves, hoping that we could obtain better results. The catalysts used are the same presented for the heterofunctionalization reactions (*Chapter 5*) and the new catalyst synthetized in *Chapter 6*.

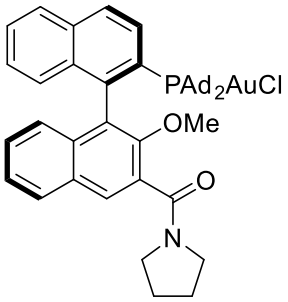

cat-17

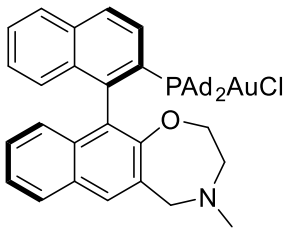

cat-22

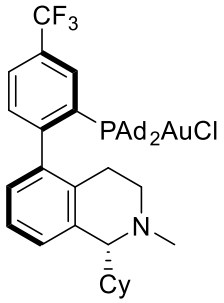

cat-23

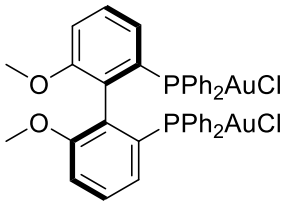

cat-24

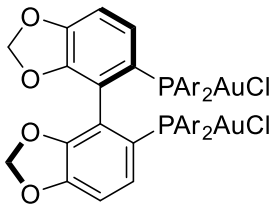

cat-25
Ar= 3,5-t-Bu-4-OMe-C_6H_4

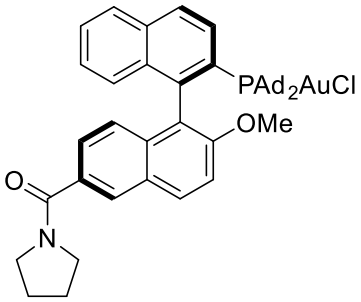

cat-26

Figure 7.1 – Chiral catalysts explored in the cyclization

Entry	Catalyst	Counteranion	T	t(h)	Conversion (%)	167 (Y%)	ee (%)
1	**cat-17**	$NaBAr_4^F$	rt	96	41	nd	nd
2	**cat-26**	$NaBAr_4^F$	rt	18	73	nd	nd
3	**cat-25**	$NaBAr_4^F$	rt	48	<5	nd	nd
4	**cat-25**	AgOTf	rt	96	12	nd	nd
5	**cat-25**	$AgNTf_2$	rt	24	64	nd	nd
6	**cat-23**	$NaBAr_4^F$	rt	96	<5	nd	nd
7	**cat-22**	$NaBAr_4^F$	rt	96	69	nd	nd

Table 7.3 – 0.1 mmol scale; catalyst 5 mol%, counterion 5 mol%, solvent 0.05M.

Despite in most of the entries we could observe the formation of a main product, we were not able to isolate it for a complete characterization because of its volatility. All the reactions needed a purification step and this one could be the limiting stage of this transformation. We also tried some purification techniques more suitable for low-boiling compounds, however we did not achieve in the product isolation.

We then explored the hydroalkoxylation reaction on ene-yne **166**, exploiting chiral Gold(I)-catalysts and by adding 3Å-molecular sieves.

Entry	Catalyst	Counteranion	T (°C)	t(h)	Conversion (%)	168a (Y%)	ee (%)
1	**cat-24**	$AgNTf_2$	rt	22	>95	49	20
2	**cat-25**	$AgNTf_2$	rt	2	>95	<5	nd
3	**cat-26**	$NaBAr_4^F$	rt	5	>95	61	90
4	**cat-26**	$NaBAr_4^F$	0	48	47	<5	nd
5	**cat-26**	$NaBAr_4^F$	rt	20	>95	34	69
6	**cat-26**	$NaBAr_4^F$	rt	28	52	21	56

Table 7.4 - 0.1 mmol scale; catalyst 5 mol%, counterion 5 mol%, solvent 0.05M.

Commercially available **cat-24** in combination with silver bis(trifluoromethylsulfonyl)imide gave a decent yield of the desired product, but unfortunately the enantioselectivity was pretty low. **Cat-25**, on the contrary, still gave a full conversion of the substrate, but we could not detect tetrahydrofuran **168a**. In fact, by TLC analysis we observed a complex mixture of products we were not able to separate, but by crude NMR analysis we could confirm the absence of significative signals. We then tried our newly synthetized catalyst **cat-26**. In combination with $NaBAr_4^F$ at room temperature, we obtained the desired product in 61% yield with a 90% *ee* value in only 5 hours. This result encouraged us in optimizing even more the reaction conditions. For this reason, we tried to lower the temperature at 0°C, but unfortunately after 48 hours of reaction, we could see only a 47% conversion and no traces of the substituted-THF **168a**. We then ran a couple of reaction at room temperature but lowering the catalyst loading at 2 mol% and 1 mol%. Both these trials gave lower yield and enantioselectivity along with longer reaction time.

In the future, we will perform an extensive substrate scope, including ene-ynes leading to tetrahydropyrans. Moreover, we will try the reaction with different nucleophiles such as acids, amines and amides.

7.3 Gold(I)-catalyzed Bromoetherification methodological study

We also thought to replicate Braddock's bromoetherification reaction on ene-ynes developing a Gold(I)-catalyzed protocol. We used the same substrates as the previous chapter and we developed a methodological study.

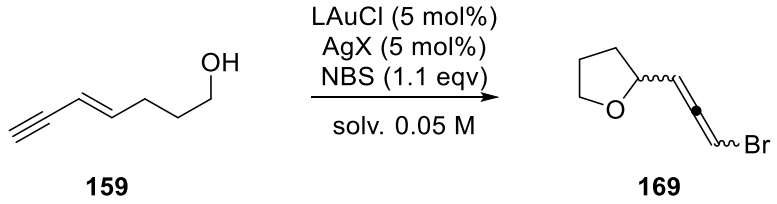

*Scheme 7.12 - Gold(I)-catalyzed bromoetherification reaction on substrate **159***

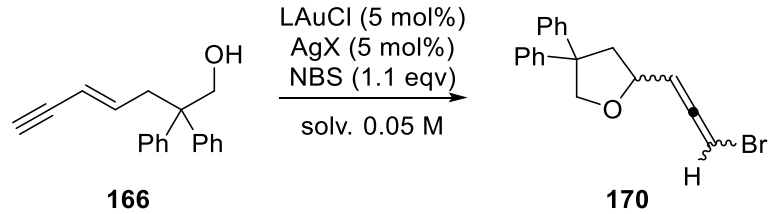

*Scheme 7.13 - Gold(I)-catalyzed bromoetherification reaction on substrate **166***

Entry	Product	Catalyst	Counteranion	T	t(min)	Conversion (%)	Y%
1	**169**	**-**	-	rt	120	>95	nd
2	**170**	**-**	-	rt	120	>95	68
3	**170**	**JohnphosAuCl**	$AgNTf_2$	rt	10	>95	62
4	**170**	**Johnphos**	-	rt	15	>95	56
5	**170**	**AuCl**	$AgNTf_2$	rt	15	>95	61

Table 7.5 – 0.1 mmol scale; Catalyst 5 mol%, counterion 5 mol%, NBS 1.1 equiv., DCM 0.05M

We began studying the reaction by just adding N-bromosuccinimide with the ene-ynes in DCM. Both reactions achieved full conversion of the substrate, however we could not get yield data about bromoallene **169** (*Table 7.5 – entry 1*), because it is quite instable compound also at lower temperature and just after purification by silica gel, we could observe the formation of a yellowish color. Moreover, 1H-NMR spectrum was quite complex as we could observe the peak relative to the desired product along with some other signals we were not able to understand. For these reasons we decided to continue our methodological study only with substrate 166, which gave some more consistent results (*entry 2*).

We then decided just to add a commercially available Gold(I)-catalyst in combination with a silver counterion (*entry 3*). We observed that after only 10 minutes full conversion of the ene-yne was achieved and we managed to obtain a 62% yield of the desired product. We thought that maybe the phosphine in the Gold(I)-catalyst could play a role as a catalyst alone. We then ran two reactions by

testing the influence of both phosphine and Gold(I) as catalyst (*entries 4-5*) and we observed that both reactions behaved quite similarly. Full conversion had been reached in just 15 minutes along with a 60% yield, meaning that both phosphine and Gold(I) have an important role and their combined effect brings only improvements in terms of yield.

Satisfied by these preliminary data, we tried the reaction in combination with chiral catalysts.

Entry	Catalyst	Counteranion	T	t(min)	Conversion (%)	170 (Y%)	ee (%)
1	**cat-23**	$NaBAr_4^F$	rt	15	>95	65	nd
2	**cat-26**	$NaBAr_4^F$	rt	15	>95	73	nd
3	**cat-24**	$AgNTf_2$	rt	60	<5	nd	nd
4	**cat-25**	$AgNTf_2$	rt	15	>95	38	nd

Table 7.6 – 0.1 mmol scale; Catalyst 5 mol%, counterion 5 mol%, NBS 1.1 equiv., DCM 0.05M

We achieved full conversion for all the entries but for **cat-24**, for which we could not observe any conversion of the substrate after 1 hour. We obtained some good results in terms of yield, however we could not get any stereoselectivity data. This problem could be related to the instability of the product in chiral HPLC analysis conditions. In fact, we could not get any reproducibility of the analysis.

In order to overcome this drawback, we envisioned to functionalize the bromoallene exploiting a stereoselective reaction so that we could transfer the axial chiral information into a stereogenic center.

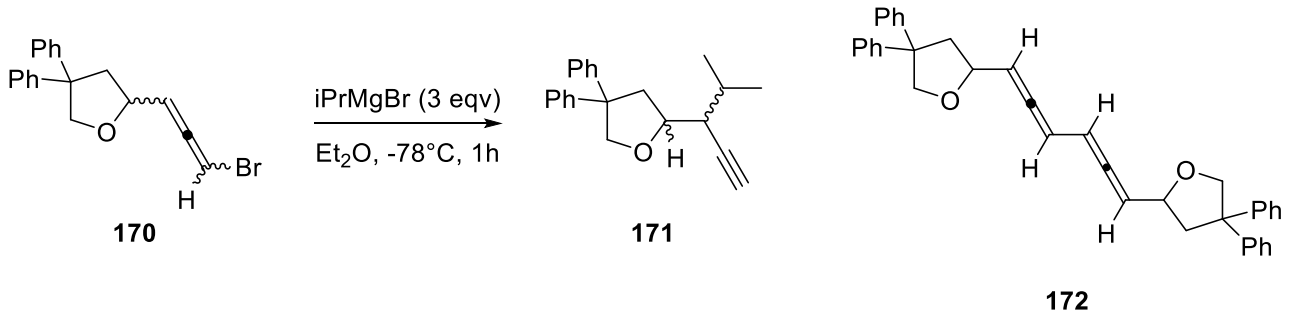

Scheme 7.14 - Functionalization attempt

We treated bromoallene **170** with Isopropyl magnesium bromide at -78°C expecting to obtain compound **171**, following a literature procedure[72], which has two stereogenic centers, one directly from the Gold(I)-catalyzed cyclization and the second one coming from the bromoallene transformation. However, the only product formed is dimer **172** coming from an *in situ* formation of the Grignard-allene reacting with another molecule of bromoallene. We decided not to investigate further because of the complexity of this product, even if it could be an interesting substrate for some cycloaddition reaction in combination with a dienophile. Moreover, we need a deeper investigation regarding the Gold(I)-catalyzed bromoetherification reaction and studies are now ongoing in our laboratories.

[72] Chemla, F.; Bernard, N.; Normant, J. *Eur. J. Org. Chem.* **1999**, 2067

8 Gold(I)-catalyzed Hydroalkoxylation of allylic alcohols

After having explored the hydroalkoxylation and the bromoetherification of ene-ynes, we envisioned a Gold(I)-catalyzed hydroalkoxylation reaction on allylic alcohols. Searching in the literature, we found Aponick's work on the Au-catalyzed cyclization of monoallylic diols, in which tetrahydropyrans are formed using $PPh_3AuCl/AgOTf$ system[73]. The proposed mechanism is shown in *Scheme 8.1*.

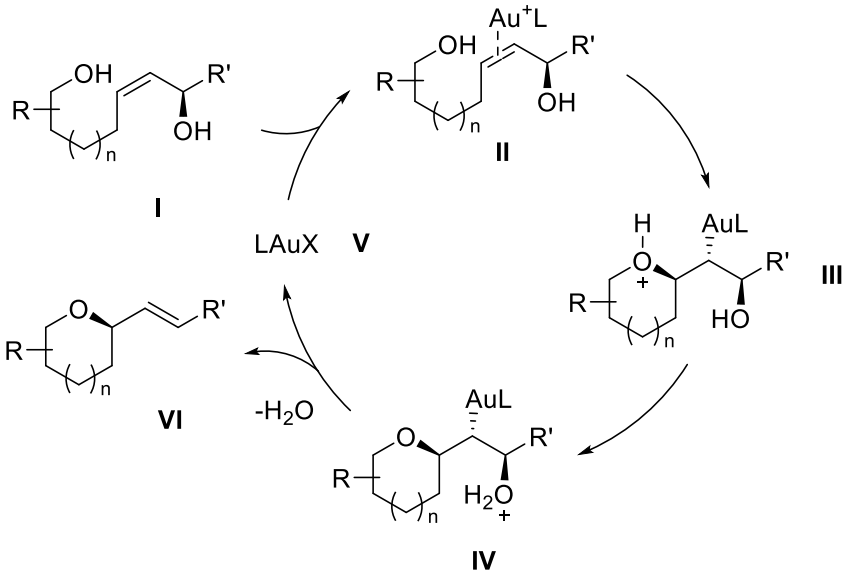

Scheme 8.1 - Aponick's proposed mechanism on Hydroalkoxylation of monoallylic diols

Gold(I)-catalyst is supposed to coordinate at the double bond, allowing the *anti*-nucleophilic attack of the furthest hydroxyl group, producing intermediate **III**. At this point, loss of water permits the de-auration step, forming the vinyl moiety on the final product **VI** and regenerating the catalyst. In this case the stereodefined allylic hydroxyl group is supposed to guide the cyclization step, selecting one of the two diastereomers of intermediate III. However, Aponick never described an enantioselective hydroalkoxylation in which the chirality transfer is mediated by a chiral Gold(I)-catalyst. For these reasons we wanted to study this reaction and to develop an enantioselective version, exploiting chiral ligands.

[73] Ghebreghiorgis, T.; Biannic, B.; Kirk, B.H.; Ess, D.H.; Aponick, A. *J. Am. Chem. Soc.* **2012**, 134, 16307

8.1 Substrate Synthesis

We envisioned a synthesis for a possible substrate. Knowing the problems we had in the past with chiral HPLC analysis, linked with the PDA detector, we decided to design a substrate with a chromophore already installed and with the least number of synthetic steps possible.

We started from the commercially available 2-allyl phenol **173** and we subjected it to a cross-metathesis reaction catalyzed by a 2nd generation Hoveyda-Grubbs catalyst in combination with ethyl acrylate. Allylic ester **174** was produced in good yield with a complete E selectivity on the double bond, as confirmed by 1H-NMR analysis.

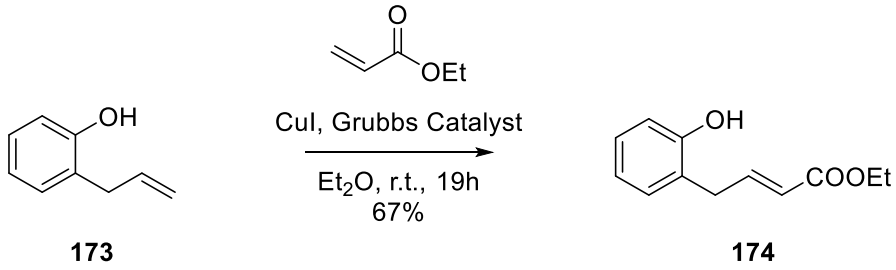

*Scheme 8.2 - Synthesis of compound **174***

Second step of this short synthesis is the reduction of the ester moiety, exploiting DIBAl-H in DCM at -78°C, producing the monoallylic diol **175**.

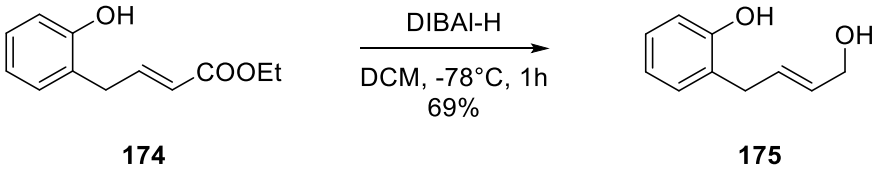

*Scheme 8.3 - Synthesis of compound **175***

8.2 Methodological study

We then begun our methodological study trying different reaction conditions, starting with 5 mol% of Gold(I)-catalyst and counterion.

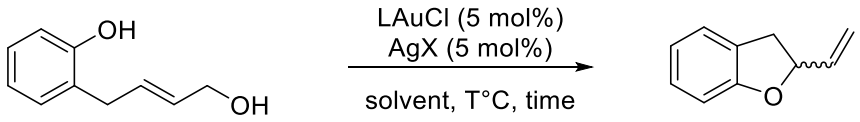

175 **176**

*Scheme 8.4 - Gold(I)-catalyzed cyclization on substrate **175***

Entry	Catalyst	Counteranion	Solvent	T	3A-MS	t(h)	Conversion (%)	176 (Y%)
1	**PPh_3AuCl**	$AgNTf_2$	DCM	rt	-	24	50	30
2	**PPh_3AuCl**	$AgNTf_2$	DCM	rt	yes	24	>95	77
3	**PPh_3AuCl**	$AgNTf_2$	Dioxane	rt	-	24	>95	>95
4	**PPh_3AuCl**	$AgNTf_2$	Dioxane	rt	yes	72	70	37
5	**PPh_3AuCl**	$AgNTf_2$	Dioxane	50	yes	72	20	21
6	**PPh_3AuCl**	AgOTs	DCM	rt	-	24	50	34
7	**PPh_3AuCl**	AgOTs	Dioxane	rt	-	8	50	31
8	**Johnphos**	AgOTs	Dioxane	rt	yes	72	>95	>95

Table 8.1 - 0.1 mmol scale; catalyst 5 mol%, counterion 5 mol%, solvent 0.05M.

Looking at results obtained in Table 8.1, we can confirm that diol **175** reacts to give the 2-vinyl benzodihydrofuran **176** in presence of a Gold(I)-catalyst. Moreover, reaction seems to be generally more efficient when molecular sieves are present in the reaction mixture. Most probably these sieves seize water coming from the deauration step, favoring the formation of new products.

We then continued our investigation with chiral catalysts following the conditions found above.

Entry	Catalyst	Counteranion	T	t(h)	Conversion (%)	176 (Y%)	ee (%)
1	**cat-17**	$NaBAr_4^F$	rt	32	10	nd	nd
2	**cat-26**	$NaBAr_4^F$	rt	32	10	nd	nd
3	**cat-26**	$AgNTf_2$	rt	24	80	77	75
4	**cat-26**	AgOTf	rt	6.5	90	>95	32
5	**cat-25**	$AgNTf_2$	rt	18	80	77	45
6	**cat-24**	$AgNTf_2$	rt	32	70	74	17
7	**cat-23**	$NaBAr_4^F$	rt	32	80	64	13

Table 8.2 - 0.1 mmol scale; catalyst 5 mol%, counterion 5 mol%, DCM 0.05M.

Cat-26 proved to be the most performing catalyst, both in yield and stereoselectivity. When used in combination with $NaBAr_4^F$ (*Table 8.2, entry 2*) it did not give satisfying results, while with a silver salt we obtained almost full conversion with high yield. $AgNTf_2$ (*entry 3*) gave the best enantiomeric excess among all the entries, even better than commercially available ligands or other similar catalysts, even

though also **cat-25** performed quite well. For these reasons we decided to continue the investigation using **cat-25** and **cat-26** in combination with $AgNTf_2$ as fixed conditions.

We then tried to change the temperature of the reaction mixture.

Entry	Catalyst	Counteranion	T	t(h)	Conversion (%)	176 (Y%)	ee (%)
1	**cat-26**	$AgNTf_2$	0	20	90	47	61
2	**cat-26**	$AgNTf_2$	-20	48	15	25	nd
3	**cat-26**	$AgNTf_2$	40	18	50	49	85
4	**cat-26**	$AgNTf_2$	60	16	>95	89	79
5	**cat-25**	$AgNTf_2$	0	22	90	84	52
6	**cat-25**	$AgNTf_2$	-20	48	15	27	nd
7	**cat-25**	$AgNTf_2$	40	5	55	50	<5

Table 8.3 - 0.1 mmol scale; catalyst 5 mol%, counterion 5 mol%, DCM 0.05M.

Initially we tried to lower the temperature with both catalysts, but we did not get any consistent improvement in yield nor in stereoselectivity. At this point we thought that maybe raising the temperature could be the trick, as it could help even more the loss of water from the system and speed up the cyclization reaction. In fact, we managed to raise up the mixture to 40°C and even 60°C and we observed a slight improvement in both yield and enantioselectivity. For these reasons we tested some other solvents in order to raise even more the temperature, without having pressure problems.

Entry	Catalyst	Counteranion	Solvent	T	t(h)	Conversion (%)	176 (Y%)	ee (%)
1	**cat-25**	$AgNTf_2$	DCE	40	18	70	11	13
2	**cat-25**	$AgNTf_2$	PhMe	40	18	70	18	65
3	**cat-25**	$AgNTf_2$	PhMe	60	16	>95	69	<5
4	**cat-26**	$AgNTf_2$	Dioxane	rt	18	<5	nd	nd
5	**cat-26**	$AgNTf_2$	PhMe	rt	16	>95	46	<5
6	**cat-26**	$AgNTf_2$	PhMe	60	16	>95	37	10

Table 8.4 - 0.1 mmol scale; catalyst 5 mol%, counterion 5 mol%, solvent 0.05M.

We tested some solvents such as dichloroethane and toluene, along with dioxane. None of these tries gave us any improvement and the best reaction conditions are the ones in Table 8.3.

Further studies are now ongoing in our lab, in order to better understand the link between enantioselectivity, solvent and temperature. Then we will produce a substrate scope to test the applicability of this transformation.

9 Conclusion

In conclusion this Ph.D. thesis discloses several strategies for the production of totally saturated heterocycles. All of these strategies are based on the powerful Gold(I)-catalysis merged with Zhang's ligand design. The directional group located on the second coordination sphere of the ligand grants access to a selective acceleration of the cyclization reaction of allenyl substrates into one prochiral allene face through general base catalysis, achieved by H-bonding with the incoming nucleophilic hydroxyl group. Thanks to these characteristics, a high level of efficiency and selectivity can be accessed, which is proved thanks to exceptional *ee* values and extremely low catalyst loading, as low as 100 ppm, already proven in 2017.

We decided to apply this designed ligand to a series of Gold(I)-catalyzed transformation, considering different nucleophiles and different π-systems.

Firstly, we managed to conclude an already begun project on the Gold(I)-catalyzed intramolecular enantioselective desymmetrization of bis-allenols (*Chapter 4*). This transformation leads to 2,4- and 2,5-substituted tetrahydrofurans in almost quantitative yields in most cases along with excellent enantiomeric excess values. On the other hand, moderate *dr* values are obtained as a consequence of poor control of the catalyst over the prochiral center present in the substrate, as can be expected.

Moreover, we managed to determine the absolute and the relative configurations of the stereogenic centers present in the 2,4-disubstituted THF core (*Chapter 4.3*). We proved that the Gold(I)-catalyzed desymmetrization allows the selective formation of *cis* products over the *trans* one. Knowing that *cis*-THFs are quite rare scaffolds and as consequence quite few methods are available in literature for their production, this transformation can be considered an innovative and efficient method in organic synthesis to build enantioselective *cis* 2,4-disubstituted THF rings. Further studies are now ongoing for the determination of the absolute and relative configuration of the 2,5-disubstituted THF cores produced with this new method.

Secondly, we investigate the heterofunctionalization of allenes with different nucleophiles, such as acids, amines and amides. Despite we could not reach the results described in the literature, it is noteworthy to point out the efficiency of the catalyst proven by the incredibly low catalyst loading (0.01 mol%). Looking at the Gold(I)-catalyzed intramolecular lactonization (*Chapter 5.1*), we performed a methodological study allowing us to better understand some mechanical feature of this reaction. Moreover, it is possible to selectively form γ-lactone or δ-lactone from the same substrate just by changing the counterion in the reaction mixture. The δ-lactone formed can be quite interesting compound as it can act as a vinyl ether, allowing several other synthetic processes, accessing late stage transformation.

As for the Gold(I)-catalyzed intramolecular hydroamination (*Chapter 5.2*), we achieved some consistent results both in yield and enantioselectivity, almost reaching the data present in the literature.

Lastly, regarding the Gold(I)-catalyzed intramolecular lactamization (*Chapter 5.3*), which at our knowledge it is an unknown transformation, we observed the formation of both γ- and δ-lactam, with a preference over the last one. Despite we could not obtain any stereoselectivity in the 5-membered ring even with chiral ligands, the 6-membered lactams are quite interesting compounds as they were not known in literature and allow the application of other transformations, increasing the molecular complexity.

Thanks to the results obtained with the Gold(I)-catalyzed heterofunctionalization of allenes, we attempt at the design of new second generation bifunctional chiral ligands (*Chapter 6*). We tried to change the directional group in order to place a stronger H-bond acceptor, however, probably for stereoelectronic issues, we could not achieve a complete synthesis. We managed, instead, to change the directional group position on the main core of the ligand, producing a new chiral Gold(I)-catalyst.

This innovative catalytic system allowed us to disclose new transformations such as the intramolecular hydroalkoxylation (*Chapter 7.1*) and the bromoetherification of ene-ynes (*Chapter 7.3*). The first reaction allowed us to obtain allene substituted THF cores in moderate to good yields with a good level of enantioselectivity. As for the bromoallene substituted THFs, we managed to isolate the desired product in good yields, however we could not observe any data regarding the stereoinduction because of the product instability in chiral HPLC analysis. Further studies are now ongoing in our laboratories in order to find an appropriate method for the detection of these compounds and to produce a substrate scope to study the applicability of the transformations.

Lastly, we begun to study the Gold(I)-catalyzed intramolecular hydroalkoxylation of monoallylic diols. We were intrigued by the fact that only two examples are reported in literature, but none of them disclose a ligand to substrate chirality transfer. We performed an optimization of the reaction conditions reaching good to excellent yields along with good enantioselectivities. Although, deeper studies are needed in order to fully investigate this transformation, especially regarding the link between enantioinduction and solvent/temperature.

To sum up, this thesis proves that gold(I) catalysis, in particular in the case of gold(I) ligand accelerative catalysis, represents a powerful and ductile tool in organic synthesis to enantioselectively build totally saturated heterocycles with an exceptionally high level of atom-economy.

10 Experimental Part

10.1 General remarks

During the execution of the experimental part of this thesis the below-listed materials and devices have been used.

For compounds characterization:

- NMR spectrometer: Varian Unity Inova 600MHz; Varian Unity Inova 500MHz; Agilent Technologies 400MHz; Bruker 300MHz; Bruker 200 MHz.

For chromatographic tecniques:

- Kieselgel 60 Merck (230-400 mesh) for standard silica gel purifications;
- Silica gel GF-254 Merck (0.25 mm) for TLCs;
- Fluorescent lamp (254 and 366 nm), vanilline solution 0.5% H_2SO_4/EtOH, solution of $KMnO_4$ in acetone for revelation of compounds in TLCs;
- Gas Chromatograph Hewlett-Packard mod. 5890 II with capillary column HP-5 (crosslinked 5% Ph-Me silicon) 25 m, 0,25 mm i.d., 0,33 μm f.t;
- Mass Spectrometer ESI-MS thermo LTQ-XL;
- MPLC Isolera One Biotage Flash Cromatography for automated preparative chromatographic purifications;
- HUPLC-MS: mass Thermo LTQ-XL; UHPLC JASCO XLC SERIES 31, pumps XLC 3080DG, column oven 3067 CO, autosampler 3159AS, column Agilent Poroshell 120 EC-18, particle size 2.7 micron, eluents H_2O-MeCN with 0.2% of HCOOH;
- Analytical HPLC: pumps JASCO PU-2080 Plus, detector diode array MD-2010 Plus, autosampler AS-2055 Plus, columns Daicel Chiralpak series;

Infrared spectra were recorded with a Perkin Elmer FT-IR spectrum 2000 spectrometer and are reported in reciprocal centimeter (cm-1);

All preparations requiring oxygen and water-free conditions have been conducted under static Argon atmosphere. Unstable substances have been handled in a glovebox under inert atmosphere. Most of the solvents have been dried through distillation over suitable drying agents under Argon atmosphere. In particular: THF, diethyl ether, and toluene from sodium/benzophenon, dichloromethane from calcium hydride. Other commercially available solvents have been employed as received, without further purification. Syringes, needles and the other glassware were dried at 140 °C for at least one night and allowed to cool in a desiccator over calcium chloride before use.

NMR spectra have been reported with chemical shift (δ, ppm) and the coupling constants (J, Hz). Signals multiplicities have been reported as: s (singlet), d (doublet), t (triplet), q (quartet), p (pentet), m (multiplet).

10.1.1 List of Abbreviations

- $(COOH{\cdot}H_2O)_2$: oxalic acid hydrate
- Ac_2O: acetic anhydride
- AcOEt: ethyl acetate
- Ag_2O: silver oxide
- Ag_2SO_4: silver sulfate
- $AgNTf_2$: silver bistriflylimide
- AgOTf: silver triflate
- AgOTs: silver tosylate
- $BF_3{\cdot}Et_2O$: boron trifluoride etherate
- Brine: aqueous saturated solution of NaCl
- BuLi: butyllithium
- CBr_4: carbon tetrabromide
- $CHCl_3$: chloroform
- $ClPPh_2$: chloro diphenylphosphine
- $CuBr{\cdot}Me_2S$: copper bromide dimethyl sulfide
- CuI: copper iodide
- DCE: dichloroethane
- DCM: dichloromethane
- DIBAl-H: di-isobutylaluminum hydride
- DIPEA: diisopropylethylamine
- dippf: di-isopropylphosphino ferrocene
- DMA: dimethylacetamide
- DMAP: 4-dimethylaminopyridine
- DMF: dimethylformamide
- DMSO: dimethylsulfoxide
- EDCI: 1-ethyl-3-(3-dimethylaminopropyl)carbodiimide
- Et_2O: diethyl ether
- Et_3SiH: triethylsilane
- EtOH: ethanol
- H_2O: water
- H_2O_2: hydrogen peroxide
- HCl: hydrochloric acid

- IBX: 2-iodoxybenzoic acid
- iPr_2NH: diisopropylamine
- iPrOH: isopropanol
- K_2CO_3: potassium carbonate
- KHMDS: potassium hexamethyldisilylamide
- KOH: potassium hydroxide
- $LiAlH_4$: lithium aluminum hydride
- $LiAl(OtBu)_3H$: lithium aluminum tri-tert-butoxy hydride
- LiHMDS: lithium hexamethyldisilylamide
- $LiOH{\cdot}H_2O$: lithium hydroxide monohydrate
- MeCN: acetonitrile
- MeI: iodomethane
- MeOH: methanol
- $MgSO_4$: magnesium sulfate
- MW: microwave
- Na_2CO_3: sodium carbonate
- $Na_2S_2O_3$: sodium thiosulfate
- $NaBAr_4^F$: sodium tetrakis[3,5-bis(trifluoromethyl)phenyl]borate
- $NaHCO_3$: sodium bicarbonate
- NaOH: sodium hydroxide
- NaOtBu: sodium tert-butoxide
- NBS: N-bromosuccinimide
- NH_4Cl: ammonium chloride
- PBr_3: phosphorous tribromide
- $Pd(OAc)_2$: palladium acetate
- $Pd(PPh_3)_2Cl_2$: palladium bis-triphenylphosphine chloride
- PPh_3: triphenylphosphine
- PPh_3AuCl: triphenylphosphine gold chloride
- TBAF: tetrabutylammonium fluoride
- TBDPSCl: tert-butyl diphenyl silyl chloride
- TBSCl: tert-butyl dimethyl silyl chloride
- THF: tetrahydrofuran
- TLC: thin layer chromatography
- $TsOH{\cdot}H_2O$: *p*-toluensulfonic acid monohydrate
- $ZrCp_2Cl_2$: zirconocene dichloride

10.2 Gold(I)-catalyzed Desymmetrization of Bisallenols

10.2.1 Substrates synthesis

10.2.1.1 Medius-based substrates synthesis

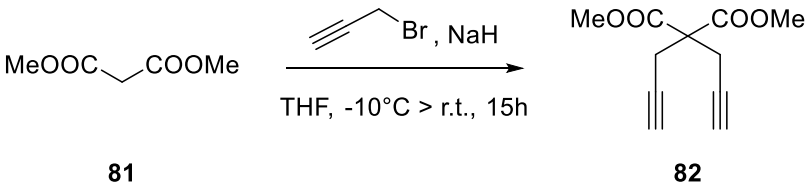

81 **82**

According to Helquist procedure[74], to a suspension of sodium hydride (60% wt in mineral oil, 63.6 mmol) in dry THF (60 mL) stirring at –10 °C, dimethyl malonate (4g, 30.3 mol) was added dropwise over 10 min. The reaction mixture was stirred at –10 °C for 5 min, and then propargyl bromide (80% wt. in toluene, 63.6 mmol) was added dropwise. The reaction mixture was warmed to 25 °C and stirred for 20 h. The reaction mixture was quenched with H_2O and Et_2O, and the layers were separated. The aqueous layer was extracted with Et_2O. The combined organic phases were dried over $MgSO_4$, filtered, and concentrated on a rotary evaporator. The product **82** was collected in quantitative yield as a light orange solid, without further purification.

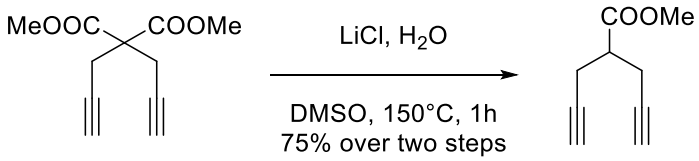

82 **83**

Compound **82** (29.6 mmol) and lithium chloride (91.9 mol) were dissolved in a solution of H_2O (74.1 mol) and DMSO (60 mL). This solution was then heated to 150°C for 1 h. After cooling, the reaction mixture was quenched with H_2O and extracted with DCM. The combined organic layers were dried over $MgSO_4$, filtered and concentrated under reduced pressure. The crude oil was purified by flash chromatography on a silica gel column using 10% Et_2O in hexanes as the eluent, to give **83** (liquid) in 75% yield in two steps;

^{1}H-NMR (300 MHz, $CDCl_3$) δ 5.07 (q, J = 6.9 Hz, 2H), 4.70 – 4.67 (m, 4H), 3.69 (s, 3H), 2.63 – 2.60 (m, 1H), 2.34 – 2.31 (m, 4H). **^{13}C-NMR (75 MHz, $CDCl_3$)** δ 208.93, 174.98, 86.85, 75.05, 51.45, 44.77, 30.08. **IR (neat)**: 3458, 3297, 2988, 2952, 1956, 1736, 1438, 1168, 847.

[74] Carney, J.M.; Donoghue, P.J.; Wuest, W.M.; Wiest, O.; Helquist, P. *Org. Lett.* **2008**, 10, 17, 3903

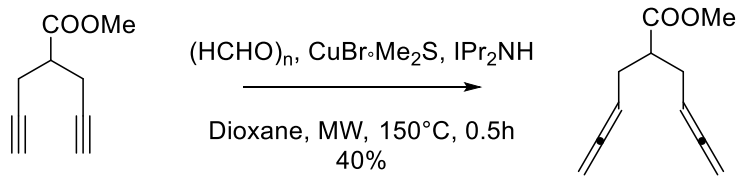

83 **84**

A solution of **83** (15.1 mmol), $CuBr{\cdot}Me_2S$ (9.03 mmol), paraformaldehyde (75.2 mmol), diisopropylamine (60.2 mmol) in anhydrous 1,4-dioxane (37 mL) was heated at 150 °C for 30 min in Microwave equipment. The crude reaction mixture was diluted with Et_2O and washed with HCl 1M. The organic phase was dried over $MgSO_4$ and evaporated under reduced pressure. The crude oil was purified by flash chromatography on a silica gel column using 5% Et_2O in hexanes as the eluent, to give **84** (liquid) in 35% yield;

^{1}H-NMR (300 MHz, $CDCl_3$) δ 5.07 (q, J = 6.9 Hz, 2H), 4.70 – 4.67 (m, 4H), 3.69 (s, 3H), 2.63 – 2.60 (m, 1H), 2.34 – 2.31 (m, 4H). **^{13}C-NMR (75 MHz, $CDCl_3$)** δ 208.93, 174.98, 86.85, 75.05, 51.45, 44.77, 30.08. **IR (neat)**: 3458, 3297, 2988, 2952, 1956, 1736, 1438, 1168, 847.

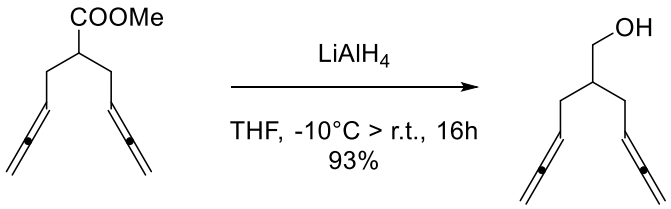

84 **79**

To a suspension of $LiAlH_4$ (6.81 mmol) in dry THF (25 mL) stirring at –10 °C, Compound **84** (4.256 mmol) was added dropwise over 10 min. The reaction mixture was warmed to r.t. and stirred for 12 h. The reaction mixture was quenched with H_2O, NaOH and H_2O and then extracted with Et_2O. The combined organic phases were dried over $MgSO_4$, filtered, and concentrated on a rotary evaporator. The crude oil was purified by flash chromatography on a silica gel column using 30% Et_2O in hexanes as the eluent, to give **79** (liquid) in 93% yield;

$_1$H-NMR (300 MHz, $CDCl_3$) δ 5.10 (p, J= 7.03Hz, 2H), 4.71 – 4.67 (m, 4H), 3.65 (d, J= 5.56, 2H), 2.15 – 2.09 (m, 4H), 1.82 – 1.74 (m, 1H). **^{13}C-NMR (75 MHz, $CDCl_3$)** δ 208.98, 87.51, 74.47, 64.77, 40.53, 29.59. IR (neat): 3339, 2919, 1955, 1438, 1031, 842.

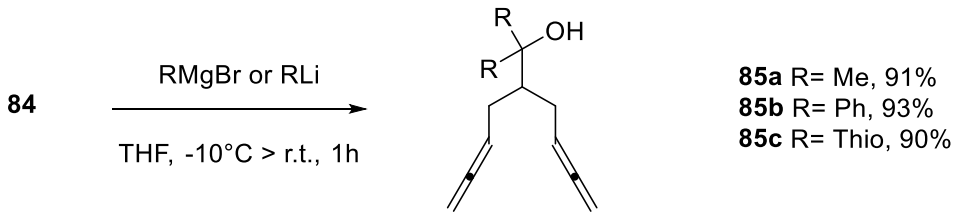

In a flamed dried flask, under Ar atmosphere, methylmagnesium bromide (3.0M in Et_2O, 1.788 mmol) was suspended in dry Et_2O (5 mL). The reaction mixture was cooled down to -40 °C and compound **84** (0.851 mmol) was added. After stirring for 1 hour, the reaction mixture was warmed to r.t. and stirred for 30 minutes. The reaction mixture was quenched with a saturated solution of NH_4Cl and then extracted with Et_2O. The combined organic phases were dried over $MgSO_4$, filtered, and concentrated on a rotary evaporator. The crude oil was purified by flash chromatography on a silica gel column using 20% Et_2O in hexanes as the eluent to give **85a** (liquid) in 91% yield;

^{1}H-NMR (300 MHz, $CDCl_3$) δ 5.20 – 5.15 (m, 2H), 4.72 – 4.68 (m, 4H), 2.32 – 2.27 (m, 2H), 2.09 – 2.04 (m, 2H), 1.66 – 1.62 (m, 1H), 1.54 (s, 1H), 1.24 (s, 6H). **^{13}C-NMR (75 MHz, $CDCl_3$)** δ 208.77, 89.25, 74.66, 73.56, 48.47, 28.84, 27.60. **IR (neat):** 3339, 2919, 1955, 1438, 1031, 842.

Compound **85b** was prepared in a similar way using phenylmagnesium bromide (93% yield); **^{1}H-NMR (300 MHz, $CDCl_3$)** δ 7.54 (dd, J = 1.23 Hz, 8.55 Hz, 4H), 7.34 (t, J = 7.88 Hz, 4H), 7.24 – 7.19 (m, 2H), 5.19 – 5.12 (m, 2H), 4.71 – 4.67 (m, 4H), 2.93 – 2.89 (m, 1H), 2.61 (s, 1H), 2.36 – 2.28 (m, 2H), 2.19 – 2.11 (m, 2H). **^{13}C-NMR (75 MHz, $CDCl_3$)** δ 208.83, 146.40, 128.17, 126.44, 125.41, 88.37, 81.52, 74.72, 45.08, 28.05. **IR (neat):** 3539, 3058, 1953, 1725, 1492, 1447, 1160, 843, 703.

Compound **85c** was prepared in a similar way using 2-thienyllithium (90% yield); **^{1}H-NMR (300 MHz, $CDCl_3$)** δ 7.24 (d, J= 4.9 Hz, 1H), 7.05 (d, J= 3.18 Hz, 1H), 7.00 – 6.97 (m, 1H), 5.13 (p, J= 7.4 Hz, 2H), 4.70 – 4.68 (m, 4H), 3.17 (s, 1H), 2.62 – 2.58 (m, 1H), 2.42 – 2.34 (m, 2H), 2.23 – 2.15 (m, 2H). **^{13}C-NMR (75 MHz, $CDCl_3$)** δ 209.27, 143.86, 140.02, 126.71, 126.48, 125.44, 88.12, 75.32, 32.37, 28.52. **IR (neat):** 3528, 3014, 2923, 1953, 1435, 1229, 846, 699.

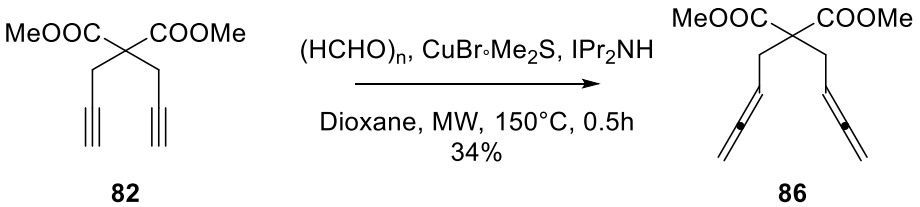

Compound **86** was prepared in a similar way as compound **84** starting from compound **82** (34% yield); **^{1}H-NMR (300 MHz, $CDCl_3$)** δ 5.01 – 4.93 (m, 2H), 4.70 – 4.67 (m, 4H), 3.74 (s, 6H), 2.69 – 2.65 (m, 4H). **^{13}C-NMR (75 MHz, $CDCl_3$)** δ 209.97, 170.79, 83.93, 74.52, 57.75, 52.34, 31.79. **IR (neat):** 2843, 1956, 1736, 1438, 1207, 846.

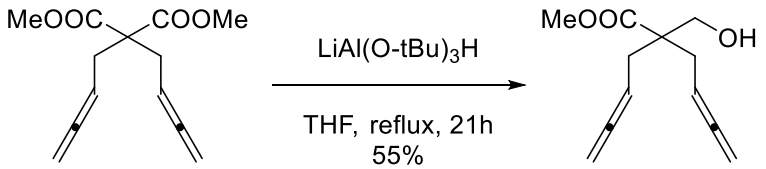

86 **87**

To a suspension of $LiAl(O\text{-}tBu)_3H$ (1.1 M in THF, 1.6 mmol) in dry THF (2.5 mL) stirring at –10 °C, Compound **86** (0.604 mmol) was added dropwise over 10 min. The reaction mixture was warmed to reflux and stirred for 12 h. After cooling, the reaction mixture was quenched with H_2O, NaOH 10% and H_2O and then extracted with Et_2O. The combined organic phases were dried over $MgSO_4$, filtered, and concentrated on a rotary evaporator. The crude oil was purified by flash chromatography on a silica gel column using 30% Et_2O in hexanes as the eluent, to give **87** (liquid) in 55% yield;

^{1}H-NMR (300 MHz, $CDCl_3$) δ 5.09 – 5.01 (m, 2H), 4.71 – 4.67 (m, 4H), 3.77 (s, 2H), 3.75 (s, 3H), 2.43 – 2.33 (m, 4H), 2.18 (m, 1H). **^{13}C-NMR (75 MHz, $CDCl_3$)** δ 209.72, 175.51, 84.60, 74.36, 64.86, 51.77, 51.64, 32.26. **IR (neat):** 3468, 2951, 1955, 1728, 1439, 1203, 1042, 844.

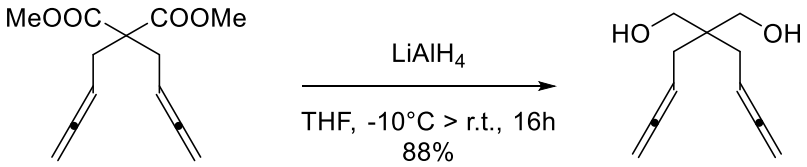

86 **88**

Compound **88** was prepared in a similar way as compound **79** starting from compound **86** (88% yield); **^{1}H-NMR (300 MHz, $CDCl_3$)** δ 5.13 – 5.05 (m, 2H), 4.71 – 4.68 (m, 4H), 3.65 – 3.64 (m, 4H), 2.13 – 2.07 (m, 6H). **^{13}C-NMR (75 MHz, $CDCl_3$)** δ 209.59, 84.74, 74.07, 67.76, 42.86, 30.60. **IR (neat)**: 3356, 2985, 1954, 1439, 1036, 842.

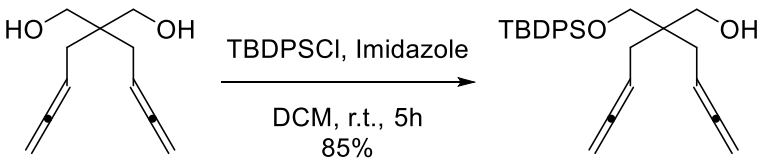

88 **89**

To a solution of **88** (2.63 mmol) in DCM (20 mL) were added TBDPSCl (2.89 mmol) and imidazole (2.89 mmol). The reaction was stirred overnight before the reaction was quenched with water. The mixture was extracted with DCM. The combined organic layer was dried over $MgSO_4$ and concentrated under

reduced pressure. The residue was purified by flash column chromatography using 10% AcOEt in hexanes as the eluent to give **89** (liquid) in 85% yield;

^{1}H-NMR (300 MHz, $CDCl_3$) δ 7.70 – 7.67 (m, 4H), 7.48 – 7.40 (m, 6H), 5.04 – 4.98 (m, 2H), 4.63 – 4.60 (m, 4H), 3.61 – 3.57(m, 4H), 2.09 – 2.06 (m, 4H), 1.56 (s, 1H), 1.10 (s, 9H). **^{13}C-NMR (75 MHz, $CDCl_3$)** δ 209.62, 135.54, 134.68, 132.85, 129.77, 127.69, 127.60, 84.80, 73.86, 67.65, 66.76, 43.37, 30.42, 26.82, 26.44, 19.15. **IR (neat):** 3354, 2930, 2857, 1954, 1428, 1112, 823, 702.

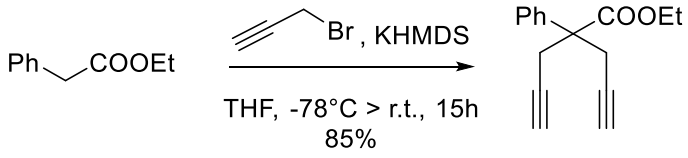

90a **91a**

To a solution of KHMDS (53.7 mmol) in dry THF (60 mL), in a flame dried flask, was added ethyl phenylacetate (24.4 mmol) at -78°C. After 1 hour, propargyl bromide (53.7 mmol) was added and the reaction was warmed to r.t. and stirred overnight. The reaction mixture was quenched with a saturated solution of NH_4Cl and then extracted with Et_2O. The combined organic phases were dried over $MgSO_4$, filtered, and concentrated on a rotary evaporator. The crude oil was purified by flash chromatography on a silica gel column using 20% Et_2O in hexanes as the eluent, to give **91a** (liquid) in 85% yield;

^{1}H-NMR (300 MHz, $CDCl_3$) δ 7.41 – 7.31 (m, 5H), 4.21 (q, J = 7.1 Hz, 2H), 3.16 (qd, J= 16.67 Hz, 2.59 Hz, 4H), 2.01 – 1.98 (m, 2H), 1.24 (t, J = 10.7 Hz, 3H). **^{13}C-NMR (75 MHz, $CDCl_3$)** δ 172.81, 139.30, 128.38, 127.49, 125.95, 79.94, 71.17, 61.45, 52.80, 25.33, 13.84. **IR (neat):** 3292, 3029, 1730, 1448, 1209, 1062, 698, 645.

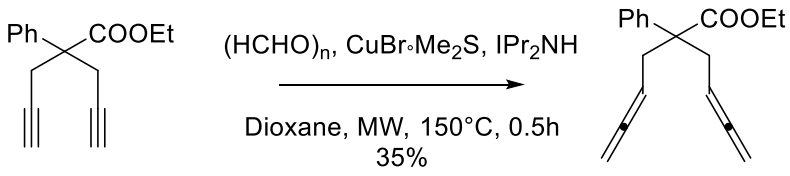

91a **92a**

Compound **92a** was prepared in a similar way as compound **84** starting from compound **91a** (35% yield); **^{1}H-NMR (300 MHz, $CDCl_3$)** δ 7.33 – 7.29 (m, 5H), 4.86 – 4.82 (m, 2H), 4.63 – 4.60 (m, 4H), 4.16 (q, J = 7.1 Hz, 2H), 2.83 – 2.80 (m, 4H), 1.21 (t, J = 7.1 Hz, 3H). **^{13}C-NMR (75 MHz, $CDCl_3$)** δ 209.91, 174.48, 141.16, 128.22, 126.81, 126.37, 84.78, 74.02, 60.81, 53.77, 34.13, 13.96. **IR (neat):** 3029, 1955, 1732, 1449, 1208, 1059, 697, 643.

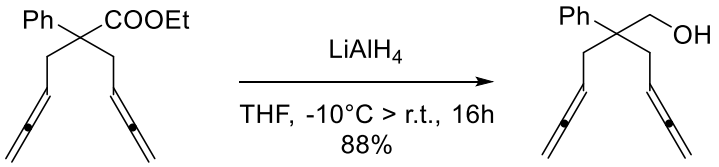

92a **93a**

Compound **93a** was prepared in a similar way as compound **79** starting from compound **92a** (88% yield); **^{1}H-NMR (300 MHz, $CDCl_3$)** δ 7.38 – 7.34 (m, 5H), 4.94 – 4.90 (m, 2H), 4.65 – 4.61 (m, 4H), 3.86 (d, J = 6.45 Hz, 2H), 2.55 – 2.52 (m, 4H), 1.39 – 1.37 (m, 1H). **^{13}C-NMR (75 MHz, $CDCl_3$)** δ 209.54, 142.69, 128.40, 126.79, 126.38, 85.20, 73.95, 67.60, 46.48, 34.34**. IR (neat):** 3406, 2985, 1954, 1444, 1038, 841, 700.

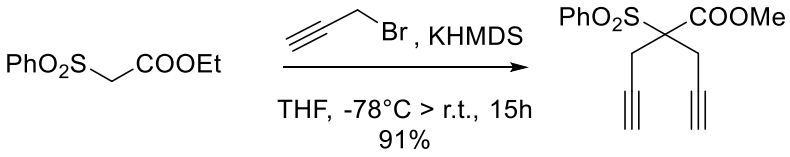

90b **91b**

Compound **91b** was prepared in a similar way as compound **91a** starting from methyl phenylsulfonylacetate (91% yield); **^{1}H-NMR (300 MHz, $CDCl_3$)** δ 7.93 – 7.90 (m, 2H), 7.76 – 7.72 (m, 1H), 7.63 – 7.58 (m, 2H), 3.75 – 3.73 (m, 3H), 3.18 (m, 4H), 2.11 – 2.09 (m, 2H). **^{13}C-NMR (75 MHz, $CDCl_3$)** δ 166.32, 135.28, 134.68, 134.56, 130.24, 129.17, 129.14, 128.92, 77.02, 73.10, 72.27, 69.00, 53.44, 21.29, 17.15. **IR (neat):** 3285, 1739, 1437, 1272, 1151, 1083, 688, 544.

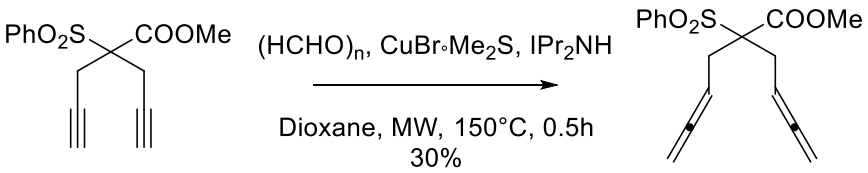

91b **92b**

Compound **92b** was prepared in a similar way as compound **84** starting from compound **91b** (30% yield); **^{1}H-NMR (300 MHz, $CDCl_3$)** δ 7.87 – 7.84 (m, 2H), 7.71 – 7.68 (m, 1H), 7.61 – 7.56 (m, 2H), 5.24 – 5.20 (m, 2H), 4.74 – 4.71 (m, 4H), 3.66 (s, 3H), 2.99 – 2.86 (m, 4H). **^{13}C-NMR (75 MHz, $CDCl_3$)** δ 210.13, 167.49, 134.19, 130.29, 130.24, 128.68, 83.70, 77.09, 75.03, 52.69, 29.73. **IR (neat):** 1958, 1735, 1447, 1309, 1147, 988, 851, 690.

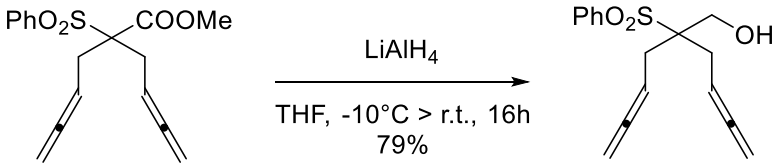

92b **93b**

Compound **93b** was prepared in a similar way as compound **79** starting from compound **93b** (79% yield); **^{1}H-NMR (300 MHz, $CDCl_3$)** δ 7.95 – 7.92 (m, 2H), 7.75 – 7.70 (m, 1H), 7.64 – 7.59 (m, 2H), 5.22 – 5.14 (m, 2H), 4.73 – 4.70 (m, 4H), 3.83 (s, 2H), 3.00 (s, 1H), 2.60 – 2.40 (m, 4H). **^{13}C-NMR (75 MHz, $CDCl_3$)** δ 210.05, 135.43, 134.20, 130.09, 129.02, 83.34, 74.97, 68.47, 63.02, 29.17. **IR (neat):** 3516, 1956, 1446, 1289, 1140, 848, 729, 691.

10.2.1.2 Remotus-based substrates synthesis

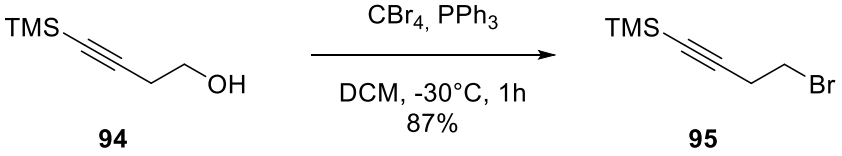

94 **95**

To a solution of 4-Trimethylsilyl-3-butyn-1-ol (3.8 g, 26.8 mmol) in dry DCM (25 mL) under argon atmosphere was added at -30 °C CBr_4 (43.03 mmol). The mixture was stirred at the same temperature for 10 min before adding a solution of PPh_3 (32.2 mmol) in DCM (25 mL). The mixture was allowed to stir at -30 °C for 2 h and then at room temperature for 2 h. Upon completion confirmed by TLC the mixture was diluted with hexanes and the solid residue was filtered off through a silica gel pad. The resulting solution was concentrated under reduced pressure. The residue was purified by flash column chromatography with hexanes (100%) to give **95** (liquid) in 87% yield;

^{1}H-NMR (300 MHz, $CDCl_3$) δ 3.45 (t, J= 7.5Hz, 2H), 2.79 (t, J= 7.5Hz, 2H), 0.18 (s, 9H). **^{13}C-NMR (75 MHz, $CDCl_3$)** δ 103.06, 80.90, 29.04, 24.17, -0.17. **IR (neat):** 3022, 2408, 1499, 1476, 1098, 777.

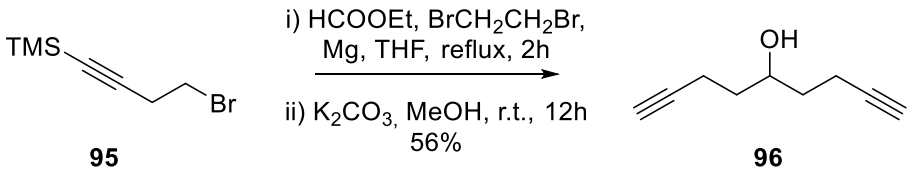

95 **96**

In a flamed dried flask equipped with condenser and septum was added magnesium turnings (14.6 mmol) in anhydrous THF (10 mL). A small portion of 1,2-dibromoethane (1.95 mmol) was added and

heated at reflux for 2 min to initiate the reaction. Afterwards a solution of **95** (2.0 g, 9.74 mmol) in anhydrous THF (10 mL) was added slowly and the mixture was heated to a gentle reflux for 1 h. The reaction mixture was cooled to 0 °C, ethyl formate (5.36 mmol) was added dropwise and the mixture was allowed to stir at room temperature for 1 h. The reaction mixture was quenched with a saturated solution of NH_4Cl and extracted three times with Et_2O. The combined organic layer was dried over $MgSO_4$ and concentrated under reduced pressure. The residue was recovered with MeOH (20 mL) and K_2CO_3 (29.22 mmol) was added. The mixture was stirred at room temperature for 12 h. Upon completion confirmed by TLC, the mixture was diluted with diethyl ether and the solid residue was filtered off through a silica gel pad and concentrated on a rotary evaporator. The crude oil was purified by flash chromatography on a silica gel column using 20% Et_2O in hexanes as the eluent, to give **96** (liquid) in 56% yield;

^{1}H-NMR (300 MHz, $CDCl_3$) δ 3.75 (p, J= 7.12 Hz, 1H), 2.27 – 2.18 (m, 4H), 1.99-1.97 (m, 2H), 1.75 – 1.70 (m, 4H). **^{13}C-NMR (75 MHz, $CDCl_3$)** δ 83.74, 69.54, 68.19, 34.85, 25.69, 17.87, 14.38. **IR (neat):** 3314, 3296, 2943, 2867, 1456, 1433, 1094, 983, 634.

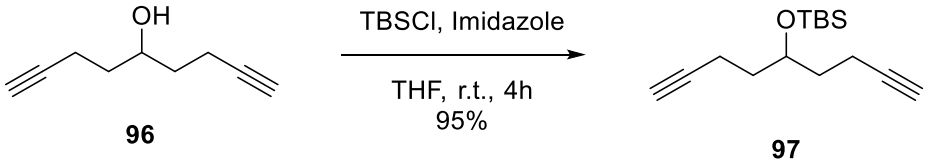

96 **97**

To a solution of **96** (358 mg, 2.63 mmol) in THF (20 mL) were added TBSCl (2.89 mmol) and imidazole (2.89 mmol). The reaction was stirred overnight before the reaction was quenched with water. The mixture was extracted with DCM. The combined organic layer was dried over $MgSO_4$ and concentrated under reduced pressure. The residue was purified by flash column chromatography with 10% AcOEt in hexanes to give **97** (liquid) in 95% yield;

^{1}H-NMR (300 MHz, $CDCl_3$) δ 3.74 (p, J= 7.08 Hz, 1H), 2.30 – 2.19 (m, 4H), 1.97-1.96 (m, 2H), 1.73 – 1.68 (m, 4H), 0.91 (s, 9H), 0.10 (s, 6H). **^{13}C-NMR (75 MHz, $CDCl_3$)** δ 84.19, 69.30, 68.27, 35.34, 25.74, 17.92, 14.21, -4.65. **IR (neat):** 3310, 2953, 2931, 2898, 1472, 1327, 1098, 1029, 836, 775, 631.

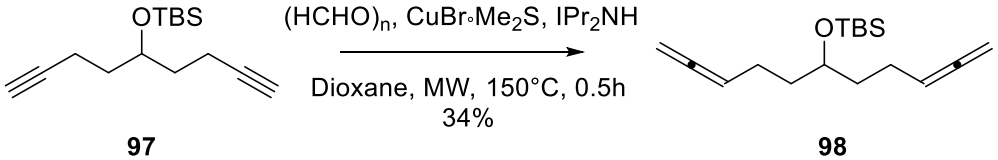

97 **98**

Compound **98** was prepared in a similar way as compound **84** starting from compound **98** (34% yield); **^{1}H-NMR (300 MHz, $CDCl_3$)** δ 5.13 (p, J= 6.67 Hz, 2H), 4.71 – 4.67 (m, 4H), 3.78 (p, J= 5.78, 1H), 2.10 –

2.01 (m, 4H), 1.62 – 1.55 (m, 4H), 0.91 (s, 9H), 0.07 (s, 6H). **^{13}C-NMR (75 MHz, $CDCl_3$)** δ 208.34, 89.88, 74.91, 70.74, 36.08, 25.81, 23.73, 17.99, -4.53. **IR (neat):** 2953, 2932, 2899, 1956, 1472, 1328, 1097, 1029, 835, 775, 630.

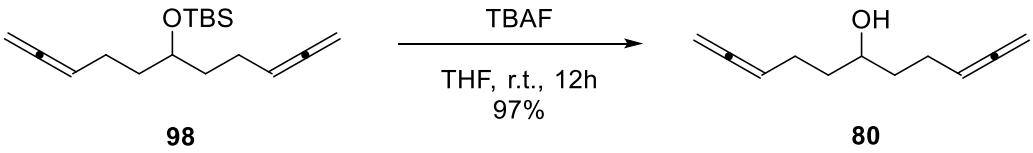

98 **80**

In a flamed dried flask under Argon atmosphere **98** (788 mg, 2.83 mmol) was dissolved in dry THF (10 mL). The mixture was cooled to 0 °C before adding TBAF (1 M in THF, 5.68 mmol) dropwise. The mixture was allowed to stir at room temperature for 12 h. The reaction mixture was quenched with phosphate buffer and the aqueous phase was extracted with Et_2O three times. The combined organic layer was dried over $MgSO_4$ and concentrated under reduced pressure. The residue was purified by flash column chromatography with 20% diethyl ether in hexanes to give **80** (liquid) in 97% yield.

^{1}H-NMR (300 MHz, $CDCl_3$) δ 5.16 (p, J= 6.67 Hz, 2H), 4.73 – 4.68 (m, 4H), 3.75 – 3.74 (m, 1H), 2.19 – 2.10 (m, 4H), 1.65 – 1.56 (m, 4H). **^{13}C-NMR (75 MHz, $CDCl_3$)** δ 208.37, 89.53, 75.04, 70.59, 36.38, 24.25. **IR (neat):** 3338, 2917, 1956, 1437, 1031, 841.

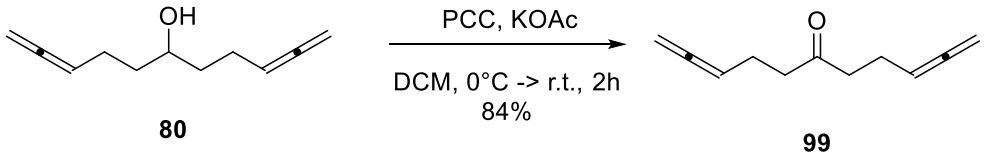

80 **99**

In a flamed dried flask, under Ar atmosphere, pyridinium chlorochromate (5.02 mmol) and potassium acetate (0.50 mmol) were dissolved in anhydrous DCM (7 mL). The reaction mixture was cooled down to 0°C and compound **80** (3.35 mmol) was added. The reaction mixture was then warmed to r.t. and stirred until completion confirmed by TLC. The mixture was filtered on a celite pad washing with DCM and the filtrate was concentrated on a rotary evaporator. The crude oil was purified by flash chromatography on a silica gel column using 10% Et_2O in hexanes as the eluent, to give **99** (liquid) in 84% yield; **^{1}H-NMR (300 MHz, $CDCl_3$)** δ 5.17 (p, J= 6.5 Hz, 2H), 4.74 – 4.69 (m, 4H), 2.57 (t, J= 7.16 Hz, 4H), 2.33 – 2.25 (m, 4H). **^{13}C-NMR (75 MHz, $CDCl_3$)** δ 209.06, 208.19, 88.97, 75.84, 53.32, 41.37, 21.74. **IR (neat):** 2921, 1956, 1715, 1434, 1410, 1369, 1091, 847.

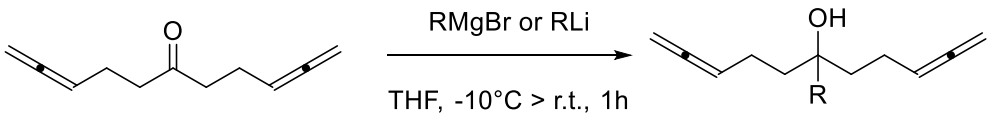

99

100a, R= Me, 93%
100b, R= Ph, 96%
100c, R= Bn, 92%
100d, R= 4-OMe-C_6H_4, 96%
100e, R= 4-Cl-C_6H_4, 94%
100f, R= 4-Me-C_6H_4, 93%
100g, R= 3-OMe-C_6H_4, 95%

In a flamed dried flask, under Ar atmosphere, methylmagnesium bromide (3 M in Et_2O, 1.35 mmol) was suspended in dry Et_2O (7 mL). The reaction mixture was cooled down to -40 °C and compound **99** (1.24 mmol) was added. After stirring for 1 hour, the reaction mixture was warmed to r.t. and stirred for 30 minutes. The reaction mixture was quenched with a saturated solution of NH_4Cl and then extracted with Et_2O. The combined organic phases were dried over $MgSO_4$, filtered, and concentrated on a rotary evaporator. The crude oil was purified by flash chromatography on a silica gel column using 20% Et_2O in hexanes as the eluent, to give **100a** (liquid) in 84% yield; **^{1}H-NMR (300 MHz, $CDCl_3$)** δ 5.18 (p, J= 6.64 Hz, 2H), 4.73 – 4.69 (m, 4H), 2.13 – 2.05 (m, 4H), 1.64 – 1.59 (m, 4H), 1.28 (s, 1H), 1.22 (s, 3H). **^{13}C-NMR (75 MHz, $CDCl_3$)** δ 208.22, 90.00, 75.20, 72.34, 40.76, 26.63, 22.57. **IR (neat):** 2920, 1955, 1716, 1434, 1410, 1368, 1091, 845.

Compound **100b** was prepared in a similar way using phenylmagnesium bromide (74% yield); **^{1}H-NMR (300 MHz, $CDCl_3$)** δ 7.42 – 7.23 (m, 5H), 5.12 – 5.06 (m, 2H), 4.69 – 4.65 (m, 4H), 2.06 – 1.99 (m, 4H), 1.86 (s, 1H), 1.85 – 1.77 (m, 4H). **^{13}C-NMR (75 MHz, $CDCl_3$)** δ 208.14, 145.25, 128.07, 126.38, 125.09, 89.87, 76.79, 75.26, 41.96, 22.15. **IR (neat):** 2921, 1955, 1716, 1457, 1434, 1410, 1368, 1091, 845, 658.

Compound **100c** was prepared in a similar way using benzylmagnesium chloride (81% yield); **^{1}H-NMR (300 MHz, $CDCl_3$)** δ 7.37 – 7.22 (m, 5H), 5.20 – 5.12 (m, 2H), 4.72 – 4.68 (m, 4H), 2.80 (s, 2H), 2.17 – 2.09 (m, 4H), 1.62 – 1.56 (m, 4H), 1.44 (s, 1H). **^{13}C-NMR (75 MHz, $CDCl_3$)** δ 208.24, 136.80, 130.48, 128.19, 126.47, 89.93, 75.24, 73.74, 45.44, 37.58, 22.43. **IR (neat):** 2922, 1955, 1714, 1457, 1431, 1410, 1364, 1091, 847, 655.

Compound **100d** was prepared in a similar way using 4-methoxyphenylmagnesium bromide (69% yield); **^{1}H-NMR (300 MHz, $CDCl_3$)** δ 7.31 – 7.27 (m, 2H), 6.90 – 6.84 (m, 2H), 5.21 – 5.07 (m, 2H), 4.76 – 4.64 (m, 4H), 3.82 (s, 3H), 2.03 – 1.78 (m, 9H). **^{13}C-NMR (75 MHz, $CDCl_3$)** δ 208.05, 141.06, 136.45, 128.72, 114.88, 90.72, 90.35, 76.74, 76.58, 43.36, 23.59. **IR (neat):** 2923, 1956, 1715, 1457, 1448, 1425, 1410, 1369, 1093, 847, 658.

Compound **100e** was prepared in a similar way using 4-chlorophenylmagnesium bromide (83% yield); **^{1}H-NMR (300 MHz, $CDCl_3$)** δ 7.34 – 7.33 (m, 4H), 5.11 – 5.05 (m, 2H), 4.69 – 4.66 (m, 4H), 2.00 – 1.82

(m, 9H). **^{13}C-NMR (75 MHz, $CDCl_3$)** δ 209.58, 145.23, 133.63, 129.61, 128.11, 91.11, 78.02, 76.80, 43.39, 23.50. **IR (neat):** 2922, 1955, 1714, 1457, 1431, 1410, 1364, 1091, 847, 655.

Compound **100f** was prepared in a similar way using *p*-tolylmagnesium bromide (78% yield); **^{1}H-NMR (300 MHz, $CDCl_3$)** δ 7.27 (d, J = 8.1 Hz, 2H), 7.17 (d, J = 8.1 Hz, 2H), 5.12 – 5.06 (m, 2H), 4.68 – 4.65 (m, 4H), 2.36 (s, 3H), 2.03 – 1.75 (m, 9H). **^{13}C-NMR (75 MHz, $CDCl_3$)** δ 208.15, 142.26, 135.87, 128.77, 125.00, 89.90, 76.69, 75.20, 41.92, 22.17, 20.84. **IR (neat):** 2922, 1953, 1714, 1457, 1431, 1415, 1364, 1090, 845, 655.

Compound **100g** was prepared in a similar way using 3-methoxyphenylmagnesium bromide (80% yield); **^{1}H-NMR (300 MHz, $CDCl_3$)** δ 7.31 – 7.25 (m, 1H), 6.99 – 6.93 (m, 2H), 6.81 – 6.78 (m, 1H), 5.12 – 5.06 (m, 2H), 4.69 – 4.65 (m, 4H), 3.84 (s, 3H), 2.04 – 1.77 (m, 9H). **^{13}C-NMR (75 MHz, $CDCl_3$)** δ 208.16, 159.50, 147.15, 129.07, 117.52, 111.46, 111.27, 89.86, 76.79, 75.24, 55.09, 41.94, 22.14. **IR (neat):** 2923, 1955, 1719, 1457, 1410, 1364, 1091, 847, 656.

10.2.2 Au(I)-catalyzed asymmetric intramolecular cyclization

General Procedure A for Au(I)-catalyzed cyclization:

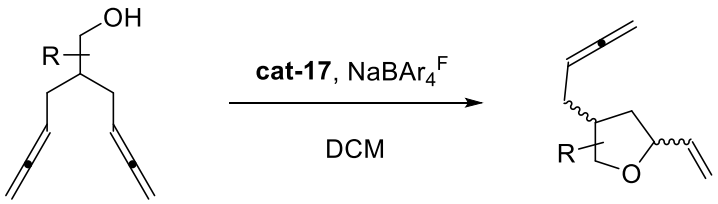

To a 3-dram vial were added an indicated volume (18.3 μL for 100 ppm) of **cat-17** solution (1 mg/mL in DCM) and 0.001 mmol $NaBAr_4^F$ (0.5 mol %) in 2 mL anhydrous DCM as solvent. The mixture was stirred at r.t. for 15 min. Then 0.2 mmol of bisallenyl alcohol were added and the reaction was cooled to -30°C and stirred at the same temperature monitoring by TLC. Upon completion, the reaction was concentrated under reduced pressure. The residue was purified by silica gel flash column chromatography to obtain pure product.

General procedure B for Au(I)-catalyzed cyclization:

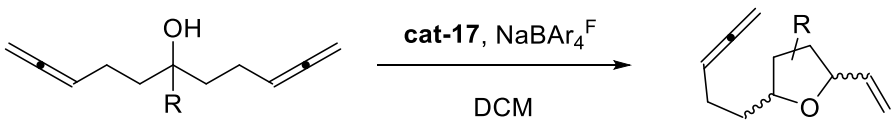

To a 3-dram vial were added an indicated volume (18.3 μL for 100 ppm) of **cat-17** solution (1 mg/mL in DCM) and 0.001 mmol $NaBAr_4^F$ (0.5 mol %) in 2 mL anhydrous DCM as solvent. The mixture was stirred at r.t. for 15 min. Then 0.2 mmol of bisallenyl alcohol were added and the reaction was stirred at the same temperature monitoring by TLC. Upon completion, the reaction was concentrated under

reduced pressure. The residue was purified by silica gel flash column chromatography to obtain pure product.

General procedure C for Au(I)-catalyzed functionalization of products:

A mixture of 1,3-bis(2,6-diisopropylphenyl)imidazole-2-yilideneAu(I)Cl (5 mol %) and AgOTf (5 mol %) in toluene (0.2 M) was stirred at room temperature for 5 min, treated with a solution of substrate (cyclized product, 1 equiv) and 3-phenyl-1-propanol (1.1 equiv) in toluene (0.2 M). The resulting suspension was stirred at room temperature for 2 h. Upon completion indicated by TLC, the reaction was concentrated under reduced pressure. The residue was purified through silica gel flash column chromatography to obtain pure product.

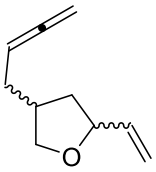

Compound **101** (liquid) was prepared in 99% yield using General Procedure A. Purification by silica gel flash column chromatography with 5% diethyl ether in hexanes. **^{1}H-NMR (300 MHz, $CDCl_3$)** δ 5.87 – 5.73 (m, 1H), 5.26 – 5.04 (m, 2H), 5.10 – 5.02 (m, 1H), 4.72 – 4.68 (m, 2H), 4.36 – 4.21 (m, 1H), 4.08 – 3.93 (m, 1H), 3.59 – 3.47 (m, 1H), 2.48 – 2.22 (m, 2H), 2.16 – 2.08 (m, 1H), 1.46 – 1.29 (m, 2H). **^{13}C-NMR (75 MHz, $CDCl_3$)** δ 208.77, 139.07, 138.97, 115.30, 114.83, 88.26, 88.19, 80.51, 79.21, 74.94, 74.93, 72.99, 72.78, 39.63, 38.82, 38.48, 37.72, 32.25, 31.95. **IR (neat):** 2837, 1964, 1438, 1426, 1207, 843, 636.

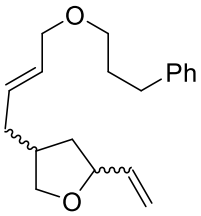

Compound **101-funz** (liquid) was prepared in 69% yield using General Procedure C. Purification by silica gel flash column chromatography with 10% diethyl ether in hexanes **^{1}H-NMR (300 MHz, $CDCl_3$)** δ 7.33 – 7.18 (m, 5H), 5.90 – 5.84 (m, 1H), 5.68 – 5.63 (m, 2H), 5.30 – 5.24 (m, 1H), 5.14 – 5.09 (m, 1H), 4.47 – 4.29 (m, 1H), 4.06 – 3.91 (m, 3H), 3.57 – 3.42 (m, 3H), 2.72 (t, J = 7.4 Hz, 2H), 2.38 – 2.16 (m, 3H), 1.98 – 1.81 (m, 3H), 1.35 – 1.29 (m, 1H). **^{13}C-NMR (75 MHz, $CDCl_3$)** δ 141.86, 139.13, 138.99, 131.72, 131.68, 128.35, 128.19, 128.07, 127.98, 125.65, 115.28, 114.79, 80.54, 79.20, 73.01, 72.80, 71.20, 69.23, 69.20, 39.59, 38.80, 38.31, 37.64, 36.10, 35.79, 32.27, 31.18. **IR (neat):** 2995, 2942, 1435, 1429, 1204, 842, 633.

dr 74:26; ee_{cis} % = 91%; ee_{trans} % = 96%;

Compound **101a** (liquid) was prepared in 96% yield using General Procedure A. Purification by silica gel flash column chromatography with 5% diethyl ether in hexanes. **^{1}H-NMR (300 MHz, $CDCl_3$)** δ 5.85 – 5.71 (m, 1H), 5.26 – 5.21 (m, 1H), 5.13 – 5.06 (m, 2H), 4.71 – 4.59 (m, 2H), 4.37 – 4.32 (m, 1H), 2.28 – 2.17 (m, 1H), 2.13 – 1.95 (m, 2H), 1.48 – 1.36 (m, 2H), 1.31 (s, 3H), 1.09 (s, 3H). **^{13}C-NMR (75 MHz,**

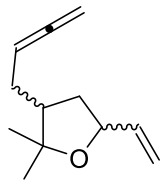

$CDCl_3$) δ 208.64, 140.20, 127.75, 114.94, 114.11, 88.68, 82.00, 77.99, 77.54, 77.02, 76.89, 74.86, 49.09, 47.06, 38.90, 37.58, 29.25, 29.15, 28.22, 24.15. **IR (neat):** 2839, 1964, 1437, 1424, 1207, 843, 636.

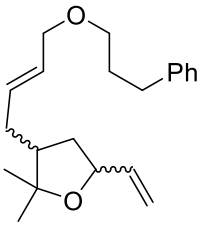

Compound **101a-funz** (liquid) was prepared in 67% yield using General Procedure C. Purification by silica gel flash column chromatography with 10% diethyl ether in hexanes. **^{1}H-NMR (300 MHz, $CDCl_3$)** δ 7.33 – 7.21 (m, 5H), 5.89 – 5.82 (m, 1H), 5.67 – 5.63 (m, 2H), 5.26 – 5.20 (m, 1H), 5.10 – 5.06 (m, 1H), 4.38 – 4.31 (m, 1H), 3.94 (d, J = 4.6 Hz, 2H), 3.44 (t, J = 6.5 Hz, 2H), 2.72 (t, J = 7.4 Hz, 2H), 2.21 – 2.18 (m, 2H), 2.02 – 1.9:1 (m, 5H), 1.29 (s, 3H), 1.09 (s, 3H). **^{13}C-NMR (75 MHz, $CDCl_3$)** δ 141.85, 140.21, 132.32, 128.34, 128.19, 127.75, 125.66, 114.93, 82.01, 78.02, 71.21, 69.21, 49.11, 38.83, 32.98, 32.26, 31.16, 28.17, 24.11. **IR (neat):** 2997, 2940, 1435, 1429, 1205, 841, 633.

dr 92:8; ee_{cis} % = 94%;

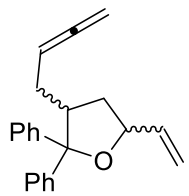

Compound **101b** (liquid) was prepared in 97% yield using General Procedure A. Purification by silica gel flash column chromatography with 4% diethyl ether in hexanes. **^{1}H-NMR (300 MHz, $CDCl_3$)** δ 7.53 – 7.16 (m, 10H), 6.20 – 6.03 (m, 1H), 5.42 – 4.97 (m, 3H), 4.70 – 4.64 (m, 2H), 4.40 – 4.29 (m, 1H), 3.16 – 3.04 (m, 1H), 2.32 – 2.25 (m, 1H), 2.03 – 1.97 (m, 1H), 1.79 – 1.71 (m, 1H), 1.59 – 1.53 (m, 1H). **^{13}C-NMR (75 MHz, $CDCl_3$)** δ 216.55, 208.87, 143.89, 140.22, 139.01, 136.63, 128.09, 127.92, 127.74, 127.57, 126.86, 126.74, 126.64, 126.49, 126.36, 126.31, 115.43, 115.06, 89.79, 88.48, 79.35, 74.84, 46.68, 45.25, 37.34, 36.55, 31.53, 29.80. **IR (neat):** 2926, 2854, 1954, 1495, 1446, 1070, 1043, 924, 843, 701.

dr 95:5; ee_{cis} % = 91%;

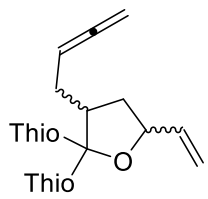

Compound **101c** (liquid) was prepared in 93% yield using General Procedure A. Purification by silica gel flash column chromatography with 4% diethyl ether in hexanes. **^{1}H-NMR (300 MHz, $CDCl_3$)** δ 7.27 – 6.79 (m, 6H), 6.16 – 6.08 (m, 1H), 5.44 – 5.38 (m, 1H), 5.26 – 5.22 (m, 1H), 5.09 – 5.01 (m, 1H), 4.72 – 4.68 (m, 2H), 4.59 – 4.55 (m, 1H), 3.02 – 2.98 (m, 1H), 2.44 – 2.23 (m, 2H), 1.85 – 1.60 (m, 2H). **^{13}C-NMR (75 MHz, $CDCl_3$)** δ 208.68, 151.15, 148.42, 137.78, 126.51, 126.33, 124.94, 124.71, 124.45, 123.77, 116.55, 88.26, 86.77, 79.44, 75.17, 51.13, 38.06, 30.52. **IR (neat):** 2960, 2925, 1955, 1434, 1229, 1038, 849, 699.

dr 97:3; ee_{cis} % = 96%;

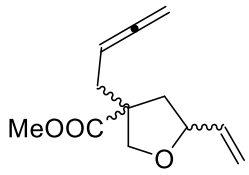

Compound **101d** (liquid) was prepared in 92% yield using General Procedure A. Purification by silica gel flash column chromatography with 7% diethyl ether in hexanes. **^{1}H-NMR (300 MHz, $CDCl_3$)** δ 5.92 – 5.83 (m, 1H), 5.33 – 5.26 (m, 1H), 5.18 – 5.14 (m, 1H), 5.07 – 4.99 (m, 1H), 4.72 – 4.68 (m, 2H), 4.46 – 4.41 (m, 1H), 4.11 (d, J = 9.0 Hz, 1H), 3.83 (d, J = 9.0 Hz, 1H), 3.75 (s, 3H), 2.67 – 2.61 (m, 1H), 2.54 – 2.51 (m, 1H), 2.44 – 2.39 (m, 1H), 1.67 – 1.59 (m, 1H). **^{13}C-NMR (75 MHz, $CDCl_3$)** δ 209.66, 175.04, 137.90, 116.09, 85.53, 80.44, 77.09, 74.88, 74.83, 55.01, 52.09, 41.28, 36.20. **IR (neat):** 2951, 2862, 1955, 1734, 1437, 1202, 1050, 848.

dr 97:3; ee_{cis} % = 99%;

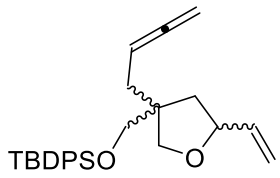

Compound **101e** (liquid) was prepared in 97% yield using General Procedure A. Purification by silica gel flash column chromatography with 1% diethyl ether in hexanes. **^{1}H-NMR (300 MHz, $CDCl_3$)** δ 7.70 – 7.65 (m, 4H), 7.46 – 7.39 (m, 6H), 5.89 – 5.73 (m, 1H), 5.24 – 4.97 (m, 3H), 4.66 – 4.62 (m, 2H), 4.41 – 4.21 (m, 1H), 3.90 – 3.87 (m, 1H), 3.73 – 3.71 (m, 1H), 3.61 – 3.52 (m, 2H), 2.38 – 2.31 (m, 2H), 2.03 – 1.91 (m, 1H), 1.54 – 1.43 (m, 1H), 1.10 – 1.09 (m, 9H). **^{13}C-NMR (75 MHz, $CDCl_3$)** δ 209.79, 138.83, 138.80, 135.54, 133.36, 133.31, 129.61, 129.57, 127.59, 127.56, 115.29, 115.22, 85.93, 85.89, 79.96, 79.81, 77.08, 74.71, 74.59, 74.06, 67.19, 66.39, 49.65, 49.59, 40.09, 39.84, 34.47, 33.56, 26.78, 19.26. **IR (neat):** 3013, 2857, 1955, 1472, 1427, 1112, 1053, 840, 824, 702, 613.

dr 61:39; ee_{cis} % = 97%; ee_{trans} % = 97%;

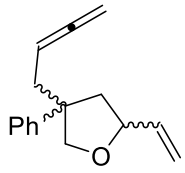

Compound **101f** (liquid) was prepared in 99% yield using General Procedure A. Purification by silica gel flash column chromatography with 5% diethyl ether in hexanes. **^{1}H-NMR (300 MHz, $CDCl_3$)** δ 7.38 – 7.15 (m, 5H), 6.02 – 5.91 (m, 1H), 5.31 – 5.26 (m, 1H), 5.17 – 5.13 (m, 1H), 4.79 – 4.73 (m, 1H), 4.61 – 4.55 (m, 2H), 4.44 – 4.38 (m, 1H), 4.17 – 3.99 (m, 2H), 2.57 – 2.44 (m, 3H), 2.05 – 1.99 (m, 1H). **^{13}C-NMR (75 MHz, $CDCl_3$)** δ 209.74, 144.51, 139.10, 139.03, 128.20, 128.13, 126.75, 126.30, 126.23, 115.53, 115.13, 85.81, 85.59, 79.83, 79.47, 77.10, 76.47, 76.25, 73.89, 51.89, 43.43, 42.40, 40.52, 39.37, 29.58. **IR (neat):** 2924, 2856, 1955, 1495, 1446, 1071, 1043, 922, 844, 702.

dr 81:19; ee_{cis} % = >99%; ee_{trans} % = 95%;

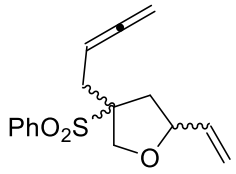

Compound **101g** (liquid) was prepared in 94% yield using General Procedure A. Purification by silica gel flash column chromatography with 30% diethyl ether in hexanes. **^{1}H-NMR (300 MHz, $CDCl_3$)** δ 7.94 (d, J= 7.5 Hz, 2H), 7.75 – 7.70 (m, 1H), 7.65 – 7.60 (m, 2H), 5.87 – 5.60 (m, 1H), 5.33 – 5.11 (m, 3H), 4.78 – 4.73 (m, 2H), 4.41 – 4.35 (m, 2H), 3.89 – 3.86 (m, 1H), 2.83 – 2.76 (m, 1H), 2.54 – 2.52 (m, 2H), 1.88 – 1.80 (m, 1H). **^{13}C-NMR (75 MHz, $CDCl_3$)** δ 210.54, 136.39, 136.30, 134.05, 133.94, 130.03, 129.87, 129.15, 129.03, 128.95, 117.22, 117.11, 83.77, 81.15, 80.87, 77.10, 75.22, 75.14, 72.67, 71.44, 71.36, 38.13, 37.97, 34.14, 32.51. **IR (neat):** 2928, 2873, 1955, 1446, 1303, 1147, 1074, 852, 691.

dr 82:18; ee_{cis} % = 97%; ee_{trans} % = 95%;

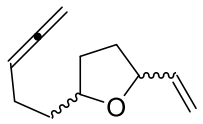

Compound **102** (liquid) was prepared in 98% yield using General Procedure B. Purification by silica gel flash column chromatography with 5% diethyl ether in hexanes. **^{1}H-NMR (300 MHz, $CDCl_3$)** δ 6.05 – 5.93 (m, 1H), 5.32 – 5.29 (m, 1H), 5.20 – 5.15 (m, 2H), 4.73 – 4.58 (m, 2H), 4.34 – 4.22 (m, 1H), 4.02 – 3.95 (m, 1H), 2.13 – 2.09 (m, 4H), 1.53 – 1.50 (m, 4H). **^{13}C-NMR (75 MHz, $CDCl_3$)** δ 208.38, 139.52, 139.43, 115.16, 114.83, 89.72, 89.70, 80.04, 79.45, 79.09, 78.56, 77.15, 75.04, 75.02, 35.20, 35.15, 32.46, 31.89, 31.73, 30.94, 24.79. **IR (neat):** 2839, 1961, 1437, 1424, 1206, 843, 635.

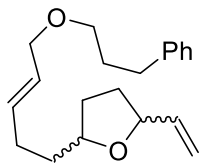

Compound **102-funz** (liquid) was prepared in 66% yield using General Procedure C. Purification by silica gel flash column chromatography with 10% diethyl ether in hexanes. **^{1}H-NMR (300 MHz, $CDCl_3$)** 7.36 – 7.21 (m, 5H), 5.89 – 5.78 (m, 1H), 5.75 – 5.68 (m, 2H), 5.29 – 5.14 (m, 1H), 5.14 – 5.03 (m, 1H), 4.40 – 4.31 (m, 1H), 4.10 – 4.02 (m, 1H), 3.94 – 3.91 (m, 2H), 3.48 – 3.42 (m, 2H), 2.75 – 2.70 (m, 2H), 2.30 – 1.93 (m, 6H), 1.77 – 1.49 (m, 4H). **^{13}C-NMR (75 MHz, $CDCl_3$)** δ 141.92, 139.49, 139.40, 133.77, 133.74, 128.36, 128.18, 126.56, 125.61, 115.05, 114.76, 79.96, 79.39, 79.10, 78.57, 76.47, 71.43, 69.14, 35.33, 35.27, 32.39, 32.28, 31.84, 31.68, 31.21, 30.90, 28.89. **IR (neat):** 2996, 2941, 1435, 1428, 1205, 842, 636.

dr 1:1; ee_{major} % = 93%; ee_{minor} % = 94%;

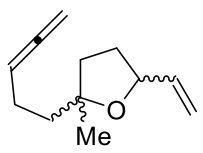

Compound **102a** (liquid) was prepared in 98% yield using General Procedure B. Purification by silica gel flash column chromatography with 5% diethyl ether in hexanes. **^{1}H-NMR (300 MHz, $CDCl_3$)** δ 5.94 – 5.77 (m, 1H), 5.30 – 5.05 (m, 3H), 4.71 – 4.66 (m, 2H), 4.41 – 4.36 (m, 1H), 2.10 – 2.03 (m, 4H), 1.92 – 1.61 (m, 4H), 1.24 (s, 3H). **^{13}C-NMR (75 MHz, $CDCl_3$)** δ 208.22, 139.97, 139.57, 115.01, 114.90, 90.17, 82.90, 82.84, 80.06, 79.31, 75.00, 74.97,

40.98, 40.38, 36.99, 36.77, 32.57, 32.49, 26.83, 26.16, 23.34, 23.26. **IR (neat):** 2837, 1960, 1438, 1422, 1205, 843, 633.

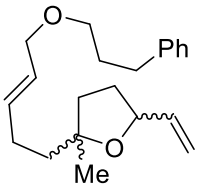

Compound **102a-funz** (liquid) was prepared in 63% yield using General Procedure C. Purification by silica gel flash column chromatography with 10% diethyl ether in hexanes. **^{1}H-NMR (300 MHz, $CDCl_3$)** δ 7.33 – 7.18 (m, 5H), 5.87 – 5.58 (m, 3H), 5.28 – 5.22 (m, 1H), 5.11 – 5.08 (m, 1H), 4.37 – 4.33 (m, 1H), 3.93 (s, 2H), 3.44 (t, J = 6.4 Hz, 2H), 2.72 (t, J = 7.4 Hz, 2H), 2.17 – 2.11 (m, 3H), 1.93 – 1.58 (m, 7H), 1.24 (s, 3H). **^{13}C-NMR (75 MHz, $CDCl_3$)** δ 141.94, 139.97, 139.60, 134.39, 128.37, 128.19, 126.16, 125.63, 115.07, 114.89, 82.95, 80.07, 79.33, 77.12, 71.50, 69.16, 41.19, 40.58, 37.00, 36.79, 32.57, 32.50, 32.29, 31.22, 29.60, 27.49, 27.41, 26.82, 26.14. **IR (neat):** 2996, 2940, 1435, 1427, 1205, 843, 636.

dr 61:39; ee_{major} % = 91%; ee_{minor} % = 75%;

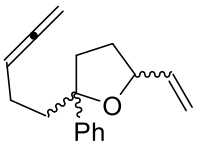

Compound **102b** (liquid) was prepared in 94% yield using General Procedure B. Purification by silica gel flash column chromatography with 3% diethyl ether in hexanes. **^{1}H-NMR (300 MHz, $CDCl_3$)** δ 7.50 – 7.21 (m, 5H), 5.99 – 5.87 (m, 1H), 5.33 – 5.29 (m, 1H), 5.15 – 5.05 (m, 2H), 4.67 – 4.53 (m, 3H), 2.27 – 1.46 (m, 8H). **^{13}C-NMR (75 MHz, $CDCl_3$)** δ 208.15, 146.97, 139.54, 139.36, 127.96, 127.74, 126.26, 126.18, 125.32, 125.08, 115.64, 114.94, 90.03, 86.85, 80.80, 79.49, 77.58, 74.98, 42.21, 41.50, 38.96, 37.88, 31.96, 31.88, 30.23, 22.97. **IR (neat):** 2925, 2854, 1955, 1495, 1447, 1070, 1043, 925, 843, 700.

dr 81:19; ee_{major} % = 96%; ee_{minor} % = 95%;

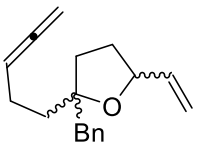

Compound **102c** (liquid) was prepared in 93% yield using General Procedure B. Purification by silica gel flash column chromatography with 3% diethyl ether in hexanes. **^{1}H-NMR (300 MHz, $CDCl_3$)** δ 7.33 – 7.24 (m, 5H), 5.94 – 5.73 (m, 1H), 5.26 – 5.07 (m, 3H), 4.70 – 4.67 (m, 2H), 4.34 – 4.16 (m, 1H), 2.90 – 2.75 (m, 2H), 2.20 – 2.13 (m, 2H), 1.92 – 1.63 (m, 5H), 1.28 – 1.15 (m, 1H). **^{13}C-NMR (75 MHz, $CDCl_3$)** 208.23, 139.44, 139.17, 138.05, 137.90, 130.62, 130.50, 127.85, 127.69, 126.08, 126.03, 115.58, 115.13, 90.08, 90.02, 85.30, 85.27, 80.68, 80.19, 77.10, 75.08, 75.02, 45.63, 45.16, 39.47, 39.22, 34.17, 33.95, 32.65, 23.07, 22.99. **IR (neat):** 2928, 2856, 1955, 1497, 1447, 1071, 1043, 924, 843, 702.

dr 56:44; ee_{major} % = 96%; ee_{minor} % = 96%;

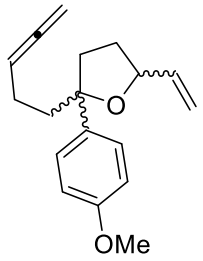

Compound **102d** (liquid) was prepared in 45% yield using General Procedure B. Purification by silica gel flash column chromatography with 3% diethyl ether in hexanes. **^{1}H-NMR (300 MHz, $CDCl_3$)** δ 7.36 – 7.28 (m, 2H), 6.90 – 6.86 (m, 2H), 5.99 – 5.86 (m, 1H), 5.34 – 5.26 (m, 1H), 5.16 – 5.05 (m, 2H), 4.67 – 4.62 (m, 2H), 4.53 – 4.42 (m, 1H), 3.82 (s, 3H), 2.21 – 1.58 (m, 8H). **^{13}C-NMR (75 MHz, $CDCl_3$)** 208.13, 158.02, 157.93, 139.60, 139.44, 139.08, 138.63, 126.39, 126.21, 115.59, 114.88, 113.28, 113.05, 90.05, 86.71, 86.62, 80.77, 79.35, 77.10, 74.95, 55.11, 42.28, 41.60, 38.89, 37.72, 31.91, 23.03. **IR (neat):** 2929, 2854, 1955, 1495, 1447, 1256, 1070, 1045, 928, 843, 700, 658.

dr 59:41; ee_{major} % = 96%; ee_{minor} % = 97%;

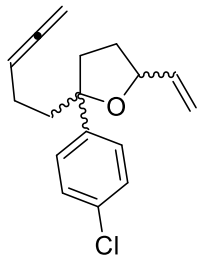

Compound **102e** (liquid) was prepared in 67% yield using General Procedure B. Purification by silica gel flash column chromatography with 3% diethyl ether in hexanes. **^{1}H-NMR (300 MHz, $CDCl_3$)** δ 7.38 – 7.28 (m, 4H), 5.97 – 5.84 (m, 1H), 5.35 – 5.27 (m, 1H), 5.17 – 5.05 (m, 2H), 4.67 – 4.63 (m, 2H), 4.57 – 4.40 (m, 1H), 2.21 – 1.58 (m, 8H). **^{13}C-NMR (75 MHz, $CDCl_3$)** δ 208.10, 145.54, 145.24, 139.25, 139.05, 132.02, 131.96, 128.09, 127.87, 126.81, 126.59, 115.92, 115.15, 89.86, 89.84, 86.57, 86.47, 80.89, 79.61, 75.15, 42.05, 41.36, 38.99, 37.94, 31.89, 31.78, 29.60, 22.86. **IR (neat):** 2925, 2855, 1955, 1495, 1447, 1072, 1043, 921, 843, 698.

dr 51:49; ee_{major} % = 97%; ee_{minor} % = 97%;

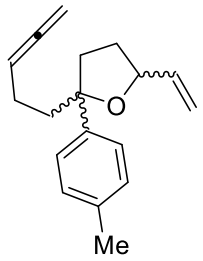

Compound **102f** (liquid) was prepared in 91% yield using General Procedure B. Purification by silica gel flash column chromatography with 3% diethyl ether in hexanes. **^{1}H-NMR (300 MHz, $CDCl_3$)** δ 7.34 – 7.28 (m, 2H), 7.16 – 7.13 (m, 2H), 5.96 – 5.87 (m, 1H), 5.33 – 5.27 (m, 1H), 5.14 – 5.05 (m, 2H), 4.66 – 4.62 (m, 2H), 4.56 – 4.41 (m, 1H), 2.36 (s, 3H), 2.25 – 1.58 (m, 8H). **^{13}C-NMR (75 MHz, $CDCl_3$)** δ 208.16, 144.02, 139.46, 135.62, 128.63, 128.41, 125.24, 125.02, 115.50, 114.81, 90.05, 86.79, 80.74, 74.89, 42.24, 41.55, 38.89, 37.77, 31.90, 22.99, 20.83. **IR (neat):** 2930, 2853, 1955, 1495, 1449, 1254, 1069, 1045, 927, 843, 700, 655.

dr 82:18; ee_{major} % = 97%; ee_{minor} % = 94%;

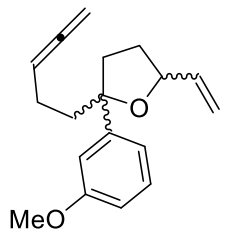

Compound **102g** (liquid) was prepared in 84% yield using General Procedure B. Purification by silica gel flash column chromatography with 4% diethyl ether in hexanes. **^{1}H-NMR (300 MHz, $CDCl_3$)** δ 7.28 – 7.23 (m, 1H), 7.06 – 6.94 (m, 2H), 6.79 – 6.77 (m, 1H), 5.98 – 5.89 (m, 1H), 5.30 (d, J= 17.1 Hz, 1H), 5.16 – 5.06 (m, 2H), 4.67 – 4.63 (m, 2H), 4.55 – 4.48 (m, 1H), 3.84 (s, 3H), 2.27 – 1.62 (m, 8H). **^{13}C-NMR (75 MHz, $CDCl_3$)** δ 208.15, 159.41, 159.18, 148.86, 148.57, 139.51, 139.34, 128.96, 128.73, 117.71, 117.55, 115.61, 114.92, 111.49, 111.34, 111.16, 90.02, 86.90, 86.82, 80.82, 79.50, 74.97, 55.10, 55.06, 42.10, 41.44, 39.01, 37.86, 31.90, 31.84, 22.96. **IR (neat):** 2925, 2855, 1956, 1495, 1445, 1072, 1041, 921, 843, 699.

dr 83:17; ee_{major} % = 96%; ee_{minor} % = 91%;

10.2.3 Absolute Configuration Determination

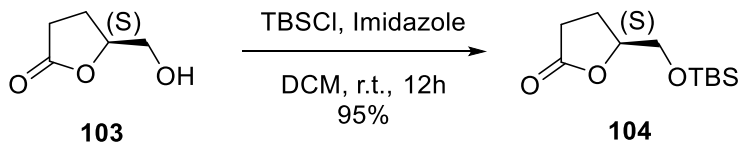

103 **104**

In a flamed dried flask under Argon atmosphere, (S)-(+)-dihydro-5-(hydroxymethyl)-2(3H)-furanone (2 g, 13.5 mmol) was dissolved in dry DCM (60 mL). The mixture was cooled to 0 °C before adding imidazole (54.0 mmol) and TBSCl (14.8 mmol). The mixture was allowed to stir at room temperature for 12 h. The reaction mixture was quenched with water and the aqueous phase was extracted with DCM. The combined organic layer was dried over $MgSO_4$ and concentrated under reduced pressure. The residue was purified by flash column chromatography with 50% Et_2O in hexanes to give **104** (liquid) in 95% yield.

^{1}H-NMR (300 MHz, $CDCl_3$) δ 4.62 – 4.58 (m, 1H), 3.88 (dd, J= 11.26, 2.95 Hz, 1H), 3.70 (dd, J= 11.27, 2.78 Hz, 1H), 2.69 – 2.42 (m, 2H), 2.35 – 2.15 (m, 2H), 0.91 (s, 9H), 0.09 (s, 6H). **^{13}C-NMR (75 MHz, $CDCl_3$)** δ 177.40, 79.94, 64.77, 28.44, 25.67, 23.45, 18.12, -5.61, -5.68. **IR (neat):** 2985, 1918, 1499, 1298, 1071.

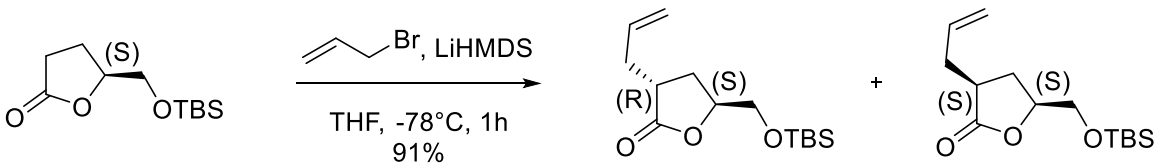

104 **105a** **105b**

In a flamed dried flask under Argon atmosphere, compound **104** (3.4 g, 12.82 mmol) was dissolved in dry THF (60 mL). The mixture was cooled to -78 °C before adding LiHMDS (14.1 mmol). The mixture was stirred at the same temperature for 40 min and then allyl bromide (19.2 mmol) was added. The reaction mixture was stirred for further 30 min. Upon completion confirmed by TLC analysis, the reaction was quenched with a saturated solution of NH_4Cl and the aqueous phase was extracted with Et_2O. The combined organic layer was dried over $MgSO_4$ and concentrated under reduced pressure. The residue was purified by flash column chromatography with 25% Et_2O in hexanes to give **105** (liquid) in 91% yield.

^{1}H-NMR (300 MHz, $CDCl_3$) δ 5.82 – 5.71 (m, 1H), 5.15 – 5.09 (m, 2H), 4.55 – 4.43 (m, 1H), 3.88 – 3.83 (m, 1H), 3.68 (dt, J= 10.78, 2.78 Hz, 1H), 2.87 – 2.56 (m, 2H), 2.35 – 2.21 (m, 2H), 2.08 – 1.88 (m, 1H), 0.89 (s, 9H), 0.06 (s, 6H). **^{13}C-NMR (75 MHz, $CDCl_3$)** δ 178.99, 178.07, 134.59, 134.51, 117.45, 117.35,

78.45, 77.97, 64.96, 63.80, 39.95, 39.00, 35.18, 34.42, 29.20, 28.90, 25.68, 18.18, 18.11, -5.46, -5.53, -5.62, -5.71. **IR (neat):** 2991, 2985, 1915, 1499, 1302, 1297, 1187, 1072.

The diastereomeric mixture was subjected to GC-MS analysis to determine the diastereomeric ratio, which turned out to be 85/15 = trans/cis, m/z : 213 [M – tBu]+.

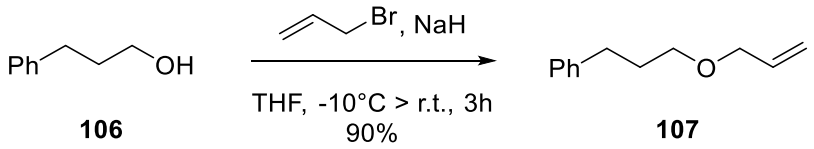

106 **107**

In a flamed dried flask under Argon atmosphere, NaH (44.1 mmol) was suspended in dry THF (75 mL). The mixture was cooled to -10 °C before adding 3-phenyl-propan-1-ol (4 g, 29.37 mmol). The mixture was allowed to stir at the same temperature for 15 min and then allyl bromide (32.3 equiv) was added dropwise. The reaction mixture was stirred at room temperature for 3 h. Upon completion confirmed by TLC analysis, the reaction mixture was quenched with water and the aqueous phase was extracted with Et_2O. The combined organic layer was dried over $MgSO_4$ and concentrated under reduced pressure. The residue was purified by flash column chromatography with 10% Et_2O in hexanes to give **107** (liquid) in 90% yield.

The spectroscopic data were in accordance with the literature data[75].

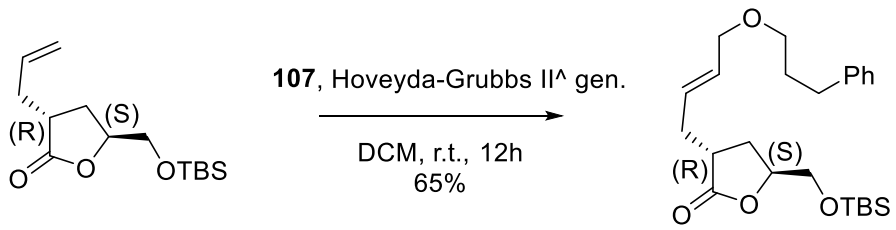

105
dr 85:15

108
dr 85:15

In a flamed dried flask under Argon atmosphere compound **105** (3.15 g, 11.67 mmol) was dissolved in dry DCM (60 mL) together with compound **107** (23.3 mmol) and the Hoveyda-Grubbs II^gen. catalyst (0.58 mmol). The mixture was allowed to stir at room temperature for 12 h. Upon completion confirmed by TLC analysis, the reaction mixture was directly purified by flash column chromatography with 30% Et_2O in hexanes to give **108** (liquid) in 65% yield.

^{1}H NMR (300 MHz, $CDCl_3$) δ 7.24 – 7.19 (m, 5H), 5.70 – 5.66 (m, 2H), 4.54 – 4.50 (m, 1H), 3.96 – 3.84 (m, 3H), 3.69 – 3.65 (m, 1H), 3.46 – 3.42 (m, 2H), 2.86 – 2.69 (m, 4H), 2.33 – 2.27 (m, 4H), 2.05 – 1.90 (m, 3H), 0.90 (s, 9H), 0.09 (s, 6H). **^{13}C NMR (75 MHz, $CDCl_3$)** δ 178.83, 141.82, 129.79, 129.49, 129.30,

[75] Yamada, K.; Hayakawa, N.; Fujita, H.; Kitamura, M.; Kunishima, M. *Chem. Pharm. Bull.* **2017**, 65, 112

128.34, 128.19, 125.65, 77.93, 77.09, 70.98, 69.32, 69.27, 64.94, 39.12, 33.74, 32.23, 31.20, 31.14, 29.24, 25.69, 18.13, -5.60, 5.70. **IR (neat)**: 2932, 2858, 1768, 1454, 1366, 1178, 1103, 701.

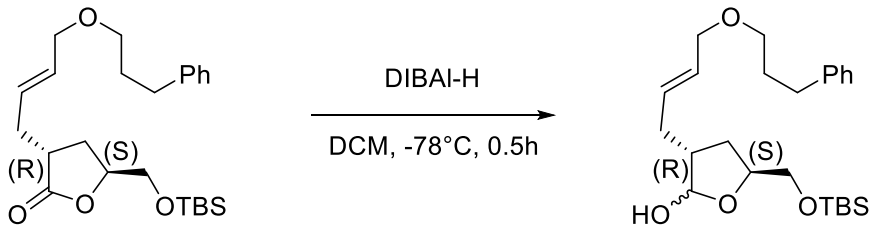

108
dr 85:15

108a
dr 85:15

In a flamed dried flask under Argon atmosphere compound **108** (3.17g, 7.58 mmol) was dissolved in dry DCM (40 mL). The mixture was cooled to -78 °C before DIBAL-H (9.1 mmol) was added. The reaction mixture was allowed to stir at the same temperature for 30 min. Upon completion confirmed by TLC analysis, the reaction mixture was quenched with water and the aqueous phase was extracted with DCM. The combined organic layer was dried over $MgSO_4$ and concentrated under reduced pressure. The crude residue was used in the next step without further purification.

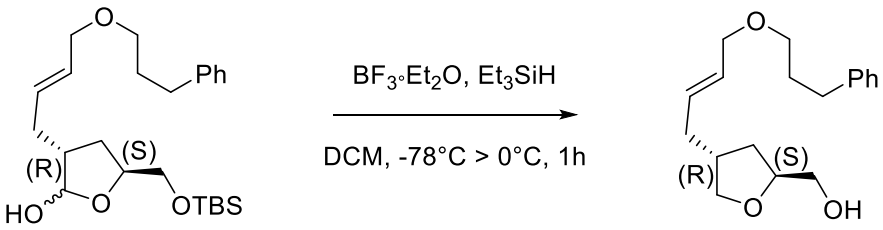

108a
dr 85:15

109
dr 85:15

In a flamed dried flask under Argon atmosphere **109** (7.58 mmol) was dissolved in dry DCM (40 mL) together with Et_3SiH (12.9 mmol). The mixture was cooled to -78 °C before $BF_3{\cdot}Et_2O$ (9.1 equiv) was added dropwise. The reaction mixture was allowed to stir at 0 °C for 1 h. Upon completion confirmed by TLC analysis, the reaction mixture was quenched with saturated $NaHCO_3$ aq. solution. The aqueous phase was extracted with DCM. The combined organic layer was dried over $MgSO_4$ and concentrated under reduced pressure. The crude residue was used in the next step without further purification.

109
dr 85:15

110
dr 85:15

In a flamed dried flask under Argon atmosphere compound **110** (7.58 mmol) was dissolved in dry DMSO (40 mmol) together with IBX (9.1 mmol). The mixture was allowed to stir at 50 °C for 3 h. Upon completion confirmed by TLC analysis, the reaction mixture was quenched with saturated $Na_2S_2O_3$ and $NaHCO_3$, and the aqueous phase was extracted with Et_2O. The combined organic layer was dried over $MgSO_4$ and concentrated under reduced pressure. The crude residue was used in the next step without further purification.

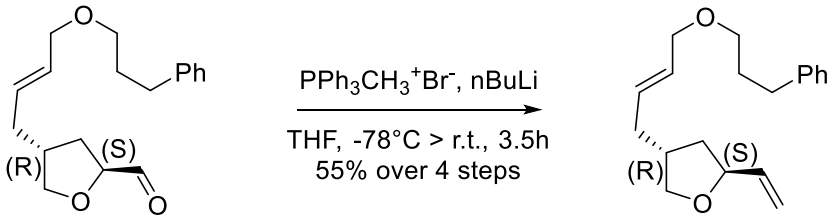

110
dr 85:15

101-funz
dr 85:15

In a flamed dried flask under Argon atmosphere triphenylphosphonium bromide (9.1 mmol) was suspended in dry THF (20 mL). The mixture was cooled to -78 °C before adding *n*BuLi (9.1 mmol) and then was allowed to stir at 0°C for 30 min. The reaction was cooled to -78 °C again and a solution of **111** (7.58 mmol) in dry THF (20 mL) was added dropwise via cannula. The reaction mixture was allowed to stir at room temperature for 3 h. Upon completion confirmed by TLC analysis, the reaction mixture was quenched with saturated NH_4Cl and $NaHCO_3$, and the aqueous phase was extracted with Et_2O three times. The combined organic layer was dried over $MgSO_4$ and concentrated under reduced pressure. The residue was purified by flash column chromatography with 10% Et_2O in hexanes to give **101-funz** (liquid) in 55% yield over 4 steps.

10.3 Gold(I)-catalyzed Heterofunctionalization of allenes

10.3.1 Gold(I)-catalyzed Lactonization

10.3.1.1 Substrates Synthesis

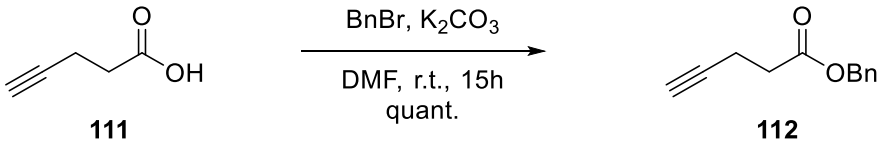

Following a reported procedure[76], 4-pentynoic acid **111** (500 mg, 5.1 mmol) and K_2CO_3 (7.65 mmol) were dissolved in DMF (5 mL). Benzyl bromide (6.12 mmol) was then added dropwise. The reaction mixture was stirred at room temperature for 15 hours. The aqueous phase was extracted with AcOEt, while the combined organic layers were washed with brine, dried over anhydrous $MgSO_4$, filtered and evaporated. The crude oil was purified by flash chromatography on a silica gel column using 10% Et_2O in hexanes as the eluent to give **112** (liquid) in quantitative yield.

The spectroscopic data were in accordance with the literature data.

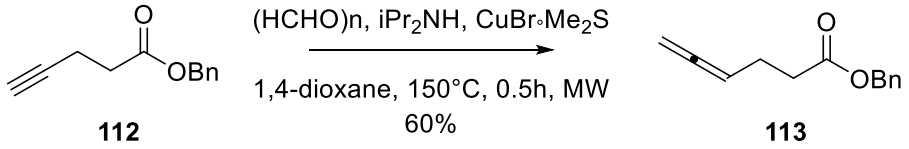

A solution of **112** (1 g, 5.1 mmol), $CuBr{\cdot}Me_2S$ (1.6 mmol), paraformaldehyde (13.4 mmol), diisopropylamine (10.6 mmol) in anhydrous 1,4-dioxane (6 mL) was heated at 150 °C for 30 min in Microwave equipment. The crude reaction mixture was diluted with Et_2O and washed with saturated $NaHCO_3$ and brine. The organic phase was dried over $MgSO_4$ and evaporated under reduced pressure. The crude oil was purified by flash chromatography on a silica gel column using 10% Et_2O in hexanes as the eluent, to give **113** (liquid) in 60% yield.

The spectroscopic data were in accordance with the literature data[77].

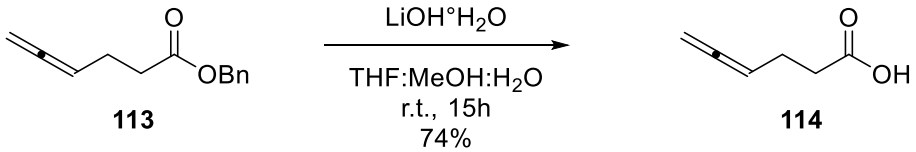

[76] Lorion, M.M.; Duarte, F.J.S.; Calhorda, M.J.; Oble, J.; Poli, G. *Org. Lett.* **2016**, *18*, 1020
[77] Wang, Z.; Nicolini, C.; Hervieu, C.; Wong, Y-F.; Zanoni, G.; Zhang, L *J. Am. Chem. Soc.* **2017**, *139*, 16064

113 (575 mg, 2.8 mmol) and $LiOH \cdot H_2O$ (17.1 mmol) were dissolved in a mixture of THF (6 mL), MeOH (4 mL) and H_2O (4 mL). The reaction mixture was stirred at room temperature for 15 hours. Et_2O was added and the solution was acidified to pH = 1. The aqueous layers were extracted with Et_2O and the combined organic layers were washed with brine, dried over anhydrous $MgSO_4$, filtered and carefully evaporated. The crude oil was purified by flash chromatography on a silica gel column using 30% AcOEt in hexanes as the eluent, to give **114** (liquid) in 74% yield.

The spectroscopic data were in accordance with the literature data[78].

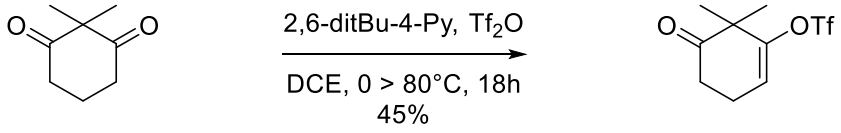

115 **116**

A stirred solution of 2,2-dimethyl-1,3-cyclohexanedione **115** (0.93 mmol) and 2,6-di-tert-butyl4-methylpyridine (2.04 mmol) in anhydrous DCE (5 mL) was cooled to 0°C. To this was added trifluoromethanesulfonic anhydride (0.33 mL, 1.94 mmol), dropwise. The reaction was then heated at 80°C for 18 h, after which it was allowed to cool to room temperature. Et_2O was added, and the white pyridinium triflate salt was removed by filtration, washing with diethyl ether. The filtrate was concentrated under reduced pressure to produce a dark oil. The crude oil was purified by flash chromatography on a silica gel column using 20% Et_2O in hexanes as the eluent, to give **116** (liquid) in 74% yield.

The spectroscopic data were in accordance with the literature data.

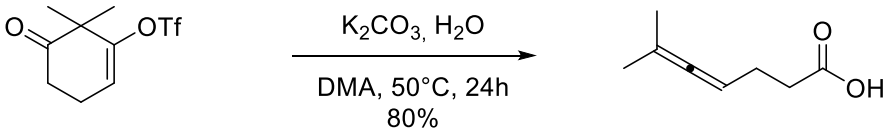

116 **117**

Following the reported procedure, enol triflate **116** (0.10 mmol) and K_2CO_3 (0.20 mmol) were weighed into a glass vial equipped with a magnetic stirring bar and sealed with a rubber septum. Then DMA (0.50 mL) and water (4.0 mmol) were added and the mixture was stirred at 50°C until completion on TLC. The reaction mixture was then diluted with AcOEt. The organic layer was washed with water, twice, brine and then dried over $MgSO_4$. After filtration, the solvent was removed in vacuo and the residue was

[78] Trost, B.M.; McClory, A. *Org. Lett.* **2006**, *8* (17), 3627

purified by silica gel chromatography using 20% Et_2O in hexanes as the eluent to give **117** (liquid) in 80% yield.

The spectroscopic data were in accordance with the literature data[79].

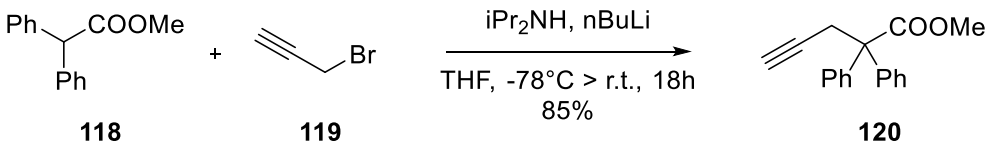

118 **119** **120**

To a solution of diisopropylamine (7.956 mmol) in anhydrous THF was added slowly nBuLi (2.5 M in hexanes, 7.293 mmol) at -30°C under Argon. The temperature was risen to 0°C and kept for 30 minutes to obtain a pale yellow solution. The reaction mixture was cooled down to -78°C and methyl 2,2-diphenylacetate **118** (1 g, 4.4 mmol) was added. After 5 hours at the same temperature, propargyl bromide **119** was added (80% w/w in toluene, 5.3 mmol) and the reaction mixture was heated up to room temperature and stirred overnight. The reaction mixture was quenched with a saturated solution of NH_4Cl and then extracted with Et_2O. The combined organic phases were dried over $MgSO_4$, filtered, and concentrated on a rotary evaporator. The crude oil was purified by flash chromatography on a silica gel column using 10% Et_2O in hexanes as the eluent to give **120** (liquid) in 85% yield.

The spectroscopic data were in accordance with the literature data.

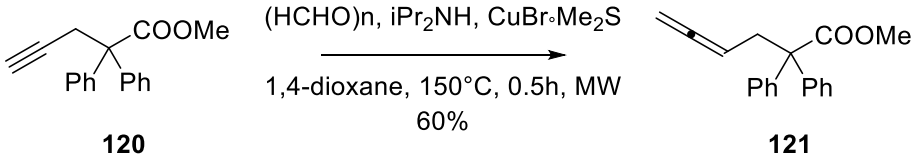

120 **121**

A solution of **120** (550 mg, 2.1 mmol), $CuBr{\cdot}Me_2S$ (0.6 mmol), paraformaldehyde (5.2 mmol), diisopropylamine (4.2 mmol) in anhydrous 1,4-dioxane (16 mL) was heated at 150 °C for 30 min in Microwave equipment. The crude reaction mixture was diluted with Et_2O and washed with saturated $NaHCO_3$ and brine. The organic phase was dried over $MgSO_4$ and evaporated under reduced pressure. The crude oil was purified by flash chromatography on a silica gel column using 5% Et_2O in hexanes as the eluent, to give **121** (liquid) in 60% yield.

The spectroscopic data were in accordance with the literature data[80].

[79] Jonasson, C.; Horvath, A.; Backvall, J-E. *J. Am. Chem. Soc.* **2000**, *122*, 9600
[80] Arbour, J.L.; Rzepa, H.S.; White, A.J.P.; Hii, K.K. *Chem. Commun.* **2009**, 136, 2538

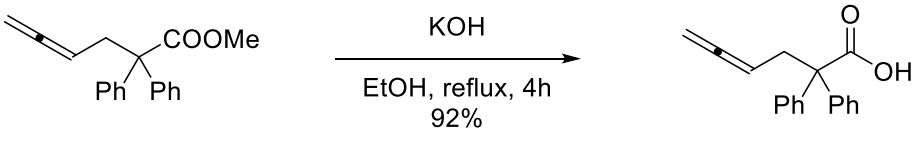

121 **122**

To a solution of **121** (260 mg, 0.93 mmol) in EtOH (10 mL) was added KOH (9.3 mmol) and the reaction mixture was heated to reflux, until completion confirmed by TLC. The reaction mixture was quenched by adding HCl 1M, until neutrality, and diluted with AcOEt. The organic phase was washed with brine, then collected and dried over $MgSO_4$. After evaporation of the solvent under reduced pressure, the crude oil was purified by flash chromatography on a silica gel column using 30% AcOEt in hexanes as the eluent, to give **122** (liquid) in 92% yield;

The spectroscopic data were in accordance with the literature data[81].

10.3.1.2 Au(I)-catalyzed cyclization reaction

General Procedure for the Au(I)-catalyzed cyclization

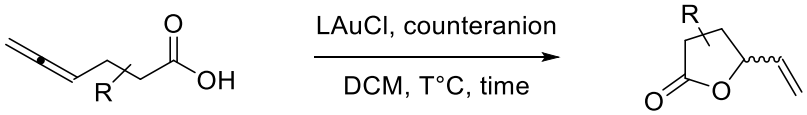

To a 3-dram vial were added the catalyst (5 mol% or 0.01 mol%) and the counterion (5 mol% or 0.5 mol %) in 2 mL anhydrous DCM as solvent. The mixture was stirred at r.t. for 15 min. Then 0.1 mmol of allenyl acid were added and the reaction was stirred at the selected temperature monitoring by TLC. Upon completion, the reaction was concentrated under reduced pressure. The residue was purified by silica gel flash column chromatography to obtain pure product.

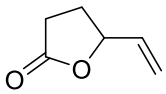

Compound **123** (liquid) was prepared in 34% yield following General Procedure, using PPh_3AuCl (5 mol%) and AgOTs (5 mol%) at room temperature (*Table 5.1, entry 1)*. Purification by silica gel flash column chromatography with 5% diethyl ether in hexanes. **^{1}H-NMR (300 MHz, $CDCl_3$)** δ 6.02 – 5.91 (m, 1H), 5.46 – 5.31 (m, 2H), 4.85 – 4.78 (m, 1H), 3.18 – 3.11 (m, 1H), 2.85 – 2.77 (m, 1H); **^{13}C-NMR (75 MHz, $CDCl_3$)** δ 176.10, 134.07, 115.30, 77.62, 28.25, 28.13. **IR (neat):** 2951, 1916, 1322, 1305, 1285.

[81] Arbour, J.L.; Rzepa, H.S.; Contreras-Garcia, J.; Adrio, L.A.; Barreiro, E.M.; Hii, K.K. *Chem. Eur. J.* **2012**, 18, 11317

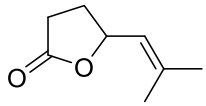

Compound **124** (liquid) was prepared in quantitative yield following General Procedure, using **cat-22** (0.01 mol%) and $NaBAr_4^F$ (0.5 mol%) at room temperature (*Table 5.2, entry 7*). Purification by silica gel flash column chromatography with 5% diethyl ether in hexanes. **^{1}H-NMR (300 MHz, $CDCl_3$)** δ 5.27 – 5.19 (m, 2H), 2.59 – 2.53 (m, 2H), 2.41 – 2.34 (m, 1H), 1.97 – 1.91 (m, 1H), 1.79 (s, 3H), 1.75 (s, 3H); **^{13}C-NMR (75 MHz, $CDCl_3$)** δ 177.09, 139.69, 122.70, 77.51, 29.19, 29.07, 25.61, 18.26. **IR (neat):** 2944, 1919, 1339, 1309, 1278.

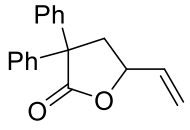

Compound **125a** (liquid) was prepared in 88% yield following General Procedure, using **cat-17** (0.01 mol%) and $NaBAr_4^F$ (0.5 mol%) at -30°C (*Table 5.4, entry 9*). Purification by silica gel flash column chromatography with 5% diethyl ether in hexanes. **^{1}H-NMR (300 MHz, $CDCl_3$)** δ 7.42 – 7.40 (m, 4H), 7.37 – 7.27 (m, 6H), 6.01 – 5.89 (m, 1H), 5.43 (d, J= 17.16 Hz, 1H), 5.33 (d, J= 10.43, 1H), 4.79 (p, J= 5.35, 1H), 3.13 (dd, J= 12.98 Hz, 5.05, 1H) 2.78 (dd, J= 12.98 Hz, 10.56 Hz, 1H); **^{13}C-NMR (75 MHz, $CDCl_3$)** δ 176.70, 141.60, 139.52, 134.84, 128.87, 128.29, 127.67, 127.60, 127.24, 127.17, 118.75, 77.39, 57.95, 43.70. **IR (neat):** 3089, 2930, 1894, 1291, 1287, 1207, 1096, 996.

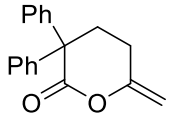

Compound **125b** (liquid) was prepared in quantitative yield following General Procedure, using PPh_3AuCl (5 mol%) and $NaBAr_4^F$ (5 mol%) at room temperature (*Table 5.4, entry 2*). Purification by silica gel flash column chromatography with 5% diethyl ether in hexanes. **^{1}H-NMR (300 MHz, $CDCl_3$)** δ 7.39 – 7.21 (m, 10H), 4.69 (d, J= 1.28Hz, 1H), 4.21 (d, J= 1.28, 1H), 2.72 – 2.68 (m, 1H) 2.57 – 2.52 (m, 1H); **^{13}C-NMR (75 MHz, $CDCl_3$)** δ 170.02, 154.53, 141.22, 128.37, 128.29, 128.03, 127.40, 93.58, 56.99, 30.91, 23.71. **IR (neat):** 3090, 2980, 1875, 1818, 1460, 1303, 1182, 978.

10.3.2 Gold(I)-catalyzed Hydroamination

10.3.2.1 Substrates Synthesis

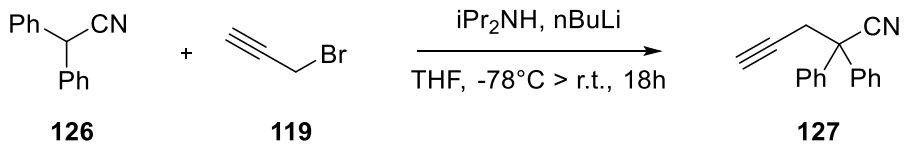

126 **119** **127**

To a solution of diisopropylamine (46.6 mmol) in anhydrous THF (60 mL) was added slowly nBuLi (11 M in hexanes, 42.7 mmol) at -30°C under Argon. The temperature was risen to 0°C and kept for 30 minutes to obtain a pale yellow solution. The reaction mixture was cooled down to -78°C and 2,2-diphenylacetonitrile (5 g, 25.9 mmol) was added. After 5 hours at the same temperature, propargyl bromide was added (80% w/w in toluene, 31.1 mmol) and the reaction mixture was heated up to room temperature and stirred overnight. The reaction mixture was quenched with a saturated solution of NH_4Cl and then extracted with Et_2O. The combined organic phases were dried over $MgSO_4$, filtered, and concentrated on a rotary evaporator. The crude residue was used in the next step without further purification.

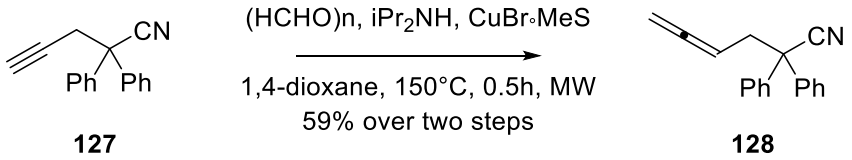

127 **128**

Compound **128** was prepared in a similar way as compound **121** starting from compound **127** (59% yield).

The spectroscopic data were in accordance with the literature data.

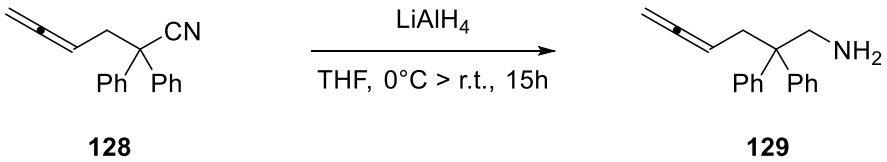

128 **129**

To a suspension of $LiAlH_4$ (22.9 mmol) in dry THF (45 mL) stirring at –10 °C, Compound **128** (1.9 g, 7.64 mmol) was added dropwise over 10 min. The reaction mixture was warmed to r.t. and stirred for 12 h. The reaction mixture was quenched with H_2O, NaOH and H_2O and then extracted with Et_2O. The combined organic phases were dried over $MgSO_4$, filtered, and concentrated on a rotary evaporator. The crude residue was used in the next step without further purification.

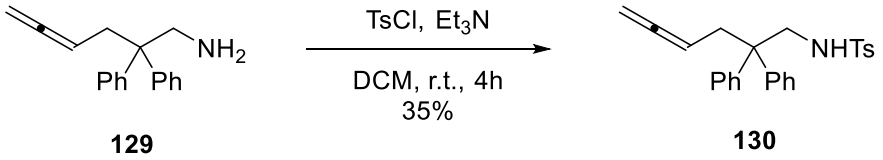

129 **130**

To a solution of **129** and triethylamine (10.7 mmol) in anhydrous DCM was added p-toluensulfonil chloride (8.02 mmol) at 0°C. After 4 hours, the reaction mixture was quenched with H_2O and diluted with DCM. The organic phase was washed with HCl 1M, collected and dried over $MgSO_4$. After evaporation of the solvent under reduced pressure, the crude oil was purified by flash chromatography on a silica gel column using 10% AcOEt in toluene as the eluent, to give **130** (liquid) in 35% yield.

The spectroscopic data were in accordance with the literature data.

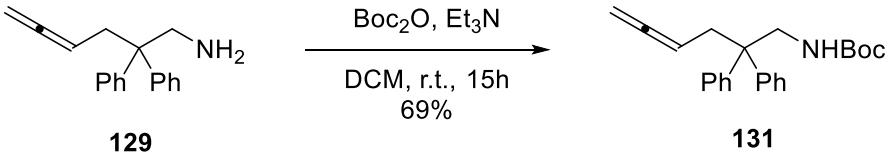

129 **131**

To a solution of **129**, triethylamine (10.7 mmol) and di-tertbutyl dicarbonate (9.17 mmol) in anhydrous DCM (35 mL) was left to stir at room temperature overnight. The reaction mixture was quenched with H_2O and diluted with DCM. The organic phase was washed with brine, collected and dried over $MgSO_4$. After evaporation of the solvent under reduced pressure, the crude oil was purified by flash chromatography on a silica gel column using 2 to 5% AcOEt in hexanes as the eluent, to give **131** (liquid) in 69% yield.

The spectroscopic data were in accordance with the literature data.

10.3.2.2 Au(I)-catalyzed cyclization reaction

General Procedure for the Au(I)-catalyzed cyclization

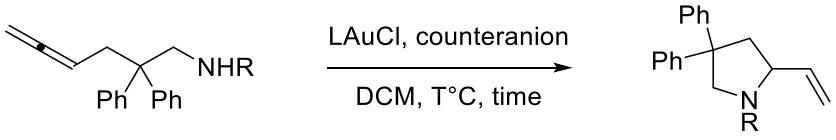

To a 3-dram vial were added the catalyst (5 mol% or 0.01 mol%) and the counterion (5 mol% or 0.5 mol %) in 2 mL anhydrous DCM as solvent. The mixture was stirred at r.t. for 15 min. Then 0.1 mmol of allenyl amine were added and the reaction was stirred at the selected temperature monitoring by TLC.

Upon completion, the reaction was concentrated under reduced pressure. The residue was purified by silica gel flash column chromatography to obtain pure product.

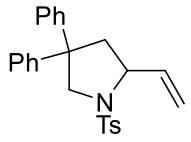

Compound **132** (liquid) was prepared in 97% yield following General Procedure, using **cat-17** (0.01 mol%) and $NaBAr_4^F$ (0.5 mol%) at -10°C (*Table 5.5, entry 6)*. Purification by silica gel flash column chromatography with 10% AcOEt in toluene. **^{1}H-NMR (300 MHz, $CDCl_3$)** δ 7.65 (d, J= 8.22, 2H), 7.31 – 7.17 (m, 12H), 5.64 – 5.55 (m, 1H), 5.16 (d, J= 17.02 Hz, 1H), 5.03 (d, J= 10.15 Hz, 1H), 4.22 – 4.08 (m, 3H), 2.84 – 2.77 (m, 1H), 2.50 – 2.43 (m; 4H), **^{13}C-NMR (75 MHz, $CDCl_3$)** δ 145.11, 144.45, 142.91, 138.59, 136.02, 129.33, 128.44, 128.40, 128.24, 127.76, 127.20, 126.60, 126.48, 126.39, 126. 31, 116.26, 61.86, 58.09, 52.43, 45.36, 26.87, 21.37. **IR (neat):** 3131, 3106, 3087, 2990, 2935, 1794, 1501, 1327, 1264, 1200, 1133, 993, 779.

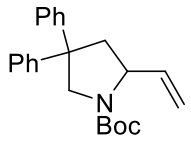

Compound **133** (liquid) was prepared in 60% yield following General Procedure, using **cat-17** (0.01 mol%) and $NaBAr_4^F$ (0.5 mol%) at room temperature (*Table 5.6, entry 4)*. Purification by silica gel flash column chromatography with 10% AcOEt in toluene. **^{1}H-NMR (300 MHz, $CDCl_3$)** δ 7.35 – 7.21 (m, 10H), 5.79 – 5.71 (m, 1H), 5.15 – 5.04 (m, 2H), 4.74 – 4.59 (m, 1H), 4.12 – 3.95 (m, 1H), 3.69 – 3.57 (m, 1H), 2.89 – 2.84 (m, 1H), 2.47 – 2.43 (m, 1H), 1.56 – 1.38 (m, 9H); **^{13}C-NMR (75 MHz, $CDCl_3$)** δ 169.05, 166.37, 155.59, 146.48, 140.52, 140.15, 138.75, 129.24, 129.20, 128.87, 128.82, 127.54, 127.30, 127.20, 127.05, 115.22, 92.92, 80.11, 79.35, 28.81. **IR (neat):** 3089, 2998, 1890, 1553, 1524, 1444, 1417, 1396, 1184, 993.

10.3.3 Gold(I)-catalyzed Lactamization

10.3.3.1 Substrates Synthesis

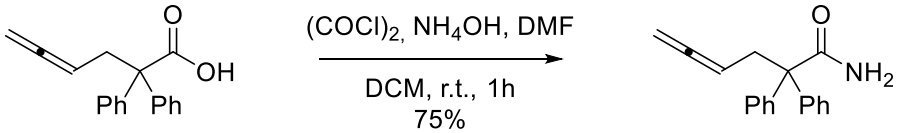

122 **134**

To a solution of **122** (270 mg, 1 mmol) in anhydrous DCM (5 mL) was added slowly oxalyl chloride (1.1 mmol) and a drop of DMF at 0°C. After 1h, solvent was evaporated and the residue was dissolved in anhydrous DCM. Ammonium hydroxide (1.2 mmol) was then added and the reaction mixture was left to stir at room temperature for 1h. Solvent was then evaporated under reduced pressure and the residue was dissolved in AcOEt. The organic phase was washed with a saturated solution of $NaHCO_3$, collected, dried over $MgSO_4$ and concentrated under reduced pressure. The crude oil was purified by flash chromatography on a silica gel column using 30% AcOEt in hexanes as the eluent, to give **134** (liquid) in 75% yield.

^{1}H-NMR (300 MHz, CD_2Cl_2) δ(ppm) 7.34 – 7.27 (m, 10H), 5.81 (bs, 1H), 5.67 (bs, 1H), 5.09 – 4.95 (m, 1H), 4.54 – 4.47 (m, 2H); 3.24 – 3.17 (m, 2H); **^{13}C-NMR (75 MHz, CD_2Cl_2)** δ(ppm) 209.49, 175.24, 142.17, 140.79, 130.17, 129.61, 129.42, 129.23, 129.09, 128.71, 89.23, 74.81, 52.65, 39.79. **IR (neat):** 3771, 3087, 2921, 2083, 1966, 1851, 1471, 1308, 1005, 993, 859.

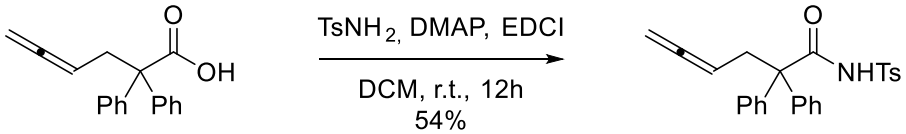

122 **135**

To a solution of p-toluensulfonamide (4.17 mmol), DMAP (8.34 mmol) and EDCI (8.34 mmol) in anhydrous DCM (90 mL) was added compound **122** (1 g, 3.79 mmol) and the reaction mixture was left to stir for 12h at room temperature. The reaction mixture was then cooled down to 5°C and HCl 10% was added to reach pH=1. Aqueous phase was extracted with a mixture of DCM/EtOH 9:1, while the organic phase was washed with H_2O and brine, collected, dried on $MgSO_4$ and concentrated under reduced pressure. The crude oil was purified by flash chromatography on a silica gel column using 20% AcOEt in hexanes as the eluent, to give **135** (liquid) in 54% yield.

^{1}H-NMR (300 MHz, CD_2Cl_2) δ(ppm) 7.98 (s, 1H), 7.75 (d, J= 8.24Hz, 2H), 4.87 – 4.83 (m, 1H), 4.51 – 4.47 (m, 2H), 3.07 – 3.02 (m, 2H), 2.49 (s, 3H); **^{13}C-NMR (75 MHz, CD_2Cl_2)** δ(ppm) 210.82, 172.04, 146.14,

140.82, 135.82, 130.22, 129.56, 129.46, 129.19, 129.05, 128.52, 88.12, 74.81, 62.55, 38.78, 22.21. **IR (neat):** 3731, 3105, 3100, 3088, 2972, 2139, 1988, 1939, 1697, 1656, 1478, 1365, 1235, 1113, 1078, 995, 951.

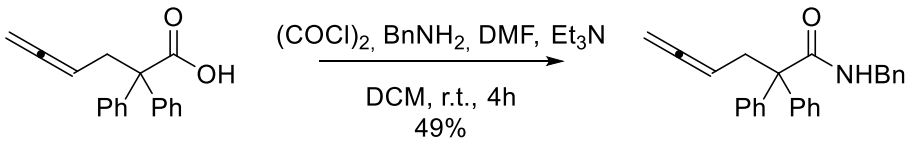

122 **136**

To a solution of **122** (allen acido) (320 mg, 1.2 mmol) in anhydrous DCM (10 mL) was added slowly oxalyl chloride (4.8 mmol) and a drop of DMF at 0°C. After 1h, solvent was evaporated and the residue was dissolved in anhydrous DCM. Benzylamine (3.6 mmol) and triethylamine (1.3 mmol) were then added and the reaction mixture was left to stir at room temperature overnight. Solvent was then evaporated under reduced pressure and the residue was dissolved in AcOEt. The organic phase was washed with a saturated solution of $NaHCO_3$, collected, dried over $MgSO_4$ and concentrated under reduced pressure. The crude oil was purified by flash chromatography on a silica gel column using 10% AcOEt in hexanes as the eluent, to give **136** (liquid) in 49% yield.

^{1}H-NMR (300 MHz, CD_2Cl_2) δ(ppm) 7.43 – 7.24 (m, 15H), 5.87 (bs, 1H), 5.12 – 4.97 (m, 1H), 4.48 – 4.41 (m, 4H), 3.27 – 3.23 (m, 2H); **^{13}C-NMR (75 MHz, CD_2Cl_2)** δ(ppm) 208.92, 175.37, 162.84, 142.23, 141.05, 130.18, 129.63, 129.44, 129.25, 129.10, 128.76, 89.34, 83.21, 75.44, 51.92, 38.41, 28.27. **IR (neat):** 3698, 3088, 2999, 2098, 1950, 1914, 1509, 1502, 1442, 1031, 992, 961.

10.3.3.2 Au(I)-catalyzed cyclization reaction

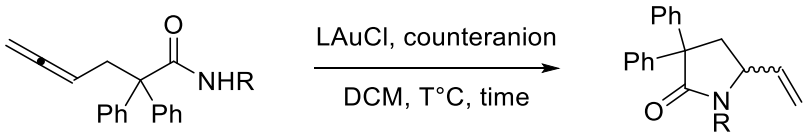

To a 3-dram vial were added the catalyst (5 mol% or 0.01 mol%) and the counterion (5 mol% or 0.5 mol %) in 2 mL anhydrous DCM as solvent. The mixture was stirred at r.t. for 15 min. Then 0.1 mmol of allenyl amide were added and the reaction was stirred at the selected temperature monitoring by TLC. Upon completion, the reaction was concentrated under reduced pressure. The residue was purified by silica gel flash column chromatography to obtain pure product.

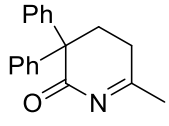

Compound **137b** (liquid) was prepared in 81% yield following General Procedure, using PPh_3AuCl (5 mol%) and AgOTs (5 mol%) at room temperature (*Table 5.7, entry 1*). Purification by silica gel flash column chromatography with 15% diethyl ether in hexanes. **^{1}H-NMR (300 MHz, $CDCl_3$)** δ 7.47 – 7.28 (m, 10H), 2.69 – 2.51 (m, 4H), 2.12 (s, 3H); **^{13}C-NMR (75 MHz, $CDCl_3$)** δ 180.10, 168.42, 141.49, 141.21, 128.47, 128.39, 128.13, 127.65, 57.10, 30.82, 28.65, 22.34. **IR (neat):** 3089, 2086, 1570, 1310, 1179, 993.

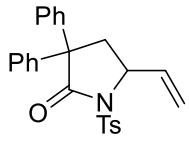

Compound **138a** (liquid) was prepared in 89% yield following General Procedure, using **cat-22** (0.01 mol%) and $NaBAr_4^F$ (0.5 mol%) at room temperature (*Table 5.8, entry 4*). Purification by silica gel flash column chromatography with 20% diethyl ether in hexanes. **^{1}H-NMR (300 MHz, $CDCl_3$)** δ 7.88 (d, J= 8.32Hz, 2H), 7.29 – 7.23 (m, 8H), 7.17 – 7.10 (m, 4H), 5.78 – 5.66 (m, 1H), 5.37 (d, J= 16.98Hz, 1H), 5.23 (d, J= 10.14Hz, 1H), 4.64 (q, J= 7.12Hz, 1H), 3.07 (dd, J= 13.23Hz, 6.99Hz, 1H), 2.61 (dd, J= 13.23 6.99Hz, 1H) 2.46 (s, 3H); **^{13}C-NMR (75 MHz, $CDCl_3$)** δ 173.99, 144.81, 141.44, 140.14, 136.73, 135.26, 129.23, 128.52, 128.41, 128.29, 127.59, 127.23, 127.13, 118.13, 59.65, 57.78, 53.29, 41.01, 21.56. **IR (neat):** 3090, 2980, 1875, 1818, 1460, 1303, 1182, 978.

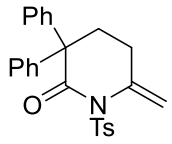

Compound **138b** (liquid) was prepared in 25% yield following General Procedure, using PPh_3AuCl (5 mol%) and AgOTs (5 mol%) at room temperature (*Table 5.8, entry 1*). Purification by silica gel flash column chromatography with 15% diethyl ether in hexanes. **^{1}H-NMR (300 MHz, $CDCl_3$)** δ 7.69 (d, J= 8.18Hz, 2H), 7.33 – 7.28 (m, 6H), 7.22 (d, J= 8.18Hz, 2H), 7.16 – 7.13 (m, 4H), 4.80 (d, J= 1.82, 1H), 4.29 (d, J= 1.82Hz, 1H), 2.71 – 2.67 (m, 2H), 2.54 – 2.49 (m, 2H), 2.40 (s, 3H); **^{13}C-NMR (75 MHz, $CDCl_3$)** δ 168.56, 153.26, 142.81, 141.48, 139.04, 128.89, 128.21, 128.17, 127.36, 126.77, 95.81, 54.69, 30.02, 23.24, 21.39. **IR (neat):** 3100, 3098, 2985, 2936, 1897, 1843, 1667, 1466, 1450, 1394, 1377, 1229, 1181, 1079, 992, 841.

10.4 Ligands synthesis

10.4.1 Synthesis Attempts for compound 145

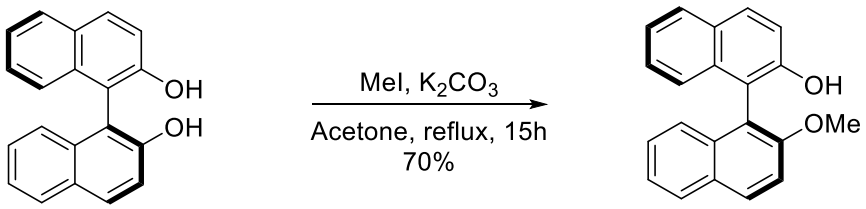

140

Compound **140** was synthetized following a reported procedure[82]. The spectroscopic data were in accordance with the literature data.

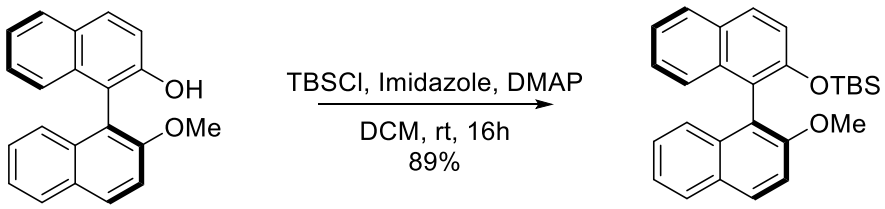

140 **141**

A solution of compound **140** (5 g, 16.6 mmol) in DCM (60 mL) was treated sequentially with imidazole (18.3 mmol), 4-N,N-dimethylaminopyridine (0.5 mmol) and tertbutyldimethylsilyl chloride (18.3 mmol). The reaction was stirred for 16 h at room temperature and concentrated to remove the solvent. The residue was then taken up in AcOEt and washed with saturated aqueous $NaHCO_3$ and brine and dried over $MgSO_4$. After concentration on a rotary evaporator, the crude oil was purified by flash chromatography on a silica gel column using 10% AcOEt in hexanes as the eluent to give **141** (liquid) in 89% yield.

^{1}H-NMR (300 MHz, CD_3CN) δ 8.05 – 8.03 (m, 1H), 7.96 – 7.90 (m, 3H), 7.55 (d, J= 9.10Hz, 1H), 7.36 – 7.32 (m, 3H), 7.30 – 7.27 (m, 2H), 7.06 – 7.04 (m, 1H), 3.76 (s, 3H), 0.47 (s, 9H), 0.00 (s, 3H), -0.06 (s, 3H); **^{13}C-NMR (75 MHz, CD_3CN)** δ 154.95, 151.08, 134.23, 133.88, 129.37, 129.31, 129.16, 129.00, 127.92, 127.84, 126.20, 126.13, 124.88, 124.87, 123.59, 123.32, 120.97, 113.65, 55.75, 24.38, 17.19, -5.21, -5.29.

[82] Tayama, E.; Sugawara, T. *Eur. J. Org. Chem* **2019**, 803

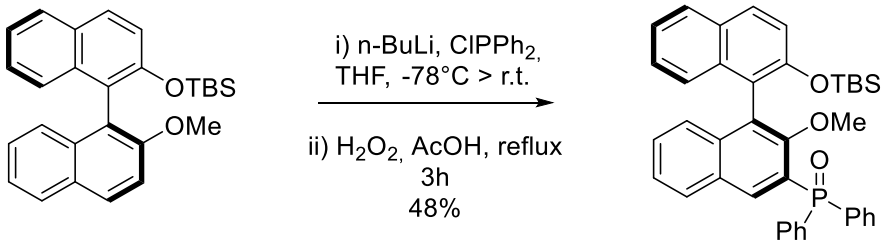

141 **142**

To a stirred solution of compound **141** (2 g, 4.82 mmol) in anhydrous THF (15 mL) at 0°C was added slowly a solution of nBuLi (8.75 mmol). Reaction was stirred for additional 2 hours and then cooled down to -78°C and $ClPPh_2$ (5.31 mmol) was added. The reaction mixture was gradually heated up at room temperature and stirred until completion, monitoring with TLC analysis. The mixture was then diluted with Et_2O and quenched with 1M HCl, extracted and the organic phases were washed with a saturated solution of Na_2CO_3 and Brine. After distillation of the solvent, the residue was dissolved in acetic acid (30 mL) and treated with H_2O_2 (0.72 mL). The reaction mixture was stirred at reflux for 3 hours and cooled down to 0°C. A solution of NaOH was added to quench the reaction, the aqueous phase was extracted with Et_2O and the combined organic phases were washed with water, dried over $MgSO_4$, filtered, and concentrated on a rotary evaporator. The crude oil was purified by flash chromatography on a silica gel column using 50% AcOEt in hexanes as the eluent to give **142** (liquid) in 48% yield.

^{1}H-NMR (500 MHz, $CDCl_3$) δ 8.81 – 8.78 (m, 1H), 8.12 – 8.07 (m, 2H), 8.03 – 7.97 (m, 2H), 7.95 – 7.90 (m, 2H), 7.68 – 7.66 (m, 1H), 7.64 – 7.61 (m, 3H), 7.58 – 7.55 (m, 3H), 7.49 – 7.46 (m, 2H), 7.42 – 7.41 (m, 2H), 7.38 – 7.32 (m, 3H), 2.70 (s, 3H), 0.57 (s, 9H), 0.24 (s,3H), 0.00 (s, 3H); **^{13}C-NMR (126 MHz, CD_2Cl_3)** δ 154.95, 151.08, 136.94, 136.88, 132.06, 131.98, 131.79, 131.70, 129.91, 129.20, 128.35, 128.25, 128.18, 128.14, 127.91, 126.68, 125.48, 125.23, 125.13, 123.84, 119.77, 53.42, 24.94, 17.33, -3.85, -4.57.

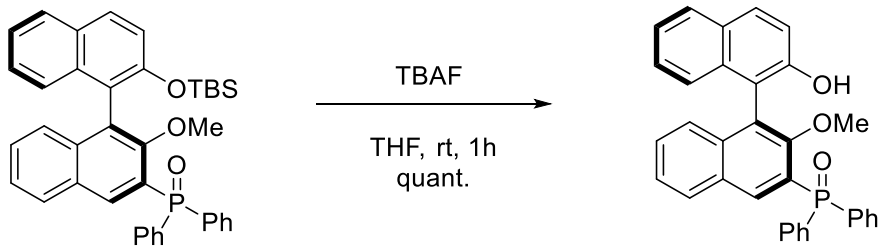

142 **143**

To a stirred solution of compound **142** (1.42 g, 2.31 mmol) in anhydrous THF (20 mL) was added a solution of TBAF (4.63 mmol). The reaction mixture was left to stir at room temperature for 1 hour, then quenched with a saturated solution of NH_4Cl. The aqueous phase was extracted with AcOEt and the combined organic phases were dried over $MgSO_4$, filtered, and concentrated on a rotary evaporator. The

crude oil was purified by flash chromatography on a silica gel column using 10% MeOH in DCM as the eluent to give **143** (liquid) in quantitative yield.

^{1}H-NMR (500 MHz, $CDCl_3$) δ 8.82 – 8.79 (m, 1H), 8.10 – 8.06 (m, 2H), 8.00 – 7.98 (m, 1H), 7.96 – 7.89 (m, 3H), 7.85 – 7.79 (m, 3H), 7.57 – 7.54 (m, 2H), 7.44 – 7.41 (m, 3H), 7.38 – 7.35 (m, 3H), 7.28 – 7.22 (m, 3H), 2.67 (s, 3H); **^{13}C-NMR (126 MHz, CD_2Cl_3)** δ 157.81, 155.09, 136.90, 136.87, 132.09, 131.91, 131.81, 131.73, 129.90, 129.17, 128.38, 128.22, 128.17, 128.13, 127.90, 126.70, 125.51, 125.20, 125.14, 123.79, 118.89, 54.52.

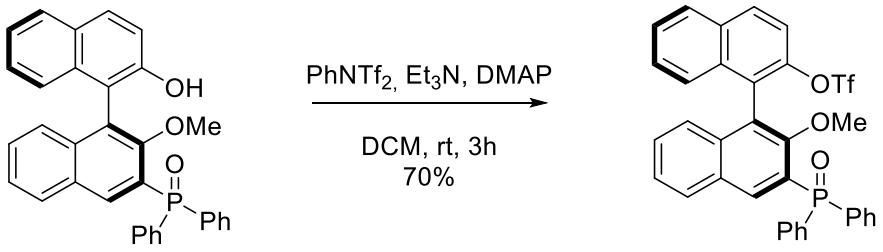

143 **144**

To a solution of **143** (1.15 g, 2.30 mmol) in dry DCM (10 mL) under Argon atmosphere N-Phenyl-bis(trifluoromethanesulfonimide) (2.76 mmol), triethylamine (3.68 mmol) and 4-N,N-dimethylaminopyridine (0.07 mmol) were added in succession and the reaction mixture was stirred at room temperature until completion reveal by TLC. The solution was poured into 0.5 N HCl and extracted with EtOAc. The organic phase was washed successively with water, 10% aqueous sodium bicarbonate and brine. The organic solution was dried over $MgSO_4$, filtered and the solvent was removed by rotary evaporation under reduced pressure. The crude product was purified by flash chromatography on a silica gel column using 30% AcOEt in hexanes as the eluent, to give **144** (white solid) in 50% yield;

^{1}H-NMR (500 MHz, $CDCl_3$) δ 8.82 – 8.79 (m, 1H), 8.09 – 8.03 (m, 2H), 7.99 – 7.97 (m, 1H), 7.94 – 7.88 (m, 3H), 7.84 – 7.77 (m, 3H), 7.59 – 7.55 (m, 2H), 7.46 – 7.44 (m, 2H), 7.40 – 7.37 (m, 2H), 7.35 – 7.31 (m, 2H), 7.26 – 7.19 (m, 3H), 2.72 (s, 3H); **^{13}C-NMR (126 MHz, $CDCl_3$)** δ 156.87, 151.43, 134.64, 133.71, 132.64, 132.06, 131.56, 129.90, 129.89, 129.07, 128.47, 128.15, 127.57, 126.46, 125.70, 125.13, 125.08, 124.69, 123.24, 117.63, 56.63.

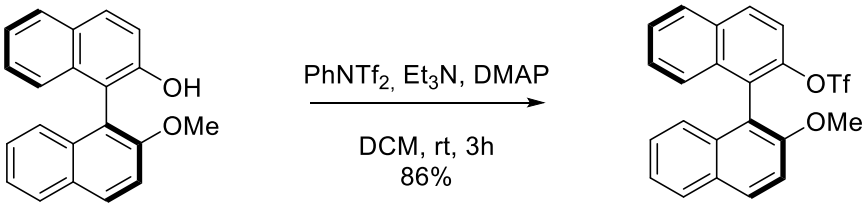

140 **146**

To a solution of **140** (3 g, 10 mmol) in dry DCM (30 mL) under Argon atmosphere N-Phenyl-bis(trifluoromethanesulfonimide) (12 mmol), triethylamine (16 mmol) and 4-dimethylaminopyridine (0.3 mmol) were added in succession and the reaction mixture was stirred at room temperature until completion reveal by TLC. The solution was poured into 0.5 N HCl and extracted with EtOAc. The organic phase was washed successively with water, 10% aqueous sodium bicarbonate and brine. The organic solution was dried over $MgSO_4$, filtered and the solvent was removed by rotary evaporation under reduced pressure. The crude product was purified by flash chromatography on a silica gel column using 10% AcOEt in hexanes as the eluent, to give **146** (white solid) in 86% yield;

The spectroscopic data were in accordance with the literature data[83].

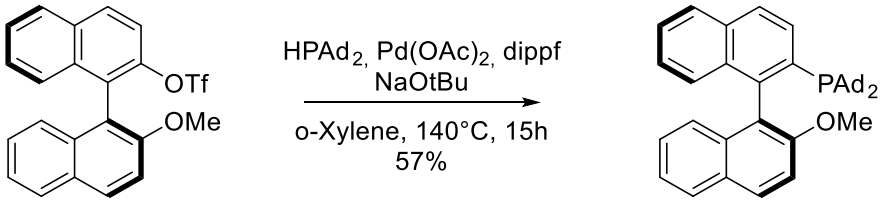

146 **147**

Under Argon atmosphere **146** (1 g, 2.39 mmol), $Pd(OAc)_2$ (0.19 mmol), dippf (0.24 mmol), di(1-adamantyl)phosphine (2.87 mmol), NaOtBu (2.51 mmol) and 10 mL dry o-xylene were added to a flamed dried Schlenk flask and the resulting suspension was stirred until apparently homogeneous (around 15 min). The reaction mixture was heated at 140°C in oil bath overnight, which then was cooled to room temperature. The residue was filtered through celite and washed with DCM. Solvent was evaporated under reduced pressure and purified by flash column chromatography on a silica gel column using 5% AcOEt in hexanes as the eluent, to give **147** (white solid) in 57% yield;

The spectroscopic data were in accordance with the literature data[84].

[83] Zhu, S.; Wang, C.; Chen, L.; Liang, R.; Yu, Y.; Jiang, H. *Org. Lett.* **2011**, 13, 5, 1146
[84] Wang, Z.; Nicolini, C.; Hervieu, C.; Wong, Y-F.; Zanoni, G.; Zhang, L *J. Am. Chem. Soc.* **2017**, *139*, 16064

10.4.2 Synthesis of cat-26

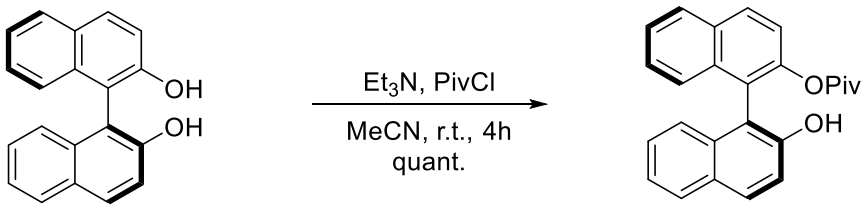

148

To a solution of (R)-Binol (5 g, 17.5 mmol) and triethylamine (52.4 mmol) in acetonitrile (50 mL) was added pivaloyl chloride (17.6 mmol) dropwise over a period of 1 h at 0°C. The mixture was allowed to warm to room temperature and stirred for 4 h. The reaction mixture was diluted with Et_2O and washed with aqueous 1N HCl, saturated aqueous $NaHCO_3$, and brine. The organic phase was dried over $MgSO_4$ and the solvent was evaporated. The crude product was purified by flash chromatography on a silica gel column using 15% AcOEt in hexanes as the eluent, to give **148** (white solid) in quantitative yield;

The spectroscopic data were in accordance with the literature data[85].

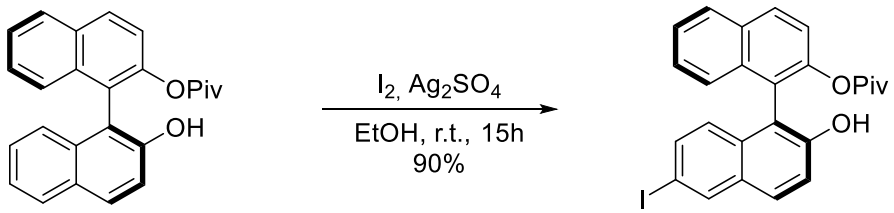

148 **149**

A mixture of I_2 (35 mmol) and Ag_2SO_4 (35 mmol) in EtOH (60 ml) was stirred until all the iodine had dissolved. Then **148** (17.5 mmol) was added and the mixture was stirred at room temperature for 15 h. After filtration, EtOH was removed by distillation. The residue was dissolved in $CHCl_3$ (50 ml) and the solution was washed with saturated $Na_2S_2O_3$. The organic layer was separated and dried over $MgSO_4$. After evaporation of the solvent, the crude product was purified by flash chromatography on a silica gel column using 5% AcOEt in hexanes as the eluent, to give **149** (white solid) in 90% yield;

The spectroscopic data were in accordance with the literature data[86].

[85] Hocke, H.; Uozumi, Y. *Tetrahedron* **2003**, *59*, 619
[86] Fehér, C.; Urbàn, B.; Urge, L.; Darvas, F.; Bakos, J.; Skoda-Foldes, R. *Tetrahedron Lett.* **2010**, *51*, 3629

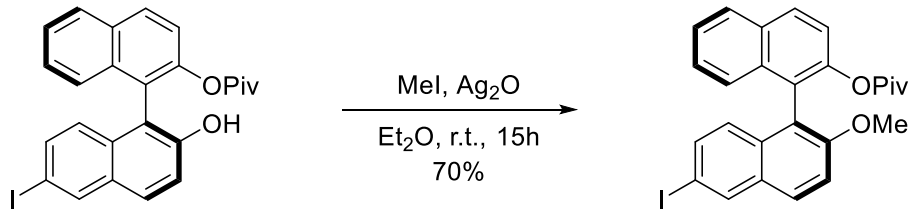

149 **150**

To a solution of **149** (7.8 g, 15.8 mmol) in Et_2O (150 mL) was added Ag_2O (38.8 mmol) and MeI (58.2 mmol). The mixture was stirred at ambient temperature for 15 h. The reaction mixture was filtered with EtOAc and washed with brine. The organic phase was dried over $MgSO_4$ and the solvent was evaporated. The crude product was purified by flash chromatography on a silica gel column using 5% AcOEt in hexanes as the eluent, to give **150** (white solid) in 70% yield;

^{1}H-NMR (500 MHz, $CDCl_3$) δ 8.24 (d, J= 6.21Hz, 1H), 8.01 – 7.94 (m, 2H), 7.87 – 7.85 (m, 1H), 7.47 – 7.40 (m, 4H), 7.33 – 7.22 (m, 2H), 6.88 (d, J= 12.11Hz, 1H), 3.77 (s, 3H), 0.78 (s, 9H); **^{13}C-NMR (126 MHz, $CDCl_3$)** δ 176.33, 155.39, 146.99, 136.26, 134.90, 133.55, 132.67, 131.70, 130.56, 129.20, 128.82, 128.21, 127.26, 126.55, 125.78, 125.47, 124.46, 123.64, 121.97, 114.30, 88.69, 56.66, 38.63, 26.53.

150 **151**

A 100 mL sealed tube equipped with a stir bar was charged with $(COOH{\cdot}H_2O)_2$ (13.1 mmol), $Pd(OAc)_2$ (0.09 mmol), PPh_3 (0.26 mmol), **150** (4.5 g, 8.75 mmol), Ac_2O (13.1 mmol), DIPEA (13.1 mmol), and DMF (40 mL) in air. The tube was quickly sealed with a Teflon® high pressure valve. The reaction mixture was then stirred in a preheated oil bath (100 °C) overnight. After filtration on a celite pad washing with Et_2O, the crude product was purified by flash chromatography on a silica gel column using 30% AcOEt in hexanes as the eluent, to give **151** (white solid) in quantitative yield;

^{1}H-NMR (500 MHz, $CDCl_3$) δ 8.15 (s, 1H), 8.00 – 7.97 (m, 2H), 7.87 – 7.85 (m, 1H), 7.45 – 7.40 (m, 2H), 7.38 – 7.34 (m, 2H), 7.33 – 7.22 (m, 2H), 6.88 (d, J= 12.11Hz, 1H), 3.75 (s, 3H), 0.77 (s, 9H); **^{13}C-NMR (126 MHz, $CDCl_3$)** δ 177.04, 169.33, 158.61, 147.23, 134.24, 133.41, 132.54, 131.42, 129.74, 129.09, 128.54, 128.21, 127.61, 126.40, 125.81, 125.02, 124.61, 123.31, 117.73, 115.98, 114.46, 114.63, 56.63, 38.37, 27.41.

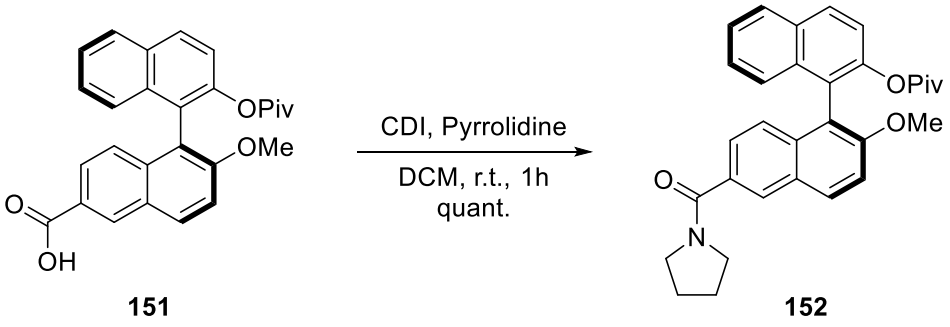

151 **152**

A solution of **151** (2.33 g, 5.4 mmol) in dichloromethane (27 mL) was treated in one portion with solid 1,1'-carbonyldiimidazole (5.97 mmol). The reaction mixture was allowed to stir at room temperature for 15 minutes. Pyrrolidine (5.97 mmol) was then added and the stirring continued for 1 hour at room temperature. The reaction mixture was then diluted with dichloromethane and washed with saturated $NaHCO_3$ solution. The organic phase was dried over $MgSO_4$ and the solvent was evaporated. The crude product was purified by flash chromatography on a silica gel column using 40% AcOEt in hexanes as the eluent, to give **152** (white solid) in quantitative yield;

^{1}H-NMR (500 MHz, $CDCl_3$) δ 8.03 (s, 1H), 7.98 – 7.95 (m, 2H), 7.92 – 7.90 (m, 1H), 7.44 – 7.41 (m, 2H), 7.38 – 7.37 (m, 1H), 7.33 (dd, J= 7.25Hz, 1.48Hz, 1H), 7.29 – 7.26 (m, 1H), 7.23 – 7.21 (m, 1H), 7.13 – 7.11 (m, 1H), 3.74 (s, 3H), 3.66 – 3.64 (m, 1H), 3.45 – 3.42 (m, 2H), 3.40 – 3.37 (m, 1H), 1.95 – 1.91 (m, 2H), 1.85 – 1.82 (m, 2H), 0.72 (s, 9H); **^{13}C-NMR (126 MHz, $CDCl_3$)** δ 178.05, 169.53, 156.81, 151.33, 134.61, 133.74, 132.54, 131.52, 129.99, 129.17, 128.51, 128.12, 127.53, 126.48, 125.74, 125.11, 124.69, 123.15, 117.43, 115.77, 114.59, 114.31, 60.41, 56.63, 53.44, 49.74, 46.33, 38.15, 27.46, 26.44, 24.46, 21.15, 14.23.

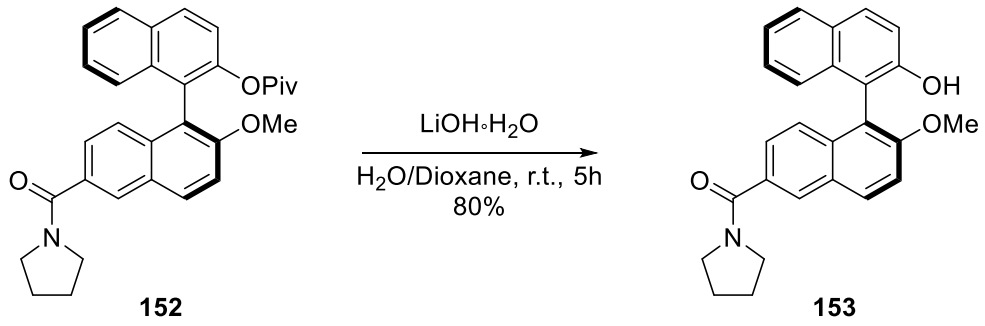

152 **153**

To a solution of **152** (1.9 g, 3.95 mmol) in 1,4-dioxane (10 mL) was added a solution of $LiOH{\cdot}H_2O$ (7.9 mmol) in H_2O (10 mL). The reaction mixture was stirred for 5 hours at room temperature. A solution of saturated NH_4Cl was added and the mixture was extracted with AcOEt. The organic phase was dried over $MgSO_4$ and the solvent was evaporated. The crude product was purified by flash chromatography on a silica gel column using 70% AcOEt in hexanes as the eluent, to give **153** (white solid) in 80% yield;

^{1}H-NMR (500 MHz, $CDCl_3$) δ 8.09 – 8.05 (m, 2H), 7.91 – 7.85 (m, 2H), 7.52 – 7.50 (m, 1H), 7.40 – 7.35 (m, 2H), 7.33 – 7.30 (m, 1H), 7.24 – 7.18 (m, 2H), 7.01 (d, J= 10,21, 1H), 3.82 (s, 3H), 3.69 – 3.66 (m, 2H), 3.50 – 3.47 (m, 2H), 1.98 – 1.96 (m, 2H), 1.88 – 1.85(m, 2H); **^{13}C-NMR (126 MHz, $CDCl_3$)** δ 169.63, 156.87, 151.43, 134.64, 133.71, 132.64, 131.56, 129.89, 129.07, 128.47, 128.15, 127.57, 126.46, 125.70, 125.08, 124.69, 123.24, 117.63, 115.83, 114.64, 114.36, 60.41, 56.63, 53.44, 49.74, 46.33, 26.44, 24.45, 21.05, 14.20.

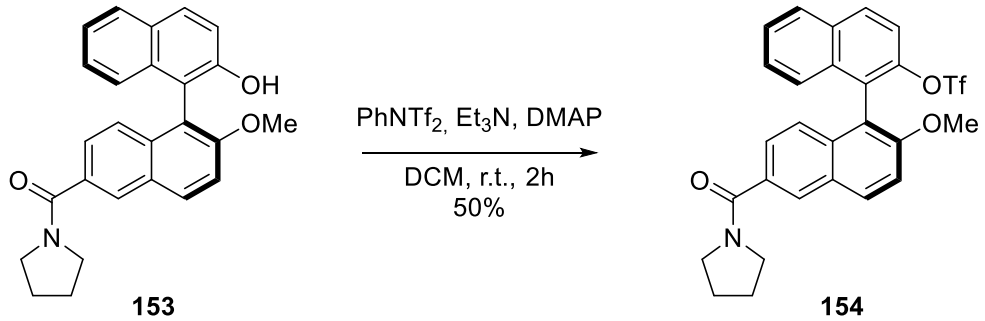

153 **154**

To a solution of **153** (1.25 g, 3.16 mmol) in dry DCM (10 mL) under Argon atmosphere N-Phenyl-bis(trifluoromethanesulfonimide) (3.82 mmol), triethylamine (5.01 mmol) and 4-dimethylaminopyridine (0.09 mmol) were added in succession and the reaction mixture was stirred at room temperature until completion reveal by TLC. The solution was poured into 0.5 N HCl (10 mL) and extracted with EtOAc. The organic phase was washed successively with water, 10% aqueous sodium bicarbonate and brine. The organic solution was dried over $MgSO_4$, filtered and the solvent was removed by rotary evaporation under reduced pressure. The crude product was purified by flash chromatography on a silica gel column using 30% AcOEt in hexanes as the eluent, to give **154** (white solid) in 50% yield;

^{1}H-NMR (500 MHz, $CDCl_3$) δ 8.01 – 7.99 (m, 2H), 7.96 (d, J= 9.13Hz, 1H), 7.89 (d, J= 8.25Hz, 1H), 7.48 (d, J= 9.05Hz, 1H), 7.46 – 7.44 (m, 1H), 7.40 (d, J= 9.13Hz, 1H), 7.32 – 7.26 (m, 2H), 7.19 – 7.17 (m, 1H), 6.94 (d, J= 8.85Hz, 1H), 3.75 (s, 3H), 3.62 – 3.58 (m, 2H), 3.44 – 3.41 (m, 2H), 1.91 – 1.86 (m, 2H), 1.82 – 1.77 (m, 2H); **^{13}C-NMR (126 MHz, $CDCl_3$)** δ 169.63, 156.87, 151.43, 134.64, 133.71, 132.64, 131.56, 129.89, 129.07, 128.47, 128.15, 127.57, 126.46, 125.70, 125.08, 124.69, 123.24, 117.63, 115.83, 114.64, 114.36, 60.41, 56.63, 53.44, 49.74, 46.33, 26.44, 24.45, 21.05, 14.20.

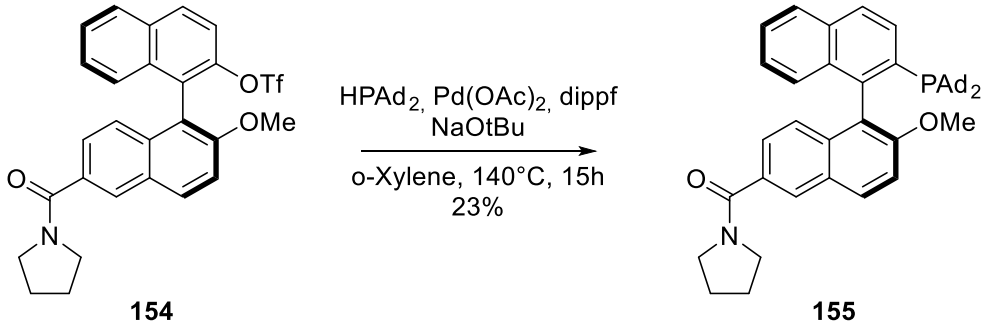

154 **155**

Under Argon atmosphere **154** (815 mg, 1.58 mmol), $Pd(OAc)_2$ (0.13 mmol), dippf (0.16 mmol), di(1-adamantyl)phosphine (1.9 mmol), NaOtBu (1.66 mmol) and 3 mL dry o-xylene were added to a flamed dried Schlenk flask and the resulting suspension was stirred until apparently homogeneous (around 15 min). The reaction mixture was heated at 140°C in oil bath overnight, which then was cooled to room temperature. The residue was filtered through celite and washed with DCM. Solvent was evaporated under reduced pressure and purified by flash column chromatography on a silica gel column using 10% AcOEt in hexanes as the eluent, to give **155** (white solid) in 23% yield;

^{1}H-NMR (400 MHz, $CDCl_3$) δ 8.05 – 7.99 (m, 3H), 7.90 – 7.86 (m, 2H), 7.44 – 7.42 (m, 1H), 7.39 (d, J= 7.57, 1H), 7.21 – 7.16 (m, 2H), 7.07 (d, J= 7.18Hz, 1H), 6.89 (d, J= 7.18Hz, 1H), 3.72 (s, 3H), 3.65 – 3.62 (m, 2H), 3.41 – 3.38 (m, 2H), 1.95 – 1.92 (m, 7H), 1.86 – 1.80 (m, 5H), 1.74 – 1.72 (m, 8H), 1.64 – 1.62 (m, 6H), 1.56 – 1.48 (m, 5H); **^{13}C-NMR (101 MHz, $CDCl_3$)** δ 170.11, 154.97, 144.41, 144.14, 134.79, 134.49, 134.27, 133.40, 133.36, 131.50, 130.20, 127.70, 127.65, 127.31, 127.20, 126.99, 126.36, 125.85, 125.43, 123.58, 112.82, 60.40, 55.18, 49.68, 46.20, 42.14, 42.04, 42.00, 41.90, 37.34, 37.22, 37.14, 37.07, 37.02, 36.93, 29.10, 29.03, 28.87, 28.80, 26.41, 24.50, 21.06, 14.21. **^{31}P-NMR (162 MHz, $CDCl_3$)** δ 27.60.

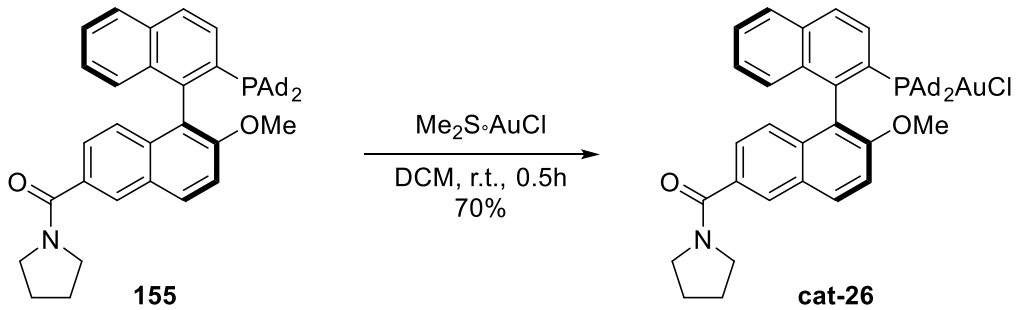

155 **cat-26**

To a solution of **155** (248 mg, 0.36 mmol) in 3 mL anhydrous DCM was added chloro(dimethylsulfide)gold(I) (0.327 mmol). The mixture was stirred for 30 min at room temperature and the solvent was evaporated off under reduced pressure. The crude gold complex was recrystallized three times with DCM and hexanes to give **cat-26** (white crystals) in 70% yield;

^{1}H-NMR (400 MHz, $CDCl_3$) δ 8.27 (s, 1H), 8.03 (d, J = 3.7 Hz, 2H), 7.98 (d, J = 8.1 Hz, 1H), 7.93 (d, J = 7.9 Hz, 1H), 7.55 – 7.50 (m, 1H), 7.42 – 7.40 (m, 1H), 7.22 – 7.18 (m, 2H), 7.01 (d, J = 8.5 Hz, 1H), 6.93 (d, J =

8.3 Hz, 1H), 3.95 (dt, J = 11.6, 6.2 Hz, 1H), 3.74 (dt, J = 12.3, 7.0 Hz, 1H), 3.66 – 3.55 (m, 2H), 3.22 (s, 3H), 2.32 – 2.11 (m, 12H), 2.04 – 1.82 (m, 8H), 1.81 – 1.74 (m, 1H), 1.74 – 1.58 (m, 13H); **^{13}C-NMR (101 MHz, $CDCl_3$)** δ 167.86, 151.74, 144.89, 144.80, 134.55, 134.48, 134.41, 134.06, 134.04, 131.27, 131.12, 130.91, 130.05, 130.03, 129.23, 128.21, 128.20, 128.11, 127.74, 127.68, 127.61, 126.81, 126.78, 126.76, 126.75, 126.57, 125.95, 125.56, 125.50, 125.21, 60.70, 48.80, 46.00, 43.54, 43.35, 42.82, 42.78, 42.76, 42.63, 42.44, 42.42, 36.45, 36.44, 36.27, 36.26, 28.80, 28.75, 28.72, 28.67, 26.00, 24.53. **^{31}P-NMR (162 MHz, $CDCl_3$)** δ 62.37.

10.5 Gold(I)-catalyzed Hydroalkoxylation of ene-ynes

10.5.1 Substrates Synthesis

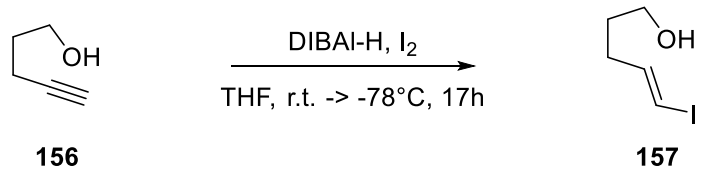

156 **157**

In a flamed round-bottom flask, to a solution of DIBAl-H (10.4 mmol) in hexanes was added 4-pentyn-1-ol **156** (250 mg, 2.97 mmol) at -20°C and then the reaction mixture was left stirring at r.t. overnight. Solvent was then evaporated under reduced pressure and the crude material was recovered using anhydrous THF (5 mL). A solution of iodine (3.57 mmol) in dry THF (4 mL) was then added to the reaction mixture at -78°C, and the reaction was left stirring for 1h at r.t.. The reaction mixture was poured into a solution of HCl (2M) and ice, and diluted with Et_2O. The organic phase was washed with brine, collected and dried over $MgSO_4$. After evaporation of the solvent under reduced pressure, the crude residue was used in the next step without further purification.

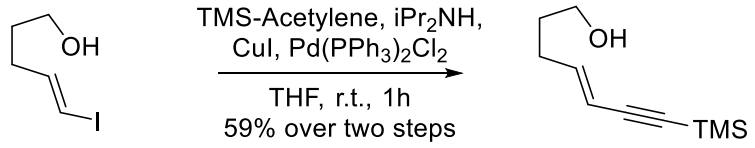

157 **158**

To a solution of **157** (2.97 mmol) in anhydrous and degassed THF (30 mL) were added $Pd(PPh_3)_2Cl_2$ (0.06 mmol), CuI (0.3 mmol), ethynyltrimethylsilane (6 mmol) and degassed diisopropylamine (22.6 mmol). The reaction mixture was left to stir for 1h at r.t.. The reaction mixture was quenched with aqueous $NaHCO_3$ and diluted with Et_2O. The organic phase was washed with a saturated solution of brine, collected, dried over $MgSO_4$ and concentrated under reduced pressure. The crude oil was purified by flash chromatography on a silica gel column using 20% AcOEt in hexanes as the eluent, to give **158** (liquid) in 59% yield over two steps.

The spectroscopic data were in accordance with the literature data[87].

[87] Ueda, Y.; Tsurugi, H.; Mashima, K. *Angew. Chem. Int. Ed.* **2020**, 59, 1552

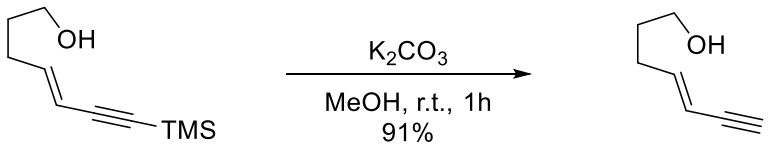

158 **159**

To a solution of **158** (320 mg, 1.75 mmol) in MeOH (6 mL) was added potassium carbonate (0.88 mmol) and stirring continued at r.t. overnight. The reaction mixture was quenched with HCl and diluted with AcOEt. The organic phase was washed with a saturated solution of brine, collected, dried over $MgSO_4$ and concentrated under reduced pressure. The crude oil was purified by flash chromatography on a silica gel column using 10% AcOEt in hexanes as the eluent, to give **159** (liquid) in 91% yield.

The spectroscopic data were in accordance with the literature data[88].

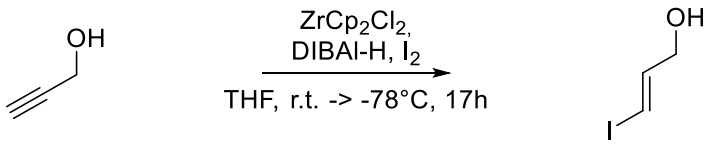

160 **161**

In a flamed round-bottom flask, to a suspension of $ZrCp_2Cl_2$ (9.81 mmol) in anhydrous THF (30 mL) was slowly added a solution of DIBAl-H (9.81 mmol) in toluene at 0°C. The reaction mixture was left to stir for 30 minutes at the same temperature and then was added propargyl alcohol (500 mg, 8.92 mmol). Temperature was risen to room temperature and stirring continued for 1 hour. A solution of iodine (11.6 mmol) in dry THF (15 mL) was then added to the reaction mixture at -78°C, and the reaction was left stirring until completion confirmed by TLC at the same temperature. The reaction mixture was poured into a solution of HCl (2M) and ice, and diluted with Et_2O. The organic phase was washed with brine $NaHCO_3$ and $Na_2S_2O_3$, collected and dried over $MgSO_4$. After evaporation of the solvent under reduced pressure, the crude residue was used in the next step without further purification.

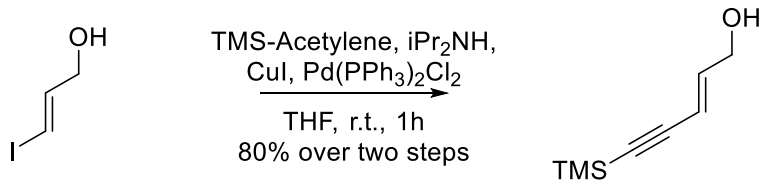

161 **162**

[88] Braddock, D.C.; Bhuva, R.; Pérez-Fuertes, Y.; Pouwer, R.; Roberts, C.A.; Ruggiero, A.; Stokes, E.S.E.; White, A.J.P. *Chem. Commun.* **2008**, 1419

To a solution of **161** (8.92 mmol) in anhydrous and degassed THF (45 mL) were added $Pd(PPh_3)_2Cl_2$ (0.18 mmol), CuI (0.9 mmol), ethynyltrimethylsilane (18.02 mmol) and degassed diisopropylamine (67.8 mmol). The reaction mixture was left to stir for 1h at r.t.. The reaction mixture was quenched with aqueous $NaHCO_3$ and diluted with Et_2O. The organic phase was washed with a saturated solution of brine, collected, dried over $MgSO_4$ and concentrated under reduced pressure. The crude oil was purified by flash chromatography on a silica gel column using 20% AcOEt in hexanes as the eluent, to give **162** (liquid) in 80% yield over two steps.

The spectroscopic data were in accordance with the literature data[89].

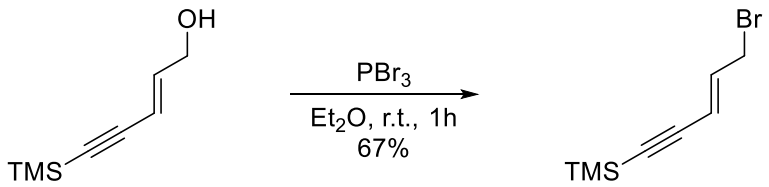

162 **163**

To a solution of **162** (1.1 g, 7.14 mmol) in anhydrous Et_2O (25 mL) was slowly added PBr_3 (3.57 mmol) at 0°C. After 30 minutes at this temperature, the reaction was heated up to r.t. and stirred for additional 30 minutes. The reaction mixture was quenched by adding ice and diluted with Et_2O. The organic phase was washed with a saturated solution of brine, collected, dried over $MgSO_4$ and concentrated under reduced pressure. The crude oil was purified by flash chromatography on a silica gel column using 5% AcOEt in hexanes as the eluent, to give **163** (liquid) in 67% yield.

The spectroscopic data were in accordance with the literature data[90].

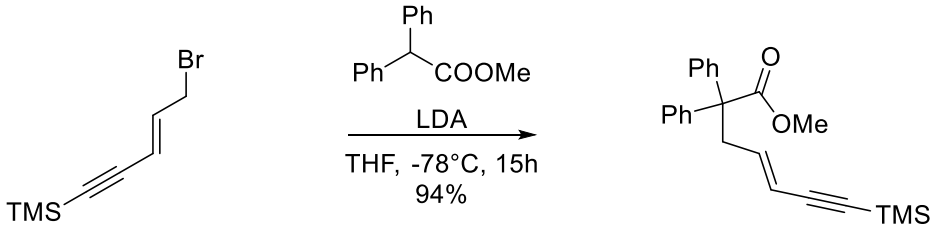

163 **164**

To a solution of diisopropylamine (8.6 mmol) in anhydrous THF (25 mL) was added slowly nBuLi (7.89 mmol) at -30°C under Argon. The temperature was risen to 0°C and kept for 30 minutes to obtain a pale yellow solution. The reaction mixture was cooled down to -78°C and methyl 2,2-diphenylacetate (5.74

[89] Trost, B.M.; Papillon, J.P.N.; Nussbaumer, T. *J. Am. Chem. Soc.* **2005**, 127, 17921
[90] Arai, S.; Koike, Y.; Hada, H.; Nishida, A. *J. Am. Chem. Soc.* **2010**, 132, 4522

mmol) was added. After 5 hours at the same temperature, bromide **163** was added (1.04 g, 4.78 mmol) and the reaction mixture was heated up to room temperature and stirred overnight. The reaction mixture was quenched with a saturated solution of NH_4Cl and then extracted with Et_2O. The combined organic phases were dried over $MgSO_4$, filtered, and concentrated on a rotary evaporator. The crude oil was purified by flash chromatography on a silica gel column using 5% AcOEt in hexanes as the eluent, to give **164** (liquid) in 94% yield.

^{1}H-NMR (300 MHz, $CDCl_3$) δ 7.37-7.25 (m, 10H); 6.02-5.95 (m, 1H); 5.44 (d, J=15.9 Hz, 1H); 3.73 (s, 3H); 3.2 (d, J=7.26 Hz, J=1.35 Hz, 2H); 0.17 (s, 9H); **^{13}C-NMR (75 MHz, $CDCl_3$)** δ 174.10, 141.90, 140.71, 128.73, 128.50, 128.49, 127.90, 127.18, 126.94, 113.00, 103.59, 93.38, 60.22, 52.38, 41.98, -0.17. **IR (neat):** 3021, 2540, 1879, 1873, 1498, 1368, 1346, 1096, 1091, 991.

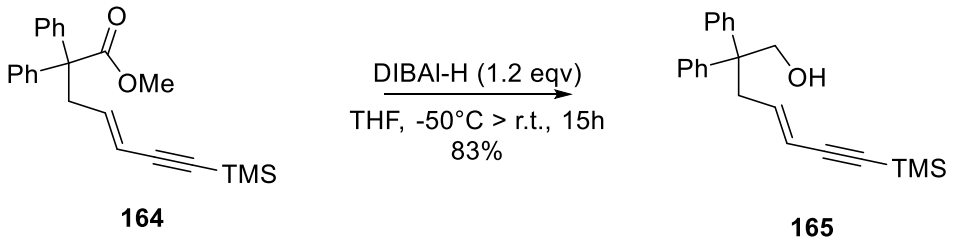

164 **165**

To a solution of **164** (1.6 g, 4.49 mmol) in anhydrous toluene (5 mL) at -50°C was added a solution of DIBAl-H (9.44 mmol) in toluene. The reaction was then stirred for 2 hours at the same temperature. The reaction mixture was heated up to 0°C and then was quenched by adding H_2O and aqueous NaOH alternatively and diluted with Et_2O. The mixture was then heated at r.t. and $MgSO_4$ was added, and then stirring for additional 15 minutes. The resulting suspension was filtered over a silica pad, washed with AcOEt and concentrated under reduced pressure. The crude oil was purified by flash chromatography on a silica gel column using 10% to 20% AcOEt in hexanes as the eluent, to give **165** (liquid) in 83% yield.

^{1}H-NMR (300 MHz, $CDCl_3$) δ 7.37 – 7.19 (m, 10H), 5.91 – 5.81 (m, 1H), 5.61 (d, J= 15.89 Hz, 1H), 4.16 (s, 2H), 3.05 (dd, J= 7.27 Hz, 1.22 Hz, 2H), 0.17 (s, 9H); **^{13}C-NMR (75 MHz, $CDCl_3$)** δ 144.67, 141.08, 128.26, 127.94, 126.47, 112.88, 103.57, 93.22, 67.89, 51.68, 40.14, -0.18. **IR (neat):** 3103, 3085, 3021, 2968, 2541, 1498, 1359, 1096, 1091, 971.

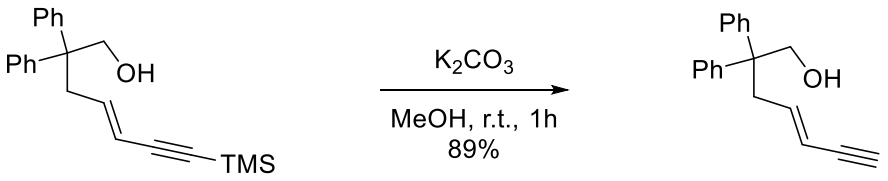

165 **166**

To a solution of **165** (1.25 g, 3.73 mmol) in MeOH (12 mL) was added potassium carbonate (1.86 mmol) and stirring continued at r.t. overnight. The reaction mixture was quenched with HCl and diluted with AcOEt. The organic phase was washed with a saturated solution of brine, collected, dried over $MgSO_4$ and concentrated under reduced pressure. The crude oil was purified by flash chromatography on a silica gel column using 10% to 20% AcOEt in hexanes as the eluent, to give **166** (liquid) in 89% yield.

^{1}H-NMR (300 MHz, $CDCl_3$) δ 7.39-7.19 (m, 10H); 5.97-5.89 (m, 1H); 5.57-5.50 (m, 1H); 4.16 (s, 2H); 3.08 (dd, J=7.37 Hz, J=0.9 Hz, 2H); 2.82 (d, J=2.18 Hz, 1H); **^{13}C-NMR (75 MHz, $CDCl_3$)** δ 145.80, 143.25, 129.04, 128.78, 127.25, 112.31, 82.85, 76.77, 68.45, 52.44, 40.61. **IR (neat):** 3907, 3321, 3104, 3089, 2961, 2447, 1795, 1247, 1222, 1192, 1030, 994, 987.

10.5.2 Au(I)-catalyzed hydroalkoxylation reaction

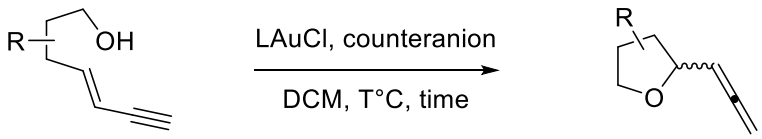

To a 3-dram vial were added the catalyst (5 mol% or 0.01 mol%) and the counterion (5 mol% or 0.5 mol %) in 2 mL anhydrous DCM as solvent. The mixture was stirred at r.t. for 15 min. Then 0.1 mmol of ene-yne were added and the reaction was stirred at the selected temperature monitoring by TLC. Upon completion, the reaction was concentrated under reduced pressure. The residue was purified by silica gel flash column chromatography to obtain pure product.

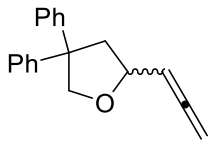

Compound **168a** (liquid) was prepared in 61% yield following General Procedure, using **cat-26** (5 mol%) and $NaBAr_4^F$ (5 mol%) at room temperature (*Table 7.4, entry 3)*. Purification by silica gel flash column chromatography with 5% diethyl ether in hexanes. **^{1}H-NMR (300 MHz, $CDCl_3$)** δ 7.35-7.20 (m, 10 H); 5.28 (q, J= 6.74 Hz, 1H); 4.85-4.77 (m, 2H); 4.66-4.56 (m, 2H); 4.19 (d, J = 8.72 Hz, 1H); 2.76-2.70 (m, 1H); 2.59-2.52 (m, 1H); **^{13}C-NMR (75 MHz, $CDCl_3$)** δ 208.19, 145.83, 145.41, 128.31, 128.25, 128.05, 127.05, 126.97, 126.39, 126.21, 92.32, 55.93, 44.80, 31.47, 29.58. **IR (neat):** 3101, 3089, 2880, 2049, 1312, 995, 986, 913.

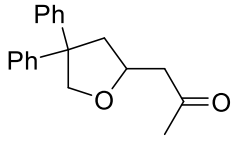

Compound **168b** (liquid) was prepared in 64% yield following General Procedure, using PPh_3AuCl (5 mol%) and $AgNTf_2$ (5 mol%) at room temperature (*Table 7.2, entry 1)*. Purification by silica gel flash column chromatography with 15% diethyl ether in hexanes. **^{1}H-NMR (300 MHz, $CDCl_3$)** δ 7.34-7.19 (m, 10H); 4.57 (d, J= 8.76 Hz, 1H); 4.49-4.43 (m, 1H); 4.21 (d, J= 8.79 Hz, 1H); 2.87-2.78 (m, 2H); 2.61 (dd, J=16.09 Hz, J=5.71 Hz, 1H); 2.33 (dd, J= 12.28 Hz, J= 9.1 Hz, 1H); 2.19 (s, 3H); **^{13}C-NMR (75 MHz, $CDCl_3$)** δ 206.92, 145.66, 128.34, 128.29, 126.99, 126.94, 126.38, 126.24, 76.67, 74.52, 55.74, 49.68, 44.57, 30.65. **IR (neat):** 3106, 3088, 2993, 2937, 2905, 1944, 1601, 1318, 1314, 995, 986.

10.5.3 Au(I)-catalyzed bromoetherification reaction

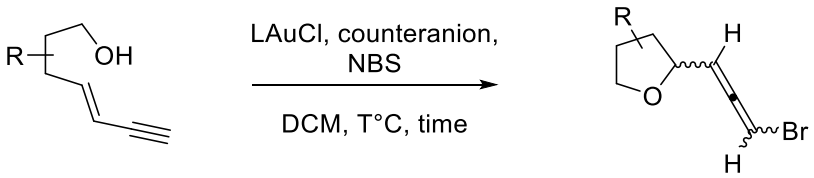

To a 3-dram vial were added the catalyst (5 mol% or 0.01 mol%) and the counterion (5 mol% or 0.5 mol%) in 2 mL anhydrous DCM as solvent. The mixture was stirred at r.t. for 15 min. Then 0.1 mmol of ene-yne and NBS (1.1 eqv) were added and the reaction was stirred at the selected temperature monitoring by TLC. Upon completion, the reaction was concentrated under reduced pressure. The residue was purified by silica gel flash column chromatography to obtain pure product.

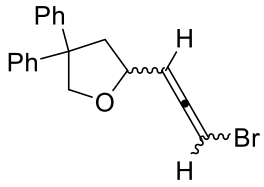

Compound **170** (liquid) was prepared in 73% yield following General Procedure, using **cat-26** (5 mol%) and $NaBAr_4^F$ (5 mol%) at room temperature (*Table 7.6, entry 2)*. Purification by silica gel flash column chromatography with 5% diethyl ether in hexanes. **^{1}H-NMR (400 MHz, $CDCl_3$)** δ 7.17 – 7.12 (m, 6H), 7.08 – 7.05 (m,4H), 5.92 – 5.84 (m, 1H), 5.37 – 5.30 (m, 1H), 4.51 – 4.48 (m, 2H), 4.07 – 4.04 (m, 1H), 2.65 – 2.59 (m, 1H), 2.46 – 2.40 (m, 1H); **^{13}C-NMR (101 MHz, $CDCl_3$)** δ 201.32, 146.69, 146.17, 129.23, 129.19, 129.07, 128.31, 128.29, 128.12, 127.99, 102.3, 75.6, 73.7, 68.2, 31.4, 25.5. **IR (neat):** 3113, 3105, 3101, 2996, 2939, 2891, 1794, 1374, 1313, 1248, 1155, 995, 987, 749.

10.6 Gold(I)-catalyzed Hydroalkoxylation of allylic alcohols

10.6.1 Substrates Synthesis

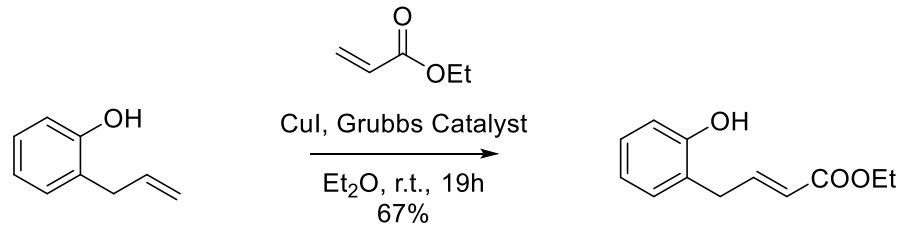

173 **174**

To a solution of 2-allyl phenol (500 mg, 3.73 mmol) in anhydrous Et_2O (50 mL) were added in order ethyl acrylate (9.32 mmol), CuI (0.075 mmol), and 2nd Generation Grubbs Catalyst (0.075 mmol). The reaction mixture was left to stir for 19 hours at room temperature and after then solvent was concentrated under reduced pressure. The crude oil was purified by flash chromatography on a silica gel column using 10% to 30% AcOEt in hexanes as the eluent, to give **174** (liquid) in 67% yield.

^{1}H-NMR (300MHz, $CDCl_3$): δ 7.20-7.40 (m, 3H); 6.70-6.85 (m, 2H); 6.5 (s, 1H); 5.80-5.90 (d, J=15.62, 1H); 4.19-4.30 (dd, J=7.13, 2H); 3.50-3.55 (d, J=5.48, 2H); 1.25-1.30 (t, J=7.15, 3H); **^{13}C-NMR (75MHz, $CDCl_3$):** δ 167.51, 153.97, 147.83, 130.42, 127.98, 124.06, 121.50, 120.48, 115.35, 77.40, 76.98, 76.55, 60.53, 33.03, 14.06. **IR (neat):** 3759, 3101, 2005, 2002, 1601, 1539, 1439, 1248, 700.

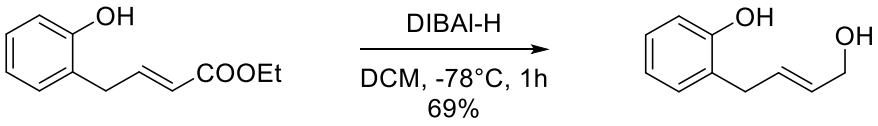

174 **175**

To a solution of ester **174** (410 mg, 2.50 mmol) in anhydrous DCM (25 mL) at -78°C was added a solution of DIBAl-H in toluene (5.24 mmol). The reaction mixture was then stirred at the same temperature until completion confirmed by TLC. The reaction mixture was quenched with MeOH and then heated up to room temperature. The organic phase was washed with a saturated solution of potassium sodium tartrate and brine, collected, dried over $MgSO_4$ and concentrated under reduced pressure. The crude oil was purified by flash chromatography on a silica gel column using 10% to 50% AcOEt in hexanes as the eluent, to give **175** (liquid) in 69% yield.

^{1}H-NMR (300MHz, $CDCl_3$): δ 7.16 - 7.11 (m, 2H); 6.90 (dt, J=7.41Hz, J=1.2Hz, 1H); 6.89 - 6.79 (m, 1H); 5.95 - 5.87 (m, 1H); 5.78 - 5.71 (m, 1H); 4.13 (dt, J=6.87 Hz, J=1.24 Hz, 3H); 3.42 (d, J= 6.14 Hz, 1H); **^{13}C-NMR (75MHz, $CDCl_3$):** δ 154.75, 131.36, 131.08, 130.96, 128.43, 126.79, 121.48, 116.24, 63.97, 33.83. **IR (neat):** 3758, 3093, 3088, 2955, 2924, 1741, 1570, 1441, 1404, 1365, 1199, 695.

10.6.2 Au(I)-catalyzed cyclization reaction

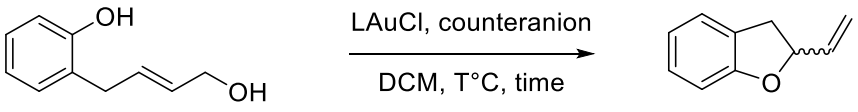

175 **176**

To a 3-dram vial were added the catalyst (5 mol%) and the counterion (5 mol%) in 2 mL anhydrous DCM as solvent. The mixture was stirred at r.t. for 15 min. Then 0.1 mmol of monoallylic diol **175** were added and the reaction was stirred at the selected temperature monitoring by TLC. Upon completion, the reaction was concentrated under reduced pressure. The residue was purified by silica gel flash column chromatography (5% Et_2O in hexanes) to obtain pure product.

^{1}H-NMR (300MHz, $CDCl_3$): δ 7.18-7.09 (m, 2H); 6.87-6.79 (m, 2H); 6.03-5.78 (m, 1H); 5.39-5.28 (m, 1H); 5.25-5.15 (m, 2H); 3.38 (dd, J = 15.4 Hz, 9.1Hz, 1H); 3.00 (dd, J = 15.4 Hz, 7.7 Hz, 1H); **^{13}C-NMR (75MHz, $CDCl_3$):** δ 137.65, 128.34, 126.77, 125.10, 120.71, 117.10, 109.64, 83.73, 36.18. **IR (neat):** 3101, 2102, 1940, 1652, 1199, 1191, 1004.

11 Appendix I – Chromatograms

11.1 Gold(I)-catalyzed Desymmetrization of Bisallenols

Scheme 4.8 - Column IB-3, flux 1 ml/min, Heptane/iPrOH=99.2/0.8, λ=208 nm

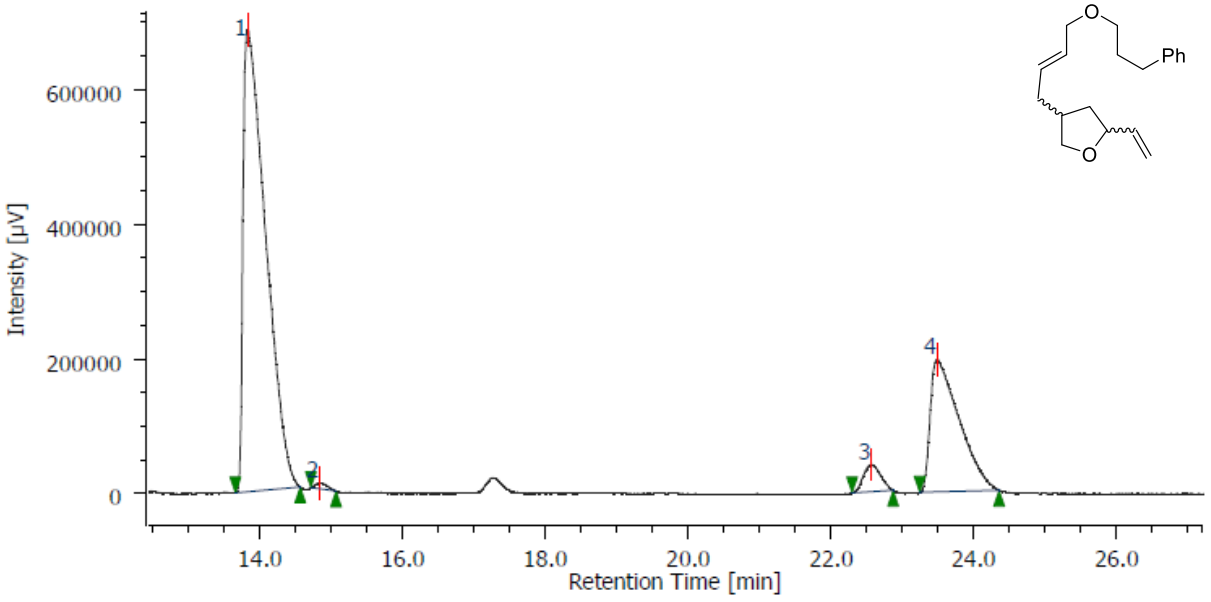

Peak	t_R (min)	Area (µV·sec)	Area %	Height %
1	13.827	15023924	70.479	73.647
2	14.840	107619	0.505	0.976
3	22.560	674136	3.162	4.316
4	23.480	5511317	25.854	21.062

Table 4.1 - Column OD-3, flux 1 ml/min, Heptane/iPrOH=98/2, λ=220 nm

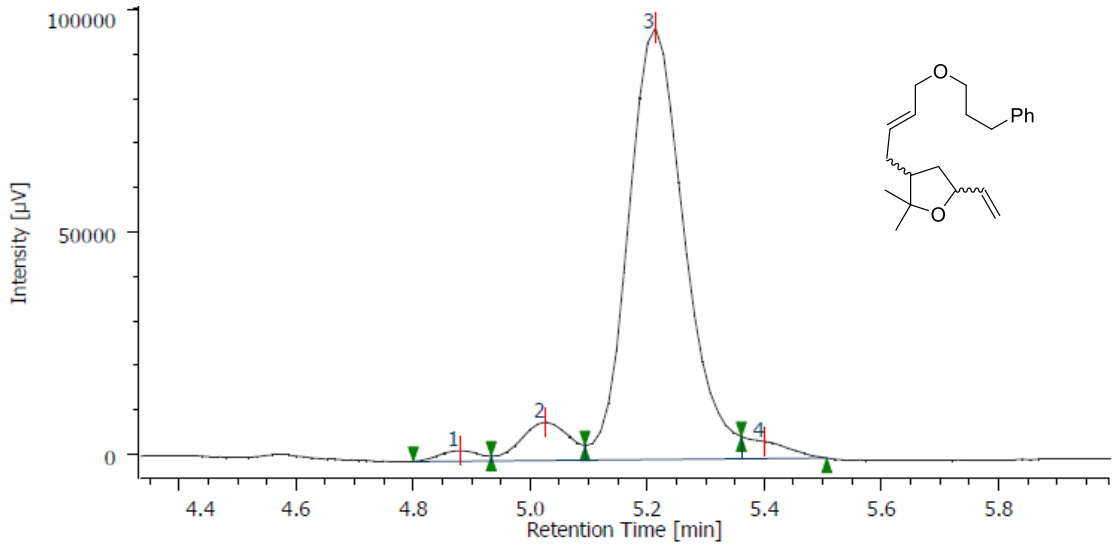

Peak	t_R (min)	Area (µV·sec)	Area %	Height %
1	4.880	11430	1.581	2.144
2	5.027	49398	6.833	7.706
3	5.213	640217	88.560	86.696
4	5.400	21878	3.026	3.454

Table 4.1 - Column OJ-3R, flux 0.8 ml/min, ACN/H_2O=40/60 12 min, 10/90, λ=220 nm

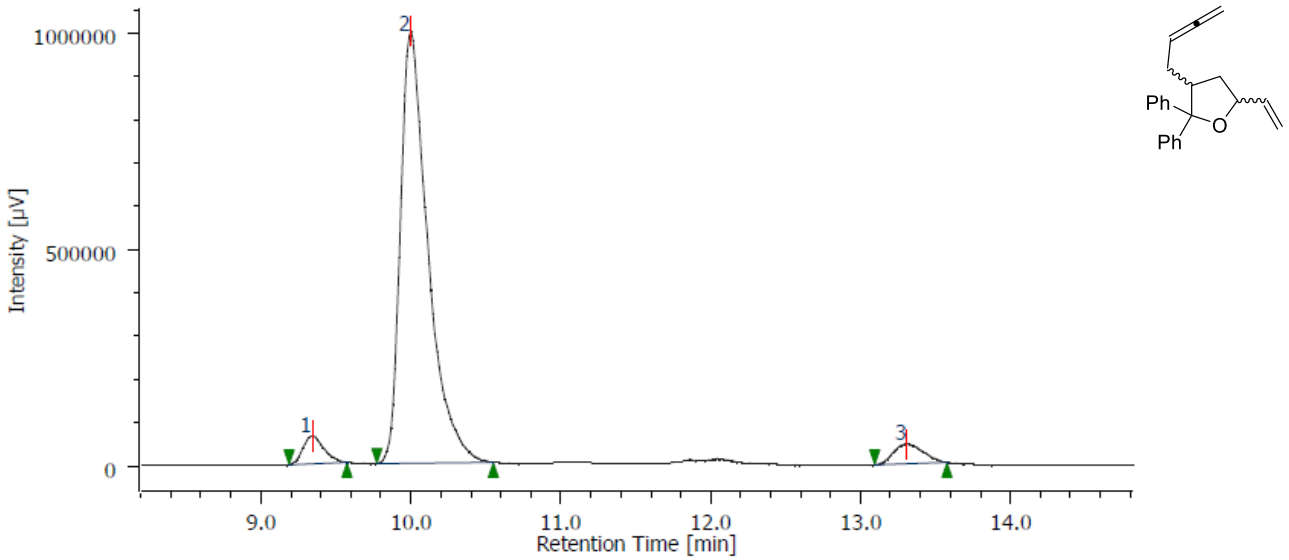

Peak	t_R (min)	Area (µV·sec)	Area %	Height %
1	9.347	626645	4.482	5.774
2	10.000	12720840	90.988	90.113
3	13.307	633292	4.530	4.113

Table 4.1 - Column OJ-3, flux 1 ml/min, Heptane/iPrOH=99/1, λ=220 nm

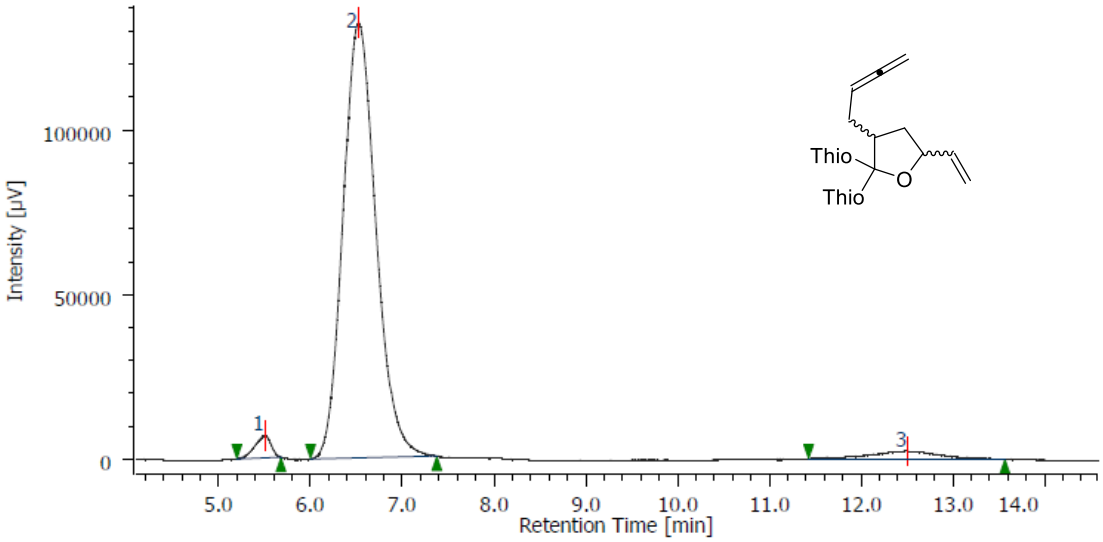

Peak	t_R (min)	Area (µV·sec)	Area %	Height %
1	5.507	80791	2.310	4.777
2	6.520	3290433	94.070	93.586
3	12.507	126622	3.620	1.637

Table 4.1 - Column GT-A 0.25, 30m, Temperature 220/100, 60min iso 8/min 170, 5min iso/350, Gas H_2 0.6 bar (Courtesy of Max Planck Institute)

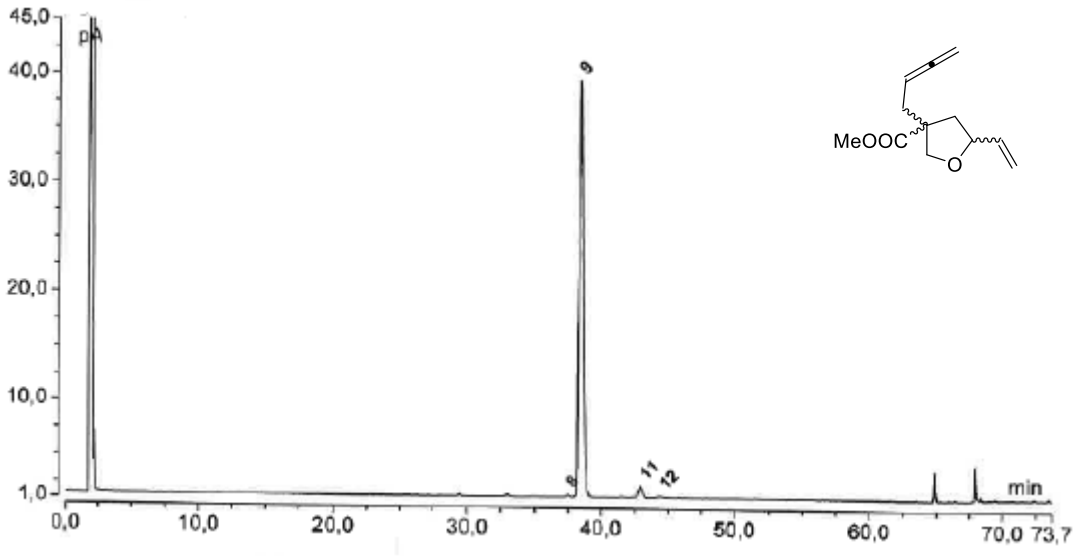

Peak	t_R (min)	Area %
8	37.45	0.32
9	38.34	96.68
11	42.94	2.64
12	44.42	0.37

Table 4.1 - Column OZ-3R, flux 1 ml/min, ACN/H_2O=99.5/0.5, λ=220 nm (Courtesy of Max Planck Institute)

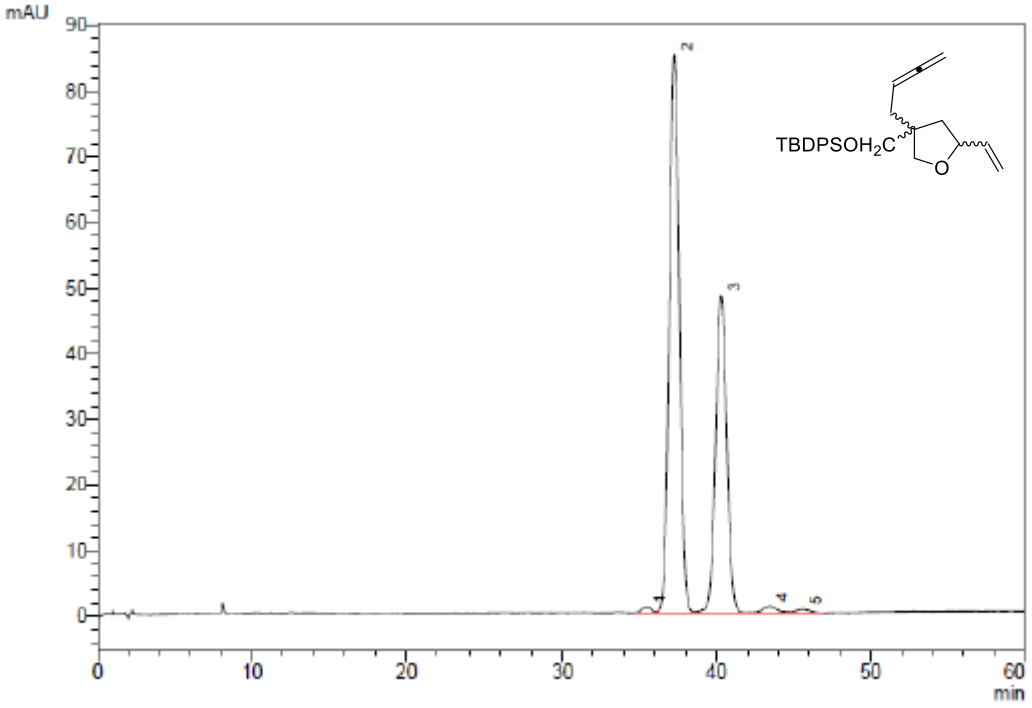

Peak	t_R (min)	Area %
1	35.49	0.61
2	37.26	60.15
3	40.32	37.61
4	43.44	1.05

Table 4.1 - Column OJ-H, flux 1 ml/min, Heptane/iPrOH=98/2, λ=208 nm

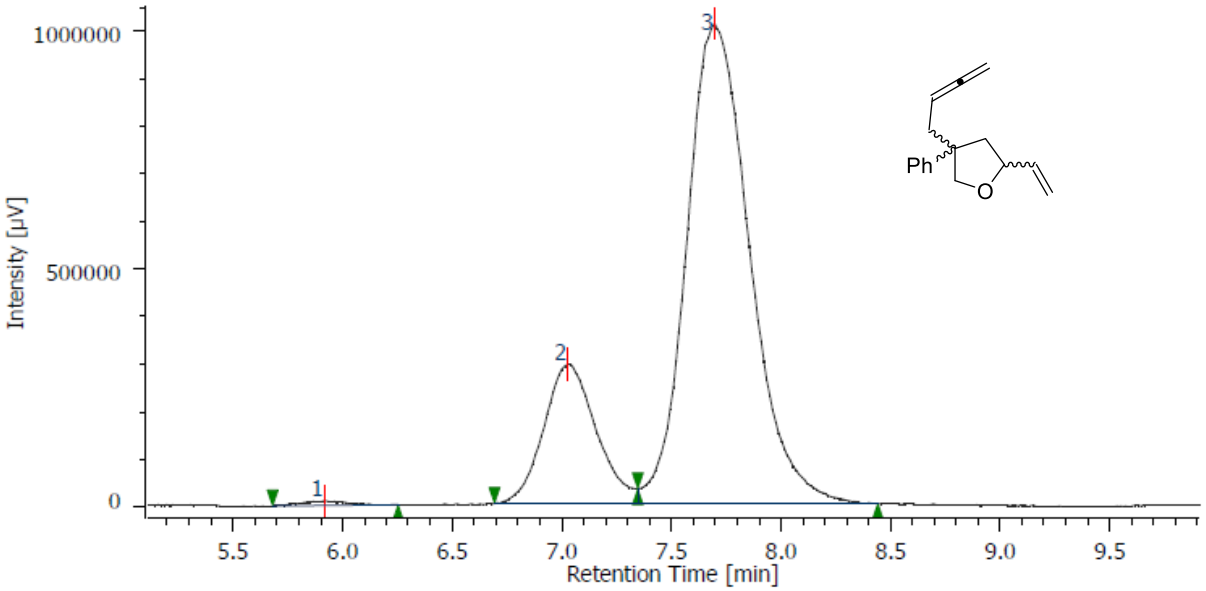

Peak	t_R (min)	Area (µV·sec)	Area %	Height %
1	5.920	129498	0.517	0.713
2	7.027	4859636	19.411	22.307
3	7.693	20046657	80.072	76.980

Table 4.1 - Column IA-3, flux 0.8 ml/min, Heptane/iPrOH=96/4, λ=220 nm

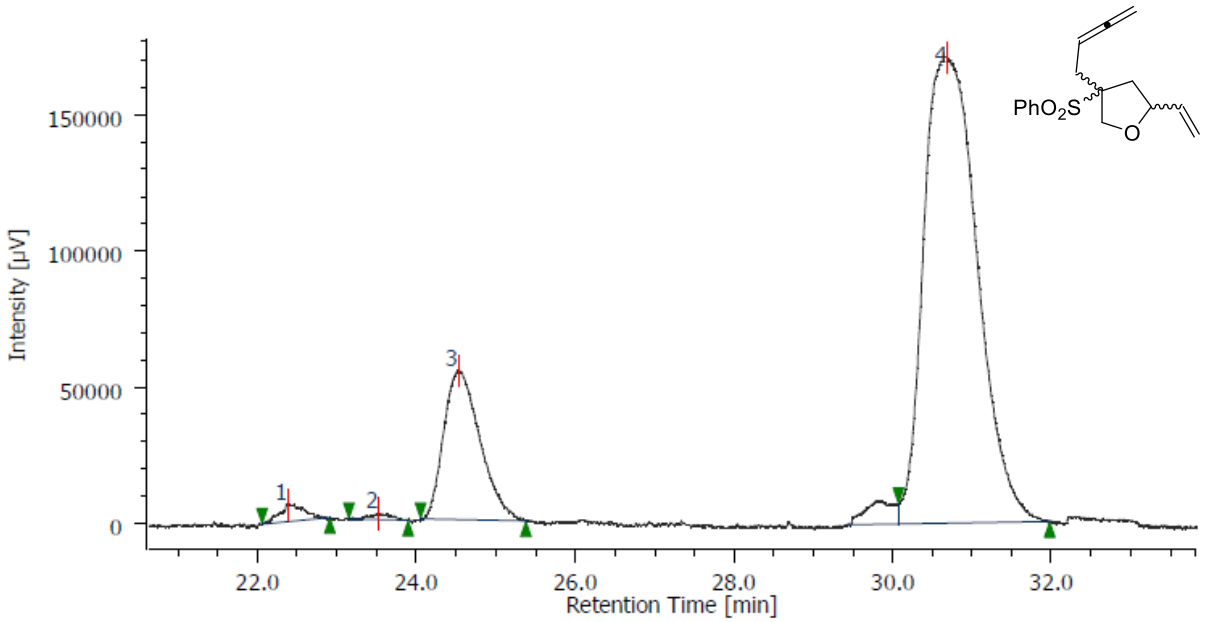

Peak	t_R (min)	Area (µV·sec)	Area %	Height %
1	22.387	136878	1.374	2.525
2	23.533	41920	0.421	0.949
3	24.533	1741794	17.480	23.447
4	30.693	8043868	80.726	73.078

Scheme 4.8 - Column IB-3, flux 0.5 ml/min, Heptane/iPrOH=99.6/0.4, λ=215 nm

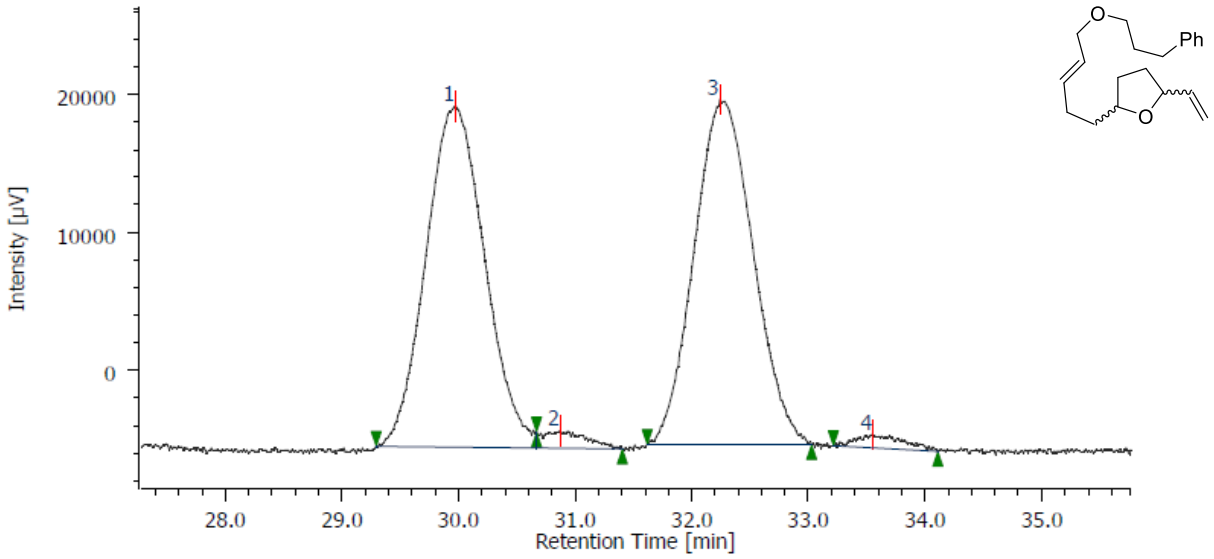

Peak	t_R (min)	Area (µV·sec)	Area %	Height %
1	29.973	866752	47.964	47.570
2	30.867	33308	1.843	2.457
3	32.240	879372	48.663	48.155
4	33.547	27647	1.530	1.817

Table 4.2 - Column OD-3, flux 0.8 ml/min, Heptane/iPrOH=99.5/0.5, λ=210 nm

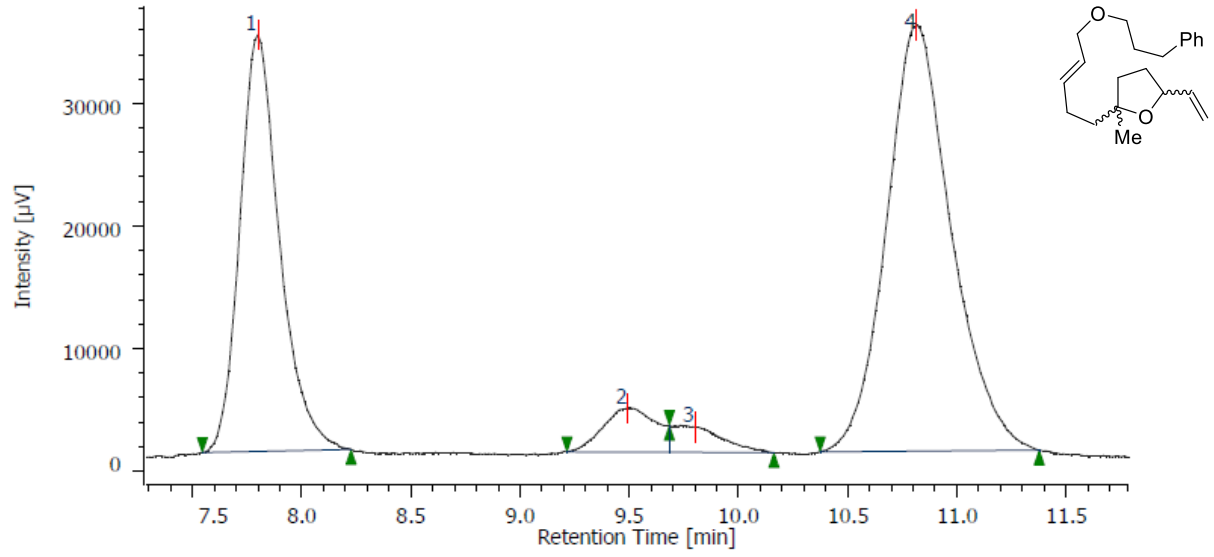

Peak	t_R (min)	Area (µV·sec)	Area %	Height %
1	7.800	428448	34.577	45.707
2	9.493	59978	4.840	4.811
3	9.800	34112	2.753	2.749
4	10.813	716566	57.829	46.733

Table 4.2 - Column BGB-176/BGB-15 0.25, 30m, Temperature 220/115 iso/350, Gas H_2 0.8 bar (Courtesy of Max Planck Institute)

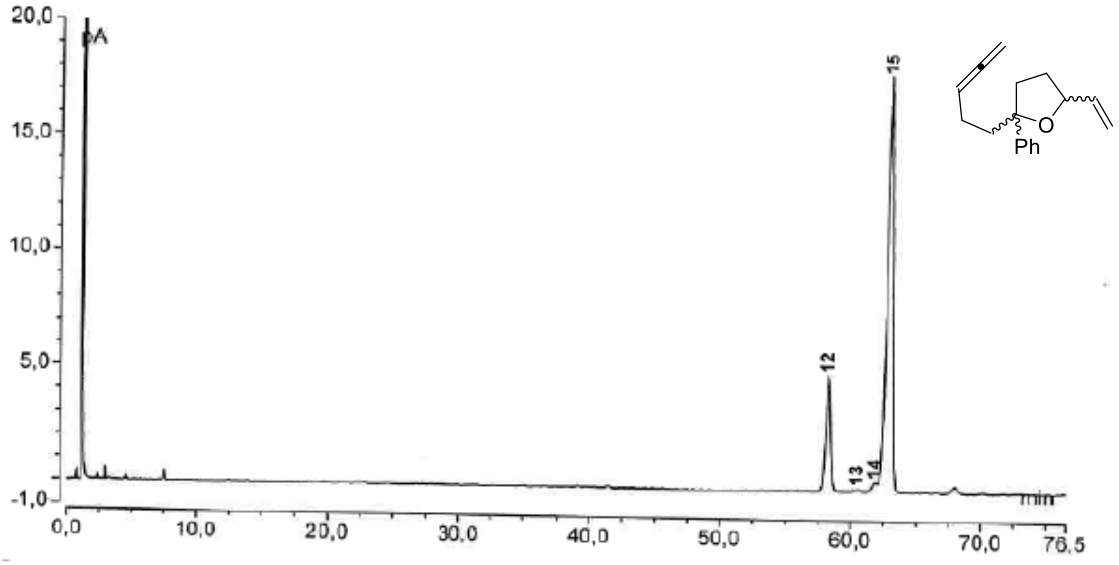

Peak	t_R (min)	Area %
12	58.26	18.72
13	60.50	0.46
14	61.86	1.52
15	62.98	79.30

Table 4.2 - Column BGB-176/BGB-15 0.25, 30m, Temperature 220/130 iso/350, Gas H_2 0.8 bar (Courtesy of Max Planck Institute)

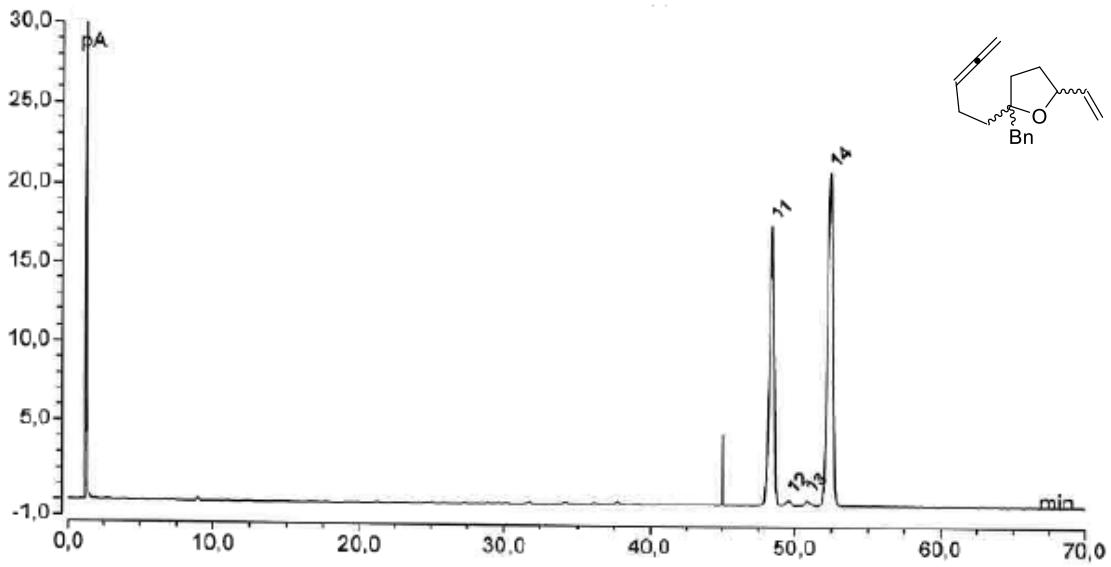

Peak	t_R (min)	Area %
11	48.38	43.21
12	49.55	0.77
13	50.83	0.97
14	52.40	55.05

Table 4.2 - Column Hydrodex-beta-TBDAc-CD 0.25, 25m, Temperature 220/130, 305min iso 9/min 220, 5min iso/ 350, Gas H_2 0.5 bar (Courtesy of Max Planck Institute)

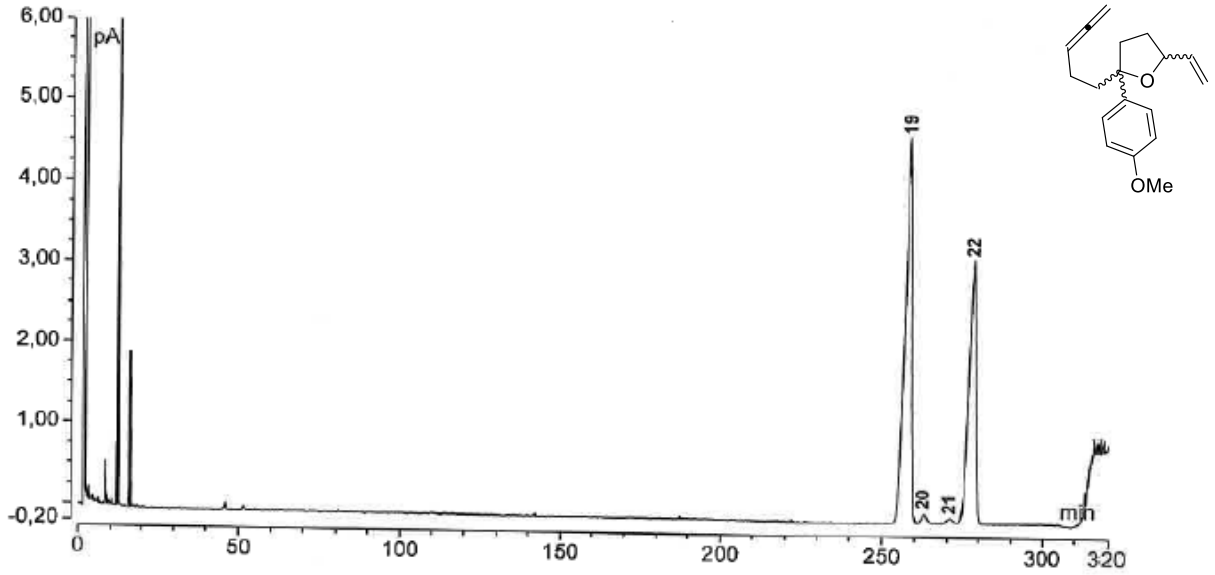

Peak	t_R (min)	Area %
19	258.23	58.34
20	262.73	1.11
21	271.01	0.66
22	278.22	39.88

Table 4.2 - Column Cyclodextrin-H in OV-1701 0.25, 25m, Temperature 220/120, 190min iso 9/min 180, 5min iso/ 350, Gas H_2 0.5 bar (Courtesy of Max Planck Institute)

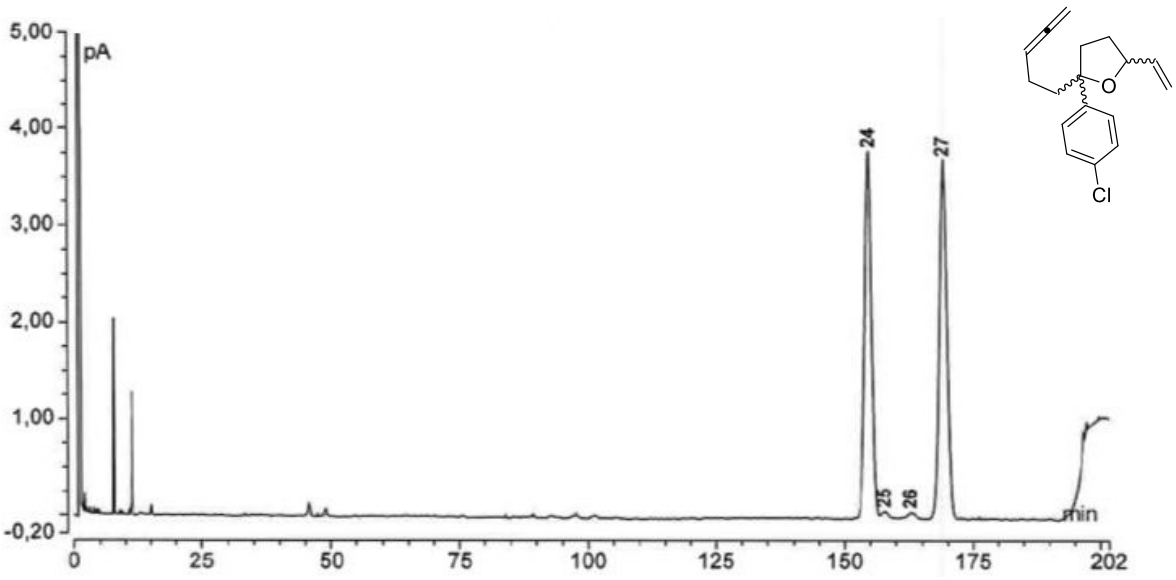

Peak	t_R (min)	Area %
24	154.86	48.02
25	157.73	0.69
26	162.86	0.65
27	169.35	50.64

Table 4.2 - Column OJ-3R, flux 1 ml/min, MeOH/H_2O=40/60 10 min, 10/90, λ=220 nm (Courtesy of Max Planck Institute)

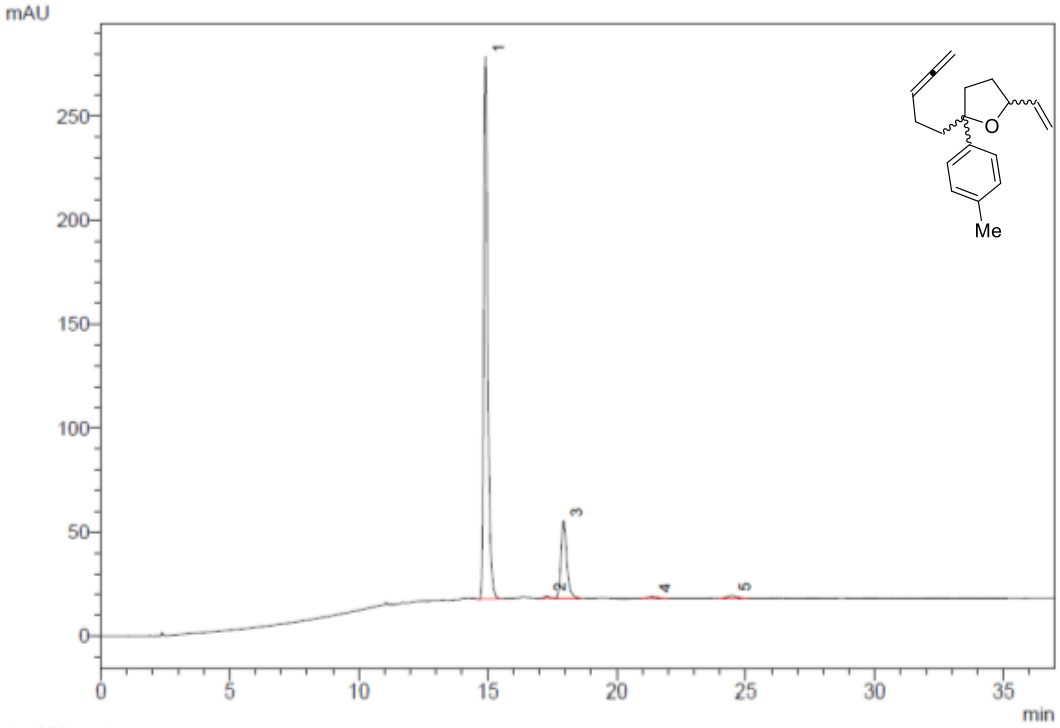

Peak	t_R (min)	Area %
1	14.91	80.87
2	17.29	0.48
3	17.94	16.77
5	24.47	1.11

Table 4.2 - Column IG-3, flux 1 ml/min, Hept/iPrOH=99/1, λ=220 nm (Courtesy of Max Planck Institute)

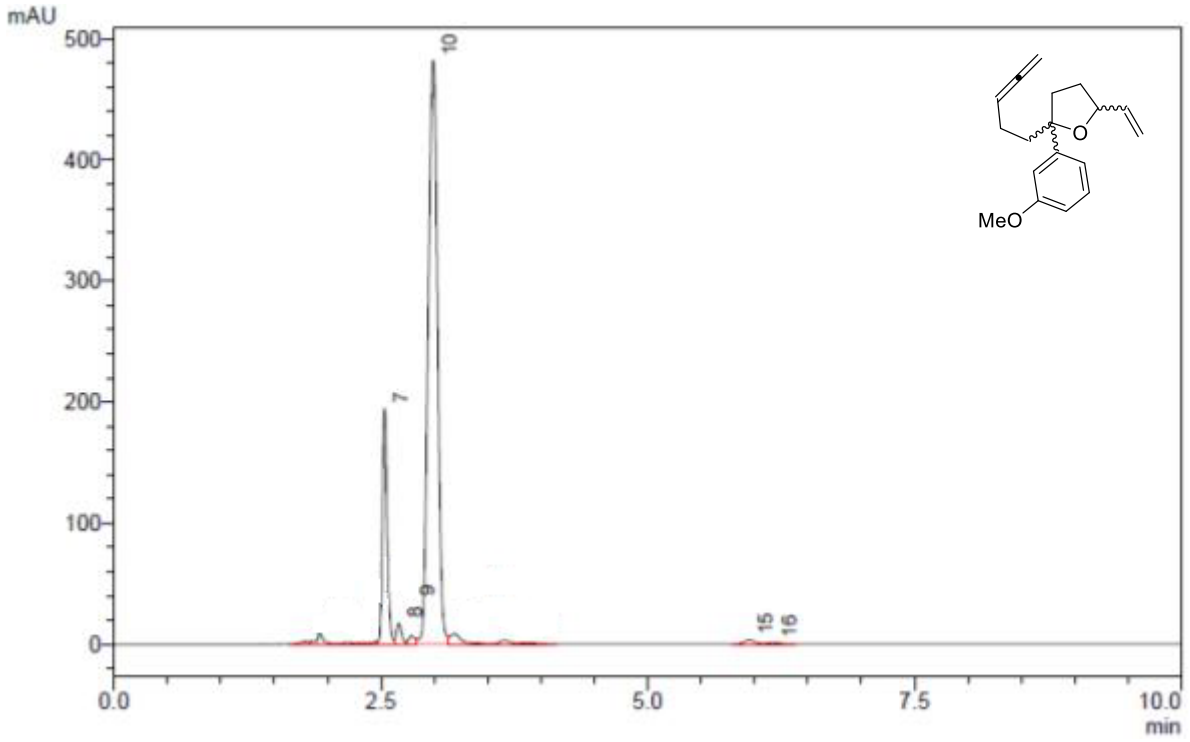

Peak	t_R (min)	Area %
7	2.53	16.07
8	2.67	1.52
9	2.78	0.72
10	2.99	76.36

11.2 Gold(I)-catalyzed Lactonization

Table 5.4, Entry 9 - Column IA-3, flux 1 ml/min, Heptane/iPrOH=99.5/0.5, λ=220 nm

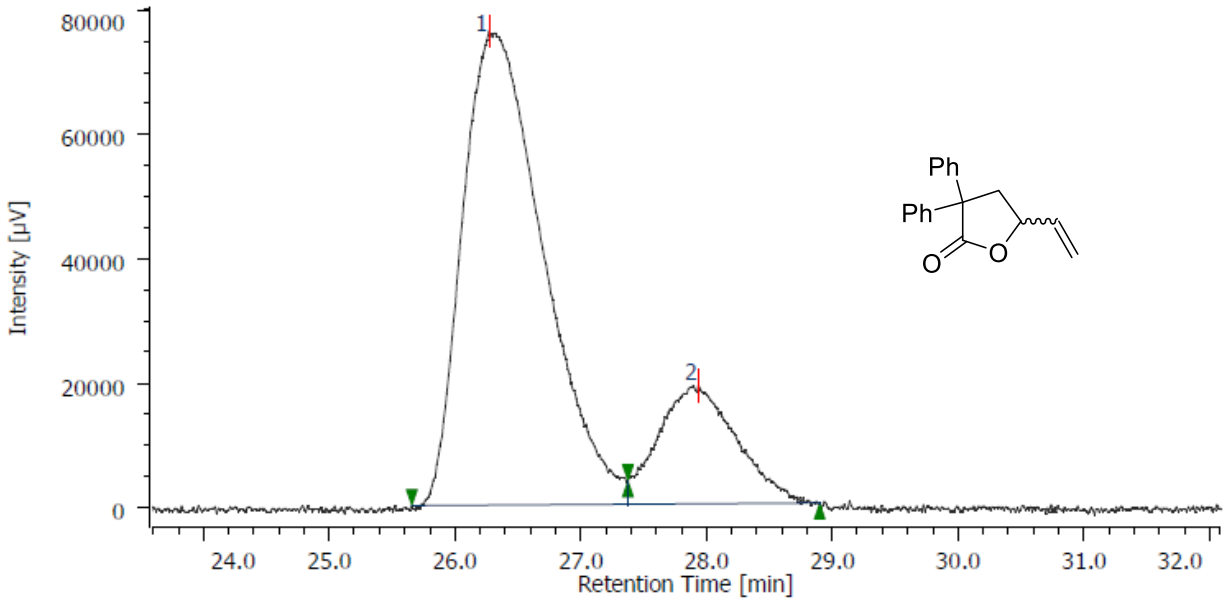

Peak	t_R (min)	Area (µV·sec)	Area %	Height %
1	26.267	3394874	80.615	80.043
2	27.933	816355	19.385	19.957

11.3 Gold(I)-catalyzed Hydroamination

Table 5.5, Entry 6 - Column IA-3, flux 1 ml/min, Heptane/iPrOH=95/5, λ=212 nm

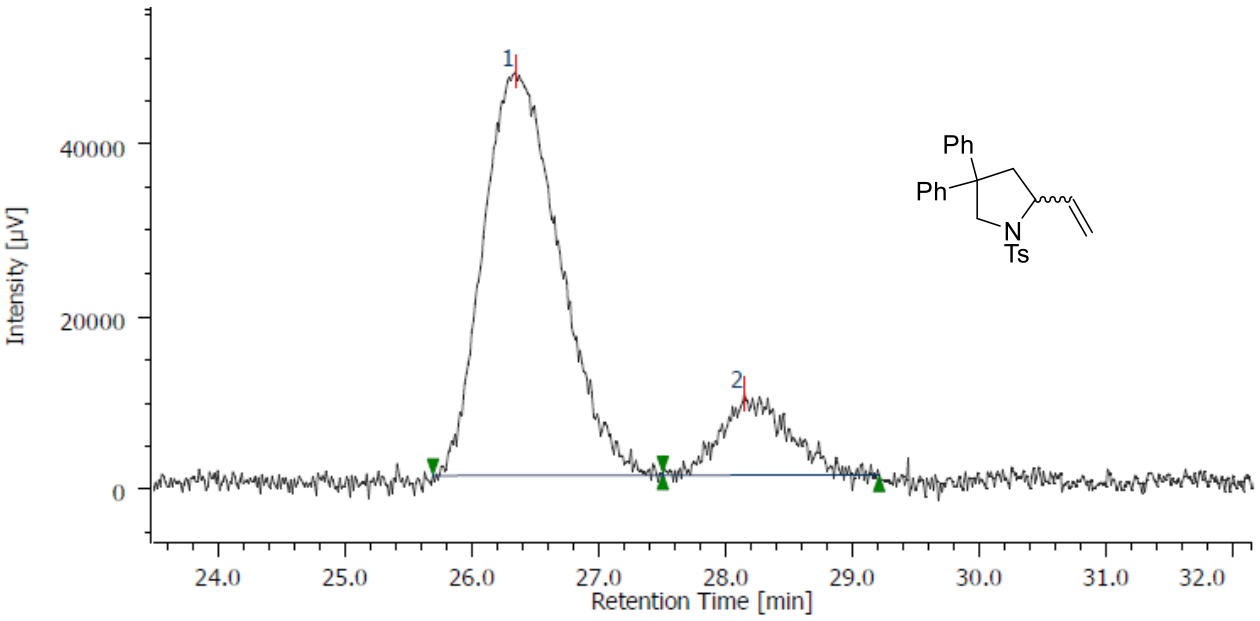

Peak	t_R (min)	Area (µV·sec)	Area %	Height %
1	26.347	1960054	85.176	83.232
2	28.147	341120	14.824	16.768

Table 5.6, Entry 4 - Column IA-3, flux 1 ml/min, Heptane/iPrOH=99.5/0.5, λ=222 nm

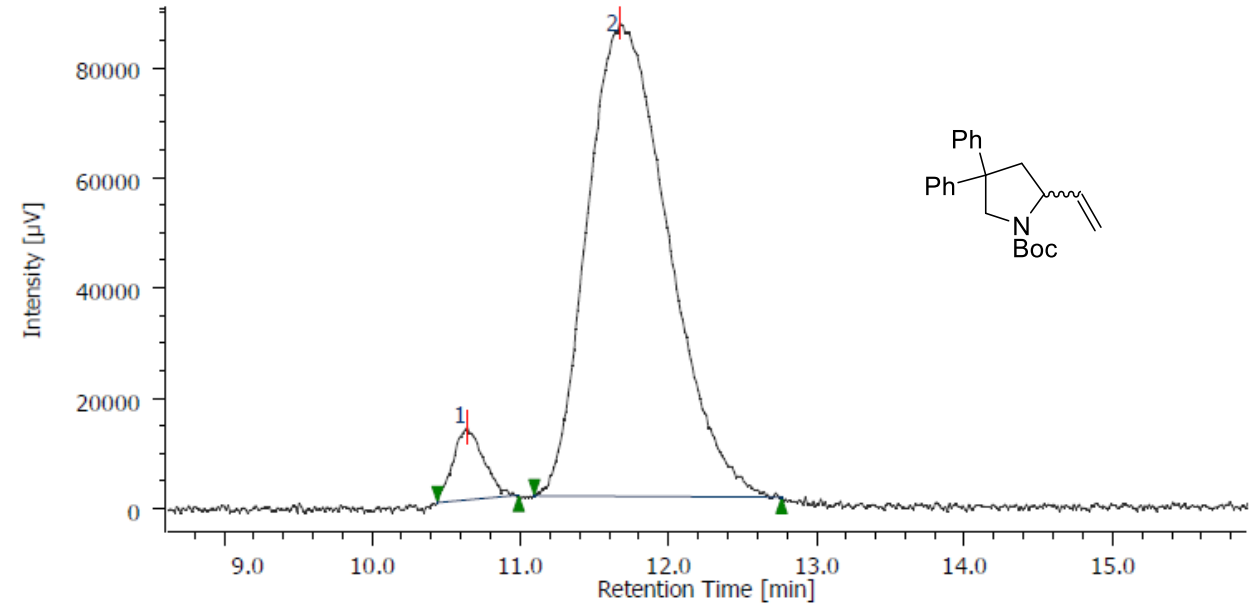

Peak	t_R (min)	Area (µV·sec)	Area %	Height %
1	10.640	186884	5.423	13.336
2	11.667	3259101	94.577	86.664

11.4 Gold(I)-catalyzed Cyclization of ene-ynes

Table X.X, Entry X - Column AS-3, flux 1 ml/min, eluent heptane/iPrOH=98:2, λ=210 nm

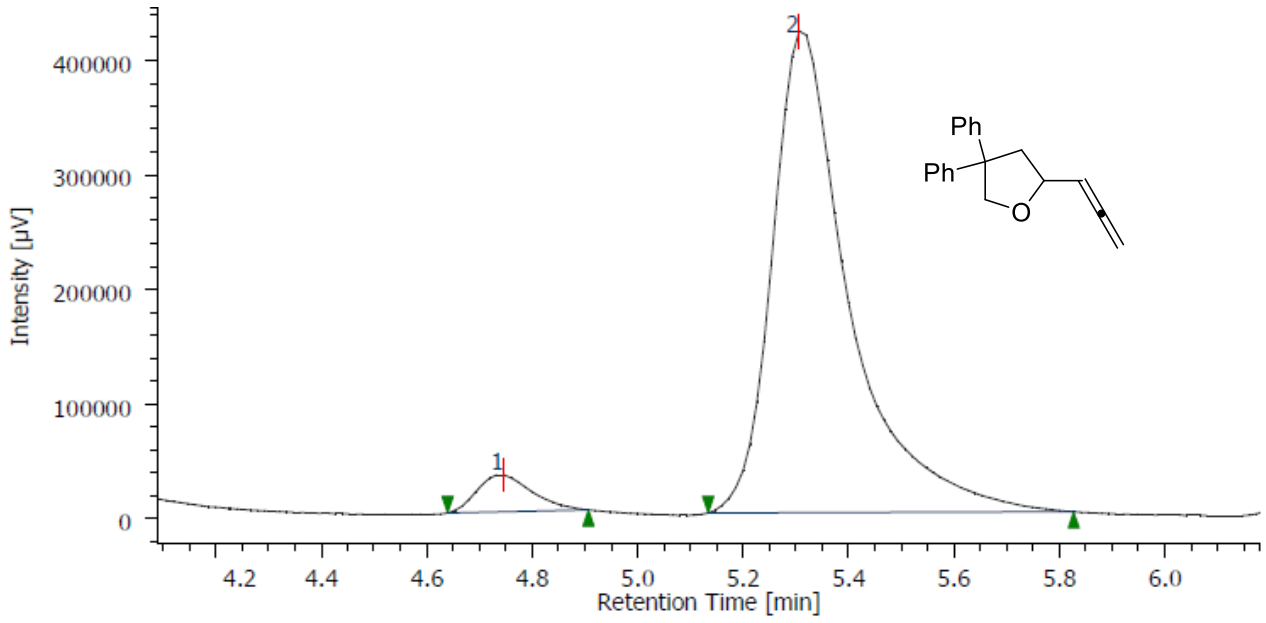

Peak	t_R (min)	Area (µV·sec)	Area %	Height %
1	4.747	232454	5.174	7.085
2	5.307	4260320	94.826	92.915

11.5 Gold(I)-catalyzed Hydroalkoxylation of allylic alcohols

Table X.X, Entry X - Column OJ-H, flux 0.5 ml/min, eluent heptane/iPrOH=98:2, λ=220 nm

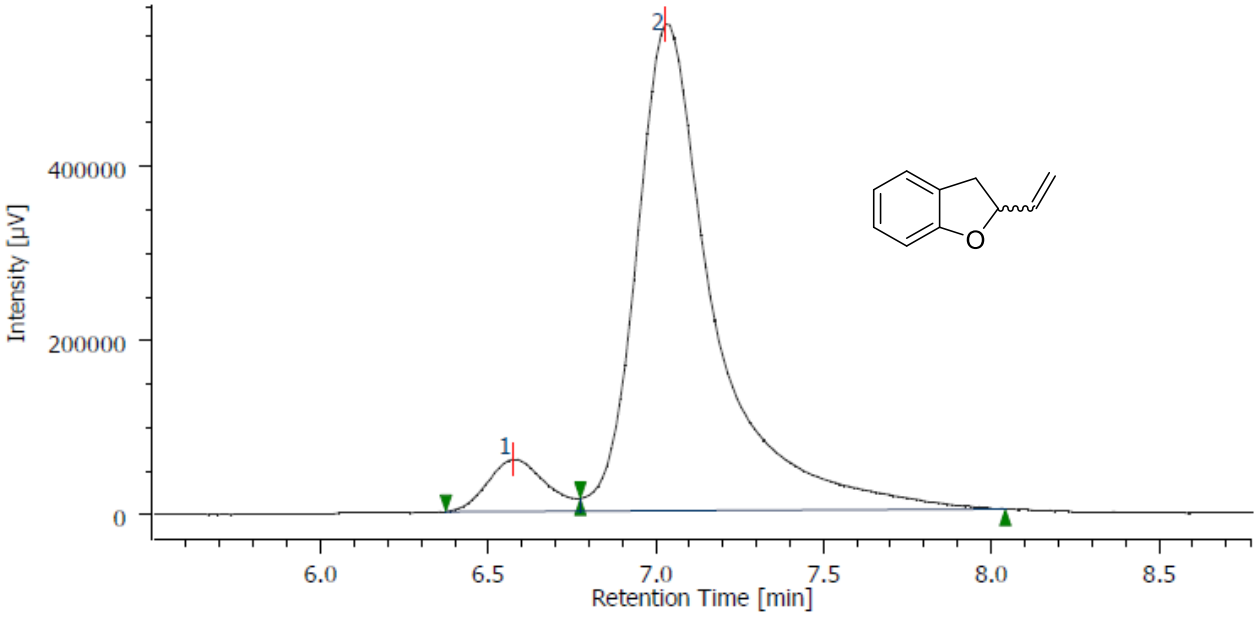

Peak	t_R (min)	Area (µV·sec)	Area %	Height %
1	6.573	720279	7.370	9.646
2	7.027	9052984	92.630	90.354

12 Acknowledgements